

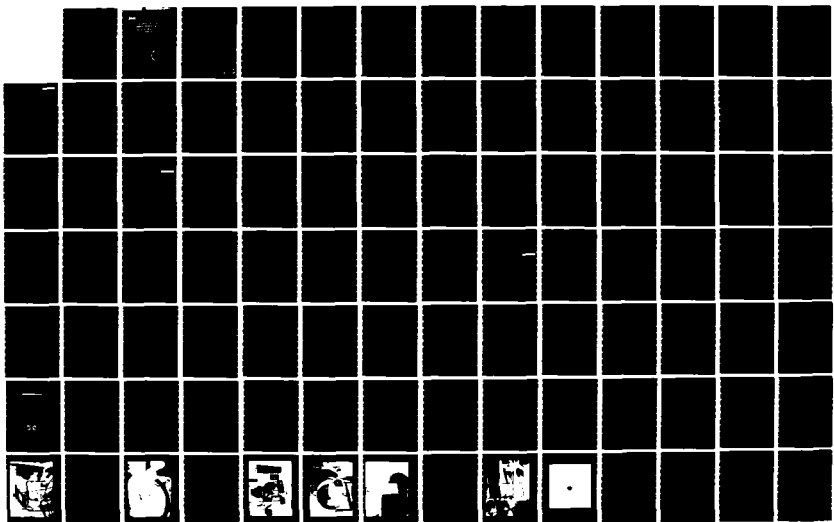
AD-A136 766

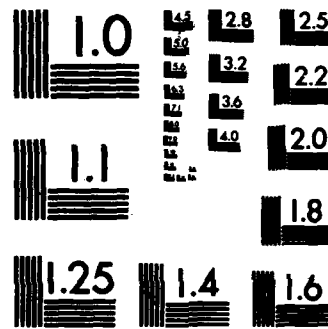
PROCEEDINGS OF THE DARPA (DEFENSE ADVANCED RESEARCH
PROJECTS AGENCY) WORK. (U) BDM CORP ALBUQUERQUE NM
B BENDOW 1982 MDA903-81-C-0151

1/4

UNCLASSIFIED

F/G 11/3 NL





MICROCOPY RESOLUTION TEST CHART
NATIONAL BUREAU OF STANDARDS-1963-A



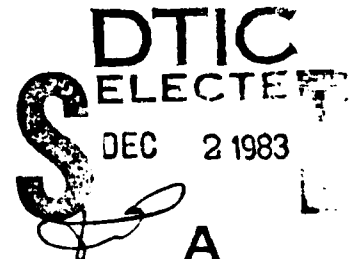
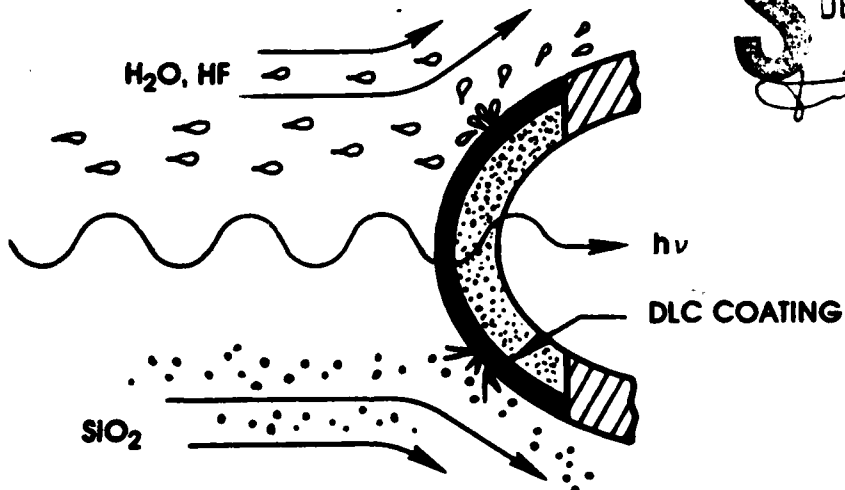
1
12

Proceedings of the DARPA Workshop on Diamond-Like Carbon Coatings

April 19-20, 1982
Albuquerque, New Mexico

A 1 3 6 7 6 6

BERNARD BENDOW, EDITOR



FILE COPY

THE BDM CORPORATION
1801 RANDOLPH ROAD, S.E.
ALBUQUERQUE, NEW MEXICO 87106

APPROVED FOR PUBLIC RELEASE
DISTRIBUTION UNLIMITED

DTIC

PREPARED FOR: DARPA UNDER CONTRACTS MDA 903-81-C-0151
AND MDA 903-83-C-0053

COMPONENT PART NOTICE

THIS PAPER IS A COMPONENT PART OF THE FOLLOWING COMPILATION REPORT:

(TITLE): Proceedings of the DARPA (Defense Advanced Research Projects Agency) Workshop
on Diamond-Like /Carbon Coatings, held at Albuquerque, New Mexico on
April 19-20, 1982

(SOURCE): BDM Corp., Albuquerque, NM

TO ORDER THE COMPLETE COMPILATION REPORT USE AD-A136 766.

THE COMPONENT PART IS PROVIDED HERE TO ALLOW USERS ACCESS TO INDIVIDUALLY AUTHORED SECTIONS OF PROCEEDINGS, ANNALS, SYMPOSIA, ETC. HOWEVER, THE COMPONENT SHOULD BE CONSIDERED WITHIN THE CONTEXT OF THE OVERALL COMPILATION REPORT AND NOT AS A STAND-ALONE TECHNICAL REPORT.

THE FOLLOWING COMPONENT PART NUMBERS COMprise THE COMPILATION REPORT:

AD#: P002 584 TITLE: Possible Applications of Diamondlike Carbon Coatings for Missile Systems and Lasers.
P002 585 Non-Conducting Hermetic Coatings for Optical Fibers.
P002 586 Hard Carbon Coatings for IR-Optical Components.
P002 587 The Properties of Hard, Insulating Carbon Coatings and Areas of Future Efforts.
P002 588 Diamond Like Carbon Films Research at NASA Lewis Research Center.
P002 589 High Energy Ion Deposited Carbon Films.
P002 590 Hard Carbon for Environmental Protection of FLIR Optics.
P002 591 Some Aspects of the Growth and Characterization of "Diamond Like" Carbon Films.
P002 592 Carbon-Coated Optical Fibers.
P002 593 Electrical and Optical Properties of "Diamond-Like" Amorphous Carbon Films.
P002 594 Ultraviolet-Laser Photodeposition.
P002 595 Carbon Film Research at Aerospace: Preparation, Characterization, and Pulsed DF Laser Damage of Coated Optics.
P002 596 Thin Film Characterization Techniques Applicable to Diamond-Like Carbon Coatings.
P002 597 Diamondlike Carbon Films in Optical Coatings.
P002 598 Surface Analysis of Diamond-Like Carbon Films.
P002 599 Raman Scattering as a Probe of Thin-Films.
P002 600 Microstructure-Property Relations in Sputtered Films.

Version For:
; GRAAI
; TAB
Encountered
Classification _____

Distribution/	
Availability Codes	
Avail and/or Special	

This document has been approved
for public release and sale; its
distribution is unlimited.

DTIC
ELECTE
S JAN 13 1984
D
A

COMPONENT PART NOTICE (CON'T)

ADM:

TITLE:

a

PROCEEDINGS OF THE DARPA WORKSHOP
ON DIAMOND-LIKE CARBON COATINGS

April 19-20, 1982
Albuquerque, New Mexico

Bernard Bendow, Editor

FOREWORD

This volume contains the proceedings of the DARPA-sponsored Workshop on Diamond-like Carbon Coatings, held at The BDM Corporation's Conference Center in Albuquerque, New Mexico on April 19 and 20, 1982. To the best of our knowledge, this was the first workshop devoted exclusively to diamond-like carbon coatings, and thus filled the need to bring together as many of the workers in the field as possible in a single forum. Included in this volume are a Foreword by D. Griscom of DARPA; a Conference Summary by B. Bendow of BDM; the texts of the majority of the papers presented at the Workshop; the Program and Abstracts from the Workshop; a list of Workshop attendees; and a partial bibliography on hard carbon coatings.

Thanks are due to the many individuals, among them authors, attendees and support personnel, who contributed to the success of the Workshop. We are also pleased to acknowledge DARPA's support for the Workshop, and BDM's assistance in providing the necessary facilities.

Bernard Bendow
Albuquerque, New Mexico
March 15, 1983

Accession Form	
Type	GRADE
PRINT	TAN
SEARCHED	<input checked="" type="checkbox"/>
INDEXED	<input type="checkbox"/>
SERIALIZED	<input type="checkbox"/>
SEARCHED INDEXED SERIALIZED	
APR 19 1982	
FBI - ALBUQUERQUE	



A-1

TABLE OF CONTENTS

<u>Section</u>		<u>Page</u>
INTRODUCTION		v
SUMMARY OF THE WORKSHOP ON DIAMONDLIKE CARBON COATINGS		1
REQUIREMENTS AND POTENTIAL APPLICATIONS		
Possible Applications of Diamondlike Carbon Coatings for Missile Systems and Lasers - H. E. Bennett		15
Non-Conducting Hermetic Coatings for Optical Fibers - H. E. Rast		20
PREPARATION AND PROPERTIES		
Hard Carbon Coatings for IR-Optical Components - A. Bubenzer, B. Dischler, P. Koidl		33
The Properties of Hard, Insulating Carbon Coatings and Areas of Future Efforts - Thomas J. Moravec		48
Diamondlike Carbon Films Research at NASA Lewis Research Center - Bruce A. Banks		58
High Energy Ion-Deposited Carbon Films - M. Stein, S. Aisenberg		78
Hard Carbon for Environmental Protection of FLIR Optics - A. Hendry, L. Taub, H. Gurev		100
Some Aspects of the Growth and Characterization of Diamond- like Carbon Films - John C. Angus		108
Carbon-Coated Optical Fibers - John M. Stevens, Martin Stein		128
Electrical and Optical Properties of Diamondlike Amorphous Carbon Films - F. W. Smith		139
Ultraviolet-Laser Photodeposition - D. J. Ehrlich, J. Y. Tsao		152
Carbon Film Research at Aerospace: Preparation, Charac- terization, and Pulsed DF Laser Damage of Coated Optics - S. T. Aminoto, J. S. Whittier, A. Whittaker, A. Chase, R. Hofland, Jr.		164

TABLE OF CONTENTS (Concluded)

<u>Section</u>	<u>Page</u>
COATING CHARACTERIZATION	
Thin Film Characterization Techniques Applicable to Diamondlike Carbon Coatings - H. E. Bennett	187
Diamondlike Carbon Films in Optical Coatings - H. A. Macleod	205
Surface Analysis of Diamondlike Carbon Films - A. K. Green, Victor Rehn	209
Raman Scattering as a Probe of Thin Films - S. R. J. Brueck	214
Microstructure-Property Relations in Sputtered Films - Russell Messier	224
APPENDIX A: PROGRAM AND ABSTRACTS	A-1
APPENDIX B: WORKSHOP ATTENDANCE LIST	B-1
APPENDIX C: PARTIAL BIBLIOGRAPHY ON DIAMONDLIKE CARBON COATINGS	C-1

INTRODUCTION

David L. Griscom
DARPA -- Defense Sciences Office

As is well known to those active in the field, the possibility of producing thin carbon films with some "diamondlike" characteristics has been known for over a decade. The reported properties of these diamondlike carbon (DLC) layers were indeed very attractive (e.g., diamondlike hardness, transparency, and corrosion resistance), leading many a program manager to consider initiating major programs to develop DLC films as useful coating materials. None of this was known to me, however, when in the fall of 1981 as a new DARPA program manager I first began putting my ear to the ground for promising "new" research opportunities. But it didn't take me long to start picking up vibrations concerning the apparently limitless potential of DLC coatings. These inputs arrived rather coincidentally from several sources, not all of which were potential vendors. Thus, diamondlike carbon appeared to be precisely the kind of opportunity I had been seeking.

As I looked deeper into the matter, it became apparent that the widespread optimism surrounding DLC was tempered by a considerable degree of uncertainty. Potential users wanted to see more samples and more research data before they became buyers. Yet, despite the demand for data and the notice generally taken by DoD program managers, there did not appear to be any major programs in place to generate the needed research. (At that time I was unaware of the substantial in-house effort at NASA-Lewis or of several smaller programs underway at other locations). For me the matter came to a head when I was paging through the preliminary program for the 1981 Boulder Laser Damage Symposium. In it I found three titles dealing with hard carbon coatings. One of these was authored by Alan Hopkins, my Air Force working partner in several

high energy laser mirror materials programs. A quick phone call to Alan led to yet another surprise: Alan was withdrawing his talk on account of receiving too few samples too late. Although this turn of events appeared to be another strike against the credibility of DLC, Alan was quick to render his assessment that diamondlike carbon had merely fallen victim again to what he termed "nickel-and-dime" funding patterns. As a result of this discussion I decided to become involved by taking a poll at the Boulder Symposium to establish how much interest there might be in holding a DARPA-sponsored workshop designed to bring together potential suppliers, researchers, and users of DLC coatings -- and hopefully some potential funding agents as well.

Encouraged by the responses elicited at an ad hoc session at Boulder, I resolved to go ahead with the organization of a workshop, with the stated objective of formulating a strategy for developing diamondlike carbon films as useful coating materials. Bernie Bendow of BDM Albuquerque agreed to take on the major logistical tasks, assist in the planning, assemble a bibliography, and prepare a final summary of the presentations and round-table discussions. To these responsibilities the task of editing the workshop proceedings was subsequently added. I think that all who attended the workshop or who peruse these proceedings will agree that Bernie's contributions have been outstanding. His summaries of the technical sessions and of overall conclusions are particularly concise and informative. For this reason I will confine my own remarks on the April 19-20, 1982 Workshop to a few salient impressions and some personal thoughts which I have had subsequently.

As apparent from the papers in this volume, diamondlike carbon obviously has many potential uses, ranging from the mundane (e.g., abrasion resistant coatings on sunglasses) to the exotic (e.g., HF resistant protective layers on high energy laser optics). Some applications seem to be within our immediate

reach (e.g., the sunglasses, or coatings for land vehicle optics) while others may require fairly long development cycles (e.g., rain-erosion resistant coatings for missile domes, or hermetic coatings for high strength optical fibers). Most intriguing in the long run is the suggestion of Hal Bennett's that DLC could become a "universal optical coating" if only the absorption coefficient could be lowered another order of magnitude to around 10 cm^{-1} . Since the refractive index can be varied by varying the hydrogen content, all-carbon AR and HR stacks might be developed which incidentally provide abrasion and corrosion resistance as well. In my view, it is here that a major research program is needed. What is the cause of optical absorption in DLC films? How is it related to stereo-chemical bonding structure? What is the nature of chemical bonding in the hard carbon films now being produced in the laboratory? What is the role of defects?

The questions which can be raised are many, and most such questions seem to lead back to fundamental questions of atomic ordering, chemical bonding, and electronic structure. These are questions which I find dear to my heart, since half of my time is still spent in the laboratory trying to determine the defect structure of fiber-optic materials such as amorphous silicon dioxide ($a\text{-SiO}_2$). Indeed, our present understanding of $a\text{-SiO}_2$ may provide, by analogy, some useful insights as we grope for the structure of amorphous diamondlike carbon. It turns out that the local atomic ordering and electronic structure of $a\text{-SiO}_2$ is very similar to that of crystalline α -quartz [I've done a review article on this subject: *J. Non-Cryst. Solids*, 24, 155 (1977)]. It is easy to visualize how a continuous random network might be constructed of perfect SiO_4 tetrahedra sharing corners. The key factor is the randomness possible in the Si-O-Si bond angle ($\sim 120\text{-}180^\circ$), coupled with the complete freedom $0\text{-}360^\circ$ in choosing the dihedral angle between tetrahedra.

By contrast, a defect-free random network of tetrahedrally hybridized carbon atoms could only be formed with gross bending of the C-C bonds. However, at present there does not appear to be any evidence for the existence of all-tetrahedrally-bonded amorphous carbon (a-C). Data obtained from Raman spectroscopy and a variety of diffraction techniques have tended to support the existence of a mixture of trigonal and tetrahedral bonds in DLC coatings. Moreover, recent reanalyses of X-ray, electron, and neutron diffraction data indicate that the bonding in bulk vitreous carbon and perhaps some hard carbon films is predominantly trigonal [D.F.R. Mildner and J. M. Carpenter, *J. Non-Cryst. Solids* 47, 391 (1982)]. A popular current model for the structure of a-C is that of a random agglomeration of small ($\sim 10\text{\AA}$) graphitic islands which might be connected by a few ($\sim 5\%$) tetrahedral bonds. Electron spin resonance (ESR) has demonstrated the presence of large numbers of unpaired electrons in dangling bonds in certain sputtered and evaporated a-C films, and this has been interpreted as indicating that the graphitic islands may not even be interconnected [Wada et al., *J. Non-Cryst. Solids* 35 & 36, 543 (1980)]. Other authors have referred to DLC films as carbynes (chain structures consisting of alternating single and triple bonds), although the supposed existence of carbyne forms of carbon in nature has recently been questioned [Smith and Buseck, *Science* 216, 984 (1982)]. To these possibilities I might add the fanciful suggestion of an a-C structure comprised of alternating two- and four-coordinated carbons; (substituting carbon for both silicon and oxygen in the $a-\text{SiO}_2$ structure would lead to a continuous random network with a density of about 1.8).

Clearly, accurate experimental determinations of the relative amounts of carbon in sp^3 and sp^2 hybridization states will be crucial to testing any structural models proposed for a-C. Diffraction methods appear to be capable of giving very precise answers if the data are obtained out to sufficiently

large values of the maximum scattering vector Q_{\max} and provided proper normalization procedures are followed [Mildner and Carpenter, loc. cit.]. The particular measurements which can be so definitive are the first- and second-shell coordination numbers determined from the radial distribution function; these are (3,6) for graphite and (4,12) for diamond. An analysis by Stenhouse and Grout [J. Non-Cryst. Solids 27, 247 (1978)] of earlier electron diffraction data for a 100Å a-C film [Kakinoki et al., Acta Cryst. 13, 171 (1959)] indicated 75% tetrahedral and 25% trigonal bonding. This outcome was tacitly questioned by Mildner and Carpenter on the normalization issue. However, based on studies of DLC films presented in Albuquerque, I get the impression that a high degree of sp^3 hybridization may indeed be possible in thin a-C films if the proper preparation procedures are employed. Of course, where the structure of the DLC coating is shown by diffraction measurements to be primarily polycrystalline diamond rather than amorphous, there can be no doubt of the predominance of tetrahedral bonding. The reasons why some DLC films are amorphous and others are crystalline comprise another issue of considerable fundamental interest.

But returning to the real world, the burning question is how this needed research is to be paid for. Despite the highly optimistic assessment of the potential of diamondlike carbon which emerged from the Albuquerque workshop, no significant sources of new funding were identified at that time. At the opening of the workshop I expressed my hope that the consensus generated by the contributors might ultimately be utilized by some appropriate funding agencie(s) as the justification for a new program of sufficient scope to get to the bottom of the major scientific and technical issues and bring DLC coatings to final maturity. I still believe this will happen, and if I have my way, DARPA may yet play a leading role as a funder of DLC research.

Summary

SUMMARY OF THE WORKSHOP ON
DIAMOND-LIKE CARBON COATINGS*

BERNARD BENDOW
THE BDM CORPORATION
ALBUQUERQUE, NEW MEXICO

*SPONSORED BY DEFENSE ADVANCED RESEARCH PROJECTS AGENCY
UNDER CONTRACT MDA 903-81-C-0151

OVERALL CONCLUSION/STATUS OF THE TECHNOLOGY

Areas of Applicability

- (a) Protection from corrosive chemical environments such as acids (HF, HNO₃, H₂SO₄, etc.)
- (b) Increased durability of glass surfaces and fibers
- (c) Abrasion-resistant, cleanable optical surfaces
- (d) AR/HR optical coatings for windows, lenses and mirrors
- (e) Heat sinks for electronics
- (f) Passivating coatings (in optical discs, solar cells, etc.)
- (g) Wear-resistant/erosion-resistant coatings
- (h) Ultrasmooth surface coatings
- (i) Space optics coatings
- (j) Surface hardening (for plastics, salts, etc.)

Current Properties

- (a) Hardness up to ~ 2x10³ Knoop
- (b) Thickness up to ~ 10-20 μm
- (c) Amorphous, but may contain some crystalline regions
- (d) Good adhesion to glass, plastic, metals, semiconductors and ionic materials
- (e) Extremely resistant to acids and bases, including concentrated HF, and sulfuric/nitric
- (f) Refractive indices between ~ 1.8-2.3
- (g) Densities up to ~ 2.8 gm/cm³ (diamond = 3.5)
- (h) Resistivities from ~ 10⁶ to 10¹⁶ Ω-cm
- (i) Pure C or doped with H, P, B; can be n or p-type semiconductor
- (j) Deposition rates up to ~ 1μm/min
- (k) Optical band gaps up to ~ 2.1 eV
- (l) High abrasion resistance compared to evaporated coatings
- (m) Lowest absorptions ~ 10² cm⁻¹ at CO₂ and DF wavelengths

Measurements or Further Measurements Required

- (a) Thermal conductivity in \perp and \parallel directions
- (b) Thermal expansion coefficient
- (c) Thermal fracture resistance
- (d) Thickness uniformity
- (e) Compositional uniformity
- (f) Impurity/defect concentration
- (g) Elastic properties
- (h) High-impact erosion resistance
- (i) Optical scattering
- (j) Laser damage
- (k) Raman spectroscopy

Fundamental Questions

- (a) sp^3 vs sp^2 bonding
- (b) Intrinsic vs extrinsic absorption
- (c) Coating microstructure, amorphousness vs polycrystallinity
- (d) Role of hydrogen
- (e) Relation of density and microstructure to deposition parameters
- (f) Dependence of properties on substrate

Priority Areas for Investigation

- (a) Absorption
- (b) Adhesion
- (c) Laser Damage
- (d) Hermiticity
- (e) Hardness/abrasion resistance
- (f) Carbon-only, high rate and high energy deposition methods
- (g) Role of implantation, surface cleaning and surface conditioning

Priority DoD Applications

- (a) AR coatings for 8-12 μm low/medium power optics
- (b) Coatings for HEL CO₂ and DF mirrors
- (c) Hermetic coatings for optical fiber
- (d) Passivating coatings for soft or reactive surfaces on laser optics, especially in chemically corrosive environments
- (e) Durability coatings for plastic goggles/canopies/domes
- (f) Coatings for optical components in salt-spray environments

SUMMARY OF TECHNICAL SESSIONS

Session on Requirements and Potential Applications

This session attempted to provide the DoD's view of requirements and potential areas of application for diamond-like carbon (DLC) coatings. Also included was a discussion of certain fundamental and practical issues which need to be addressed in this connection as the technology evolves. D. Griscom's talk reviewed some of the history leading up to the workshop, especially the preliminary discussions in an ad hoc meeting set-up at the 1981 Boulder Conference between representatives of DARPA, AFWL, AFWAL, AFOSR, NWC and other organizations. There was overall agreement on the potential significance of the technology for DoD, and the need for further discussions and planning aimed at validating and exploiting the technology. H. Winsor's talk provided a broad range of observations and thoughts on the subject. He pointed out the importance of enhancing both the mechanical and chemical durabilities of exposed optical components such as mirrors, windows and domes, especially those operating in corrosive environments such as salt spray, or impact-erosion-prone ones such as in airborne vehicles (rain, insects) and battlefield vehicles (sand). Surfaces must also stand up to repeated cleanings for use in many scenarios. Adhesion is an essential characteristic, and one should assess the potential advantages of amorphous as opposed to polycrystalline carbon coatings in this regard. Hydrogenation may reduce dangling bonds in the amorphous form. The durability provided by DLC could allow exploitation of materials like alkali halides which have excellent transparency but are too soft and/or hygroscopic for operational systems. Another matter which merits investigation is the potential, by analogy to a-Si, for improved optical performance of the coating in the space nuclear environment. Analogies with silicon may be useful in analyzing carbon, but the smallness of the carbon atom and its many allotropes are important differences to keep in mind. We may also be able to gain insights from glassy metals, which develop tight bonds

upon quenching. AFOSR's interest is primarily in the why, not what, of carbon coating formation and properties. H. Bennett addressed the potential application of DLC coatings for missiles and lasers. Potential properties of DLC which could be exploited in this connection are hardness, adhesion, high refractive index, low absorption, high thermal conductivity, modest thermal expansion, hydrophobicity, and chemical inertness, for example. Some requirements include resistance to erosion, minimization of scattered light, low emission (and therefore absorption) if supersonic, and good optical homogeneity. Even at Mach-2 stagnation temperatures of over 200°C need to be accommodated at sea level, with more demanding requirements at higher speeds; thus, good resistance to thermal shock is required. The anticipated high thermal conductivity of DLC could be exploited in this connection for sufficiently thick coatings. The thermal radiation problem requires as low an absorption as possible, preferably $\sim 10^{-1} \text{ cm}^{-1}$. The high index of DLC is an advantage for HR coatings but limits their use in AR coatings to high index substrates. Requirements for laser optics are similar, but also include requirements for high damage threshold, and low wavefront distortion (quiescent as well as under thermal load). Bennett also pointed out that coating pairs with large index differences are desirable because they lower the effective coating absorption. It is also essential for laser optics to maintain tight tolerances on coating thickness uniformity to achieve acceptable figure (phase) control. For the IR this translates to a uniformity requirement of $\sim 1\%$.

A. Guenther reiterated some of the previous points, but addressed various new ones as well. He felt that the terminology question was still open: just how diamond-like is DLC? Guenther commented on information given to him that Zeiss in Jena has been coating large size components of CaF_2 and alkali halides for environmental protection with "pinhole-free" DLC. He also mentioned work underway in the UK, at Barr and Stroud (tens of microns thick coatings) and Spectron. Returning to issues, the compatibility between coating and substrate, and the specificity

thereof, needs to be considered. C-films appear to be smoother than their substrates, and may thus themselves serve as substrates for other films. A potential advantage of high index materials for coatings is the reduced thicknesses required, limiting impurity size and thus damage susceptibility. He pointed out that an important reason that DLC coatings should be pursued is that DLC is one material which people are satisfied can achieve environmental protection of components.

H. Rast described the Navy's requirements for underwater fiberlinks and especially for load-bearing fiber. Applications include torpedo missiles, sonabouys, bottom-laid cable, towed arrays and mine countermeasures. In order to lock-in high strength and maintain it (i.e., eliminate fatigue) in fibers, a non-damaging hermetic coating is required. Such a coating must be insulating, adherent, chemically inert, pinhole free, uniform/smooth, concentric, immune to cyclic fatigue, easily spliced, deposited in-line, moderate in cost (< 5% cost of fiber), and non-damaging to the strength and optical properties of the substrate fiber. DLC is one of the coating materials which offers promise for satisfying these criteria.

Session on Preparation and Properties

A. Bubenzier et al described investigations of hydrogenated a-C coatings deposited from an RF-excited discharge from benzene vapor on negatively biased substrates. The main parameters determining film properties appeared to be negative bias and gas pressure. Deposition rates of ~ 500Å/mm were achieved, which implies about a half hour for $\lambda/4$ coating at 10.6 µm, at gas pressures of ~ .03 to .1 Torr. The refractive index and the visible absorption vary linearly and the absorption of the CH stretching band inversely with H content. Significantly, the refractive index can be tuned as required between about 1.8 and 2.2 with relatively small effects on absorption at long wavelengths. For n=2, e.g., a-C is an ideal AR coating for Ge, and the authors obtained promising results by replacing a ZnSe layer in an AR stack with a-C. The absorption is

still higher than desired but they are optimistic about reducing it. An interesting test was performed with a 600W CO₂ laser incident on a 1 μm carbon coating on Si, which indicated that the coating burns off very cleanly, with virtually no damage outside of the beam spot.

T. Moravec described coatings produced by low energy ion beam deposition and plasma induced CVD via decomposition of hydrocarbon gas. The deposition rates were very slow, 100's Å/hr and chamber wall deposits were a problem. DLC coatings were shown to provide decreased reflection and increased durability for solar cells. Auger analysis indicated features intermediate between diamond and graphite. By varying gas pressure and power one is able to produce coatings with variable refractive index (~ 1.7-2.3) and hardness (up to ~ 1850 Knoop). Calorimetry measurements for coatings on CaF₂ revealed absorptions in the 400 cm⁻¹ range at 1.3 and 2.9 μm , and 121 cm⁻¹ at 3.8 μm . They experienced difficulties coating high thermal expansion ionics such as CaF₂ due to large compressive stresses building up in the coatings, ~ 20-30x10⁹ dynes/cm². Structural studies including X-ray diffraction indicated the films were amorphous, but contained some crystalline regions.

B. Banks described NASA's interests and project work on DLC coatings. Their primary application areas are passivating/protective coatings and/or heat sinks for spacecraft electronics (microwave diodes, etc.) and other components requiring high thermal conductivity (e.g., as a filler in diamond flake composites). They have experimented with many different methods of coating production. These include deposition via Ar-ion source (low rates); DC hydrocarbon plasma; RF sputtering with either hydrocarbons and/or carbon target; dual-beam methane and argon sources; argon source with carbon target; vacuum arc carbon source (high rate deposition); coaxial carbon plasma gun source (currently under construction); and a projected carbon ion beam source currently in the planning stage. A range of values were achieved for resistivities

(10^{10} - 10^{12} $\Omega\text{-cm}$), densities (1.9-2.8), and refractive indices (1.75-2.30). The resistance to sulfuric + nitric acid was very good. Adhesion was found to vary with the particular substrate, but ion beam cleaning of the surface was invariably helpful in achieving good adhesion. The objective is to concentrate on the pure C-sources based on the supposition that predominantly C films are denser and thus more tetrahedral (closer to diamond) and that hydrogen reduces thermal conductivity. Nevertheless, if the films are imperfect, hydrogen can be beneficial in binding up the structure, but the "fully" densified pure-C films should be best. The arc and plasma gun techniques are attractive because they combine pure C-films with high deposition rates. Very high rate processes may provide the advantage of depositing a coating before chamber contamination can become a problem.

M. Stein described the use of ion-plasma (non-equilibrium) deposition techniques. The high energy of ion deposition (up to KeV's) can be used to implant C into substrates, establishing "roots" which enables subsequent deposition of a well-adhering coating at lower energies. The method is especially useful for ionic substrates where the bonding to C is poor, and has been used at G+W to produce high-adherence coatings on CaF_2 , for example. Auger measurements reveal a graded profile in C-concentration as a function of depth into the substrate for these coatings (no sharp interface). Ion-deposited coatings can be prepared with or without hydrogen, and show excellent corrosion resistance to both organic and inorganic acids and bases. Coatings have been applied to glass, polycarbonate, metals, semiconductors and ionic materials. Raman spectra indicate the presence of both diamond and graphite-type vibrations in DLC, suggesting it is chemically somewhere in-between the two.

H. Gurev described development of $\lambda/4$ AR coatings for Ge at $10.6 \mu\text{m}$ in support of RSRE in UK. The Holland/Lettington patents were licensed and RF glow discharge employed in an "upside-down" configuration for coating

large parts up to ~ 8"/side. The films contributed about 2-4% absorption in the 7-10 μm range and < 1% from 4-6 μm , hardness was about 1800-2000 Knoop, and deposition time for the AR coating was ~ 1/2 hr. The most spectacular property of the coating was its abrasion resistance. The coated window, which was envisioned for military land vehicle applications, showed virtually no degradation in performance after close to 10^5 cycles of a wiper with 40 gm load cleaning off a water and sand slurry from the window; while alternative evaporated coatings degraded rapidly after an order of magnitude less cycles.

J. Angus discussed various aspects of the chemistry of DLC coatings. He pointed out that thermal deposition (evaporation, thermal decomposition) results in coatings which are non-insulating, non-dense, soft and susceptible to acids, while non-thermal deposition (ion beams, RF glow discharge, etc.) result in coatings which are insulating, dense, hard and acid-resistant. These observations suggest that thermal films are dominated by sp^2 trigonal bonding, while the non-thermal are dominated by sp^3 tetrahedral bonding. There is little memory expected of the original source in deposition because energy is quickly dissipated on impact with the surface. It is likely that sputtering and deposition occurs simultaneously. Molecular dynamics calculations were employed to investigate the stability of potential bonding configurations, and the most stable dimer was found to be a linear configuration normal to the surface. Preliminary conclusions are that non-tetrahedral structures sputter away preferentially, and that positive ions are not responsible for DLC, rather negative species may play a role in stabilizing the structure. DLC films revealed no structure under SEM/electron diffraction. Auger must be used with care because sputtering can induce graphitization and thereby provide false readings. SIMS is difficult because of slow sputter rate, but is useful for qualitative identification of additives and/or impurities such as hydrocarbons. IR absorptance can be used to identify the type of C-H bonding in hydrogenated films.

R. Jaeger of Spectran presented the paper by Stevens and Stein on DLC-coatings for optical fiber. He described the development of a plasma-ion coating module for applying thin DLC coatings (100's Å) to fibers in-line subsequent to draw. The coating module has two stages for deposition of different materials. The objective is to obtain a hermetic coating which reduces static fatigue and does not degrade the original fiber strength. Very good improvements in lifetime were obtained with a double stage of C, followed by In coating, although the original strength was degraded by a third or more. C alone was less effective in improving the lifetime, but less damaging to the initial strength. The authors hypothesize that the DLC coating contains pinholes and thus does not provide as much lifetime improvement as expected. The pinholes could allow In to react with the fiber and reduce the initial strength. The pure-DLC coating, when optimized, should increase lifetime substantially with little degradation of the initial fiber strength.

G. Wehner reported on a paper given by Weisenthal at another conference in April 1982. Weisenthal described several deposition schemes, one of which is reactive triode sputtering deposition using a perforated anode in-between a hot cathode and the substrate (maintained at negative voltage). Deposition rates were \sim 300-800 Å/min. Wehner suggested that it might be better to hide the anode. Two other schemes which were less successful included a combined ion beam/sputtering with laser assist (rate \sim 10 Å/min); and coaxial sputtering with a C anode in-between hollow cathodes (\sim 100 Å/min). The refractive indices were similar to other DLC coatings but surprisingly low densities (\sim 2gm/cm³) were reported. Models with 3 to 8-fold coordinated rings were invoked to interpret the observations. Finally, internal stress problems were noted with the films. Wehner then described a patent issued to him in 1962 for a deposition process involving Hg discharge at low pressures. He envisions exploiting the higher kinetic energy of atoms sputtered from a target obliquely to selectively deposit higher energy C atoms and

thereby obtain a harder, more diamond-like coating. Use of pulse deposition ($\sim 10^3$ KeV per pulse, 10 \AA thickness per pulse) is an attractive option. A thin target with long sheath geometry was suggested.

F. Smith described a-C films prepared by dc glow discharge decomposition of ethylene, with deposition rates $\sim 200\text{\AA}/\text{min}$. The film properties, including optical energy gap and electrical conductivity are strong functions of the preparation conditions. The conductivity, e.g., varied from 10^{-16} to $10^{-6}\Omega^{-1}\text{cm}^{-1}$ as deposition temperature varied from 75 to 350C. Stabilization of the structure by incorporation of hydrogen was observed. The possibility of incorporating F instead of H to achieve higher band gaps was proposed. The ability to dope with P and B and thereby tailor the conductivity, was demonstrated by thermopower measurements.

D. Ehrlich described "cold" photodeposition (1-10°C temp rise) using visible/UV selective laser-induced surface reactions. The method has been successfully demonstrated for a variety of surface reactions on semiconductors. Laser induced photoreaction of adsorbed hydrocarbons is suggested as a method for attaining DLC coatings. The temperature of the substrate and the surface chemical reaction can be controlled independently in an attempt to optimize the coating process.

S. Aminoto described deposition of DLC coatings of 0.1 to 0.2 μm thickness on CaF_2 windows and polished copper mirrors using a rapid quench of laser-heated C gas. Adhesion was excellent (~ 60 -400 kg/cm^2) on these as well as other types of substrates and the coating displayed high resistance to chemical attack by acids such as concentrated HF. Absorption ranged from $\sim 10^5$ at 1 μm to $\sim 10^3 \text{ cm}^{-1}$ at 10 μm . The coatings were subjected to single pulse DF damage tests. Damage levels $\sim 25\text{J}/\text{cm}^2$ were obtained for CaF_2 , with similar damage levels for uncoated CaF_2 . The damage levels for coated Ca mirrors was $\sim 10\text{J}/\text{cm}^2$ as opposed to $\sim 58\text{J}/\text{cm}^2$ uncoated. This decrease, and the cause of damage in both

cases, was believed to be graphite inclusions from the C-source. When cleaned up from defects and particulates, DLC should be effective as a protective coating for laser components to withstand corrosive F₂-DF gas mixtures at high pressures and at high laser fluence.

Session on Coating Characterization

This session discussed various methods of characterizing coatings which are being used, or could be used, to characterize DLC coatings.

Bennett's paper outlined some of the principal properties and tools available for measuring them. Among the properties of interest for optical coatings are thickness, refractive index, absorption, structure, surface irregularities/defects, scattering and laser damage threshold. Thickness can be measured by a variety of methods including transmission vs wavelength, interferometry, ellipsometry and taper-sectioning. Ellipsometry is especially of interest for measuring relative thickness uniformity for which it is a very sensitive measurement (~ 0.1% accuracy possible). Coating, surface and interface absorptions can be studied by calorimetry, nuclear resonance (for H⁺), ATR and profiling SIMS. Wedged coatings facilitate the measurement of absorption vs coating thickness. Impurities and structure can be studied by electron diffraction, Auger, XPS, SIMS, electron microscopy, nuclear methods (neutron activation, nuclear resonance and Rutherford back-scattering, e.g.), and laser desorption to name a few. Surface irregularities can be detected by interferometry and stylus profiling. In short, a virtual plethora of characterization techniques are available for studying coating and coating surface properties.

A. Macleod indicated the importance of columnar growth in coatings and their potential influence on coating properties. Variations in density (voids) can have a major effect on optical, physical and chemical

characteristics of coatings, especially if water is incorporated in low density regions, breaking bonds (affecting adhesion) or promoting recrystallization.

A. Green described the application of electron spectroscopy to surface characterization of DLC coatings. XPS spectroscopy was difficult to use because of the very small shifts among different C allotropes (~ .1 volt). Auger, on the other hand, displays well-defined changes as a function of C chemistry. Application of Auger to a variety of DLC coatings indicated a combination of both diamond-like and graphitic spectral features. When properly cleaned in UHV, DLC coating surfaces display distinctive C-KLL spectral features similar to diamond surfaces.

S. Brueck described the application of Raman Scattering to nondestructive characterization of thin films. The Raman spectrum is sensitive to properties such as local structure, stress, and defect density. It is possible to scan the surface with submicron resolution and, moreover, the film can be scanned as it is deposited by using an OMA. The method is also attractive because it is nondestructive, low laser powers can be used, and special surface preparation is not required. Brueck's reported measurements were on Si surfaces, but he believes the method should be equally applicable to DLC.

R. Messier discussed methods of classifying the microstructure of vapor deposited thin films and relating microstructure to chemical, mechanical and electrical properties of films. The universal parameters are normalized preparation temperature and sputtering gas pressure. The model implies that C, with a high melting point can access relatively dense structures at low equilibrium temperatures. A wide variety of film microstructure, including columnar growth and nodular growth can be analyzed within this context.

Roundtable Discussions

The preparation-properties discussion resulted in an enormous matrix of preparation methods and properties to which noncontroversial values could not easily be assigned. The matrix will be sent out to authors to fill in any blanks of their choice, and hopefully a consensus will emerge on at least some points. Some "best" values were agreed on, including hardness ~ 2000 Knoop, CO_2 and DF absorptions $\sim 10^2 \text{cm}^{-1}$, size of substrate coated $\sim 8"$ on a side, and thickness $\sim 10\text{-}20 \mu\text{m}$, for example. The discussion on future directions centered on problem areas requiring improvement and/or resolution. Some of the key properties which need to be pinned down quickly are absorption (is it extrinsic and if so what's the cause?), hermeticity, adhesion, hardness, surface roughness and abrasion resistance. All of these have to be related quantitatively to preparation conditions.

Requirements and Potential Applications

REQUIREMENTS AND
POTENTIAL APPLICATIONS

REQUIREMENTS AND POTENTIAL APPLICATIONS

ADP002584

Possible Applications of Diamondlike Carbon Coatings
for Missile Systems and Lasers

H. E. Bennett

Optical Component Technology Program Office
Naval Weapons Center, China Lake, California 93555

If hard carbon or "diamondlike carbon" films that have primarily sp^3 bonding rather than the sp^2 bonding of graphite and conventional amorphous carbon can be prepared with low optical absorption coefficients, they will have many optical applications. Among these are (1) hermetic protective coatings for optical fibers, (2) antireflective protective coatings for germanium windows used in FLIR search sets, (3) hard coatings for goggles, tank windows, and plastic parts, and (4) coatings for various other optical components. Barr and Stroud Ltd. produces coatings for military optics for the United Kingdom.¹ Spectran Corporation of this country is setting up a commercial plant to coat optical fibers with hard carbon coatings using present technology.² Two very important component applications may be (1) protective coatings for missile domes and (2) coatings for laser optics; these two applications are the subject of this paper.

Rain and dust or sand erosion are significant operational problems for missile domes. If the missile is carried on an aircraft, the dome normally is uncovered during flight and thus is exposed to sand erosion during takeoff and landing operations. In addition, salt spray and contact with seawater can be problems in ocean operations. During captive flight, the missile dome can be exposed to rain erosion as the aircraft flies through clouds and weather.

The requirement for erosion resistance can occur for other reasons also. For example, in a Navy Telex dated 4 April 1981 from CG FMFPAC to COMNAVAIRPAC San Diego, which that Command forwarded to COMNAVPAIRSYSCOM Washington, DC, problems

with inadequate erosion resistance on some aircraft optics are described. The Telex to Washington, DC reads, in part,

"... request task appropriate activity to investigate the feasibility of design changes which can be implemented so that the lens/windows will withstand rocket motor damage ..."

Hard carbon coatings, which are highly resistant to erosion damage and which are chemically inert, would probably solve this problem. Another application is the protection of systems exposed to a marine environment. Stachiw and Bertic^{3,4} investigated the problem of germanium windows exposed to seawater. The windows, which are used in several systems under development at the Naval Ocean Systems Center, are fouled and made inoperative by seawater after only a few months' exposure. However, germanium windows coated with hard carbon by Honeywell did not foul over extended periods of time except at pinholes in the film. By understanding the growth process and thus developing the ability to produce low-absorption pinhole-free films, this fouling problem could be eliminated. Many other examples could be cited, but perhaps one will suffice.

Many of the new generation of infrared missiles are expected to travel much faster and farther than current designs and to operate in the 8-12 μm wavelength range as well as in the 3-5 μm wavelength range. Problems with thermal shock, erosion, and aerothermal heating are thus greatly increased. This increase occurs not only because of the increased speeds, but also because transmission at the longer wavelength is usually accompanied by weaker chemical bonding in the dome material. Thus, 8-12 μm materials tend to have lower fracture toughness than the best 3-5 μm materials. The best currently available 8-12 μm dome material is zinc sulfide. It is significantly softer (200-355 Knoop) than the currently used IRTRAN-1 (magnesium fluoride) domes (575 Knoop) which operate in the 3-5 μm range and are themselves too sensitive to erosion. Developmental materials for

the 8-12 μm region such as calcium lanthanum sulfide are better but are still only about as hard as IRTRAN-1. Their erosion resistance is also about the same as IRTRAN-1. It is not clear that nature will allow us to find other more erosion-resistant materials which still have adequate transmission in the 8-12 μm region. The other option is to develop a coating which will reduce the erosion problem. On the basis of present information, hard carbon offers the best hope for such a coating. Thus, the feasibility of 8-12 μm missile systems now under development may be enhanced significantly if a hard carbon coating program is initiated and proves successful.

The most ambitious application of diamondlike carbon films is as an optical coating material for high flux density lasers. Successful coating materials for this application have absorption coefficients under 50 cm^{-1} , and most are under 10 cm^{-1} . There is a need for a high index material with good damage resistance and good environmental properties, including hardness and encapsulation, to prevent penetration by water into possibly hygroscopic inner layers. Hard carbon films potentially have these properties. The laser damage resistance of most currently deposited carbon films is relatively low. However, available evidence suggests that the observed thresholds are not intrinsic. S. T. Amimoto and colleagues at the Aerospace Corporation report² that absorbing graphite particles in films they tested are the primary cause of damage at DF laser frequencies. In recent tests at the Naval Weapons Center on hard carbon coatings from a variety of sources, one coating from RCA Laboratories was found to exhibit an order of magnitude higher damage threshold at DF frequencies than any of the other carbon coatings tested.⁵ Its damage threshold was higher than coatings of aluminum oxide, silicon, or silicon oxide, all typical laser coating materials.⁵ Thus, there is the potential to develop high damage-resistant hard carbon laser coatings for this critical wavelength region.

In addition to damage resistance, coatings for high flux density lasers must, in some cases, operate in a reactive gas environment. Thus, important advantages of carbon film coatings in this application are their chemical inertness and their ability to be deposited in a nearly pinhole-free condition. They can thus act as an encapsulant for the other coating layers. Finally, their relatively high index is an advantage since fewer layers must be deposited to obtain a given reflectance if the spread between indices of the high and low index coatings is large.

Good adhesion and thermal shock resistance are needed for high flux coatings. Hard carbon coatings often exhibit good adhesion, a definite advantage. The high stress level of typical hard carbon films is, however, a problem. Another problem is the necessity to obtain a very uniform coating thickness over large areas on high flux density laser mirrors. Nonuniform film thicknesses cause an apparent figure change in the mirror⁶; to meet typical figure specifications, the film uniformity must often be about 1%, a difficult task. The most important problem with present hard carbon coatings, however, is their high absorption coefficient. For good results, the absorption coefficient of the as-deposited film should be $1-10 \text{ cm}^{-1}$ or less. Thus, an order-of-magnitude improvement in the absorption coefficient of present hard carbon films is required. Since the absorption in the HF-DF wavelength region appears to be extrinsic, not intrinsic, there is hope that such an improvement can be made.

To conclude, hard carbon coatings appear to be quite promising candidates for a variety of applications which include obtaining (1) more erosion-resistant missile domes and (2) higher flux density laser coatings. Problems such as thickness uniformity, film stress, and absorption coefficient still have to be worked out. If they can be overcome, better infrared optical components will emerge.

References

1. Dr. Keith Lewis, Royal Radar Establishment, Malvern, England (private communication).
2. B. Bendow, "Summary of the Workshop on Diamond-Like Carbon Coatings," DARPA Contract MDA 903-81-C-0151 (1982).
3. J. D. Stachiw, *High Pressure Viewports for Infrared Systems: Phase I - Germanium*, Naval Ocean Systems Center TR 565, September 1980.
4. J. D. Stachiw and S. L. Bertic, *Resistance of Coated and Uncoated IR Windows to Seawater Corrosion: Phase V - Summary*, Naval Ocean Systems Center TR 633, February 1981.
5. J. O. Porteus, Naval Weapons Center, China Lake, Calif. (private communication).
6. H. E. Bennett and D. K. Burge, "Multilayer Thickness Uniformities Required to Meet Wave Front Error Tolerances in Laser Mirrors," in *Laser Induced Damage in Optical Materials: 1980*, H. E. Bennett, A. J. Glass, A. H. Guenther, and B. E. Newnam, eds. (National Bureau of Standards Special Publication 620, October 1981), pp. 356-368.

AD P002585

Non-Conducting Hermetic Coatings for Optical Fibers

H. E. RAST

Naval Ocean Systems Center, San Diego, CA 92152

A number of military systems incorporating fiber optics require long lengths of high strength fibers. These fibers, like other silicate derived glasses, suffer from the phenomenon of stress corrosion or static fatigue. The observed fatigue occurs when fibers are subject to tensile stresses in a humid environment. None of the currently used organic buffer and overcoating materials is impermeable to water and, therefore, to provide hermetic protection, one must look to other materials. Among the more promising materials are metals, silicon nitride, and diamond-like carbon. The requirements and possible behavior of suitable coatings will be discussed in terms of performance, expected reliability, and economic considerations.

INTRODUCTION

Many of the applications of fiber optics to military systems involve the use of long lengths (> 5 km) of optical fibers having high strength and long term durability.^[1] As opposed to permanently installed, static data links, these applications require cables which may be frequently moved or, perhaps, used as a data link between moving platforms. Consequently, an extra measure of survivability is needed. One may roughly categorize fiber cables into two types: those having load-bearing members and those in which the optical fiber, itself, is the load-bearing element. Table I represents a selected number of such systems according to this division.

Table I.

OPTICAL FIBER CABLES

Cabled structures with load-bearing members:

- Towed array.
- Bottom laid communications (retrievable).
- Mine countermeasures.
- Work Systems.
- Intelligence Gathering
- Submarine Communications Buoy.

Load-bearing fiber:

- Torpedo
- Missile
- Sonobuoy
- Bottom laid (nonretrievable)
- Swimmer

In the case of cables with load-bearing elements, an important consideration is the strain at which a load-bearing material yields or fails. In order to maintain optical continuity, it is requisite that the optical fiber strain-to-failure exceed that of the load-bearing members in tension. Table II lists a number of load-bearing materials and their approximate failure strains. Most optical fibers are composed of doped-silicate glasses protected by organic buffers. Since the modulus of silicate glasses is approximately 10^7 psi (or 70 G Pa), a 1% strain on a silica glass fiber represents a stress of 100,000 psi.

Table II
LOAD-BEARING MATERIALS

<u>MATERIAL</u>	<u>STRAIN AT FAILURE %</u>
Ultra Strength Steel	1.0
Boron Composite	1.0
Graphite Composite	1.0
Kevlar-49 Composite	2.2
S-Glass Composite	4.5

In the last few years, considerable progress has been achieved in improving the strength of optical fibers.^[2] For many years it has been known that brittle ceramic materials fail under tension because of the presence of microscopic surface and volume defects. By carefully controlling the fiber drawing process, optical fiber manufacturers have been able to reduce the densities of larger flaws which lead to failure. As a result, the strengths of fibers have steadily increased. Many vendors now routinely proof-stress their fibers to a moderately high level, say 75,000 or 100,000 psi. While these levels are satisfactory for most non-military applications, the severe requirements of defense systems demand higher levels of assurance. It is reasonable to ask, however, what the limits of this improvement effort may be or, indeed, if it is practical and economically feasible to demand higher proof levels.

The theoretical bond strength of silica is approximately 2.5×10^6 psi or approximately 25% tensile strain.^[3] Thus, from the standpoint of ultimate fiber strength, the limits of attainability have not been approached. In short lengths, fibers have been drawn which have median strengths approaching 1×10^6 psi (7 G Pa). Longer lengths are weaker because the probability of occurrence of flaws is proportional to the length. The longer the fiber, the more apt one is to have a large flaw which leads to tensile failure. In terms of the stress, σ , at which a fiber of length L fails, the probability of failure is given as:^[4]

$$\psi(\sigma, L) = 1 - \exp \left\{ - \left(\frac{\sigma - \sigma_p}{\sigma_0} \right)^M \left(\frac{L}{L_0} \right) \right\} \quad (1)$$

In Equation (1), σ_0 is a scale parameter, σ_p is the proof-stress, and L_0 is the initial length. Thus, the chance of failure increases exponentially with length.

Ideally, one would desire proof-tested fibers. Because of the aforementioned length dependence of the survival, however, the additional manufacturing cost of assuring defect-free fibers also rises exponentially. A practical compromise, therefore, would seem to be to splice together proof-tested segments of, say, 5 km if a fairly long, high strength fiber was needed. The solution to these problems appears to be within reach. Recent work at Bell Telephone Laboratories was reported to have exceeded 12 km at a 200,000 psi proof level in a continuous run.^[5] This is an important milestone with promising implications for military applications.

STRESS CORROSION IN OPTICAL FIBERS

Assuming that strong optical fibers can be drawn is the first half of the problem. The second part is to preserve this initial strength and this leads to the issue of hard, insulating coatings. It is well known that ceramic materials, under stress in the presence of water, suffer a diminution of strength through the phenomenon of stress corrosion or static fatigue.^[6] Fibers are coated with buffering materials as they are drawn. These coatings serve to prevent micro-bending optical losses and to protect against abrasion. There is a trade-off as to the thickness of such coatings, the greater the thickness, the better the fiber is protected against abrasion damage (which introduces flaws, thereby weakening the fiber). On the other hand, it should not be so thick that one ends up with dimensions on the order of conventional coaxial or twisted pair wires which fibers are intended to replace. However, from the standpoint of strength preservation, these coatings, which are organic polymers, are all permeable to water and, therefore, do not prevent stress corrosion.

The time to failure, t_f , of a fiber under a static stress, σ , can be estimated from the fracture mechanics relation,^[7]

$$t_f = \frac{2}{YA(N - 2)} \sigma^N \left(\frac{K_{IC}}{\sigma_{IC}} \right)^{2-N} \quad (2)$$

in which Y is a dimensionless geometric constant, K_{IC} is the characteristic critical stress intensity factor for the fiber material, and σ_{IC} is the strength of the fiber in an inert environment. The numbers A and N are constants, but N is environmentally dependent. In fact, N is a figure of merit as to the resistance of the material to static fatigue. For silica materials in an ambient environment N has a value of about 20. Hermetically-coated fibers have larger values of N and this translates into substantially longer times-to-failure.

Figures (1) and (2) are respectively plots of the cumulative failure probabilities of a non-hermetic fiber and a hermetically-coated fiber. These were taken in decades of stressing rate. The data points indicated by the symbol N were taken in dry nitrogen. It is clear from a comparison of the two plots that the hermetically-coated fiber is less dependent on stressing rate and more closely approaches the behavior observed in an inert environment.

If one now plots the median strengths versus the stress rate or, alternatively fitting the differentiated Equation (2) to stressing rates, the diagrams in Figures (3) and (4) are obtained. The inverse of the slope is the parameter N discussed above. The larger value of N, for hermetically-coated fibers, is indicative of stress corrosion resistance.

To achieve hermeticity in optical fibers, the Department of Defense has supported several research efforts aimed at coatings other than polymer-based materials. One approach involved the in-line application of metals. While these metallic coatings offered a fairly high level of protection from stress corrosion, they suffered from other problems which offset the advantage of improved resistance to static fatigue. Among these problems were excessive microbending losses, poor concentricity, cyclic failure, plastic flow under tension, and electrical conductivity. While some of these objections have since been overcome, there still remains the problem of electrical conductivity which is totally incompatible with all-dielectric waveguides.

Alternative approaches using dielectric coatings are currently under investigation. The first of these is the in-line chemical vapor deposition of silicon nitride.^[8] This technique has the advantage of rapid coating at fiber drawing rates. At the same time, results of fatigue testing yield values of N on the order of 100 which significantly extend the estimated times-to-failure. One of the disadvantages with the SiN, however, is that the median strengths of fibers is halved. While this intrinsic strength reduction is acceptable for moderate strength applications, it is unsatisfactory for those applications where proof-stress levels in excess of 200,000 psi are required. Figure (5) depicts the drawing system and Si_3N_4 in-line reactor for hermetically-coating fibers as developed at Hewlett-Packard Laboratories.^[8]

Another approach involves the ion plasma deposition of dielectric materials.^[9] This technique offers the advantage of drawing and coating fibers in a high vacuum which should dramatically improve the attainable pristine strength, in addition to hermeticity, since a major source of surface flaws has been traced to airborne particulates. Preliminary results are very interesting, but whether deposition

rates will be fast enough is still uncertain. Inadequate quantities of coated fibers have been available for extensive mechanical or optical characterization. Another advantage of this approach is the fairly large number of dielectric, as well as metallic materials that could be investigated. To date, only hard carbon coatings and indium were attempted.

Thin coatings of diamond-like carbon would seem to offer solutions to the optical fiber problem. In addition to hermeticity, the hardness should serve to prevent abrasion enabling one to reduce the thickness of the polymer overcoating. Chemical inertness and insulating behavior are further attractive features.

Table III lists some of the properties that would be essential for such coatings.

Table III
PREFERRED CHARACTERISTICS OF HERMETIC COATINGS

- Thin (300 - 600 Å[°])
- Uniform/smooth/concentric
- Pin-hole free
- Stress-free
- Chemically inert
- No cyclic fatigue
- Fast in-line deposition
- No diminution of fiber strength
- Easily spliced
- Low cost

FUTURE WORK

Numerous ideas have been proposed by several investigators for hermetic coatings. These proposals suffer primarily from the fact that the investigator does not have access to a fiber drawing facility. In order to fully and properly characterize coatings, one must have the capability of in-line coating and control of the many variables involved in drawing fibers. To date, many of the large optical waveguide vendors have been unresponsive to the DOD's need for fatigue-resistant, high strength fibers. However, as the military and commercial markets expand for these fibers, greater interest in solving these problems can be expected.

REFERENCES

1. H. E. Rast, "Military Systems Requirements for Strong Optical Fibers," Guided-Wave Optical and Surface Acoustic Waves Devices, System and Applications, SPIE 239, 261(1980).
2. C. R. Kurkjian and H. E. Rast, "Recent Progress in the Strength of Fibers," International Conference on Integrated Optics and Optical Fiber Communication, San Francisco, CA, April 27-29(1981).
3. W. C. LaCourse, "The Strength of Glass," in Introduction to Glass Science, L. D. Pye, H. J. Stevens and W. C. LaCourse, eds., Plenum Press, N.Y.(1972).
4. B. Justice, "Strength Considerations of Optical Waveguide Fibers," Fiber and Integrated Optics, 1, 115(1977).
5. S. R. Nagel, K. L. Walker and J. B. MacChesney, "Current Status of MCVD: Process and Performance," reported at the Topical Meeting on Optical Fiber Communication (OFC '82), Phoenix, AZ, April 13-15(1982).
6. R. J. Charles, "Static Fatigue of Glass," J. Appl. Phys., 29, 1549,1554(1958).
7. J. E. Ritter, "Probability of Fatigue Failure of Glass Fibers," Fiber and Integrated Optics, 1, 387(1978).
8. C. A. Schantz, E. G. Hanson and R. Hiskes, "Properties of Silicon Oxynitride Coated Fatigue-Resistant Fibers," Topical Meeting on Optical Fiber Communication, Phoenix, AZ, April 13-15(1982).
9. M. L. Stein, S. Aisenberg and J. M. Stevens, "Ion Plasma Deposition of Hermetic Coatings for Optical Fibers," in Physics of Fiber Optics, B. Bendow and S. S. Mitra, eds., American Ceramic Society, Columbus, OH (1981).

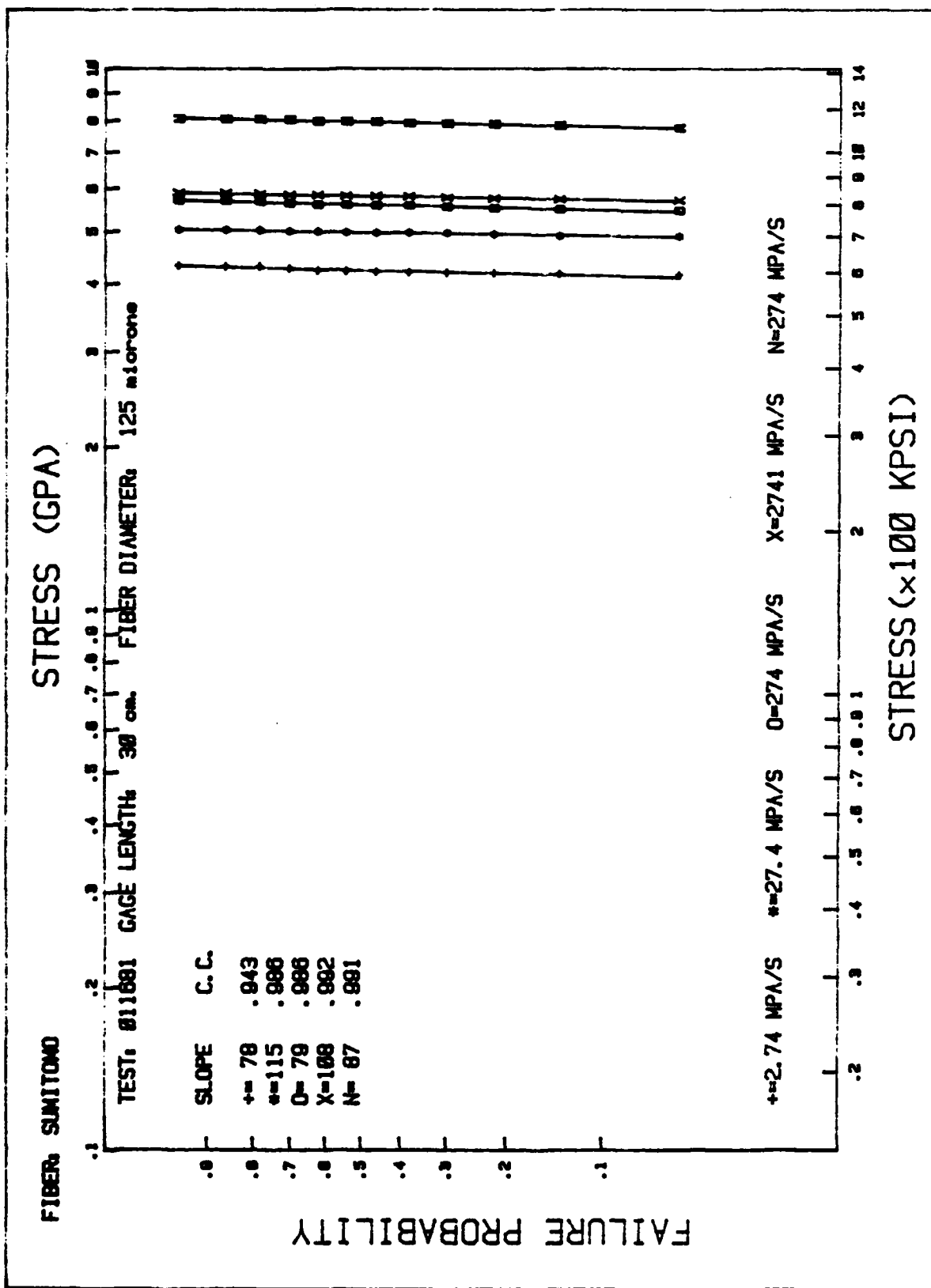


Figure 1. Cumulative Failure Probabilities of a Non-Hermetically-Coated Fiber at Different Stressing Rates

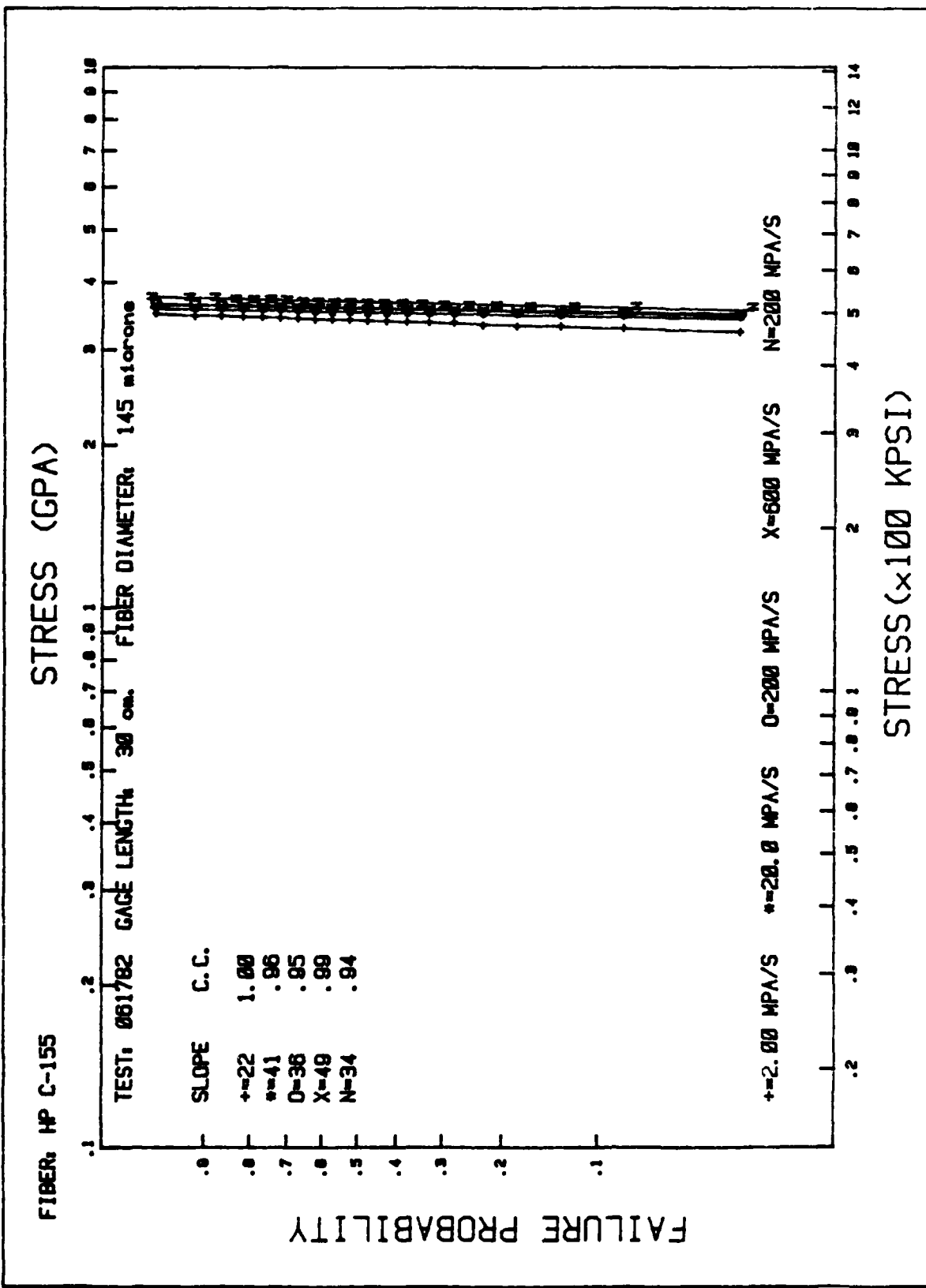


Figure 2. Cumulative Failure Probabilities of a Hermetically-Coated Fiber at Different Stressing Rates

DYNAMIC FATIGUE FOR N VALUES

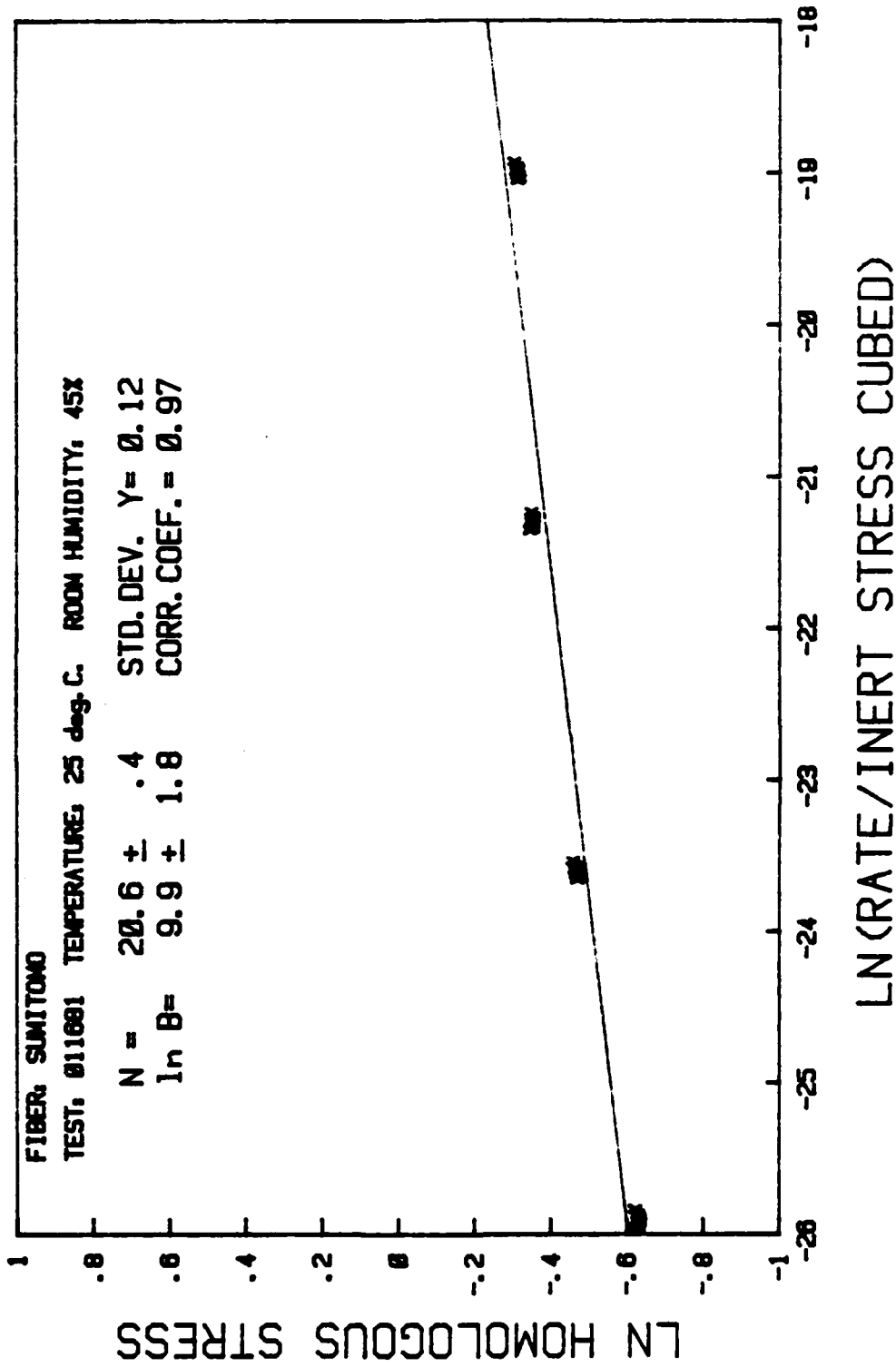


Figure 3. Plot of the Homologous Strengths (Determined at Different Stress Rates) of a Non-Hermetically-Coated Fiber versus Stress Rate

DYNAMIC FATIGUE FOR N VALUES

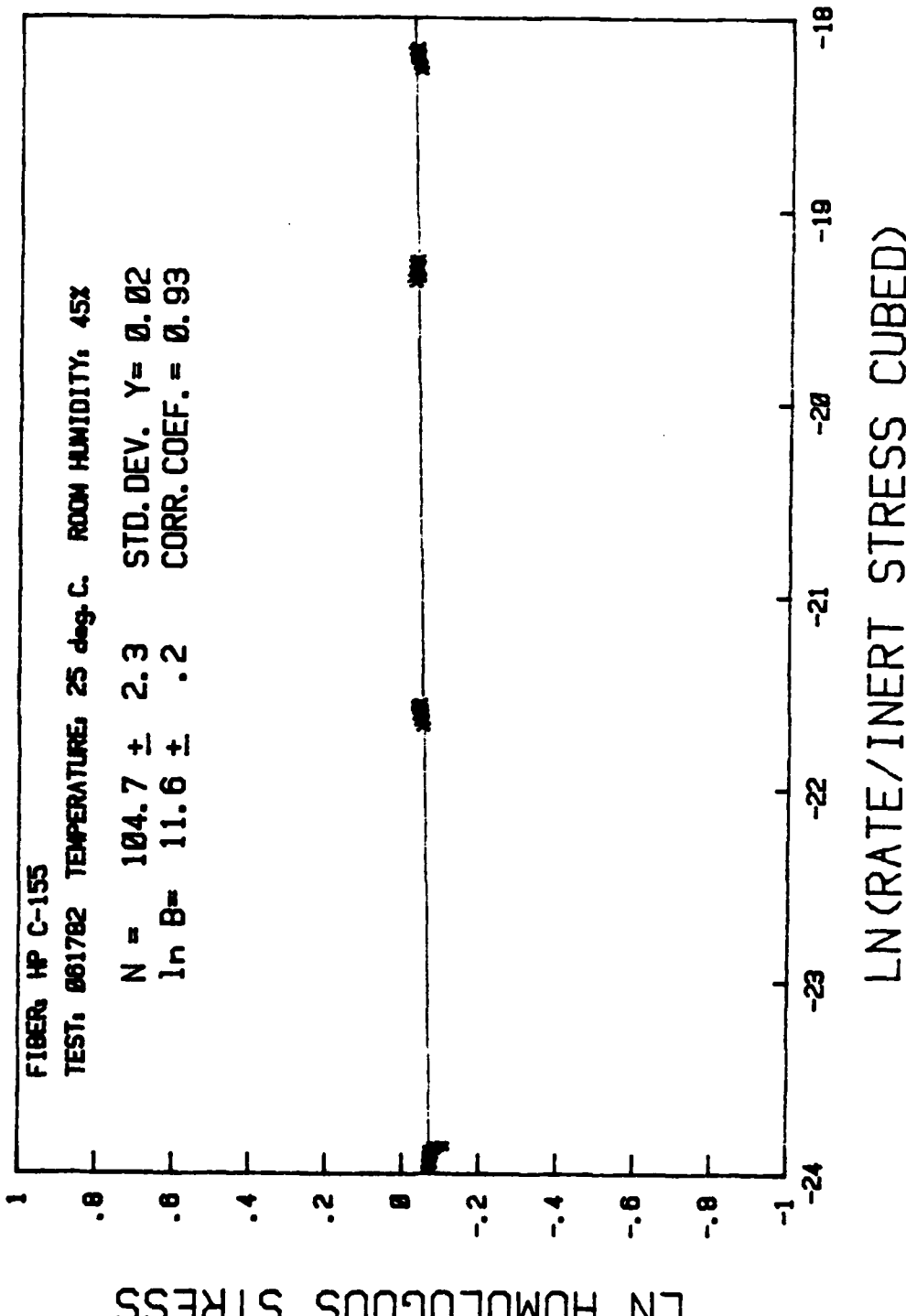


Figure 4. Plot of the Homologous Strengths of a Hermetically-Coated Fiber Versus Stressing Rate

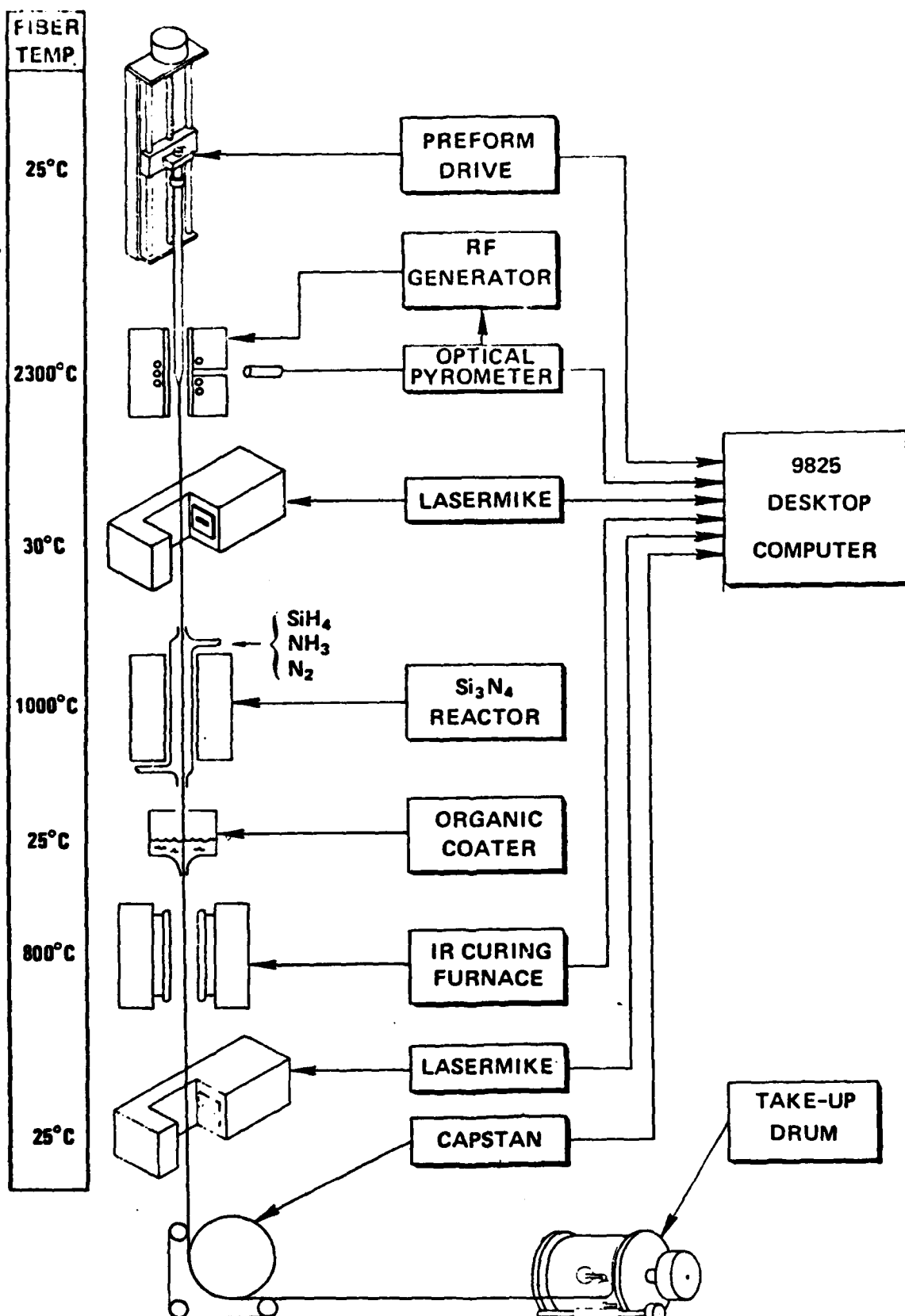


Figure 5. Diagram of the In-Line Coating of an Optical Fiber with Si₃N₄ (from Hewlett-Packard, ref. 8)

Preparation and Properties

PREPARATION AND PROPERTIES

PREPARATION AND PROPERTIES

AD P 002586



Hard Carbon Coatings for IR-Optical Components

A. Bubenzer, B. Dischler and P. Koidl

Fraunhofer-Institut für Angewandte Festkörperphysik,
Eckerstr. 4, D-7800 Freiburg, West-Germany

Hydrogenated amorphous carbon films (a-C:H) were deposited on glass, silicon and germanium substrates. The films are transparent in the IR and are extremely hard. The a-C:H films were homogeneously deposited at a rate of about 500 Å/min in an RF excited discharge from benzene vapour. The characteristic features of this deposition method are discussed.

Thickness, short wavelength absorption, refractive index ($2 - 10 \mu\text{m}$) and relative hydrogen content were determined. Variations in short wavelength absorption, IR-refractive index and relative hydrogen content could be correlated with deposition conditions. The refractive index of a-C:H can be tuned to be exactly 2, thus a-C:H is an ideal single layer AR-coating for germanium ($n = 4$). Laser calorimetric measurements of optical absorption at $10.6 \mu\text{m}$ give an absorption coefficient of 250 cm^{-1} . The application of a-C:H as single layer AR coating on Ge and as outside layer of a multi-layer coating is demonstrated.

Introduction

During the recent years a special form of carbon thin films received an increasing attention /1-23/. These films were called diamondlike carbon, or since this term is slightly misleading, it was also named I-Carbon, hard carbon or a-C. Because there is a strong analogy to the well known amorphous silicon thin films (a-Si) /24,25/ the name a-C appears to be adequate. The most important analogy between a-Si and a-C is the potential of incorporating large amounts of Hydrogen (up to about 25% /8/). This is especially important when a-C coatings are deposited from Hydrocarbon-gases. Here the name a-C:H is more precise.

There is one important exception to the analogy however: The thermodynamically stable form of carbon at normal pressure is graphite and not diamond. A graphite like structure does not exist for silicon. Due to these two totally different carbon modifications a-C:H thin films can differ significantly in their properties. Depending on the preparation conditions the material is either on the graphite side (electrically conducting, optically opaque) or on the diamond side (electrically insulating, optically transparent). The most valuable inheritance from the diamond side is the exceptional hardness of a-C:H thin films which is on the order of 1400 kp/mm² knoop hardness /26/.

Preparation

a-C:H coatings on glass, Si, Ge were deposited in an RF plasma sustained by benzene vapour. This method offers the potential of producing a-C:H coatings with desirable optical and mechanical properties: if the appropriate deposition parameters are chosen, homogeneous large area coatings with high electrical resistivity ($10^{12} \Omega\text{cm}$) can be deposited. Figure 1 shows the coating apparatus. The hydrocarbon gas is leaked into the glow discharge chamber with one electrode grounded and the other one which is capacitively coupled to the RF source (MHz range) serving as the substrate carrier. In the discharge region the hydrocarbons are ionized and the positively charged C, C-H and H particles are accelerated towards the substrate under the negative cathode self bias /27,28/ and thereby form a carbon film.

Figure 2 shows the effect of the negative self bias on voltage waveform (right) and average time distribution of voltage within the discharge (left). A DC bias V_B of slightly less than the half peak to peak voltage $2 V_0$ develops on the powered electrode. This means, there is a high average potential V_B between substrate and plasma and a low average potential V_p between anode (i.e. metal vacuum chamber) and plasma. Thus there is much less interaction between plasma and vacuum chamber walls (i.e. less sputtering and less contamination) than between plasma and substrate. Deposition and sputtering is almost totally restricted to the small powered electrode with the substrate on top.

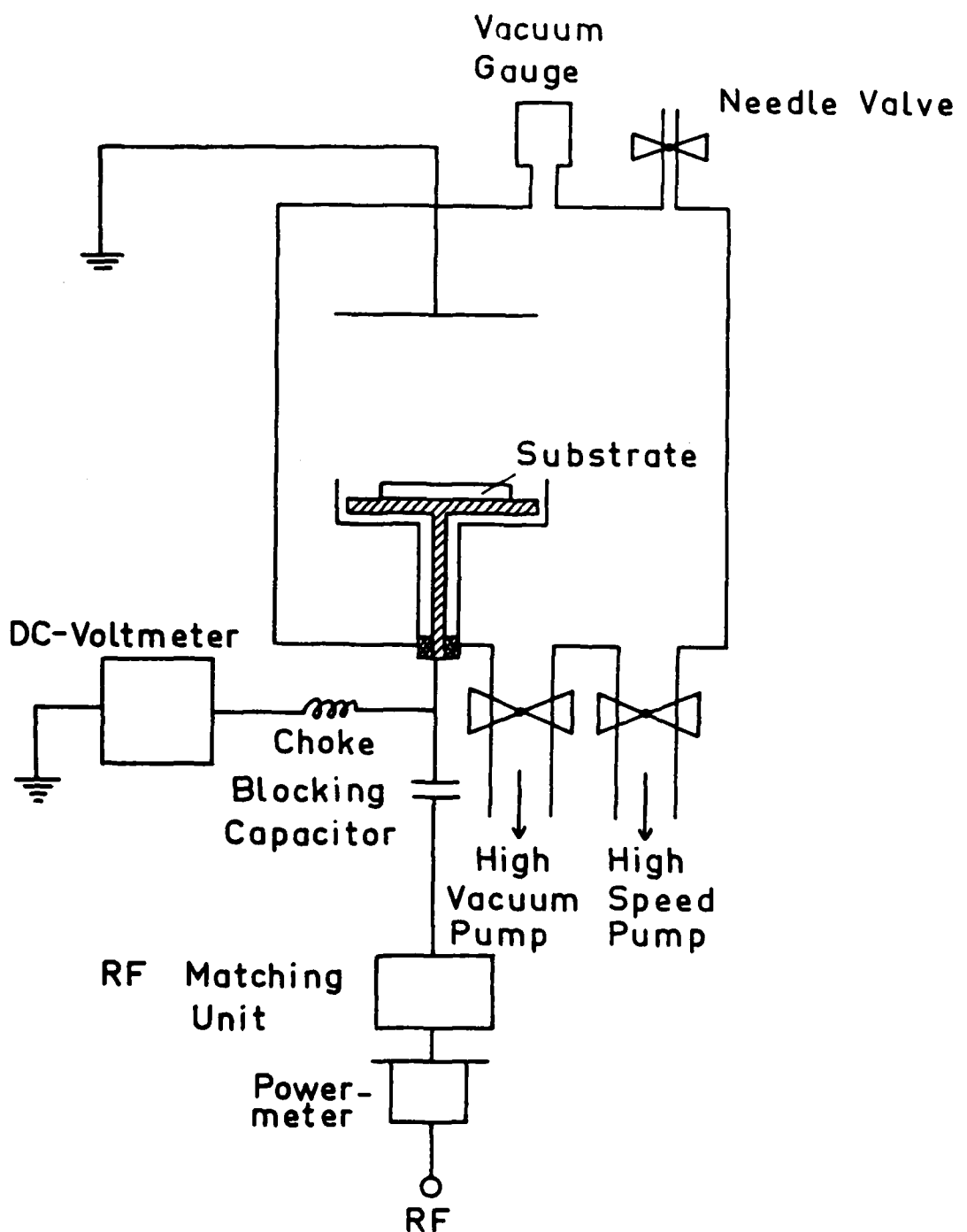


Figure 1: Outline of the coating apparatus

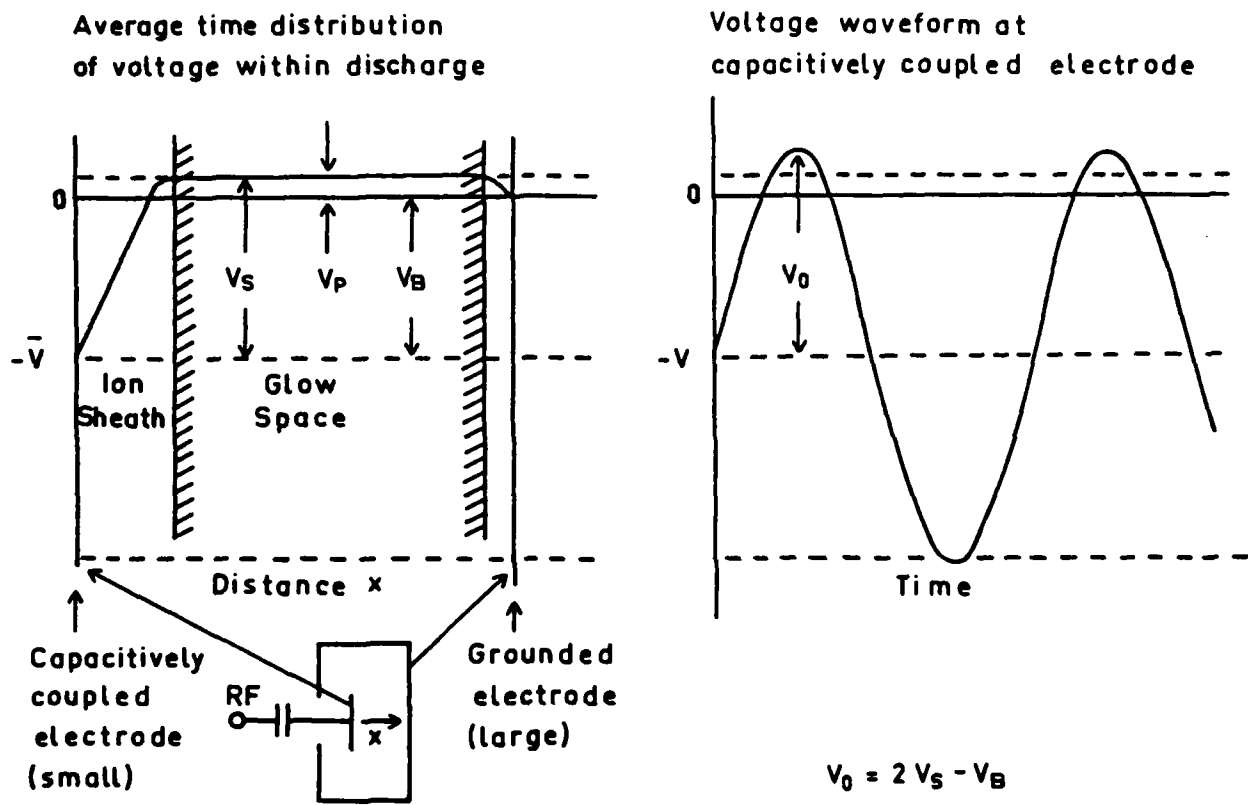


Figure 2: Time average voltage distribution between RF powered electrode and grounded metal walls of plasma chamber (left)
DC self biased RF voltage (right)

In order to produce carbon coatings of reproducible quality, standard deposition conditions have to be established which should be independent of the particular coating apparatus.

Figure 3 gives all the "knobs" which can be turned during RF plasma deposition of hard carbon or which during the construction of the apparatus are tied to a certain value. Geometry of reactor (this means mainly the ratio of the anode to cathode area) is a constant as well as probably in most cases the pumping speed. Gas flow rate and pumping speed however can be tuned although these quantities do not give sufficiently meaningful parameters. What finally determines the average energy of the ions impinging on the substrate and thus the coating properties are the sheath potential V_S in which the ions are accelerated and the mean free path of the ions (i.e. the inverse pressure).

In asymmetric systems (small capacitively coupled electrode, large grounded electrode, which is the total metal vacuum chamber) V_p is on the order of only a few percent of V_B (3% in our system). Therefore the sheath potential $V_S = V_B - V_p$ is sufficiently accurately determined by the negative self bias V_B .

Thus there are two basic process parameters negative self bias V_B and pressure P the quotient of which V_B/P in our experiments has proven to be a leading parameter determining coating properties.

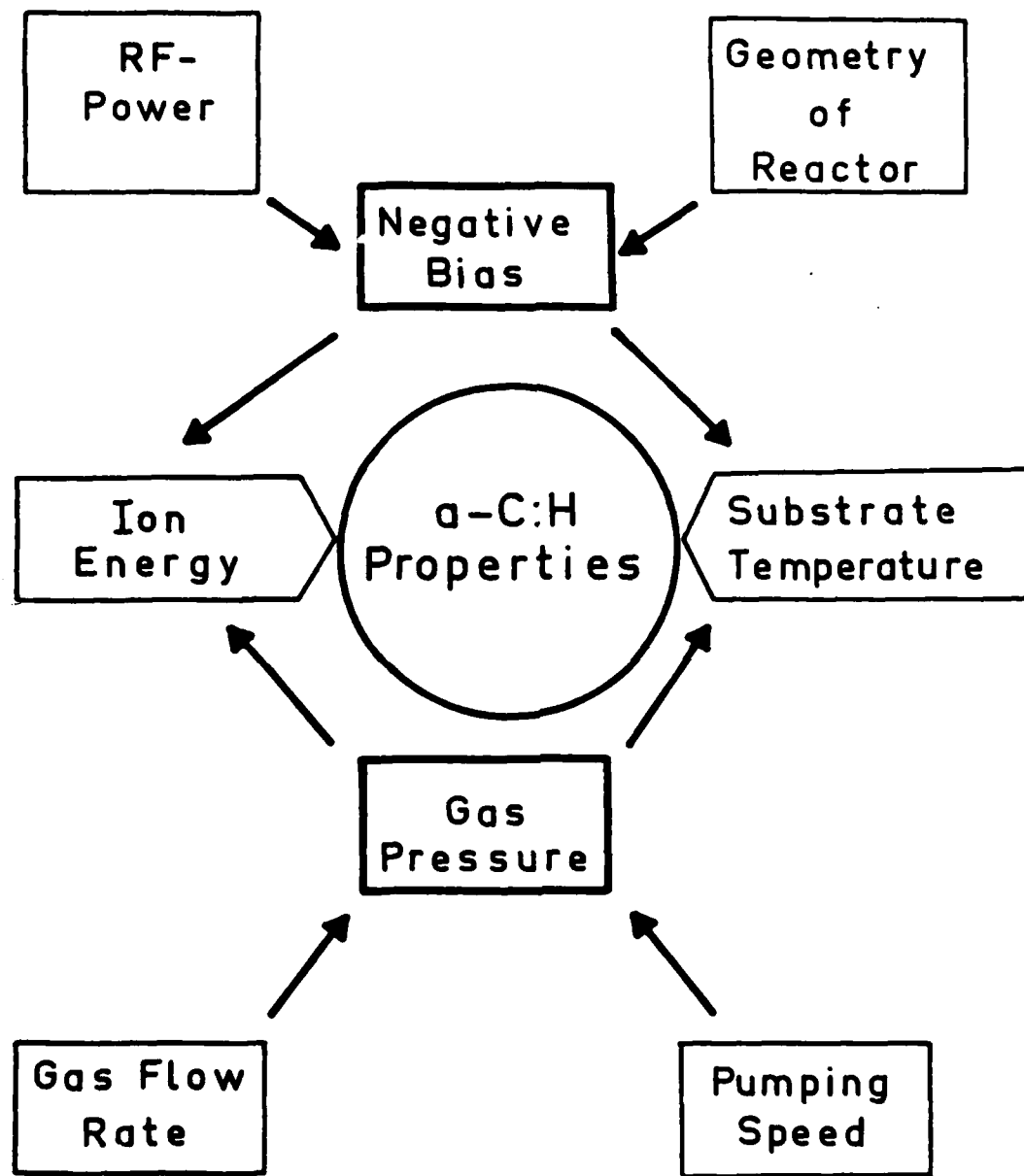


Figure 3: Parameters of the RF plasma deposition process. DC negative self bias on the RF powered electrode and hydrocarbon gas pressure being the parameters by which a-C:H properties can be controlled.

Optical properties

Figure 4 demonstrates the influence of the leading deposition parameter V_B/P on a-C:H coating properties.

The refractive index at 1 μm (Fig. 4(a)) determined from thin film optical interference ranges from 1.86 to 2.24 thus approaching the diamond value of 2.4 for high V_B/P . The dispersion between 1 and 10 μm is negligible.

For applications of a-C:H as AR coating its refractive index can thus reproducibly be tuned to the desired value (e.g. $n = 2$ for AR coatings on germanium) by choosing the appropriate deposition parameters V_B and P .

Due to the high hydrogen content of a-C:H coatings the 3.4 μm C-H stretch vibration is a prominent feature of the IR spectrum. The strength of the C-H stretch vibration (Fig. 4(b)) - and thus the amount of chemically bonded hydrogen in a-C:H - decreases with increasing V_B/P .

Finally the optical absorption edge changes with V_B/P (Fig. 4(c)): Films produced under increasing V_B/P change their color from yellow to black. This means, the short wavelength optical absorption edge is shifting to longer wavelength with increasing V_B/P .

Applications

a-C:H with refractive index $n = 2$ is an ideal single layer AR coating for germanium with $n = 4$. Figure 5 shows the (1-reflection) (1), transmission (2) and loss (3) spectrum of a 1 mm Ge disc coated on both sides with a quarter wave a-C:H coating for 10.6 μm . The reflection at 10.6 μm is less

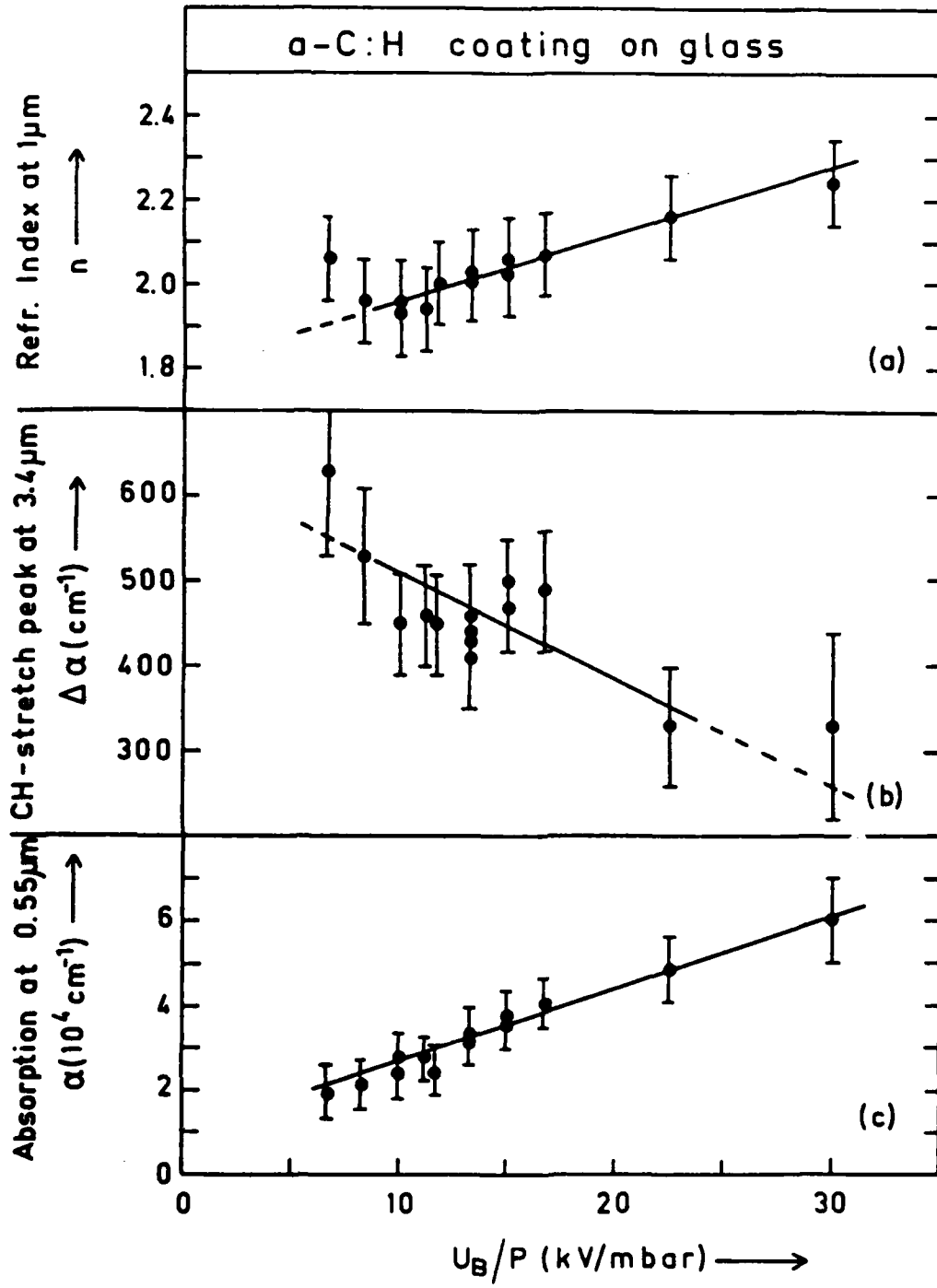


Figure 4: Dependence of a-C:H thin films properties on deposition parameters
 V_B/P = negative self bias/gas pressure.
(a) refractive index at 1 μm ; (b) strength of C-H stretch vibration at 3.4 μm ; (c) absorption coefficient at 550 nm showing the shift of the short wavelength absorption edge.

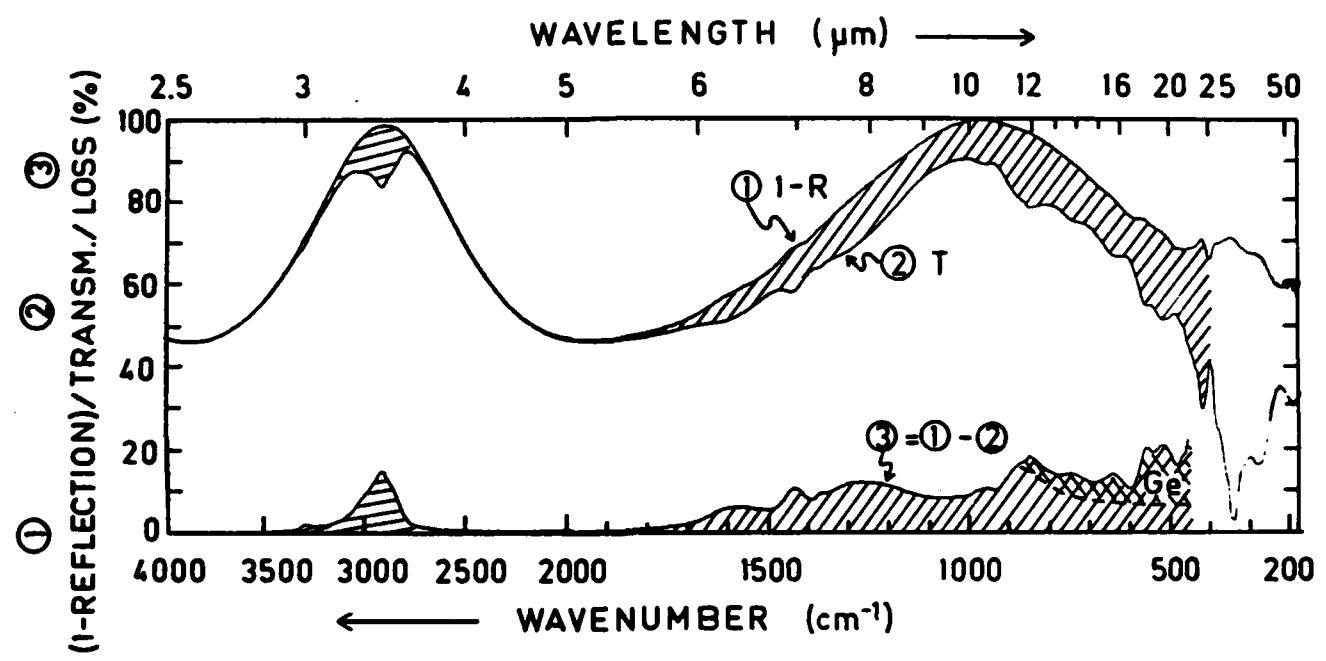


Figure 5: Spectral dependence of (1-reflection) (1), transmission (2) and losses (3) of a Germanium disk with an a-C:H $\lambda/4$ coating for 10.6 μm on each side.

than 0.3 %, this means the refractive index is very well tuned to the right value of $n = 2.0$. The losses between 6 and 12 μm are due to C-C vibrations as well as to C-H deformation bands, the losses above 12 μm are mainly intrinsic absorptions in the Ge substrate. Independent laser calorimetric measurements at 10.6 μm give a total loss of 8 % in the two a-C:H coatings of this sample. Taking into account interference effects this yields an absorption coefficient of 250 cm^{-1} .

The optical performance of a single layer AR coating is not adequate for many applications. Thus an a-C:H coating was used as an outside layer of a conventional multilayer stack (Fig. 6). This coating consists essentially of an alternating stack of Ge and ZnS layers (Fig. 6, T1 and R1). Its outside ZnS layer was dissolved in hydrochloric acid leaving the next Ge layer exposed (Fig. 6, T2 and R2). The multilayer stack was then coated with an a-C:H coating ($n = 2.2$) the thickness of which was adjusted such that it had the same nd product of 3 as the original ZnS layer. From Fig. 6, R3 it is seen that the reflection spectrum of the remodelled coating comes close to the original one, the transmission however being lower due to the a-C:H losses (Fig. 6, T3).

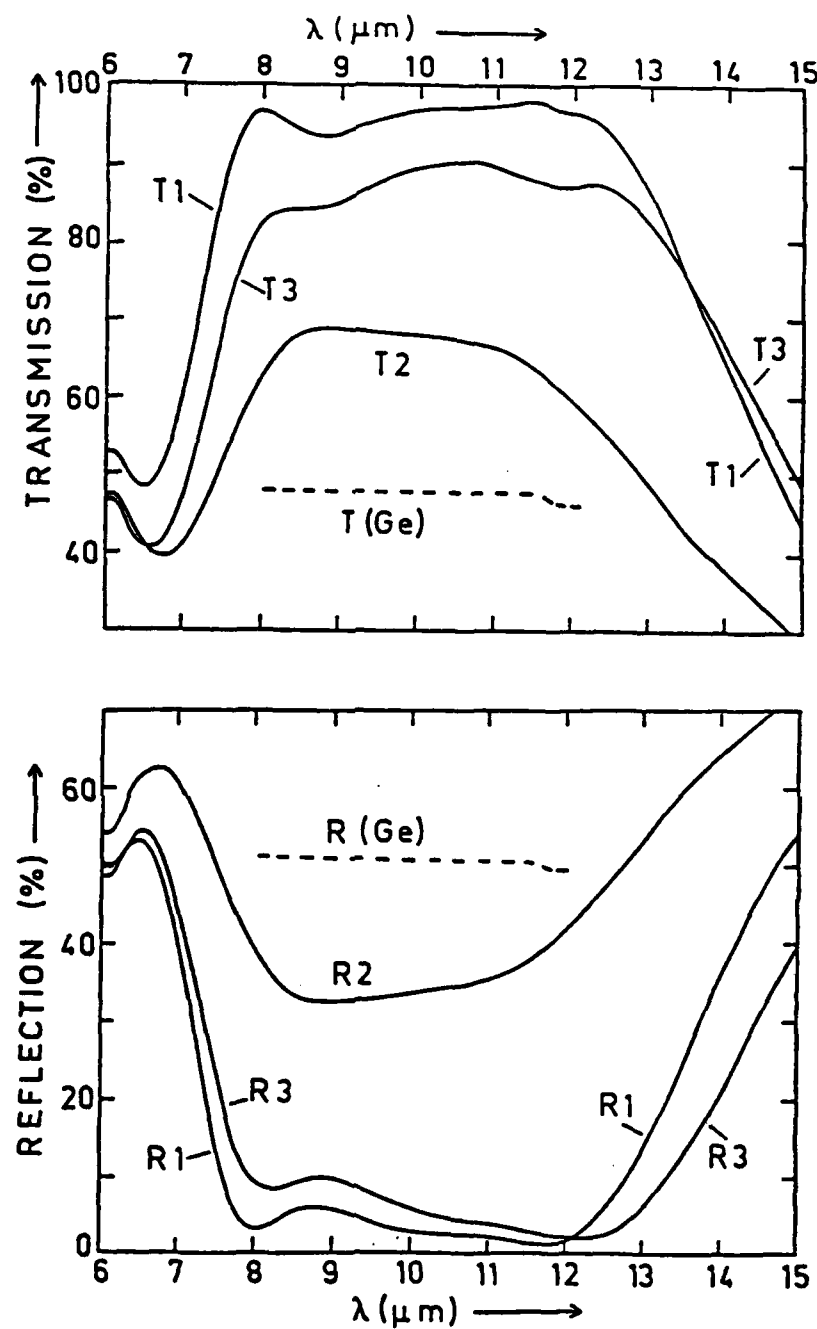


Figure 6: Remodelling of a multilayer coating:
 Transmission (T1) and reflection (R1) of original coating.
 The outside ZnS layer was removed (T2, R2) and then replaced
 by an optically equivalent a-C:H layer (T3, R3).

Conclusion

It could be shown that physical properties of a-C:H thin films such as refractive index, content of bonded hydrogen and optical gap can be tuned by deposition parameters. An increase in ionic energy increases the refractive index and decreases the content of bonded hydrogen as well as the optical gap.

Two applications of a-C:H were demonstrated: a-C:H coatings were used as single layer AR coatings on Ge for 10.6 μm , giving a reflection of less than 0.3 % at 10.6 μm .

An a-C:H coating was designed which successfully replaced an outside ZnS layer of a conventional multilayer broad band AR coating for the 8 to 12 μm range.

References

- /1/ S. Aisenberg and R. Chabot, J. Appl. Phys. 42 (1971) 2953
- /2/ L. Holland, Brit. Pat. No. 15 82 231 (Appl. 1976)
- /3/ L. Holland and S.M. Ojha, Thin Solid Films, 38 (1976) L17
- /4/ S.M. Ojha and L. Holland, Thin Solid Films, 40 (1977) L31
- /5/ S.M. Ojha and L. Holland, Proc. 7th Int. Vacuum Congr. and 3rd Int. Conf. on Solid Surfaces, Vienna (1977), Berger, Vienna (1977) p. 1667
- /6/ L. Holland and S.M. Ojha, Thin Solid Films, 48 (1978) L21
- /7/ L. Holland and S.M. Ojha, Thin Solid Films, 58 (1979) 107
- /8/ S.M. Ojha, H. Norström and D. McCulluch, Thin Solid Films, 60 (1979) 213
- /9/ L.P. Andersson and S. Berg, Vacuum, 28 (1978) 449
- /10/ L.P. Andersson, S. Berg, H. Norström, R. Olaison and S. Towta, Thin Solid Films, 63 (1979) 155
- /11/ C. Weissmantel, Thin Solid Films, 58 (1979) 101
- /12/ C. Weissmantel, G. Reisse, H.-J. Erler, F. Henny, K. Bewilogua, U. Ebersbach and C. Schürer, Thin Solid Films 63 (1979) 315
- /13/ R.J. Gambino and J.A. Thompson, Solid State Commun., 34 (1980) 15
- /14/ B. Meyerson and F.W. Smith, Solid State Commun., 34 (1980) 531
- /15/ B. Meyerson and F.W. Smith, J. Non-Cryst. Solids, 35-36 (1980) 435

- /16/ K. Enke, H. Dimigen and H. Hübsch, Appl. Phys. Lett., 36 (1980) 291
- /17/ K. Enke, Thin Solid Films 80 (1981) 227
- /18/ E.J. Alessandrini, R.J. Gambino, C.C. Tsuei and J.M. Viggiano, IBM Technical Disclosure Bulletin 23 (1980) 387
- /19/ H. Vora and T.J. Moravec, J. Appl. Phys. 52 (1981) 6151
- /20/ T.J. Moravec and J.C. Lee, J. Vac. Sci. Technol. 20 (1982) 338
- /21/ M.L. Stein, S. Aisenberg and B. Bendow, 13th International Symposium on Materials for High Power Lasers, Boulder (1981), NBS Special Publication
- /22/ A. Bubenzer, B. Dischler and A. Nyairesh, 13th International Symposium on Materials for High Power Lasers, Boulder (1981), NBS Special Publication
- /23/ A. Bubenzer, B. Dischler and A. Nyairesh, Thin Solid Films 91 (1982) 81
- /24/ M.H. Brodsky, R.S. Title, K. Weiser and G.D. Petit, Phys. Rev. B1 (1970) 2632
- /25/ Eva C. Freeman and William Paul, Phys. Rev. B20 (1979) 716
- /26/ G. Brandt, IAF Freiburg, private communication
- /27/ J.W. Coburn and Eric Kay, J. Appl. Phys., 43 (1972) 4965
- /28/ J.W. Vossen, J. Electrochem. Soc., 126 (1979) 319

AD P002587

AD P002587

The Properties of Hard, Insulating Carbon Coatings
and Areas of Future Efforts



by

Thomas J. Moravec

Honeywell Corporate Technology Center
10701 Lyndale Ave. So.
Bloomington, MN 55420

Workshop Abstract

The electrical, optical, and mechanical properties of hard, insulating carbon coatings will be reviewed from data collected over the last several years at Honeywell. Then areas of future research efforts will be discussed that will be important for the application of these coatings to different substrates. These areas include stress and adhesion of these films.

Summary

Through the past five years, Honeywell has been involved in research to study the preparation and properties of carbon thin films that have been described as having diamond-like properties. The bulk of this work has been published in the open literature. The titles and abstracts of these papers are listed below. Following that are several figures of viewgraphs presented at the workshop with figure captions. These are intended to be self explanatory and to summarize the bulk of the work done to date. Future research should be directed towards fundamental studies of the nucleation and growth of these carbon films. Practical applications are presently limited by the poor adhesion to some substrate materials (e.g., alkali halides) and the large compressive stresses that these films possess.

References

T.J. Moravec, Thin Solid Films, 70, L9 (1980), "Color Chart for Diamond-like Carbon Films on Silicon".

T.J. Moravec and T.W. Orent, J. Vac. Sci. Technol., 18, 226 (1981)", Electron Spectroscopy of Ion Beam and Hydrocarbon Plasma Generated Diamondlike Carbon Films",

"Mechanically hard, electrically insulating (diamondlike) carbon thin films have been produced by low energy carbon ion beam deposition and by decomposition of butane gas. Deposition parameters are presented for these two methods. The ion beam films can be produced with or without a secondary discharge in the ion source and the parameters are given for these two modes of operation. ESCA and electron energy loss (EELS) techniques have been used to examine the electronic character of these films. ESCA carbon (1s) spectra show that the films are composed mostly of C-C bonds and that a negative bias is important to eliminate C-H bonds from the butane generated films. EELS data show that the films are more diamondlike in that the strong graphitic feature at 6.5 eV is not evident in these films. Among the other measured properties of these films, a refractive index (2.3 at 5 μ m) and hardness (1850 knoop) are in keeping with the diamondlike character of these films."

H. Vora and T.J. Moravec, J. Appl. Phys. 52, 6151 (1981), "Structural Investigation of Thin Films of Diamondlike Carbon",

"Diamondlike carbon films produced both by ion-beam technique and by radio-frequency (rf) plasma decomposition of hydrocarbon gases (C_4H_{10} , C_2H_6 , C_3H_8 , and CH_4) have been examined using the technique of transmission electron microscopy. Although these examinations indicate that these films are predominantly amorphous, both single-crystal and polycrystalline diffraction patterns have been obtained from forms of both types that indicate formation of several different phases. Some of these phases appear to be cubic and could be new forms of carbon. The results of secondary ion mass spectrometric analysis of carbon films produced by rf plasma decomposition of hydrocarbon gases are also discussed."

T.J. Moravec and J.C. Lee, J. Vac. Sci. Technol., 20, 338 (1982), "The Development of Diamond-like (i-Carbon) Thin Films as Antireflecting Coatings for Silicon Solar Cells",

"There is a need for stable, single layer antireflecting (AR) coatings for low cost terrestrial silicon solar cells. Diamondlike (i-Carbon) carbon thin films produced by decomposition of hydrocarbon gases have been studied to determine if these films can be developed into AR coatings for silicon. Such coatings would require a refractive index, $n(\text{film}) \approx 1.9 = \sqrt{n(\text{silicon})}$. We determined the optical constants n and k over a large range of process parameters and source gas for the diamondlike carbon films and will report these results. The degree of hydrogen incorporation in these films has also been studied by SIMS analysis. It was found that the lower visible light absorbing films contain more hydrogen. This does not, however, manifest itself in fundamental C-H absorption bands in the infrared. Very efficient single-layer quarterwave i-C AR coatings $n \approx 1.9$ have been produced on single crystal and silicon-on-ceramic Si solar cells. An increase in cell efficiency of 40% over uncoated cells has been achieved."

T.J. Moravec, Proc. 13th Boulder Damage Symposium, NBS Special Publ. (1982) (to be published), "The Deposition of Diamondlike Carbon Thin Films on CaF₂".

"As part of an AFML program, deposition conditions were studied to produce diamondlike carbon thin films on CaF₂. Halide materials are difficult to deposit diamondlike carbon coatings onto because of the moderate or large coefficient of thermal expansion of the halides which causes thermal induced separation of the coating. In addition, the adhesion of the carbon films to CaF₂ is poor. Several pretreatments were attempted to improve adhesion without much success. We describe a simple thermal technique that resulted in carbon films adhering most of the time to CaF₂ mechanical test bars and optical discs. The problem of adherence, however, has not been solved for this film-substrate system."

T.J. Moravec, in Proc. SPIE, Vol. 325, Optical Thin Films, (1982), ed by R. Seddon, "diamondlike Carbon Thin Films from Ion Activated Techniques."

"Diamondlike carbon thin films can be made by several different processes. We discuss two methods we have used to produce these films: deposition by low energy carbon ion beam and rf decomposition of hydrocarbon gases. In many ways, the films made by the two methods are similar, but there are some slight differences. The films have been characterized by electron spectroscopy, optical spectroscopy and transmission electron microscopy, and these measurements will be discussed. The films are mechanically hard, resist abrasion, transparent in the infrared and less in the visible with a refractive index that can be varied between 1.8 and 2.3. Very efficient single layer quarterwave AR coatings have been produced on silicon solar cells. Other applications will be discussed."

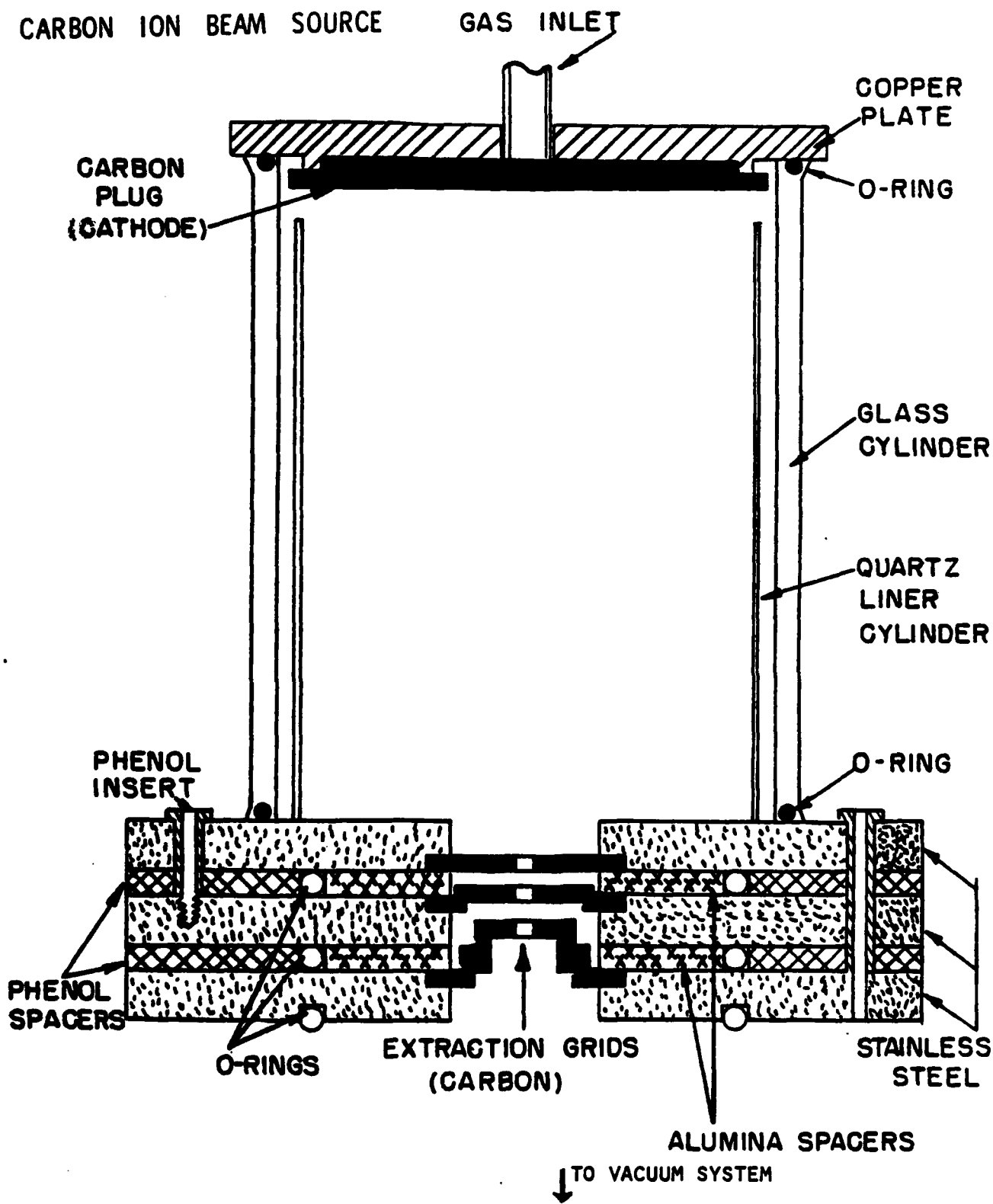


Figure 1. Deposition by direct carbon ions. Argon gas is inlet through a carbon disk electrode into glass cylinder discharge chamber maintained by a high voltage arc. Carbon ions and neutrals sputtered off the electrode are extracted by grids and nucleate film on substrate (not known) placed below grids.

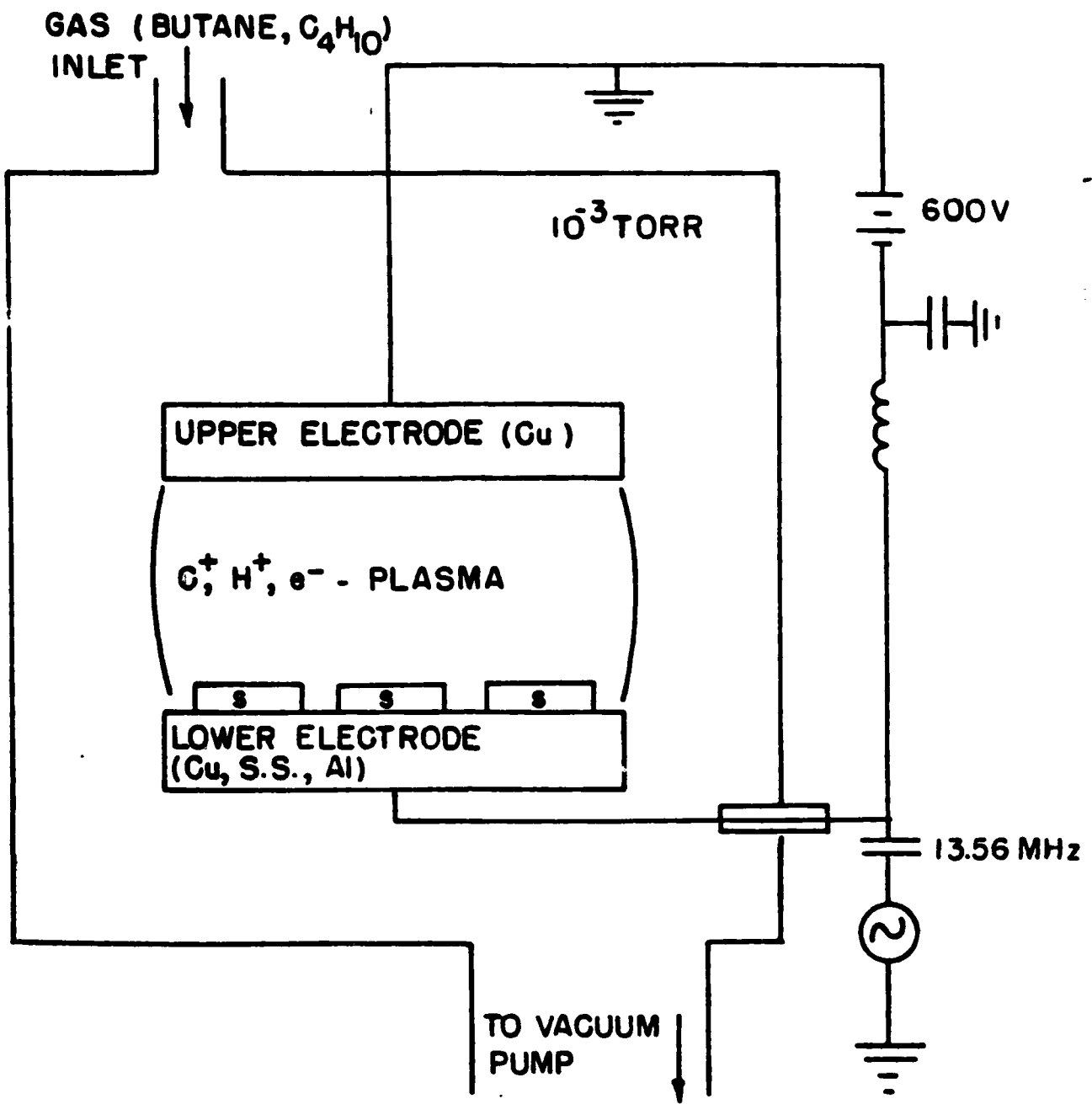


Figure 2. Schematic of rf plasma reactor for producing diamond-like carbon (DLC) films from butane (or any other hydrocarbon gas).

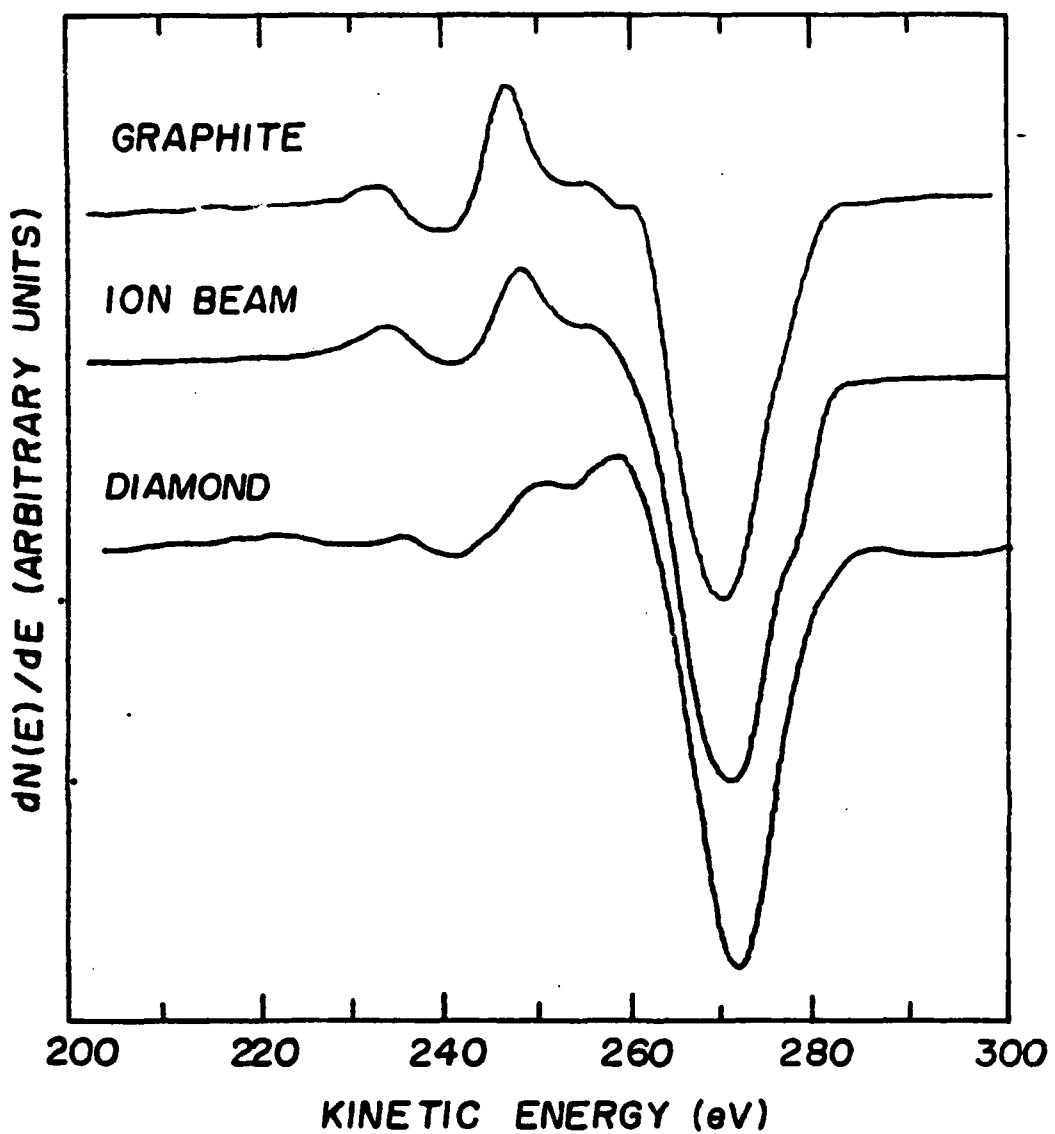


Figure 3. Carbon Auger spectra ($E_p = 3$ deV; 2 V_{pp}) from graphite, ion beam carbon film and diamond. The peaks have been aligned to the graphite position.

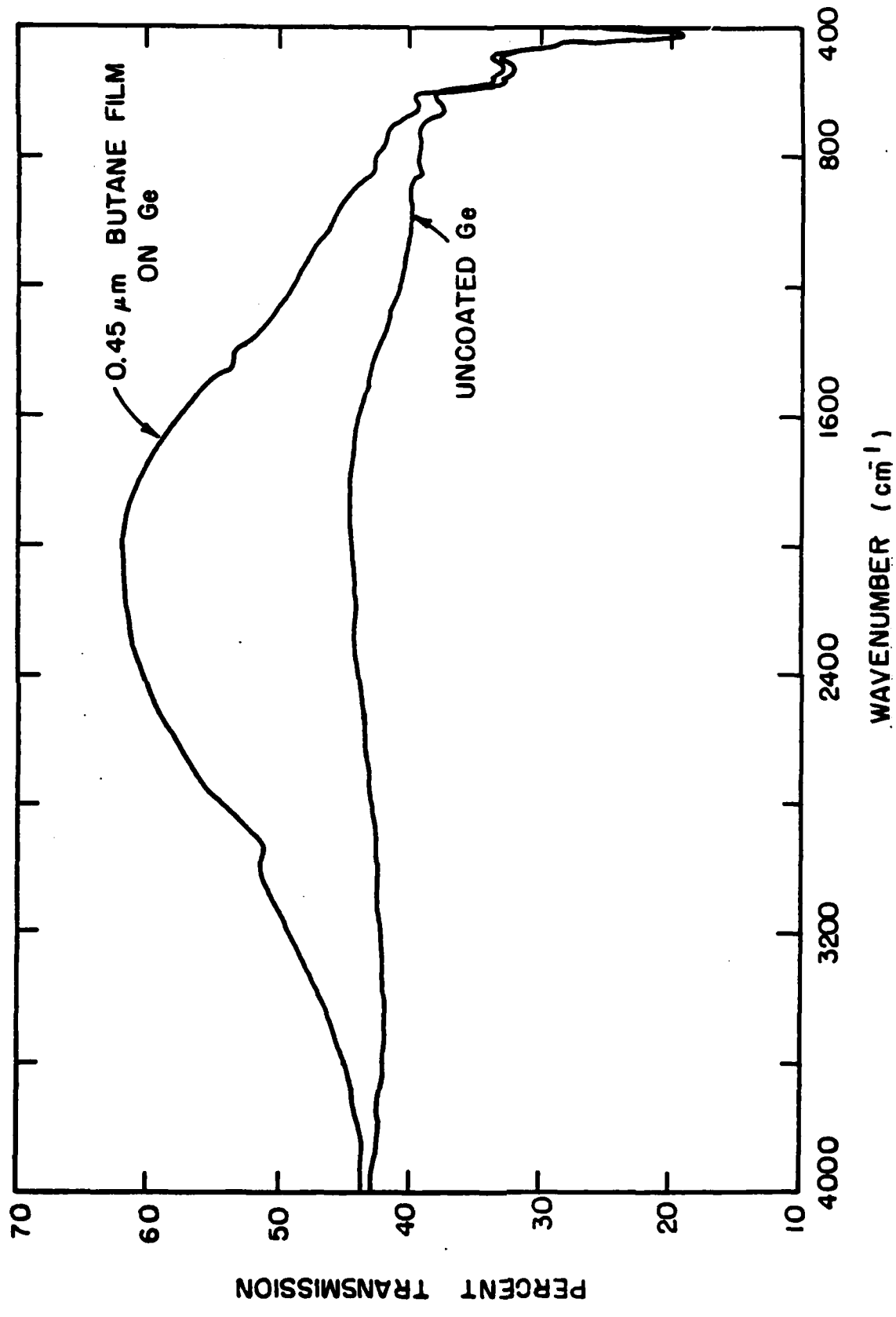


Figure 4. Infrared transmission of a $0.45 \mu\text{m}$ DLC film generated by the method of Figure 2 on germanium. This shows broad transmission from 2.5 to 25 μm (4000 to 400 cm^{-1}) of the DLC with a refractive index of 2.3.

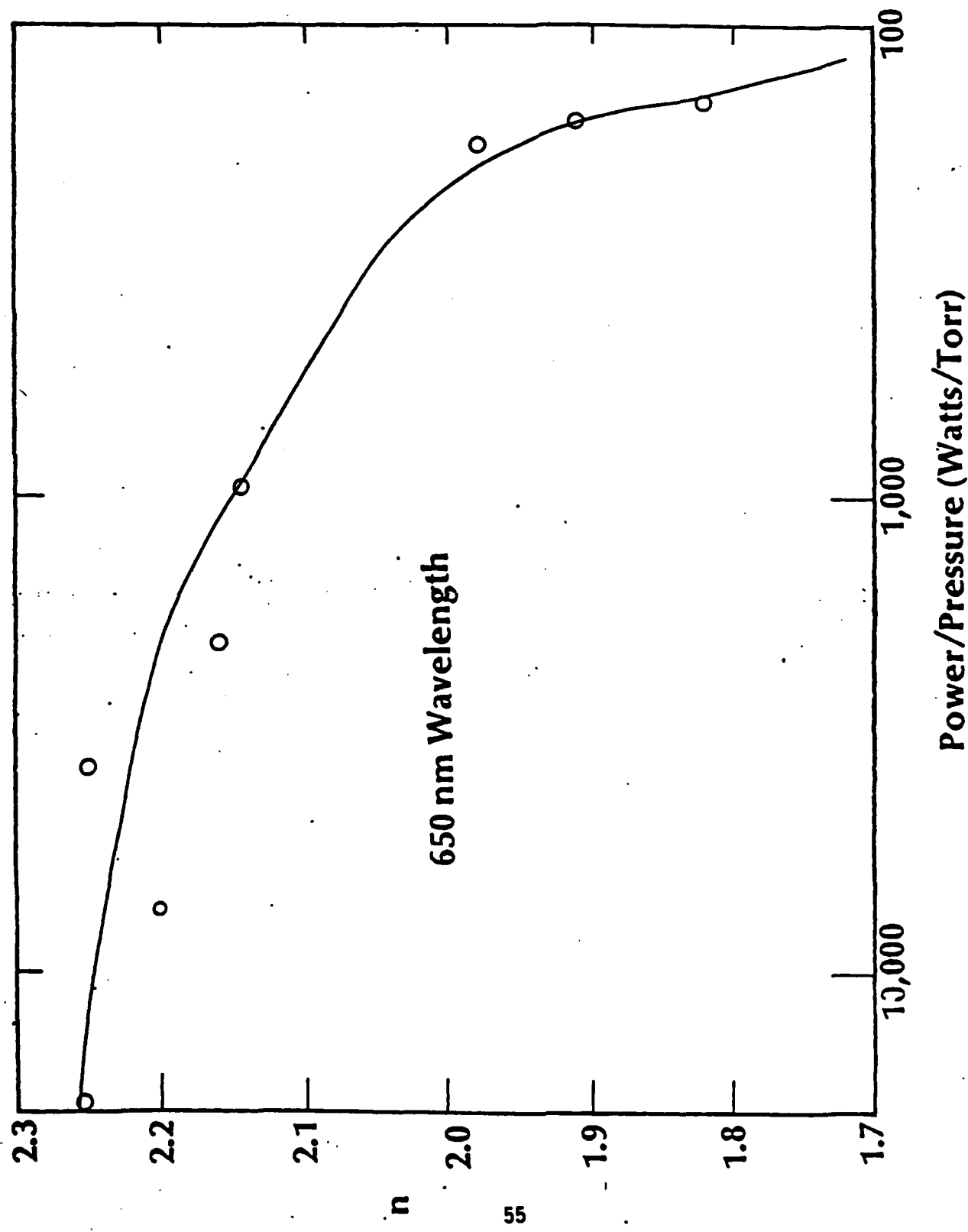


Figure 5. Variation of refractive index n versus power/pressure at .650 micrometer wavelength for films made by method of Figure 2. Power/pressure scale is logarithmic and electrode is 12.7 cm in diameter. Below 100 watts/Torr, the films are mechanically soft.

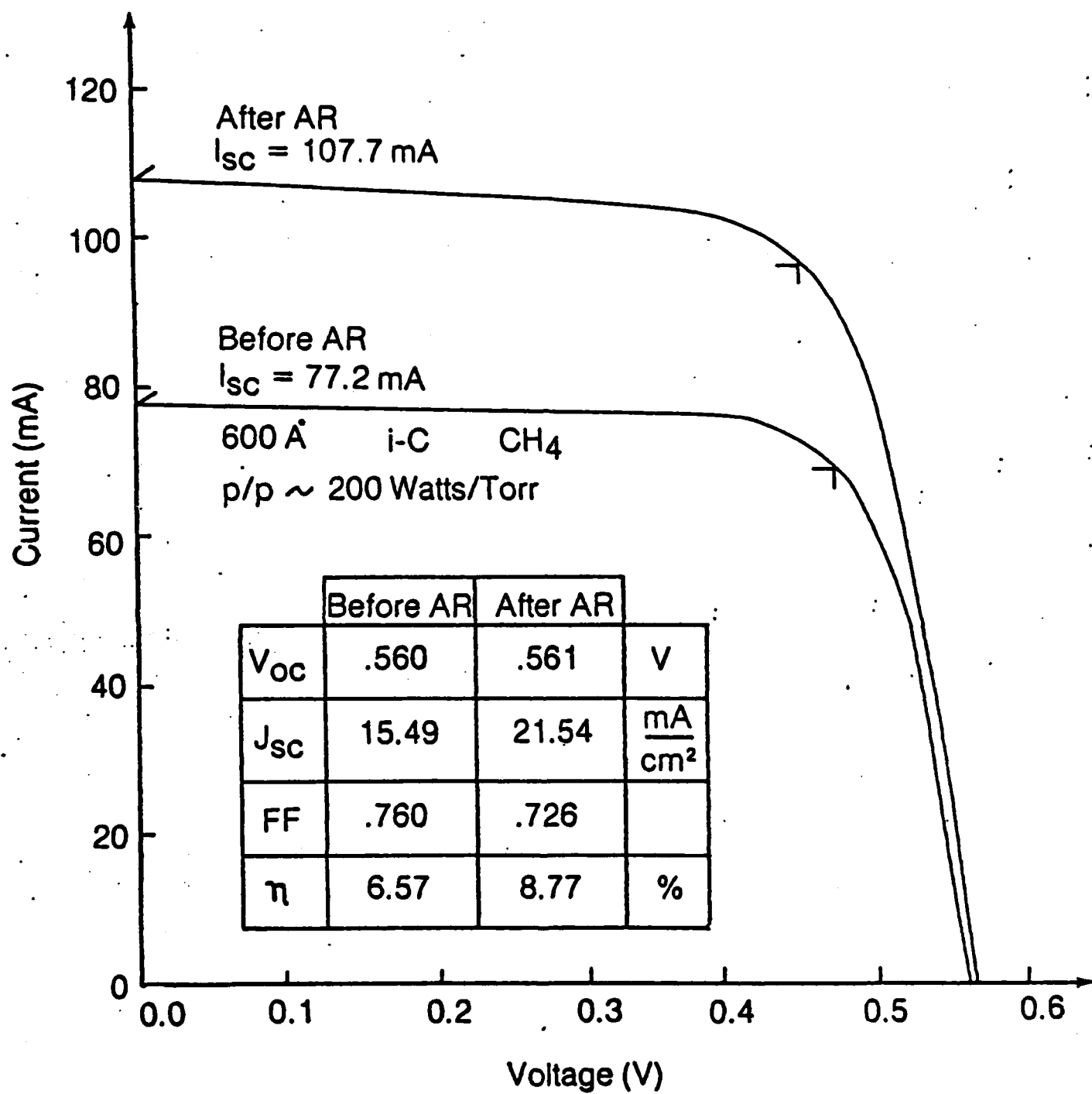


Figure 6. Based upon optical properties shown in Figure 5, very efficient single layer antireflective coatings have been produced on silicon solar cells. Here we show the current-voltage relationship of a Honeywell SOC (silicon-on-ceramic) solar cell before and after AR coating by i-C CH_4 demonstrating a 40 percent increase in J_{SC} with AR coating. Symbols are defined as follows: V_{OC} , open circuit voltage; J_{SC} , short circuit current; FF, fill factor; η , efficiency.

**Summary Table of Properties of Hard Carbon (DLC; i-C)
Films Produced at Honeywell**

Refractive Index, n	Vary between 1.8 and 2.3
Hardness	1850 Knoop
Structure	Amorphous with crystalline regions
Composition	Carbon with up to 20 percent hydrogen
Stress	Compressive: $20-30 \times 10^9$ dynes/cm ²
Solubility	Insoluble in acids or bases
Laser Calorimetry Absorption	1.3 μm : 446 2.9 μm : 429 3.8 μm : 121

ADP002588

Diamond Like Carbon Films Research
at NASA Lewis Research Center

by

Bruce A. Banks

NASA Lewis Research Center

Cleveland, Ohio

Interest in diamond-like films at NASA Lewis Research Center has been based on potential applications that might advantageously utilize the electrical, optical, thermal, mechanical, or chemical properties of these films. Over the past two years a focussed effort has been established at NASA Lewis to investigate the feasibility of using such films for power electronics devices such as heat conductor for semiconductors or as doped semiconductors themselves. If the diamond like films exhibit high thermal conductivities then applications as a heat spreader to cool semiconductor junctions may be attractive. Doping of diamond-like films as an integral part of a vacuum deposition process may enable cost effective production of a new class of semiconductors. The realization of practical application of diamond-like films will be in part dependant upon the ability to reliably and economically produce diamond-like films having satisfactory characteristics. Investigations of the various deposition techniques reported in this paper were performed by B. Banks, S. Domitz, M. Mirtich, J. Kolecki, and S. Rutledge of NASA LeRC.

Figure 1 is a list of current and planned vacuum processes being investigated at NASA-Lewis for the production of diamond-like films. The top six approaches have been tested to date. The coaxial carbon plasma gun source is under construction. The carbon ion beam source is being designed. Figure 2 is a schematic drawing of the carbon-argon ion source. The source is of the general type used by many researchers in which sacrificial sputtering of cathode potential surfaces is used to produce carbon atoms which are then ionized and accelerated along with an inert gas ions. The rates of deposition of are quite low with this technique and the inert gas arrival rate is typically greatly orders of magnitude greater than the carbon ion arrival rate.

Figure 3 shows a schematic drawing of a DC hydrocarbon plasma source. Electron bombardment of the organic gas molecules produces free carbon atoms and ions which can be deposited on a target which may be AC or DC biased. Depending upon the deposition conditions films may be slowly deposited which range from a crosslinked hydrocarbon polymer to diamond-like carbon. Figure 4 is a photograph of the plasma source lifted up from its position for deposition.

Figure 5 shows two RF sputtering methods used to produce diamond-like films. The method on the left being the most popular technique used throughout the world. Use of the carbon electrode in the configuration on the right enables one to increase the carbon to hydrogen ratio of the depositing species.

The use of two ion beams as shown schematically in Figure 6 and in a photograph in Figure 7 have been successfully used to produce diamondlike films. The large ion source is a 30 cm diameter ion source with its optics masked to produce a 10 cm diameter ion beam. It was operated with methane fed directly into the discharge chamber and argon fed in through the ion source hollow cathode. The ratio to methane to argon feed molecules was 28 percent.

Carbon, hydrogen, argon, and perhaps more complex hydrocarbon ions are accelerated at low energies (100 to 150 eV) to impinge on a substrate. Simultaneously a more energetic (600 eV) argon ion beam from a 8 cm diameter ion source also bombards the substrate. Deposition rates of diamond-like carbon film were of the order of 1 A/sec. Densities of carbon films produced by this deposition technique were approximately 1.9 gm/cm^3 .

Figure 8 is a schematic drawing of a single ion beam sputter deposition technique that utilizes the fringe of the ion beam for simultaneous ion bombardment of carbon films being deposited. Such simultaneous bombardment of the depositing carbon films produces densities of 2.2 grams/cm^3 compared to 2.1 grams/cm^3 for simply sputter deposited films. Deposition rates ranging from approximately 0.1 to .3 A/second were measured using this deposition technique depending upon the relative carbon arrival to removal rates. Figure 9 is a photograph of the vacuum facility showing the ion beam source in place source in place and the adjoining ion source power supplies. Figure 10 is a photograph of the 8 cm argon ion source used with a hot wire neutralizer. Figure 11 shows the configuration of the actual sputter deposition (with simultaneous ion bombardment) experimental apparatus. The deposition substrates were mounted on a motorized disk behind a pyrolytic graphite adjustable transparency comb which served to adjust to the desired carbon arrival to removal ratio.

Figure 12 and 13 are a schematic drawing and photograph of a vacuum arc carbon source used to deposit diamond-like carbon films. Typically a 20 to 30 volt arc is struck (by means of a striking electrode) between a carbon cathode and an anode ring. The high current (50-200 Amp) vacuum arc causes a very hot cathode spot to form which evaporates the carbon which also may be then ionized. Deposition rates of the order of $10^3 \text{ Angstroms/sec}$ can easily be

achieved. Resulting films have densities up to 2.8 grams/cm³. In addition to single carbon atom or ion arrival at the target, very large polyatomic can be observed being ejected from the cathode hot spot and are found in abundance in the resulting films. Figure 14 is a photograph of the vacuum arc in operation which also illustrates the tracer-like paths taken by the hot polyatomic particles.

Figure 15 is a schematic drawing of a diamond-like film deposition technique which uses the Lorentz force to accelerate a pure carbon plasma. The central graphite electrode is moved forward until it allows an arc to strike between it and the outer graphite electrode. This pulse deposition technique is currently under construction at NASA-Lewis.

Figure 16 shows a pure carbon ion beam concept in which carbon vapor is ionized to then be accelerated to allow energetic carbon ion deposition.

Figure 17 is a table comparing some of the characteristics of diamond and graphite with the diamond-like films produced at NASA Lewis.

A comparison of the optical absorption properties (in the visible region) of diamond-like films is shown in Figure 18 for the single ion beam technique (of Figures 8-11) and the dual ion beam technique (of Figures 6 and 7).

In summary a variety of vacuum deposition techniques are currently being investigated or are planned which hold promise for the deposition of diamond-like carbon films. Densities clearly in excesses of that of graphite have been observed along with other properties which are indicative of sum degree of tetragonal bonding. Additional research on deposition techniques and characterization is needed and is being planned to fully access the scope of applications of these films.

- **CARBON-ARGON ION BEAM SOURCE**
- **DC HYDROCARBON PLASMA SOURCE**
- **RF SPUTTERING WITH HYDROCARBONS**
- **DUAL BEAM METHANE AND ARGON ION SOURCE**
- **ARGON ION SOURCE WITH CARBON TARGET**
- **VACUUM ARC JET CARBON SOURCE**
- **COAXIAL CARBON PLASMA GUN SOURCE**
- **CARBON ION BEAM SOURCE**

Figure 1. LeRC Approach for Synthesis of Diamondlike Films

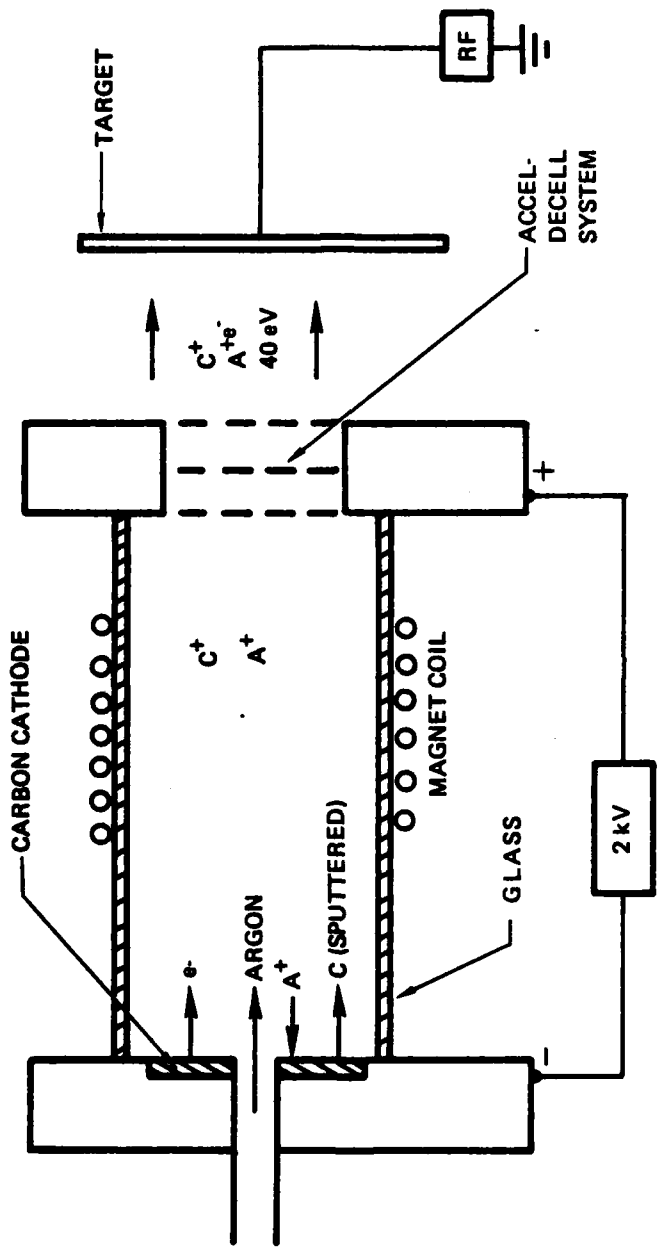


Figure 2. Carbon-Argon Ion Source

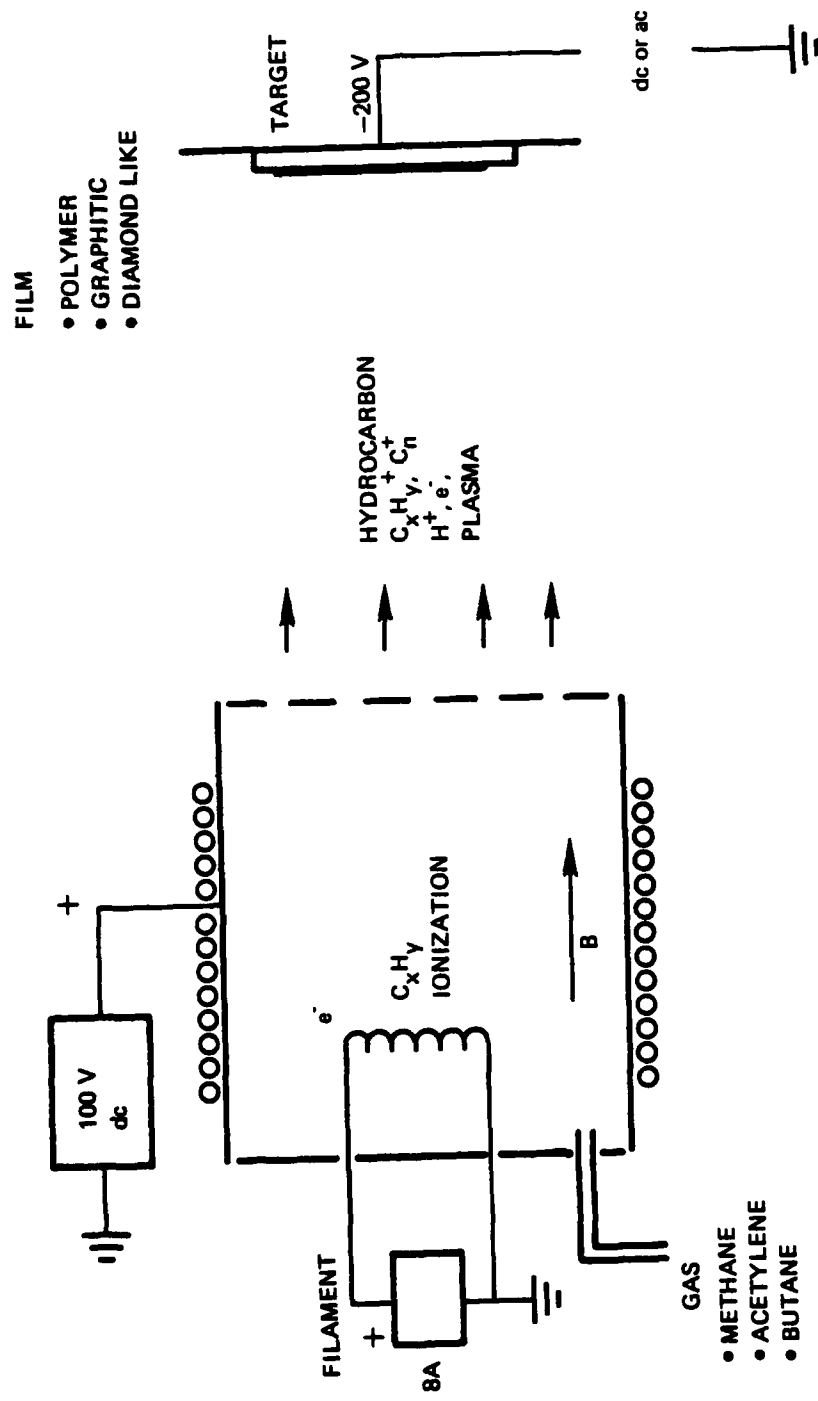
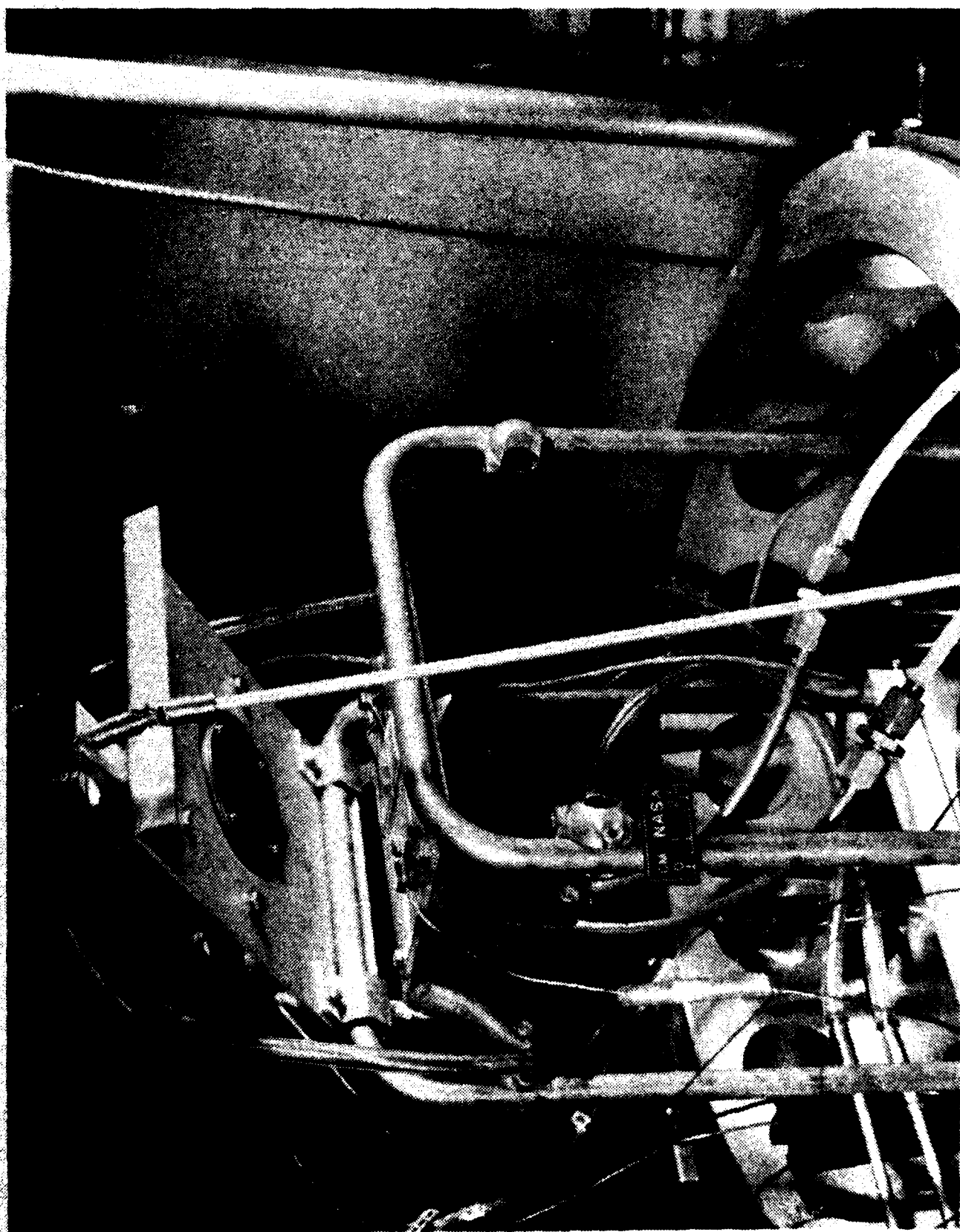


Figure 3. DC Hydrocarbon Plasma Source

Figure 4



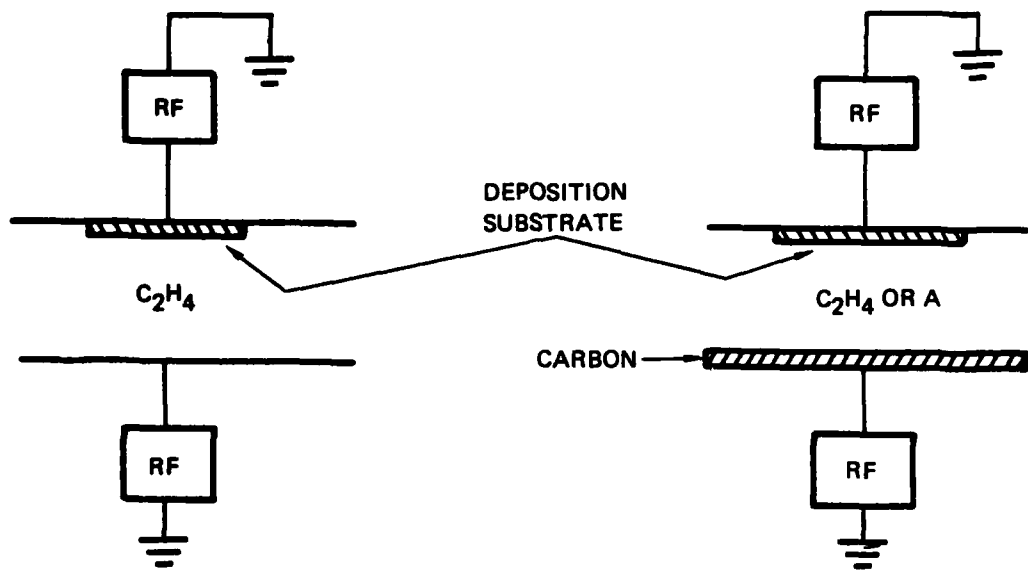


Figure 5. RF Sputtering with Hydrocarbons

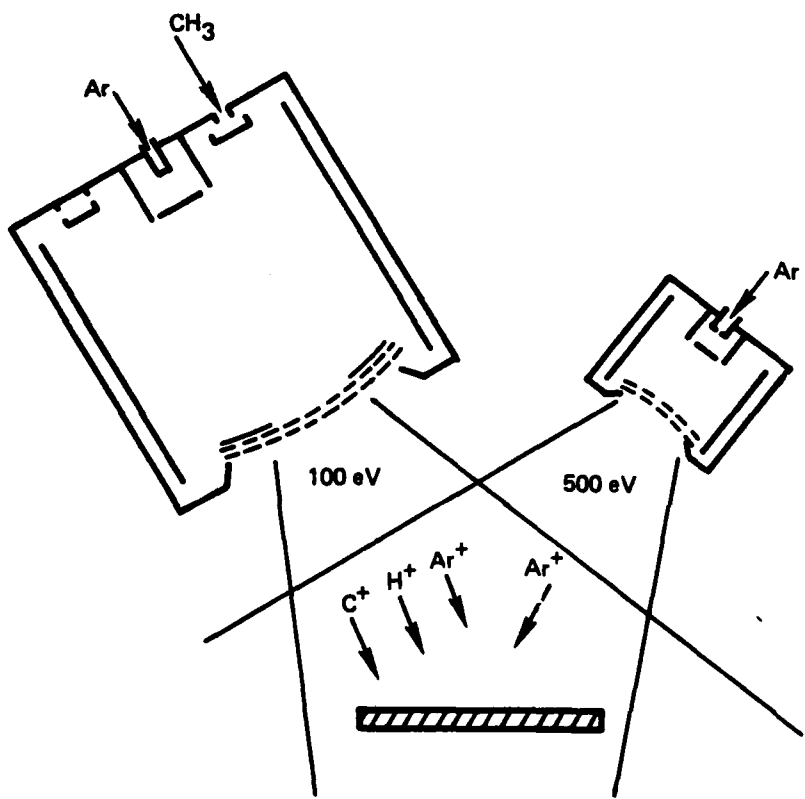


Figure 6. Dual Beam Methane and Argon Ion Sources

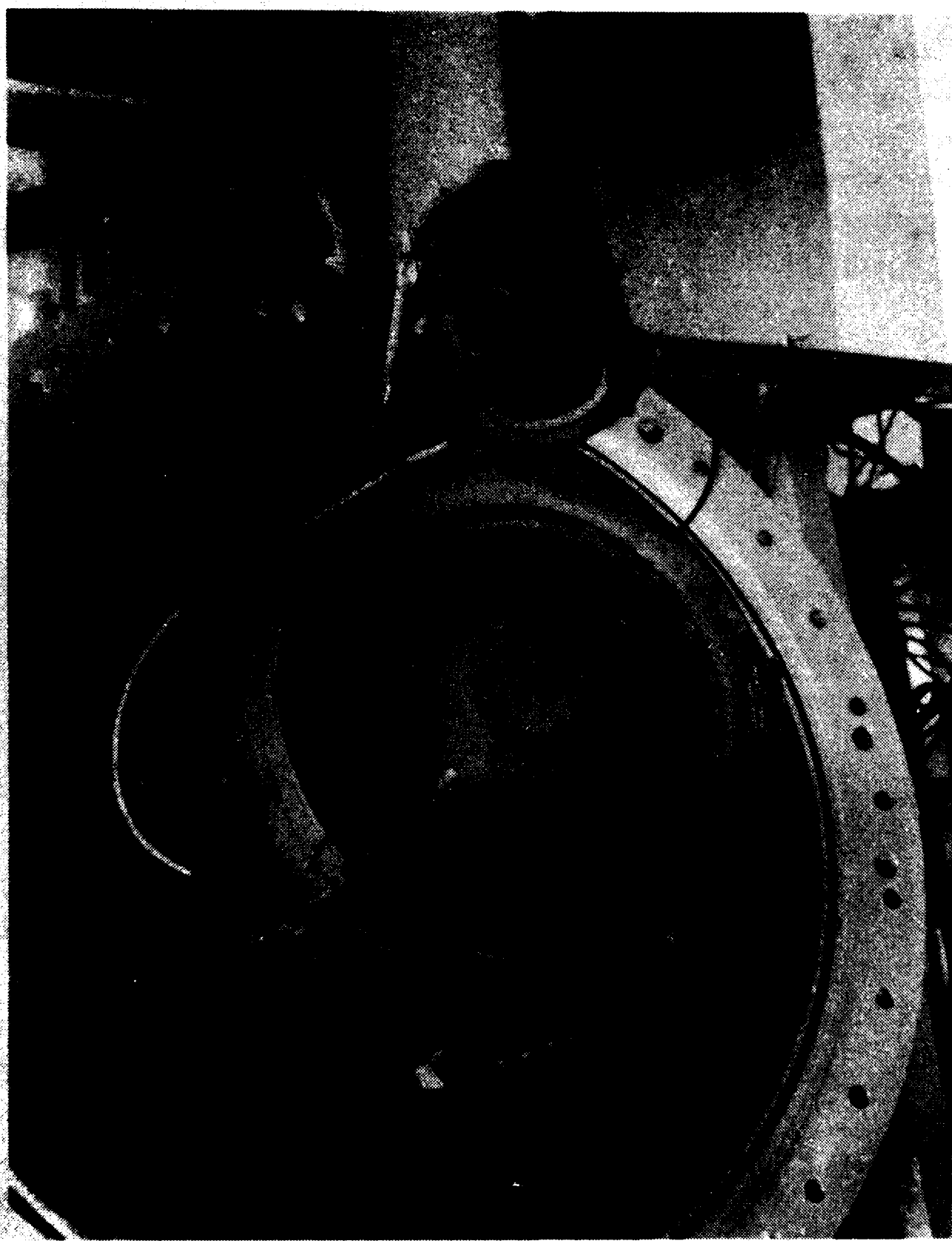


Figure 7

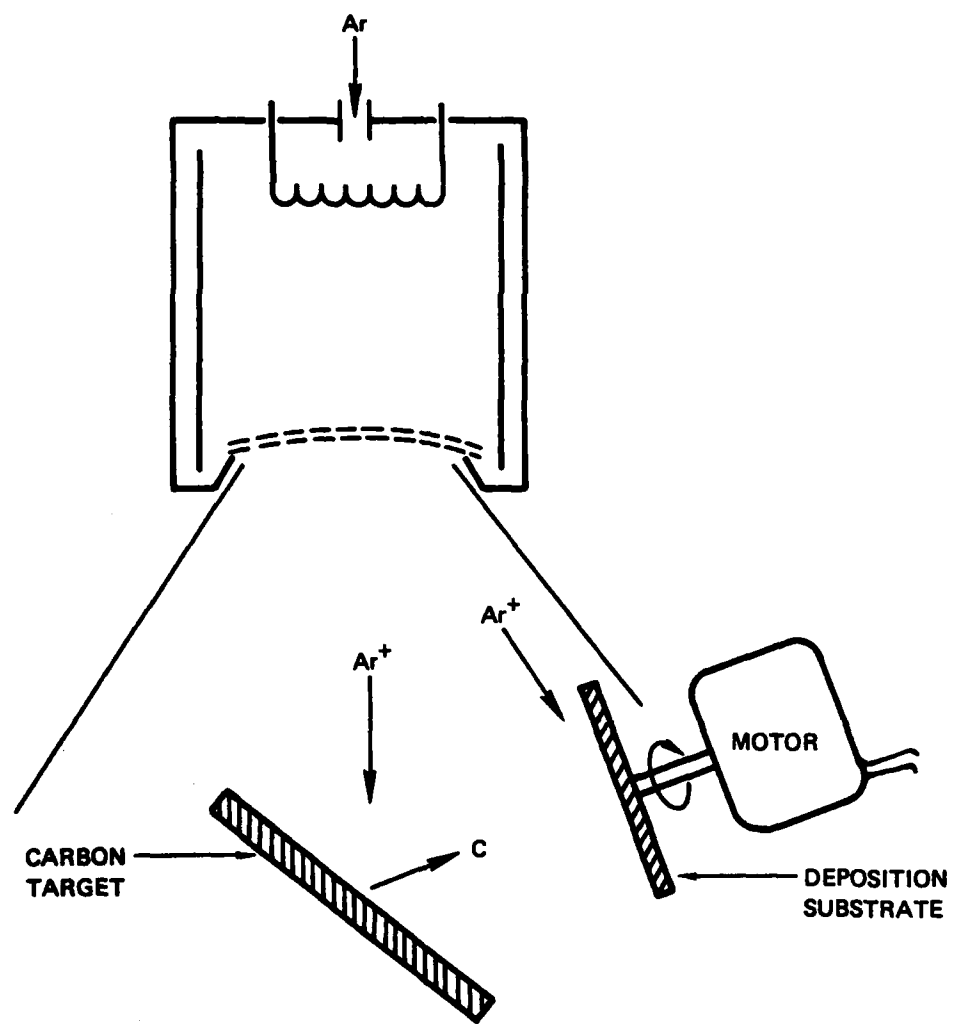


Figure 8. Argon Ion Source with Carbon Target

NASA
C-02-167

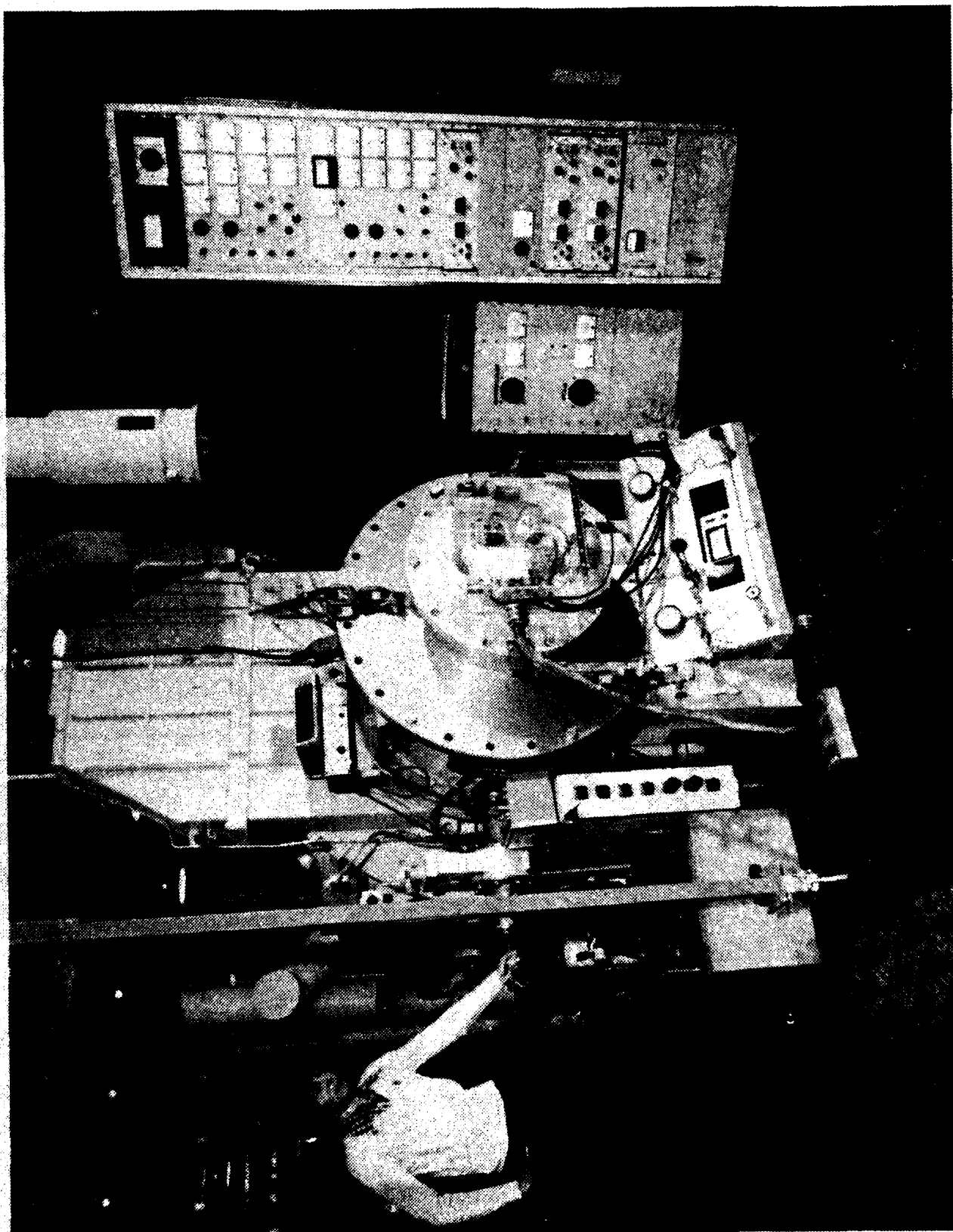
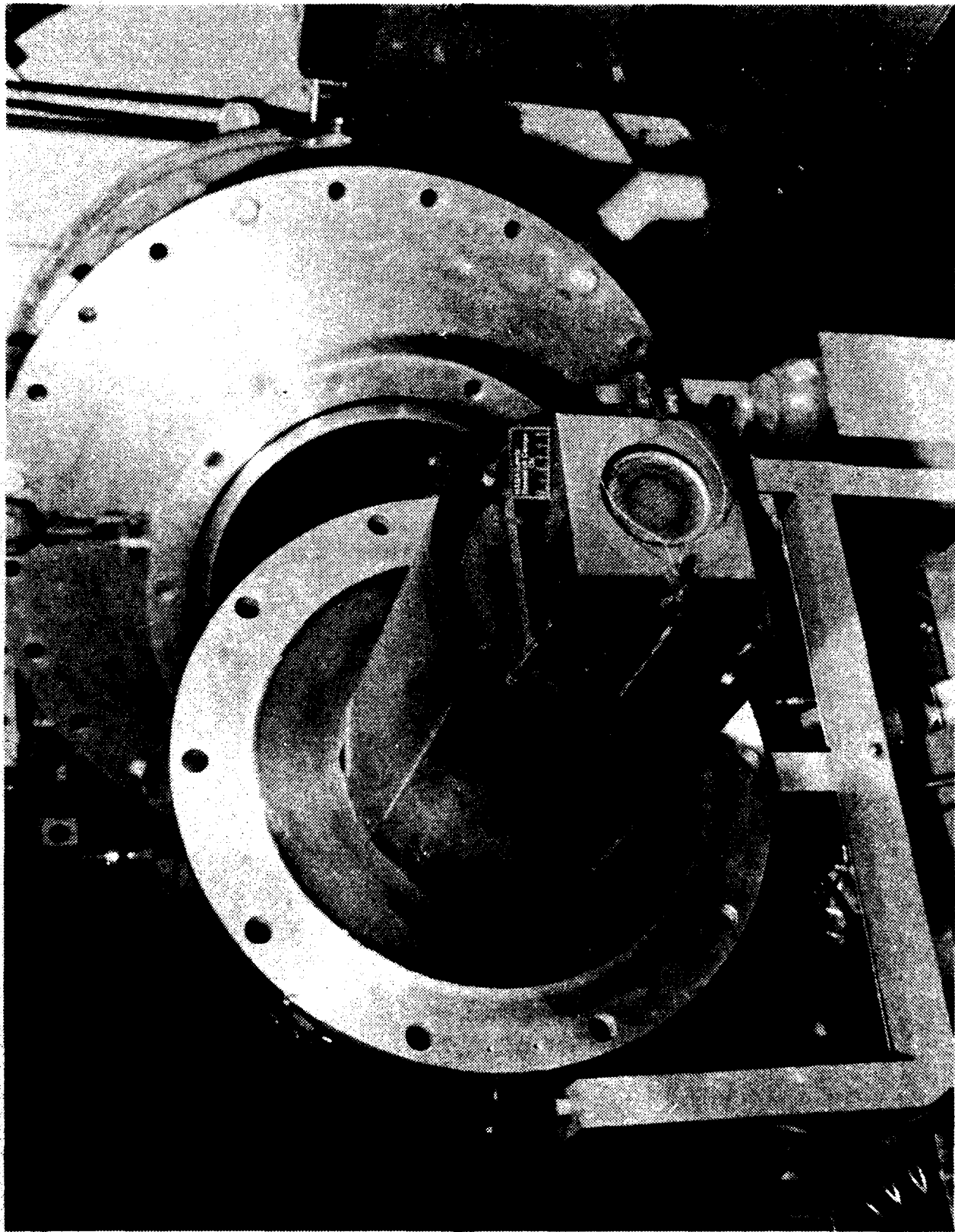


Figure 9

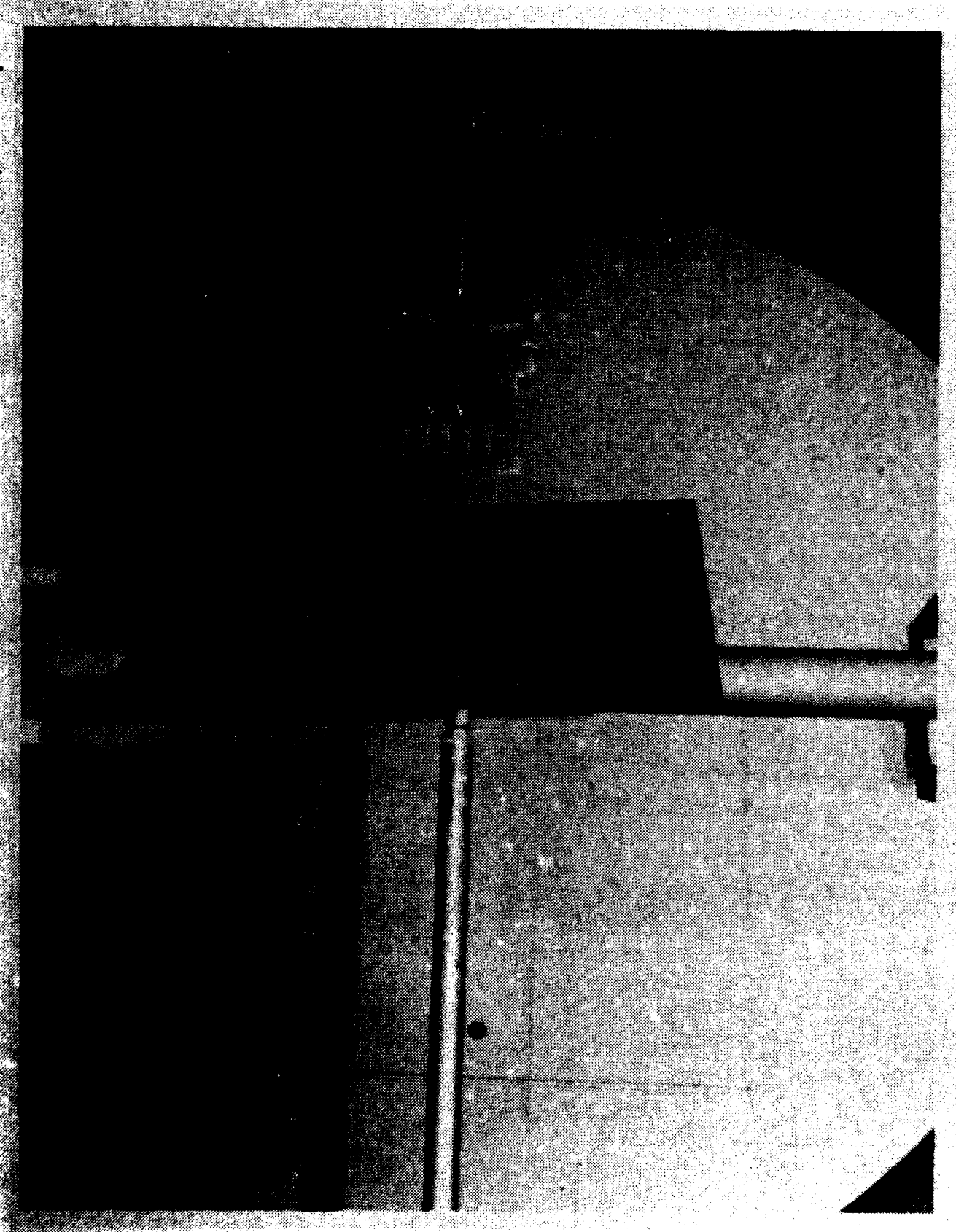


NASA
C-82-1675

Figure 10

C-82-162
NASA

Figure 11



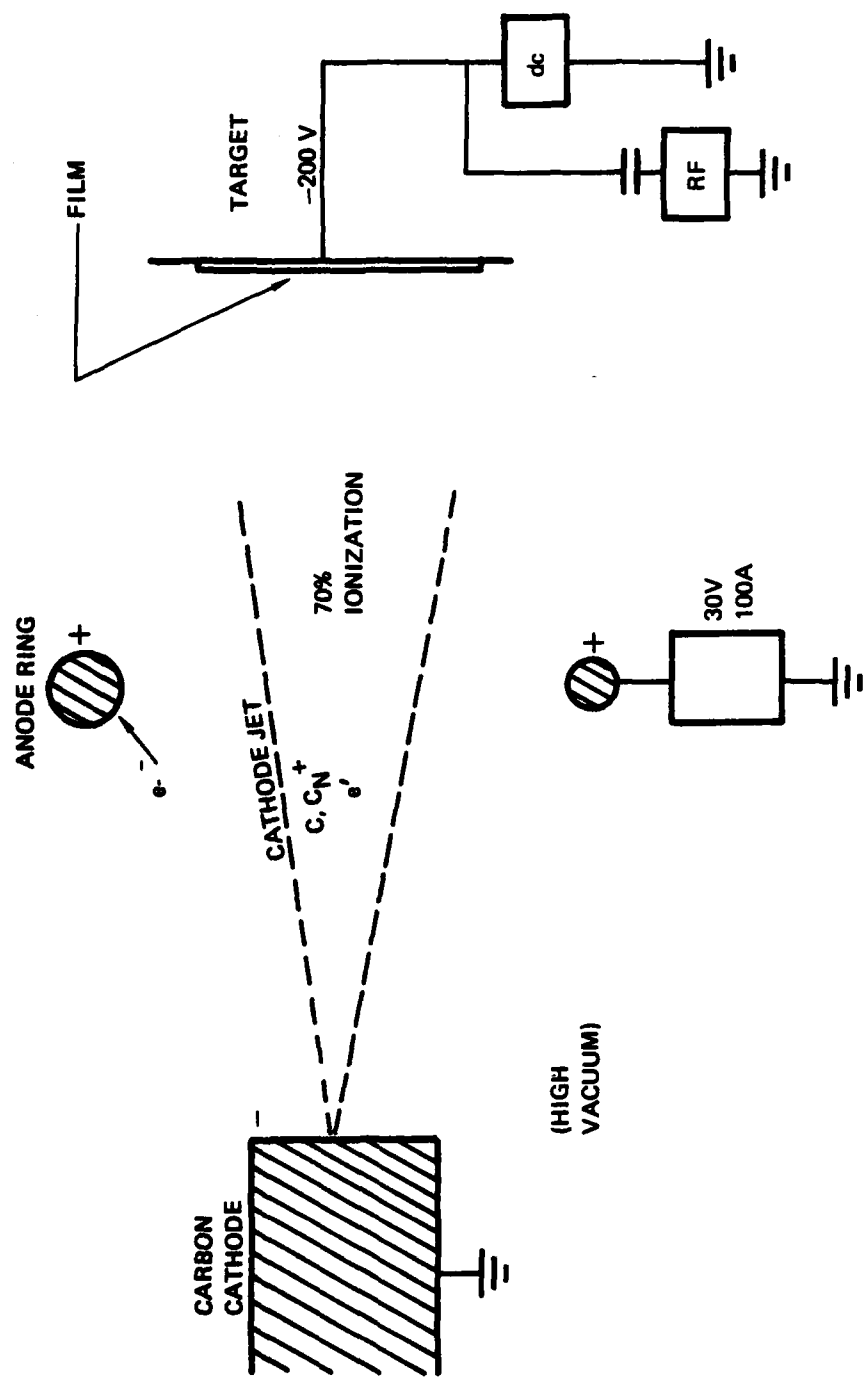


Figure 12. Vacuum Arc Carbon Source

NASA
C-82-1856

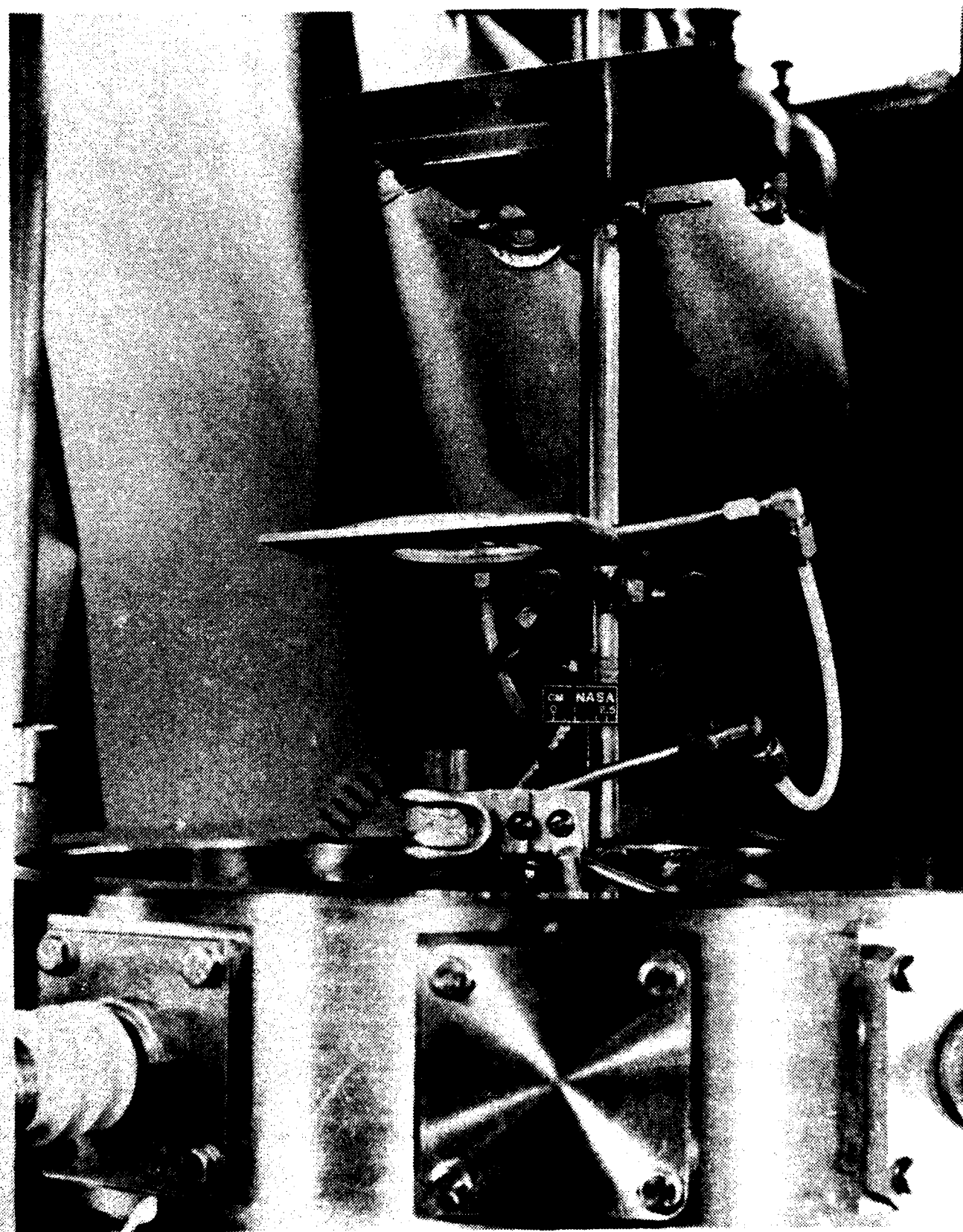


Figure 13

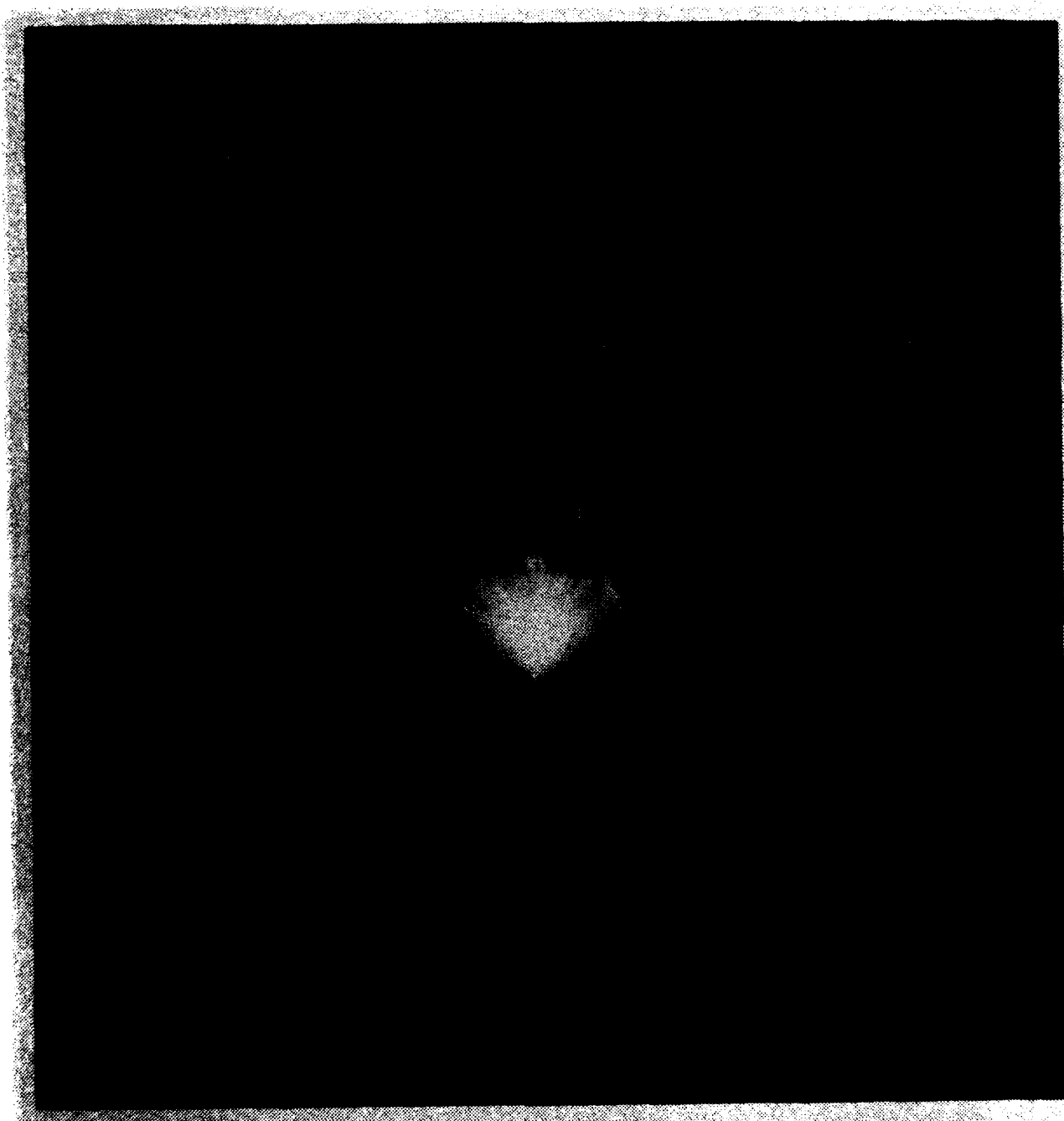


Figure 14

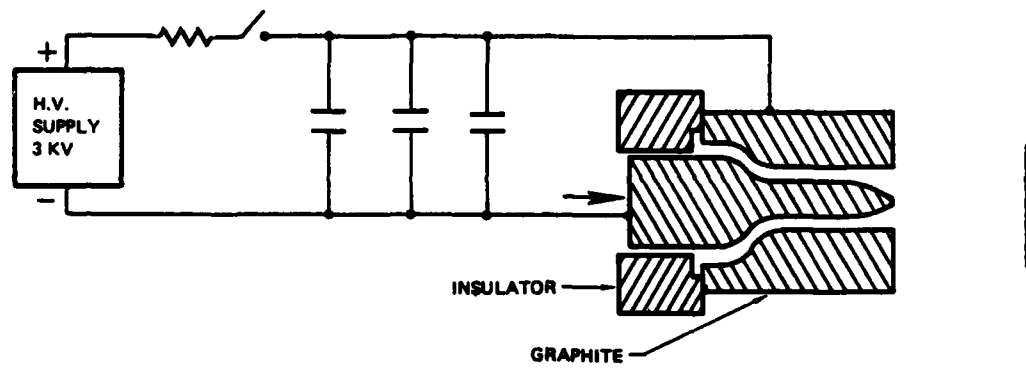


Figure 15. Coaxial Carbon Plasma Gun Source

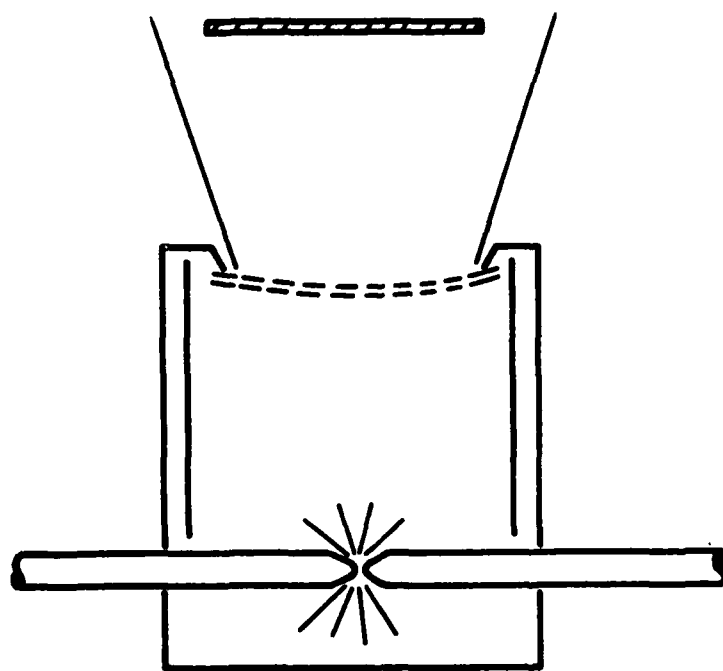


Figure 16. Carbon Ion Beam Source

DIAMOND-LIKE FILM CHARACTERISTICS

<u>PROPERTY</u>	<u>DIAMOND-LIKE FILM</u>	<u>DIAMOND</u>	<u>GRAPHITE</u>
INDEX OF REFRACTION	1.3 - 1.7	2.4	—
RESISTIVITY, CM	10^{10}	10^4 TO 10^{16}	10^{-5}
RESISTANCE TO $3H_2SO_4-HNO_3$	YES	YES	NO

Figure 17. Diamond-like Film Characteristics

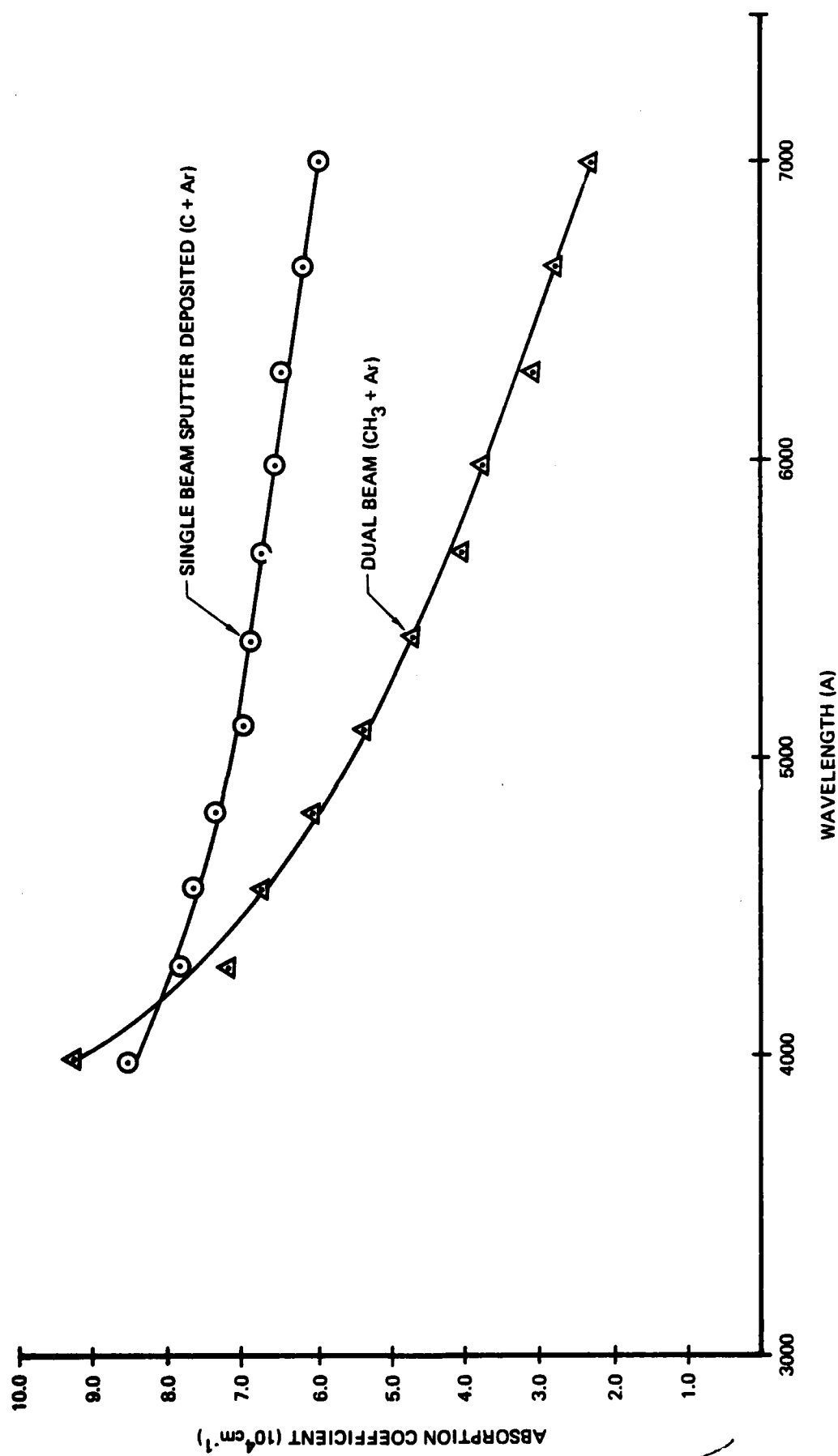


Figure 18

AD P002589



HIGH ENERGY ION DEPOSITED CARBON FILMS

By:

M. Stein and S. Aisenberg
Applied Science Laboratories
335 Bear Hill Road
Waltham, Massachusetts 02154

INTRODUCTION

Diamond-like carbon films have been grown successfully for almost two decades. Although complete characterization of the films is still lacking, many of the properties have lead to the phrase "diamond-like" in describing these thin coatings. One commonality among the many preparation techniques for these films is that the mass is transferred through charged particles to form the coating on the substrate.

We have used many processes for producing the diamond-like carbon coatings. These have included ion beam deposition, RF and DC plasma deposition using sources of sputtered carbon, evaporated carbon and plasma hydrocarbon decomposition. In spite of the deposition technique used, it was found that many of the diamond-like properties were maintained over a broad range of system parameters. The energy of the mass/charge transfer particle was found to be a useful indicator to characterize the deposition process.

AD-A136 766

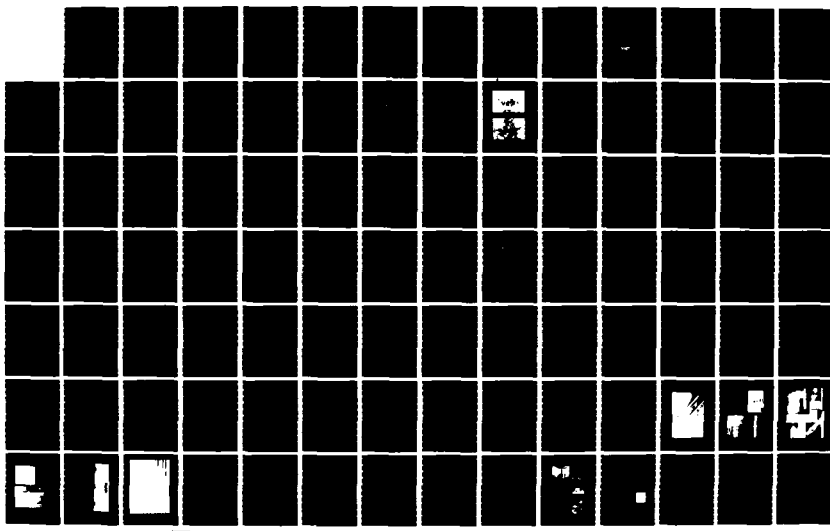
PROCEEDINGS OF THE DARPA (DEFENSE ADVANCED RESEARCH
PROJECTS AGENCY) WORK. (U) BDM CORP ALBUQUERQUE NM
B BENDOW 1982 MDA903-81-C-0151

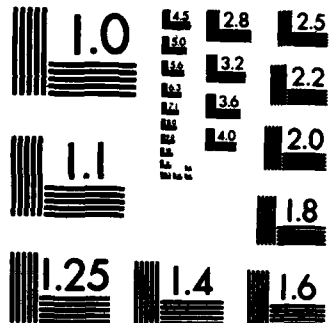
2/4

UNCLASSIFIED

F/G 11/3

NL





MICROCOPY RESOLUTION TEST CHART
NATIONAL BUREAU OF STANDARDS-1963-A

EXPERIMENTAL APPROACH

The ion beam technique provided the greatest versatility for controlling the mass/charge ratio since the incoming ion energy to the substrate could be varied over many orders of magnitude. Furthermore, many of the energy ranges used for this work could also be duplicated using various plasma techniques. This allows greater versatility in setting up many of the experiments for coatings. Consequently, the primary deposition technique used for this work is an ion beam source which allows separate control of ion species and deposition rate.

One of the problems typically encountered with an ion beam source is the limited coverage of the coating. To resolve this problem we have developed an extended ion source which has a 1 x 70mm exit aperture. This source permits coating larger surfaces by moving the substrate perpendicular to the plain of the ion beam as illustrated in Figure 1. The ion source used for this work also contains features for energy control and separation of the ion trajectory down stream from the source. The ion source assembly is housed in a stainless steel, cryopumped coating chamber which exhibits adequate cleanliness for experimental coating work.

ENERGY DEPENDENCE

Typical properties which make this film desirable for several

applications are listed in Figure 2. Depending upon application, the importance or quality of particular properties may vary greatly. Obviously dielectric applications require a good insulator, while optical loss is often not a significant factor. Typically for all applications of any type coating, good adhesion to the substrate is vital to performance of the film-substrate system.

Figure 3 schematically illustrates the modification of the top surface layer on a calcium fluoride window before and after coating. The coating process modifies the surface below as well as above the original surface, as indicated by the darker horizontal line. The extent of modification below the original surface depends upon several factors such as substrate pretreatment, temperature, and chemical reaction, all of which may occur to some extent.

Using the ion beam technique, the depth of surface interaction can be controlled by controlling the energy of the bombarding ions. In Figure 4 the particular energetic ion process occurring is plotted as a function of incoming energy and penetration depth for carbon ions in silica. The coatings themselves may form at many bombardment energies. Whether or not a coating forms is determined by the ratio of masses and sticking coefficient of the incoming ions or particles.

When energies of the incoming ions exceed 2 1/2 electron

volts, sputtering may occur. This process is exhibited when the ion energy exceeds the surface binding energy. The sputter yield tends to increase with atomic number as illustrated in Figure 5, for ion bombardment of copper. For an incident energy of 10 kilovolts, 5 atoms are ejected for every incoming Argon ion. This ratio is about 1 to 1 for carbon. The sputter yield tends to decrease slightly with increasing incident ion energies over about 20 keV for carbon.

The sputter yield will also vary with crystalline orientation as well as incoming incidence angle. Typically the higher incident angles will result in a greater number of particles ejected. The relationship between crystalline orientation is illustrated in Figure 6 (Snouse, T.W., and Haughney, L.C., 1966). A four-fold change in sputtering rate can occur based on crystalline orientation.

Another process occurring at energies greater than 20 eV is radiation damage wherein successive atoms in the lattice are dislocated and expend their kinetic energies propagating the damage. This tends to produce a fine amorphous structure as the upper surface layers are bombarded.

As energies are increased typically into the keV range, ion implantation ensues. Implantation does not produce a coating but modifies the original surface by ion stuffing. This can change the surface properties as well as the behavior of a final coating.

Ion implantation can thereby inhibit the formation of a sharp interface between the substrate and coating. This may help improve adhesion and reduce localized stress concentrations. Additionally, it is possible to make depth concentration profiles by varying the energy, composition, and dosages of the incoming ions. Figure 7 illustrates the theoretical penetration depth for positive carbon ions of various incident energies in copper. The profiles are typically of gaussian distribution; however in application these profiles are rarely realized due to other atomic effects, such as sputtering, coating, etc.

COATINGS ANALYSIS & RESULTS

Energies of only 50 keV are required to produce a mean implantation depth of 1000 angstroms in many materials. An example of the concentration gradient appears in the following transition zone analysis which was performed by auger electron spectroscopy (AES). This coating followed implantation at approximately 4 keV to produce the transition zone as illustrated in Figure 8. As can be seen, the concentration is about 50 atomic percent carbon at 100A into the film surface. The gradient is constant and appears to have the anticipated gaussian profile. At depth 0 the true coating would normally start. The coating at this point can be deposited to the desired thickness, once this transition zone has been established.

Several techniques have been used to determine film

composition. The films are typically found to be essentially pure carbon, while TEM analysis indicates rings assignable to diamond. The films can form chemical bonds with some substrates such as silicon or germanium resulting in very tenacious, adherent films. The bonds can also be formed with hydrogen and oxygen resulting in a hydrocarbon surface as well as in the bulk, if these hydrocarbons are present during deposition and the bombarding ions are of low energies (several eV).

AES spectral surveys were made for ion deposited carbon films, both as received and after sputtering, and for graphite. A comparison of these spectra is shown in Figure 9. Obviously, there is very little difference in peak geometry or in energy. It is interesting to note that the shape of the slope for the major peak contains an extra dip for the coating after argon ion bombardment. This dip is similar to that found in the pure graphite sample. An ESCA survey was also made on the sample received and on graphite. These spectra are illustrated in Figure 10. The graphite peak appears to be shifted in energy with respect to the coated sample peak by approximately 1/2 eV. There is a portion of the graphite spectrum which is labeled surface hydrocarbons due to hydrogen bonding on the graphite surface. The AES and ESCA surveys are typical of what other investigators have found.

Raman spectra were also made on this film on silicon. The spectra indicate that peaks assignable to both diamond and

graphite are detectable as is illustrated in Figure 11.

The optical properties of the carbon film are receiving current interest. Typically, the film appears transparent to yellow when freestanding with no detectable IR activity for low hydrogen samples. The films appear amorphous and free from defects. Calcium Fluoride windows coated by this technique have shown no increase in detectable scatter. The refractive index can range from about 2.0 to 2.4 at 5000A. The absence of IR activity is illustrated in Figure 12 which shows the spectra for two samples of the film on a 3mm calcium fluoride wafer. Multiple spectral traces were made with no variations assignable to any optical activity.

An initial measurement was also made to compare the IR absorption on the half coated calcium fluoride disk. At wavelengths of 2.9 and 3.8 microns, the absorption increased about 3 to 4 times with the coating. It is inconclusive what the cause of the attenuation was and what proportion was surface and what proportion bulk.

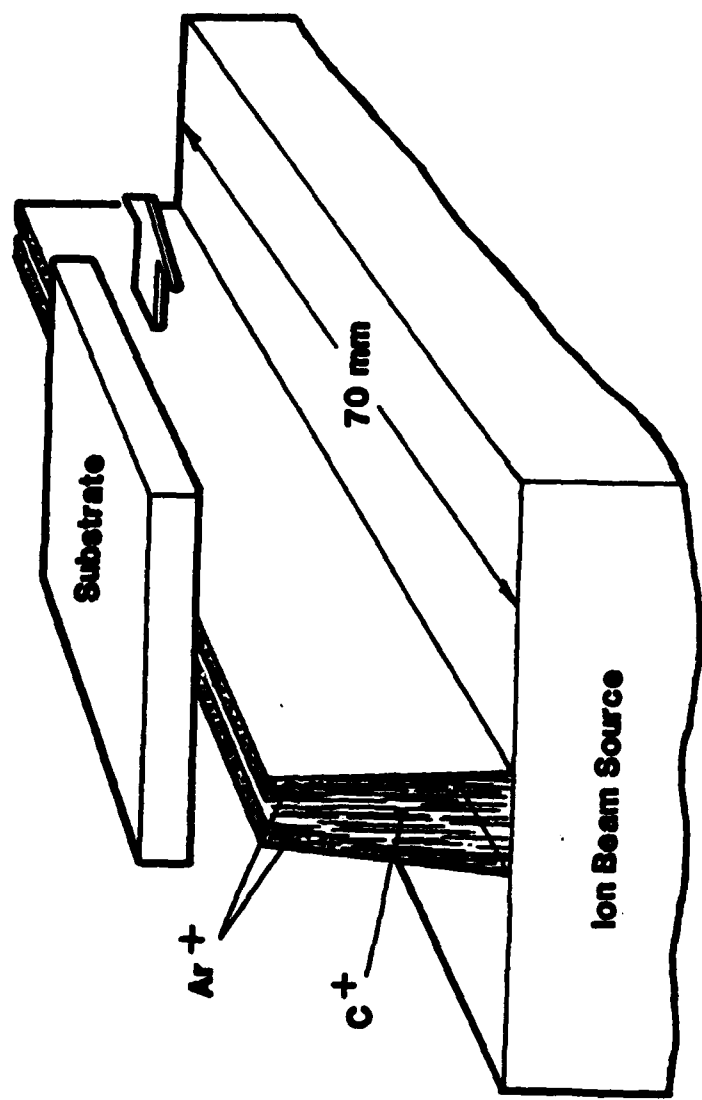
EXPERIMENTAL CONCLUSIONS

↓ The nature of the substrate preparation also appears to be important. This is illustrated in Figures 13 and 14 which show two topographies of diamond turned copper surfaces. In Figure 13, the nature and presence of grain boundaries is very evident ↓

following coating. It appears that some grains received no coating while others have a substantial coating. This was apparently due to delamination of certain grains following a cleaning of the coated surface. Figure 14 shows a similar diamond turned copper surface coated to the same thickness using a 4 keV carbon implant prior to deposition. This resulted in much better adhesion of the coating on the surface with improved uniformity of the various grains. Although the sharp edges of the diamond turning process appeared to be detrimental with respect to coating adhesion, greater uniformity and adhesion can be obtained when higher energy implantation occurs first.

REFERENCES

1. Wehner, G.K., *Appl. Phys.* **30**, 1762 (1959).
2. Aisenberg, S., and Stein, M., *Laser Induced Damage in Optical Materials*, NBS SP 620, pp. 313-318 (1980).
3. Wilson, R.G., and Brewer, G.R., *Ion Beams With Applications to Ion Implantation*, R.E. Krieger Publishing Co., Huntington, N.Y., 1979.
4. Snouse, T.W., and Haughney, L.C., in "Ion Beams With Applications to Ion Implantation" (Wilson, R.G., and Brewer, G.R., eds.), R.E. Krieger Publishing Co., Huntington, N.Y., 1979.
5. Vossen, J.L., and Kern, W., *Thin Film Processes*, Academic Press, New York, 1978.
6. Hirvonen, J.K., *Treatise on Materials Science and Technology*, Volume 18, *Ion Implantation*, Academic Press, New York, 1980.

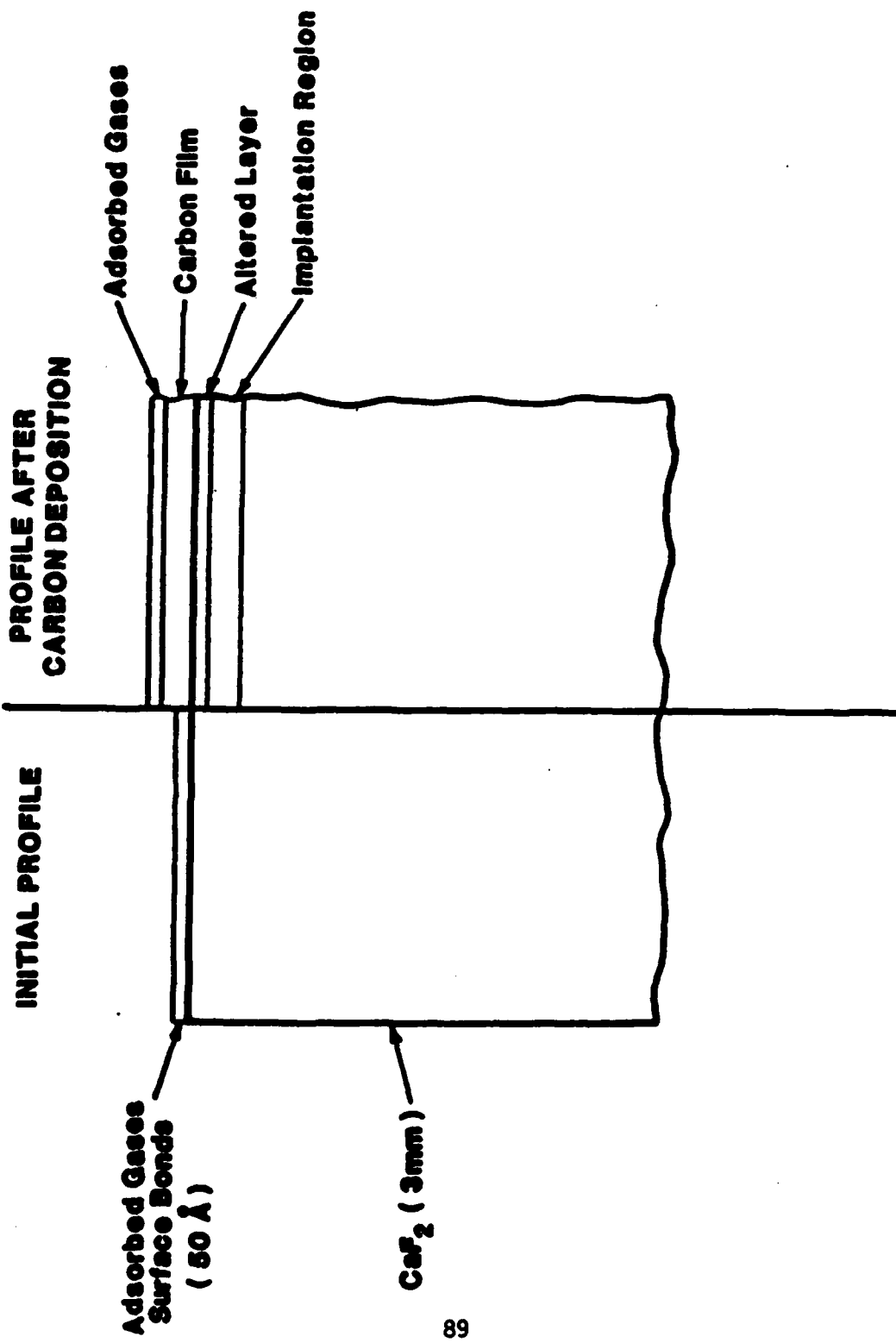


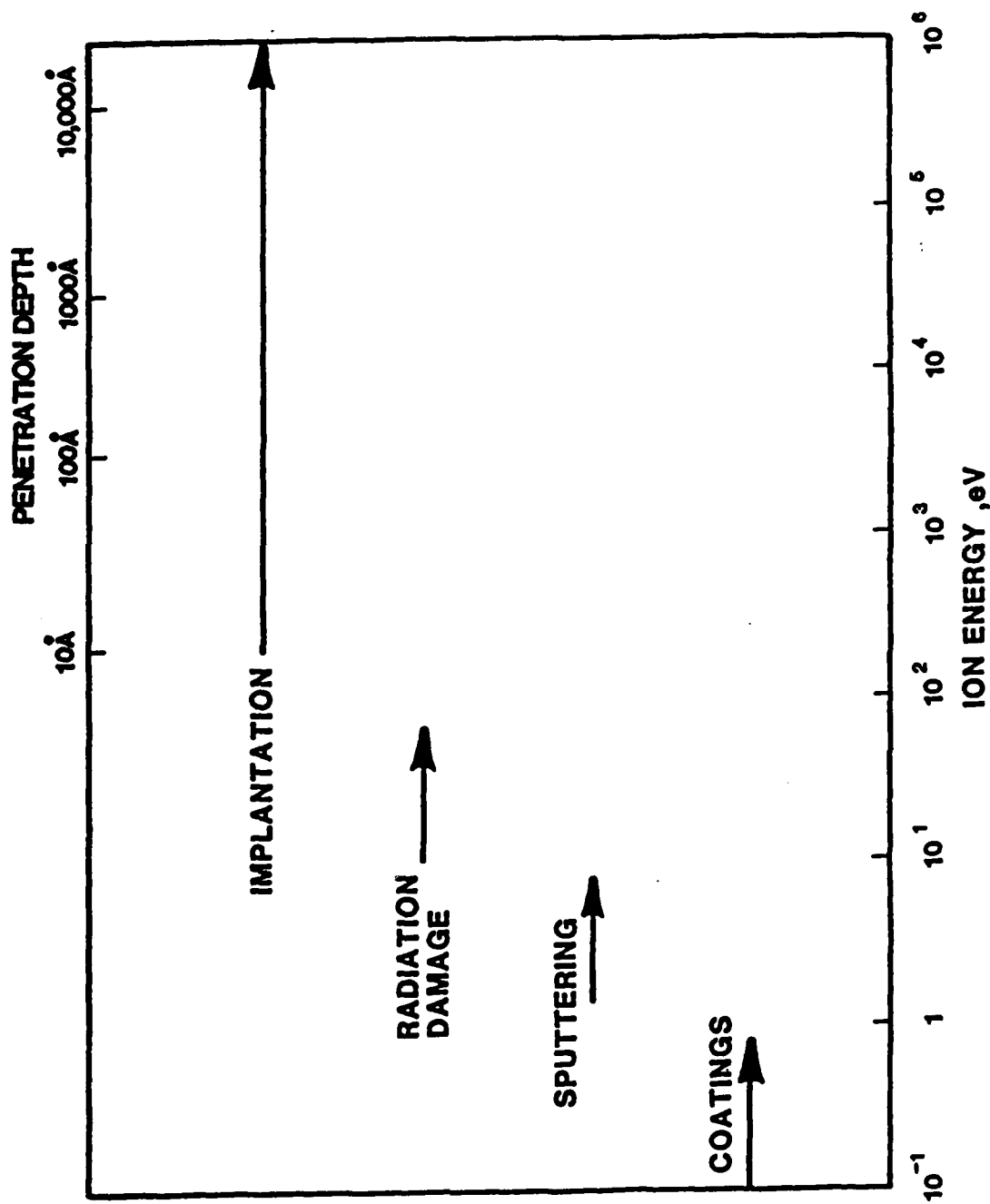
ION BEAM DEPOSITION PROCESS

DIAMOND-LIKE CARBON FILM PROPERTIES

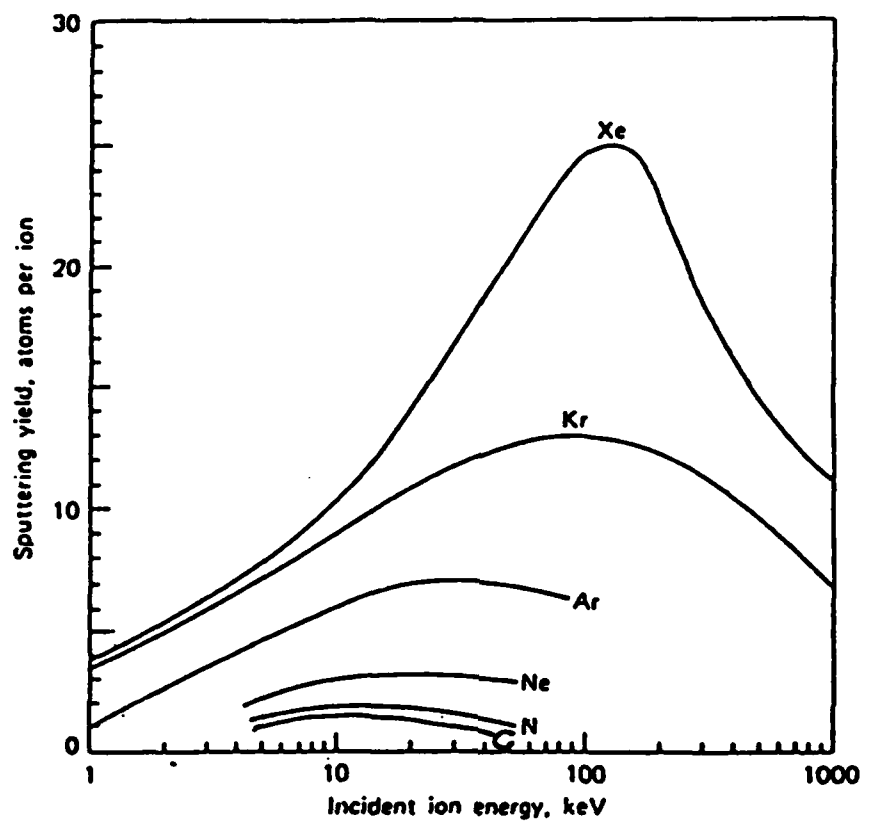
- **INSULATING (10^{11} - 10^{12} OHM - CM)**
- **GOOD ADHESION TO SUBSTRATE (5,000 PSI)**
- **DURABLE**
- **CHEMICALLY INERT TO ACIDS, BASES, AND SOLVENTS TESTED
(HF, HNO_3 , H_2SO_4 , HCOOH, BASES, ACETONE, ETC.)**
- **SMOOTH FILM**
- **DIAMOND-LIKE STRUCTURE X-ray DIFFRACTION LINES, TEM
50-100A SIZES**
- **BARRIER PROPERTIES**
- **LOW OPTICAL LOSS**

Surface Modification and Coating of CaF_2 Window

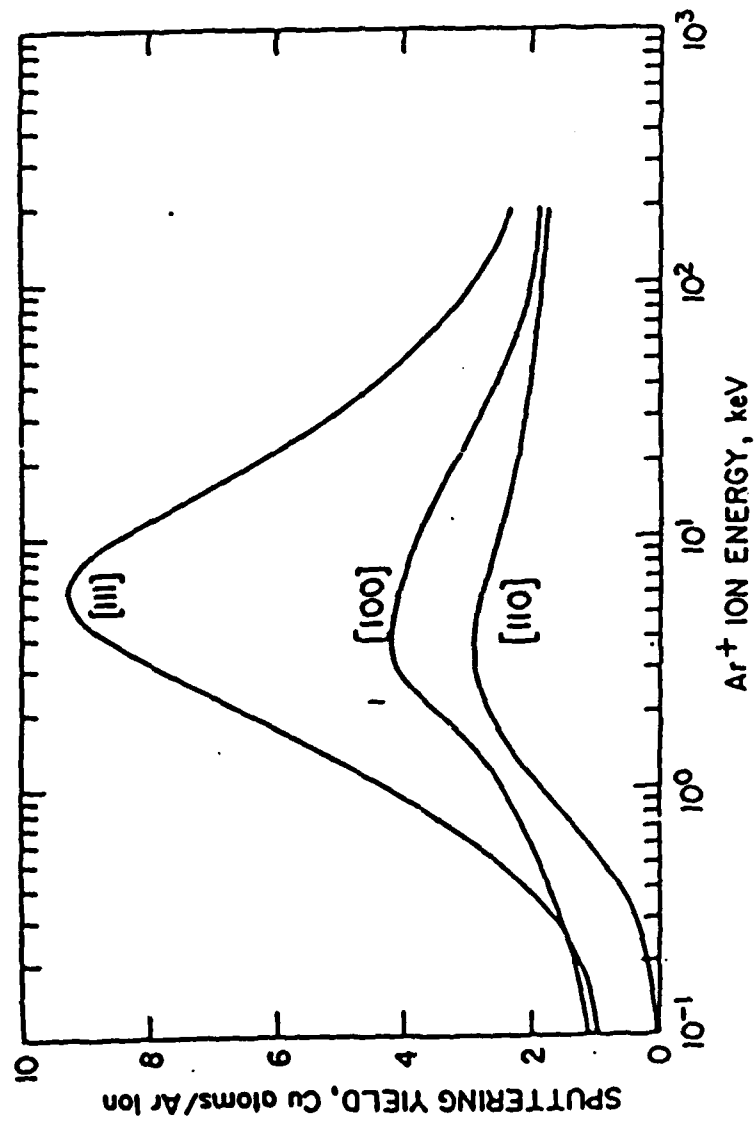




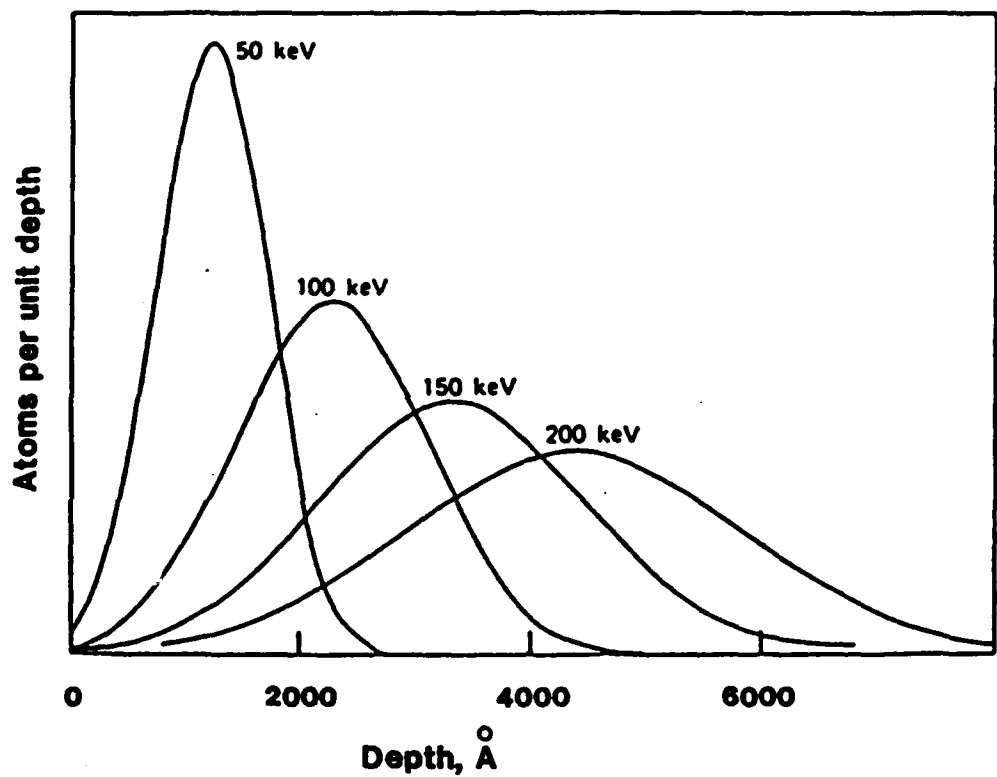
Ion Process vs Energy and Penetration Depth



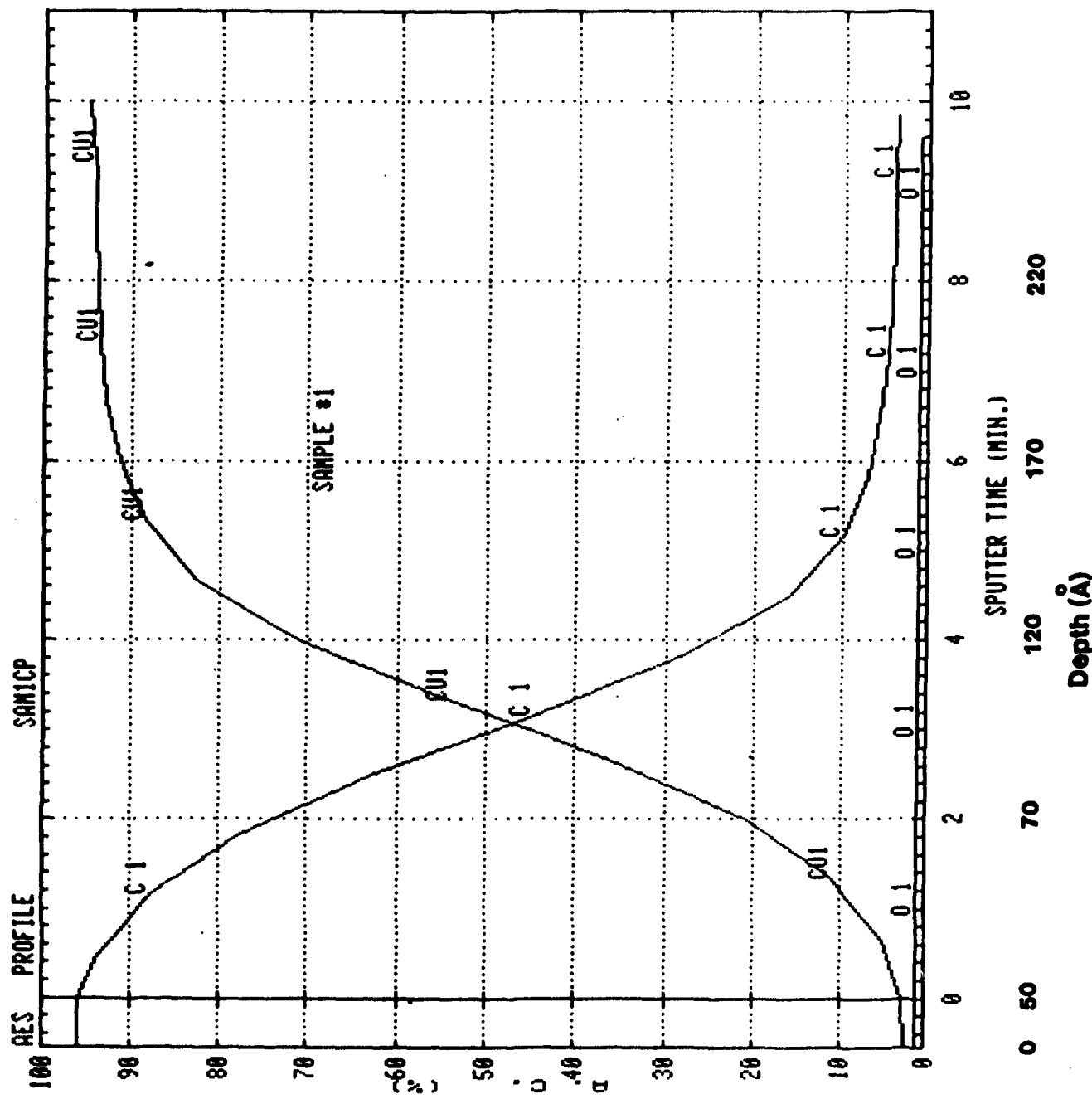
The sputtering yield S for polycrystalline copper as a function of incident ion energy or various ion species

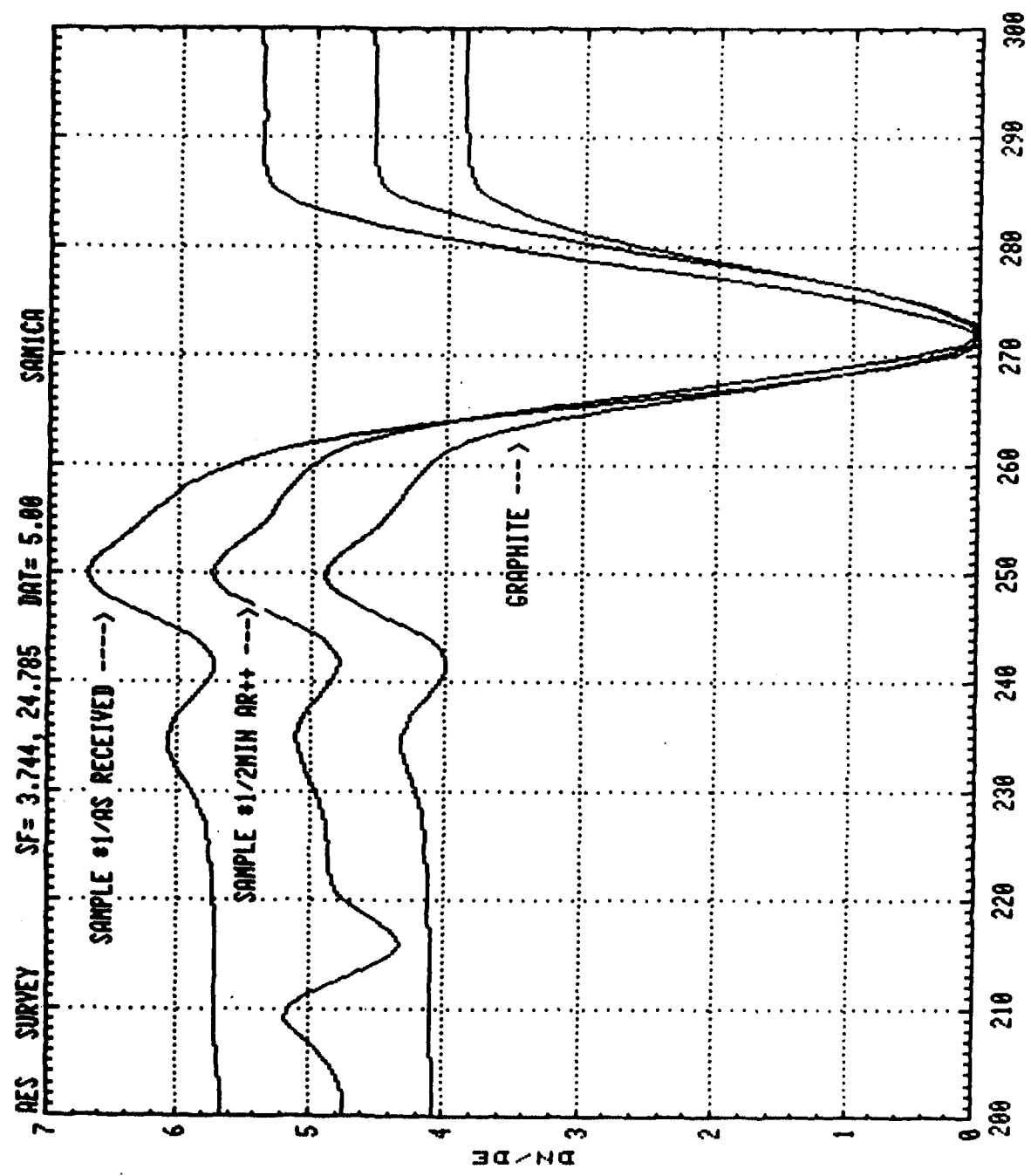


Sputtering yield of copper sputtered by argon ions, showing the effect of different crystal directions (from Snouss and Haughney 1966)

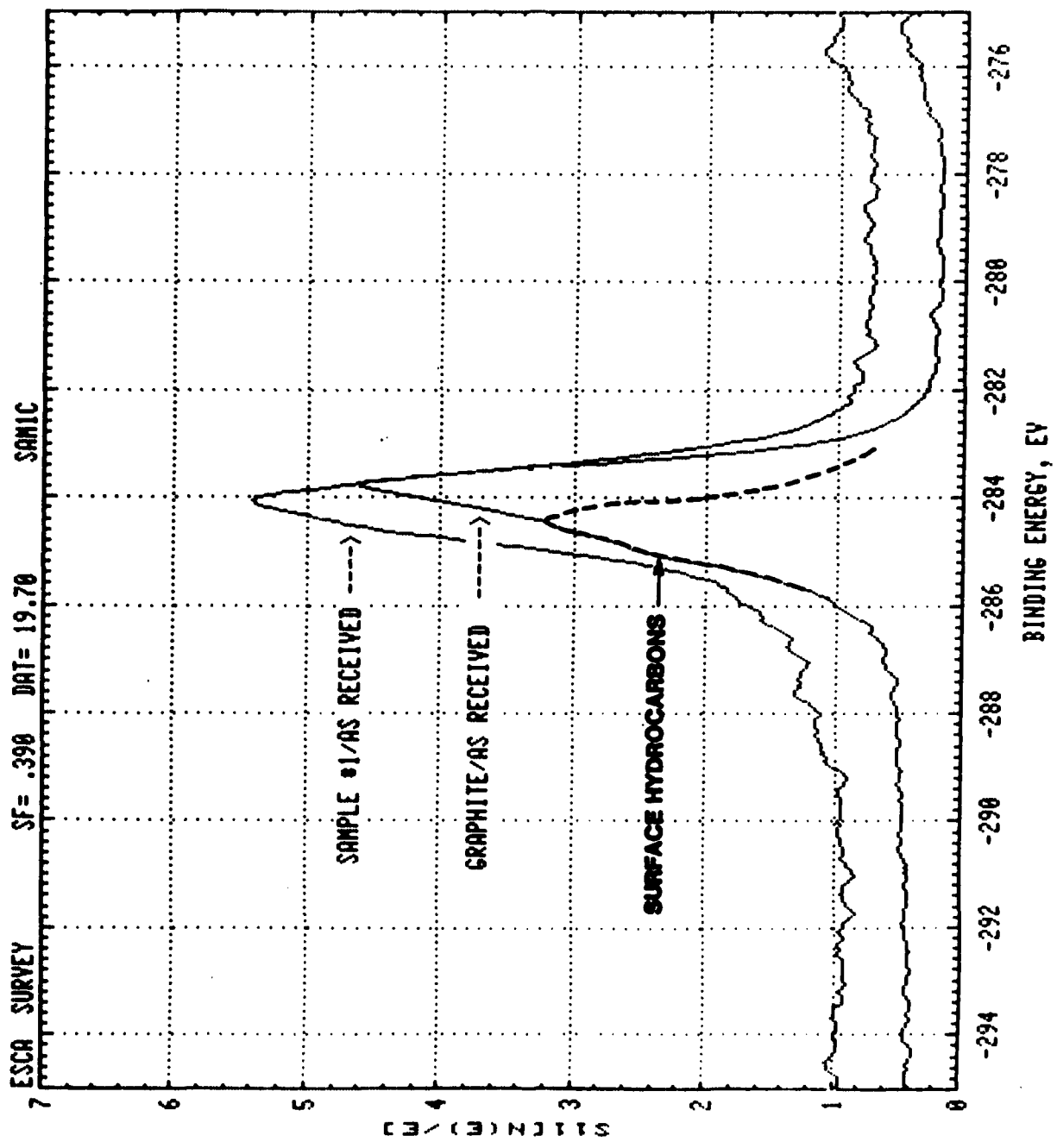


**Penetration Depth for C⁺ ions of various
incident energies in copper**

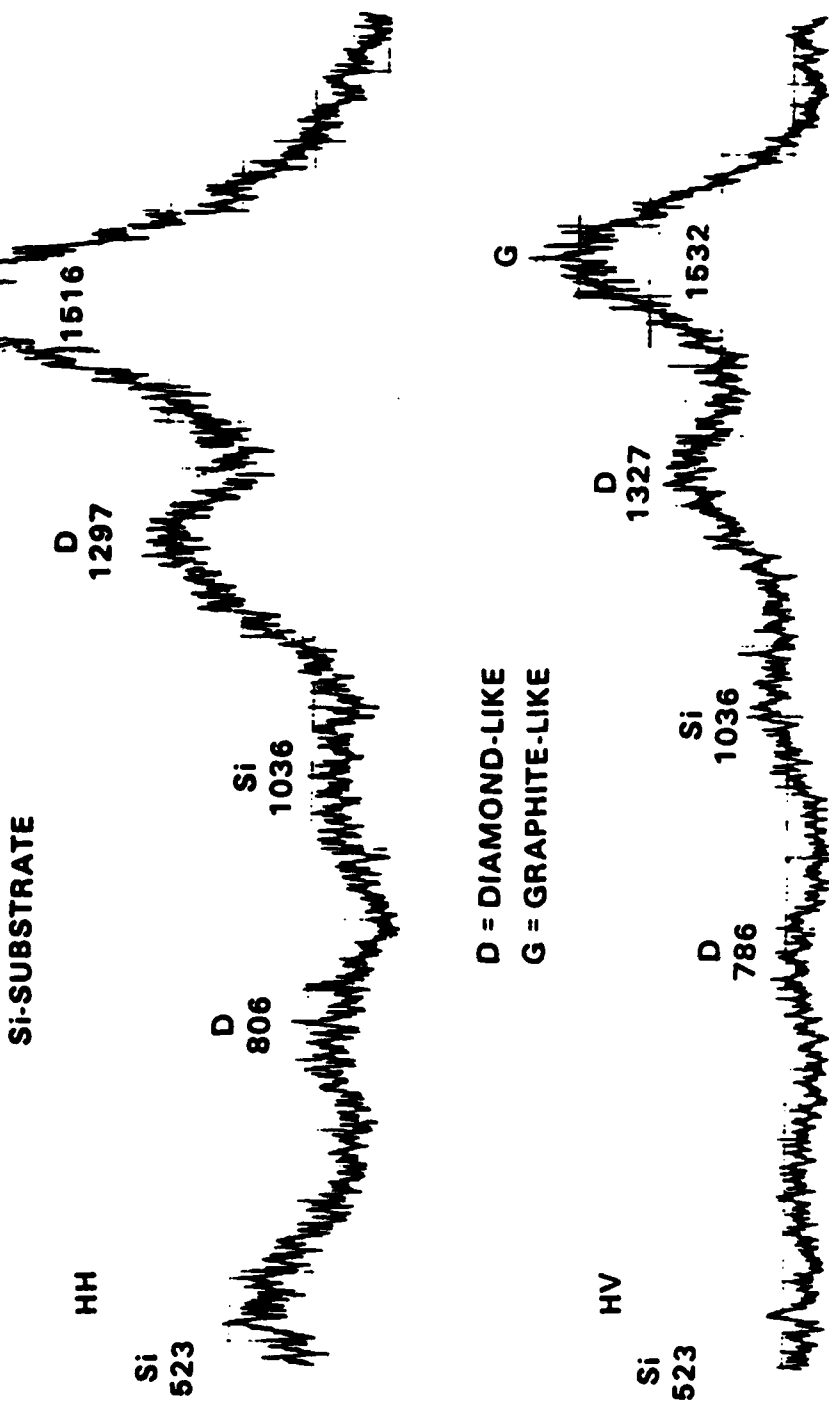




AES Survey Comparison



RAMAN SPECTRA OF DIAMOND-LIKE CARBON



8DMIA-81-6909

**ABSENCE OF IR ABSORPTION BANDS IN ION PLASMA DEPOSITED
CARBON FILMS ON CaF₂ WINDOWS**

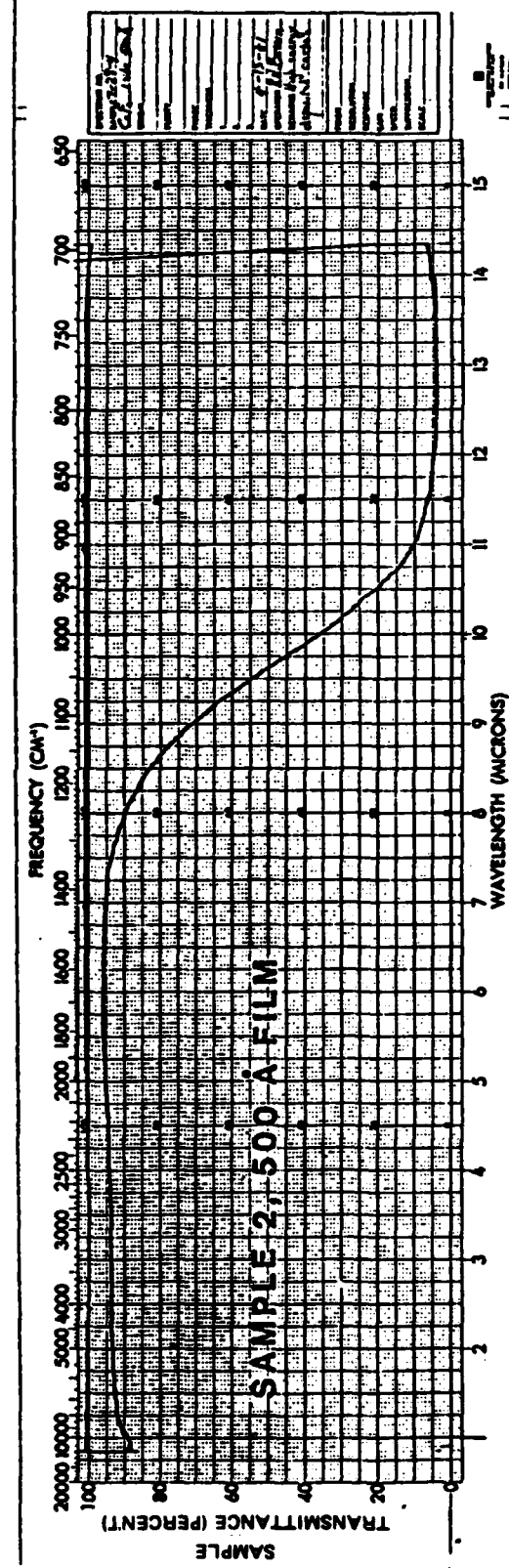
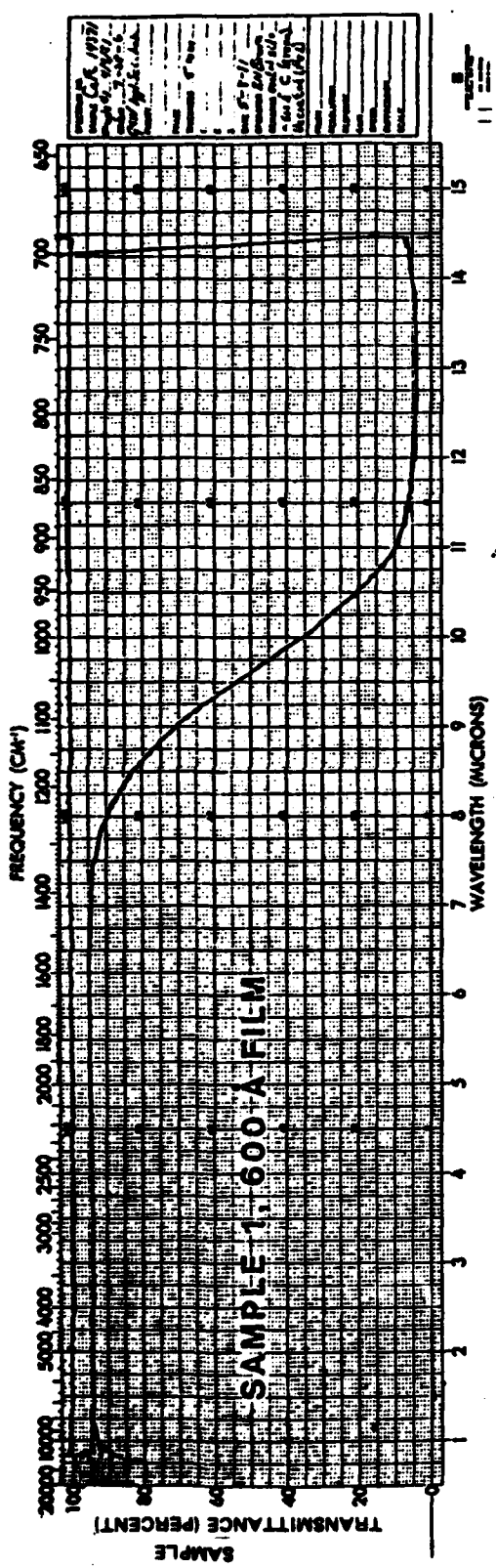




Figure 13. Diamond Turned Copper Surface with 0.1 Micron Carbon Coating

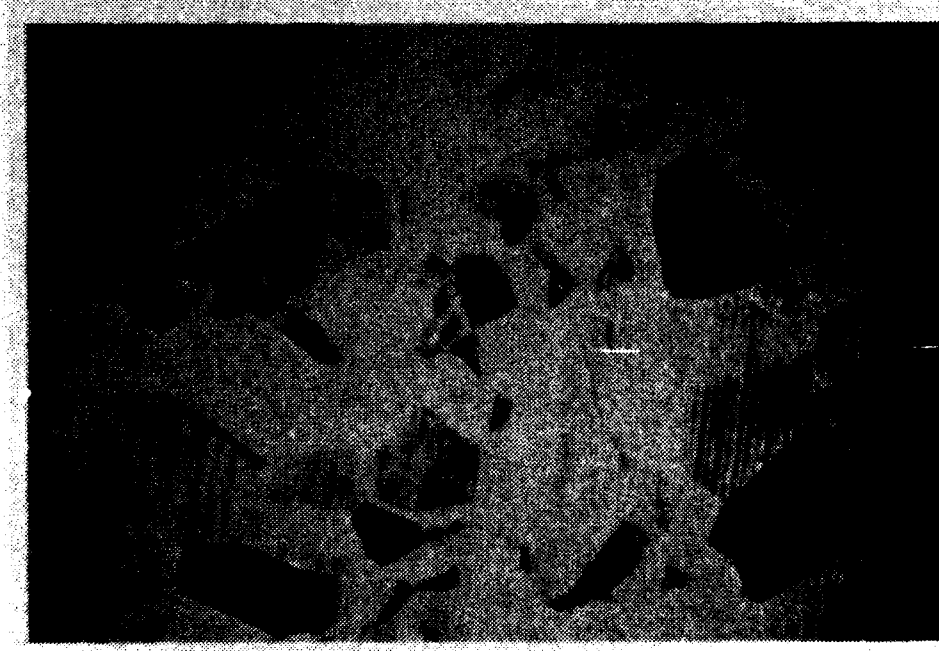
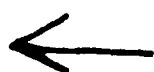


Figure 14. Same as Figure 13 with Carbon Ion Implantation Prior to Coating.



ADP002590



HARD CARBON FOR ENVIRONMENTAL
PROTECTION OF FLIR OPTICS

BY: A. Hendry*
L. Taub*
H. Gurev**

* OCLI - Hillend, Dunfermline, Fife, Scotland

** OCLI - 2789 Northpoint Parkway, Santa Rosa, California

INTRODUCTION

OCLI has been involved in the development of hard carbon, primarily as a protective optical coating. We have been working in conjunction with the Royal Signals Radar Establishment (RSRE) under license of the British Ministry of Defence. Coating development has been pursued both at Santa Rosa and at Hillend, and a production facility has been established at the latter site.

These results were obtained using an r.f. glow discharge plasma to "crack" a hydrocarbon gas to form the C-H compound which has been termed hard carbon.^{1, 2}

The properties of interest of films produced in this manner are the inherent high microhardness, optical transparency, the refractive index, and the general chemical inertness of the coating. The refractive index of the film is such that it acts as an efficient single layer antireflection coating on germanium when coated with the appropriate quarter wave optical thickness.

DEPOSITION PROCEDURE

The schematic diagram in Figure 1 shows the production system used to coat diamond-like carbon onto germanium and metal.

The coating chamber is initially evacuated by a diffusion pump to about 10^{-4} torr. The vacuum pump is then throttled from the reaction chamber by a butterfly valve located at the pump orifice to prevent backstreaming of the D.P. oil. Prior to the introduction of the hydrocarbon gas the substrates are pre-cleaned by sputter etching with argon gas. The hydrocarbon gas (99.0% n-butane in this case) to be decomposed is introduced through a needle valve in the side of the chamber and the r.f. power applied to the upper electrode holding the substrates. The r.f. power is tuned into the plasma by

Hard Carbon For Environmental Protection of FLIR Optics

matching the impedance of the plasma via an appropriate tuning network. Deposition thickness is controlled by monitoring reaction times.

Typical deposition parameters are listed in Appendix 1.

RESULTS

The performance of an extremely durable antireflection coating on germanium between 8 and 11.5 microns is described below. OCLI has coated up to 8 X 7½ inch windows.

(a) Spectral

When coated with a hard, durable carbon layer front surface and a high efficiency antireflection rear surface the performance obtained is shown in Figure 2. Transmittance of greater than 88% average from 8-11.5 microns is regularly achieved. The inherent absorption in the coating is about 4% at 10 microns wave length.

(b) Environmental

The coating has been found to be extremely durable, inert to chemical attack and abrasion resistant. It passes all the standard environmental tests.

Adhesion	MIL-M-13508C	para. 4.4.6
Abrasion	MIL-C-675A	para. 4.6.11
Humidity	MIL-C-675A	para. 4.6.9
Solubility	MIL-C-675A	para. 4.6.8
Salt Spray	MIL-C-675A	para. 6.6.10
Temperature Cycle	MIL-M-13508C	para. 4.4.4

Hard Carbon For Environmental Protection of FLIR Optics

The coating will also withstand windshield wiper action and chemical attack from acids. The wiper action is tested on an experimental rig called the "Grittington Abrasion Tester" developed at RSRE. This wipes the coating with a mixture of sand (sieved through an eight thousand mesh size) and water at a prescribed load and number of revolutions. We have found the coating to regularly withstand 5000 revolutions at 40 grams load. The optical degradation of the carbon coating compared with that of state-of-the-art thermal evaporation is shown in Figure 3.

Extensive Grittington Abrasion tests were carried out to determine effects of prolonged abrasion and increased loading on the sample. The thermally evaporated coating degrades for all loads applied whereas the carbon remains stable for loads up to 20 grams and only deteriorates after prolonged subjection at 40 grams. Slight pitting was noticed after prolonged exposure ($>100,000$ revolutions) at 10 and 20 grams load but no optical deterioration in performance was measured.

Microhardness measurements have been made with a Knoop indenter at 5 to 10 gram loads. Typical values of 1800-2000 KHN were measured for 10μ QWOT hard carbon films.

(c) Structural Analysis

The film microstructure is being studied by transmission electron microscopy. Initial results³ suggest that crystallites of a cubic diamond structure, approximately 500\AA in diameter, are embedded in an amorphous carbon matrix.

CONCLUSIONS

micrometers

A production process for coating hard carbon on germanium has been developed. Coating with a 10 μ m QWOT has been shown to provide an efficient single layer antireflection coating which has about 4% absorption at that wavelength.

This carbon coating has been found to have outstanding environmental resistance especially towards particulate abrasion as measured by the "Grittington Abrasion Test".

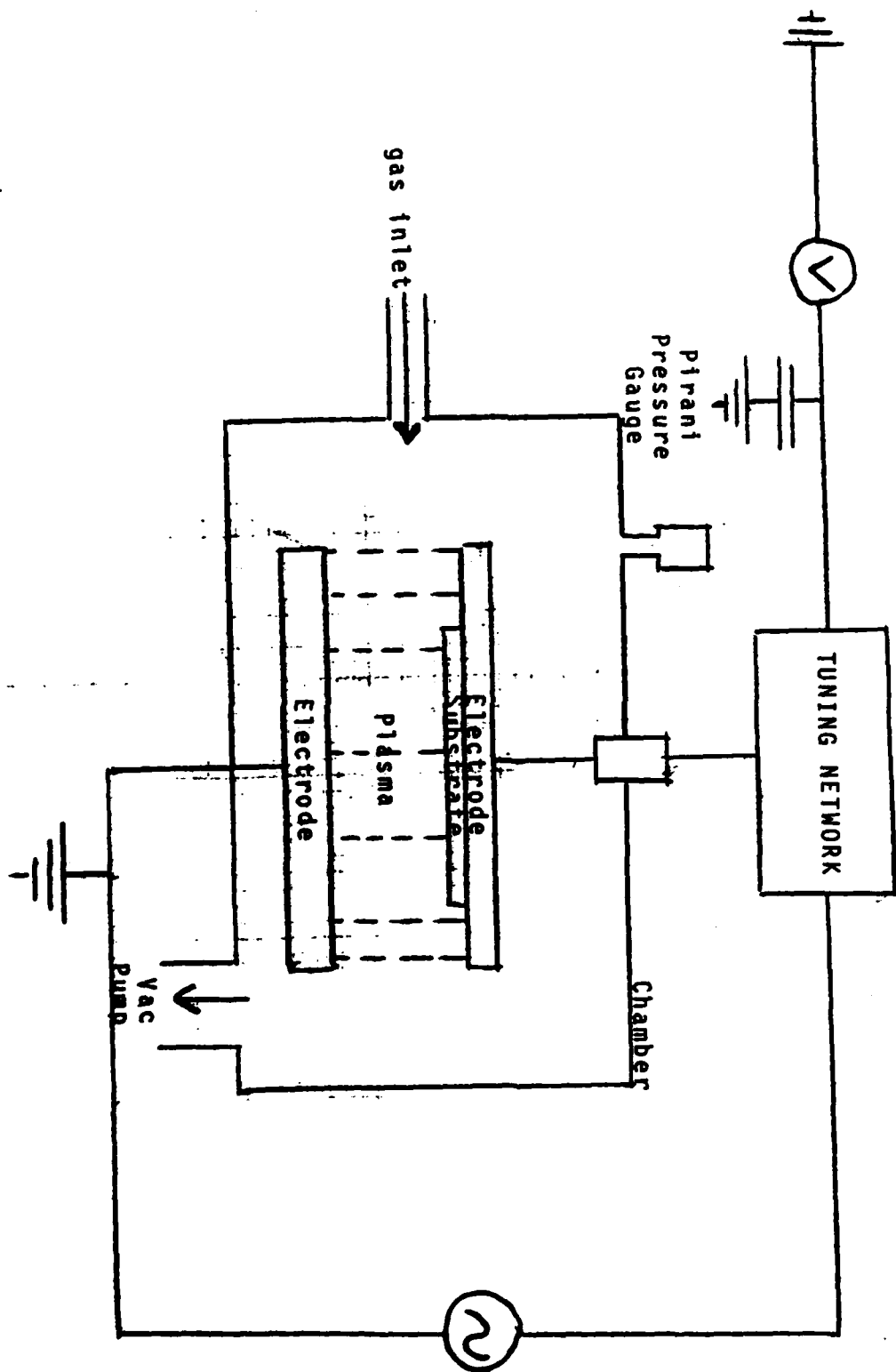
REFERENCES

- 1) L. Holland, Provisional UK Patent 33794, 1976
- 2) S. Berg and L.P. Andersson, Thin Solid Films, Vol. 58, pp. 117-120, 1979
- 3) R. G. Faulkner, University of Technology, Loughborough, Private Communication

APPENDIX 1. PROCESS PARAMETERS FOR SLAR ON GERMANIUM

DC. Bias Voltage	1300 Volts
R.F. Frequency	13.56 MHz
R.F. Power	750 Watts
Butane Pressure	20 microns
Deposition rate	1.5 μ m/hour
Electrode size	38cm diameter
Argon Pre-etch	10 minutes, 1300V, 5 microns 600 Watts.

Figure 1. Schematic Diagram of Production System



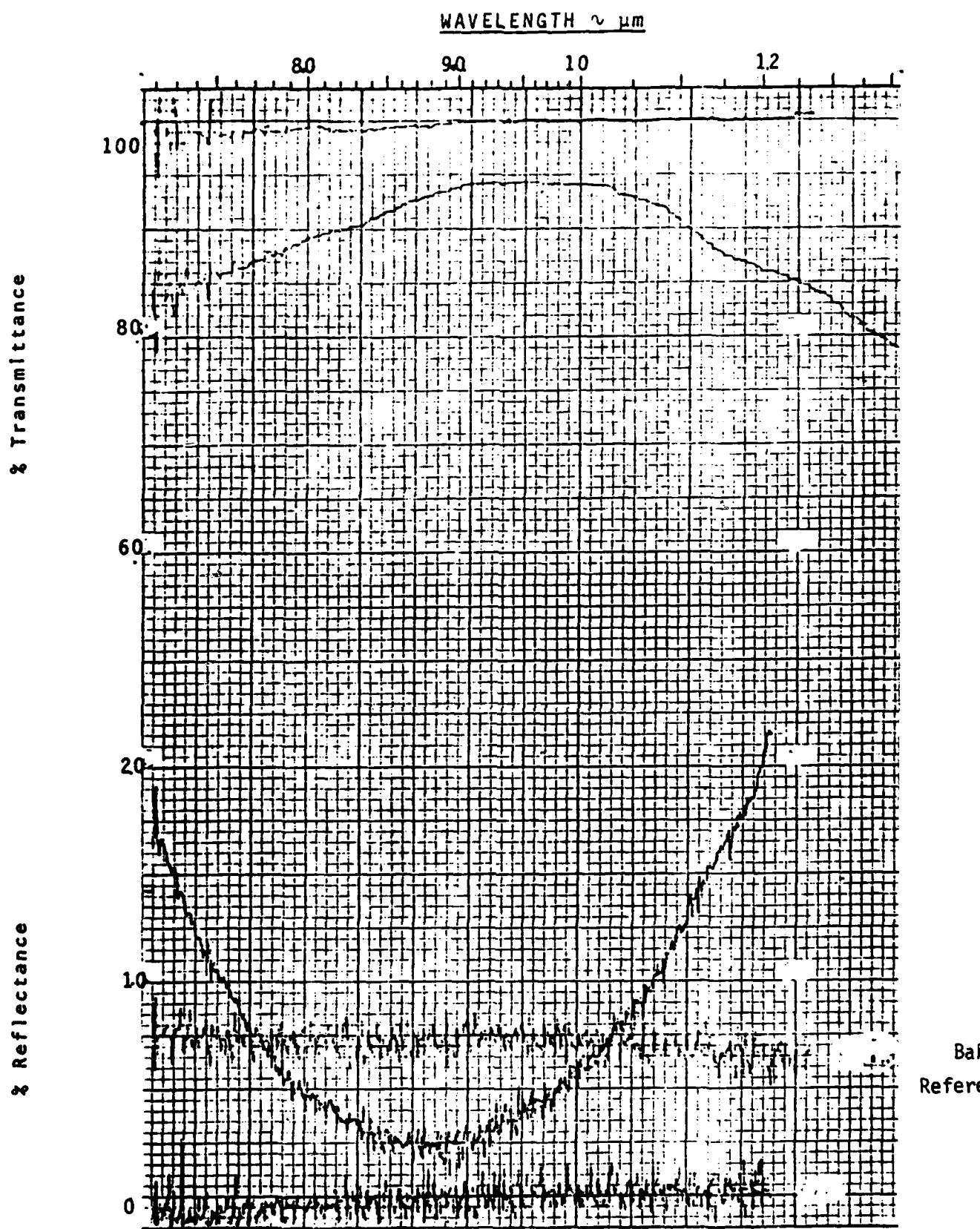


Figure 2. Reflectance and Transmittance of Germanium Coated with Hard Carbon and MLAR Surfaces

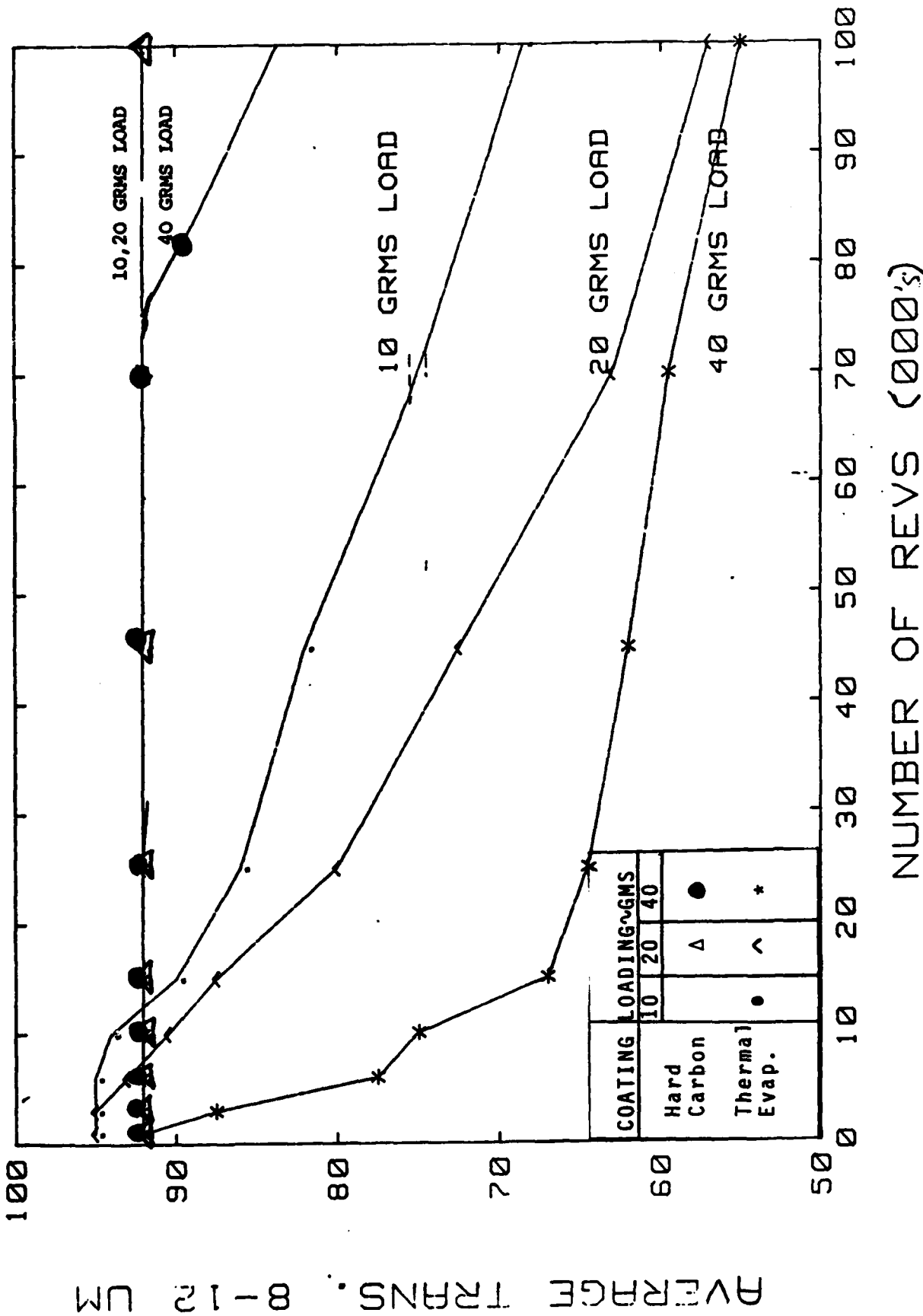


Figure 3. Optical Degradation of Carbon and Conventional Thermally Evaporated Coatings with Wiper Action

AD P002591

SOME ASPECTS OF THE GROWTH AND CHARACTERIZATION OF "DIAMOND LIKE" CARBON FILMS

John C. Angus
Chemical Engineering Department
Case Western Reserve University
Cleveland, Ohio 44106

I INTRODUCTION

This paper will cover three topics: (1) the general properties and categorization of types of carbon films, (2) a discussion of some factors that must influence the growth of the so called "diamond like films", 3) some results of characterization of "diamond like films" grown from low energy ion beams.

II PROPERTIES AND CATEGORIZATION OF CARBON FILMS

Carbon films have been grown by many varied techniques including: chemical vapor deposition from hydrocarbons, evaporation (carbon arc, resistance or electron beam), ion beams, RF and glow discharge in hydrocarbons and various types of sputtering processes. This is not the place for an exhaustive survey of the literature, but representative works are those listed in references 1-17. A good review of the literature prior to 1973 is given by McLintock and Orr (18).

Although properties of the films vary widely, they can be grouped, roughly, into those produced by low energy or thermal sources (chemical vapor deposition and evaporation) and those produced in a non-thermal, higher energy environment (ion beams, discharge processes and sputtering). The differences between these films are summarized in Table 1. In not all cases do the films fall neatly into one category or the other. For example, diffraction maxima at both 1.16 Å and 3.36 Å are sometimes found.

The most logical and simplest explanation for the differences is that the "thermal" films are dominated by sp^2 , trigonal bonds, whereas the films produced by non-thermal means are dominated by sp^3 , tetrahedral type bonding. It should be emphasized, however, that the structure of the films has not yet been unambiguously determined and that this conclusion is arrived at by somewhat indirect evidence. However, it is clear that the "thermal" films grow in an environment where the molecules and molecular

Table I
**Differences Between Amorphous Carbon Films Produced
 by Thermal and by Non-Thermal Means**

<u>"Thermal" Films^a</u>	<u>"Non-Thermal" Films^b</u>
electrically conductive, $\rho = 1$ to $10 \Omega \text{ cm}$	electrical insulators, $\rho = 10^{12}$ to $10^{16} \Omega \text{ cm}$
optical absorption coefficient at 5461 \AA , $\alpha \approx 10^5 \text{ cm}^{-1}$	optical absorption coefficient at 5461 \AA , $\alpha \approx 10^4 \text{ cm}^{-1}$
less resistance to chemical attack, $3\text{H}_2\text{SO}_4/1\text{HNO}_3$ at 80°C	very resistant to chemical attack, $3\text{H}_2\text{SO}_4/1\text{HNO}_3$ at 80°C
softer	harder
less dense (?)	more dense (?)
presence of $\sim 3.36 \text{ \AA}$ diffractive line	absence of $\sim 3.36 \text{ \AA}$ diffraction line presence of $\sim 1.16 \text{ \AA}$ diffraction line

- a. These include films produced by thermal decomposition of hydrocarbons and by evaporation of carbon.
- b. These include films produced from ion beams, glow or RF discharge and by dual beam ion sputtering.

fragments have relatively low energies, i.e., less than 1 eV. On the other hand, with non-thermal sources the surface is continually bombarded with energetic species, e.g., 10 to 500 eV depending on the process. It has been suggested that this unusual growth environment is likely responsible for the production of films dominated by sp^3 tetrahedral structures (7). Other structures, e.g., graphitic, olephinic and cumulene, are sputtered away by the high energy ions impinging on the surface.

Although Table 1 indicates that the films can be categorized into one of two groups, it is probable that there is a spectrum of structures ranging from those dominated by trigonal sp^2 bonding to those dominated by tetrahedral sp^3 bonding. There will be appreciable electronic conductivity when there is significant orbital overlap from the graphitic type structures.

It has been suggested that the so-called "diamond-like" carbon films be called i-carbon. This name was derived from the belief that ionized species were responsible for the formation of the films. It is perhaps more reasonable to categorize the films on the basis of the energies of the impacting species. The ions are important only in so far as they allow one to easily achieve non-thermal energies. A further discussion of these questions is given in the following section.

III FACTORS THAT INFLUENCE THE FORMATION OF DIAMOND-LIKE CARBON FILMS

Mass spectra of ionized carbon vapor show the presence of carbon clusters (19,20,21). For clusters of up to 9 carbon atoms, the odd number species are more abundant than the adjacent even number species. The first break in this regularity occurs at C_{10}^+ , whose abundance reaches a local maximum. After C_{10}^+ , there is a recurring periodic maximum with every 4 additional carbon atoms, i.e., at C_{14}^+ , C_{18}^+ , C_{22}^+ and C_{26}^+ .

The structure of these charged carbon nuclei has, unfortunately, not been unambiguously established. There does seem to be general agreement that the smaller species, C_9^+ and smaller, are linear chains. The maxima at C_{10}^+ , C_{14}^+ etc. may be caused by the presence of monocyclic or polycyclic ring structures. There is not evidence in the literature, or from our calculations which are reported in the next section, to support the view that these clusters have a diamond-like, tetrahedral structure. Moreover, since the bond energies are on the order of 1 to 2 eV, clusters with an energy of 100 eV would almost certainly break up upon impact with the surface.

We therefore believe that the mechanism of film formation on the surface has little memory of structures present in the primary ion beam.

In Table 2 the energies of various processes of importance to film growth are listed. It is very suggestive that the preferred ion energy, from 50 to 100 eV, is just above the sputtering threshold for carbon, just at the reported displacement energies and significantly below the energy where the sputter yield is greater than unity. These considerations indicate that both sputtering and deposition must take place simultaneously during film growth.

Table 2
Energies of Various Processes

<u>Item</u>	<u>Energy, eV</u>
Energy of incident carbon ion beam	50 to 150
Displacement energy of carbon atoms in diamond	80 (ref. 22)
Displacement energy of carbon atoms in graphite	25 (ref. 23)
Bond energy of diamond	3.60 (ref. 24)
Interplanar bond energy in graphite	0.43 (ref. 25)
Threshold energy for graphite sputtering	15 (ref. 23)

Simple calculations show that 100 eV carbon ions are stopped within 8 Å of the surface. The beam energies and beam currents that are employed correspond to very low energy fluxes but very large momentum fluxes. There is a very high rate of energy dissipation in the outermost surface layers being bombarded by the ion beam. In our experiments (see Section V) a current density of $300 \mu\text{A}/\text{cm}^2$ and an ion energy of 100 eV were employed. Therefore about 4×10^5 watts/cm³ are dissipated within 8 Å of the surface. It is within this outer layer that thermalization of the incident ion beam occurs and the momentum transfer takes place which leads to ejection of sputtered species.

IV MOLECULAR ORBITAL CALCULATIONS

Molecular orbital calculations using the atomic superposition electron delocalization (ASED) method (26-30) were performed for various carbon clusters. The results of some of the calculations are shown in Table 3. In all cases the linear configuration is the most stable. The charge state of the cluster

Table 3
Relative Energies of Isolated Carbon Clusters

<u>Species</u>	<u>Configuration</u>	<u>Energy, ev</u>	<u>Energy, kcal/gmole</u>
C_3	linear triangular	0 1.99	0 45.89
C_4	linear diamond square trigonal (pyramid) tetrahedral	0 4.30 5.15 unstable	0 99.3 118.9
C_4^{-1}	linear trigonal (pyramid) diamond square	0 4.98 5.74	0 114.8 132.3
C_4^{+1}	linear diamond square trigonal (pyramid)	0 3.33 3.75	0 76.4 86.6
C_5	linear pentagon capped pyramid tetrahedron trigonal bipyramide	0 6.39 10.28 11.78 15.25	0 147.4 236.6 271.6 351.7
C_5^{+1}	linear pentagon square capped pyramid tetrahedron trigonal bipyramide	0 5.25 9.49 10.44 unstable	0 121.2 218.8 240.9

Note: The parameters used for carbon and hydrogen are:

element	orbital	Slater exponent	ionization potential
carbon	s	1.658	-20.00 eV
	p	1.618	-11.26 eV
hydrogen	s	1.200	-13.60 eV

did not change this conclusion. These results are in general agreement with the conclusions of prior workers and also support the view that positively charged clusters do not prefer a tetrahedral arrangement.

In addition to the study of isolated clusters described above, carbon nuclei bonded to a model diamond substrate were also considered. The model of the diamond surface is shown in Figure 1. Carbon atoms were brought up to this surface and the preferred orientation of bonded clusters was obtained. Figure 2 shows the preferred orientation for a single adatom. Not surprisingly, the preferred position is directly above one of the vacant lattice sites on the model diamond surface. The bond length of 1.61 Å is longer than the diamond bond length of 1.54 Å and the bond energy of 3.15 eV is less than the diamond bond energy of 3.6 eV. In Figure 3 the most stable attached dimer is shown. Note that the dimer is bonded more weakly to the surface than the monomer shown in Figure 2. The bond length to the surface has increased to 1.87 Å and the bond energy has been reduced to 2.11 eV.

Several four atom nuclei are shown in Figures 4, 5 and 6. The four atom configuration shown in Figure 4 is less stable than the "bridge and sentry" configuration of Figure 5. In turn, the bridged configuration is less stable than four atom "tent" configuration shown in Figure 6.

The results of the molecular orbital calculations tend to indicate that: 1) positively charged ions are not directly responsible for the formation of diamond-like films and 2) non sp^3 structures are bonded less strongly to diamond surfaces and therefore may be more susceptible to sputtering.

There are a number of significant unanswered questions. First, the mechanism for the nucleation of the precursor sp^3 bonded clusters is not understood. It may involve the presence of negatively charged carbanions or residual hydrogen on the surface, both of which will promote sp^3 bonding. (Because of the details of the calculational procedure some uncertainty of the structure of negatively charged species remains.) Secondly, the condensation of acetylenic species to form graphitic type nuclei was not explicitly considered in these preliminary calculations.

V SOME PROPERTIES OF FILMS GROWN FROM LOW ENERGY ION BEAMS

Detailed characterization of "diamond-like" carbon films produced by low energy ion beam deposition was performed (15,16,17). The films were grown by Mr. Michael J. Mirtich of the NASA Lewis Laboratories, Cleveland, Ohio.

The films were grown from an ion beam of 100 eV energy derived from a CH_4/Ar discharge. The current density was approximately $300 \mu\text{A}/\text{cm}^2$ and the growth rates were approximately $0.3 \mu\text{m}/\text{hour}$. The ion source is a converted ion thruster.

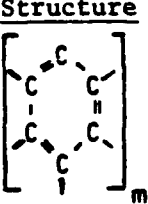
General Observations. Films were grown on silica and silicon substrates. Optical absorption measurements on the former showed increasing absorption towards the blue end of the spectrum giving the films a characteristic yellowish color in transmission. The films on silicon substrates gave beautiful interference colors. Electron microscopy showed the films to be essentially featureless. Repeated electron diffraction experiments showed no evidence of crystallinity in any of the films. These results are described in more detail in reference 15, 16 and 17.

The resistance of the films to a reagent comprised of $3\text{H}_2\text{SO}_4/1\text{HNO}_3$ by volume at 80°C is a particularly useful test. Graphitic and hydrocarbon based polymers are readily attacked by this reagent while diamond-like carbon films are not. The reagent does not attack macroscopic diamond crystals and attacks glassy carbon slowly. The transparent ion beam deposited films were untouched by this reagent; however, in some films there was a small dark patch which was removed.

The presence of the diffraction line at 1.16 \AA in diamond-like films is also quite characteristic. By analogy to studies on amorphous germanium (31), it may be inferred that this diffraction maximum is a composite of the reflections from the (311) and (220) planes which occur at 1.07 and 1.26 \AA respectively. More work, however, is required to confirm this speculation.

Density Measurements. Density measurements are a very important and somewhat neglected characterization method. Carbon has a limited number of bonding schemes available to it. Therefore, confirmation that a film is essentially all carbon plus a density measurement is very instructive. A summary of reported densities for carbon with various types of bonding is shown in Table 4. Densities significantly greater than that of graphite would be strong, but not conclusive, evidence for the presence of tetrahedral,

Table 4
Densities of Carbon Phases

<u>Phase</u>	<u>Structure</u>	<u>Density, g/cm³</u>
Graphite		2.26
Diamond		3.515
"Amorphous Carbon"		1.5-2.0
Polyyne	{C≡C-C≡C} _m	1.97 (ref. 32)
Polycumulene	{C=C=C=C} _m	2.25 (ref. 32)
Chaoite	hexagonal	3.43 (ref. 33 and 34)
Carbon VI	Hexagonal	>2.9 (ref. 35)

sp^3 , bonding. Note in this connection that there are many more possible crystal structures than there are bond types. For example, a carbon crystal comprised entirely of sp^3 tetrahedral bonding can be either the normal cubic diamond or the so-called hexagonal diamond. These two modifications are analogous to the zinc blende and wurtzite structures of zinc sulfide. In cubic diamond the (111) layers are stacked in an abcabc sequence; in hexagonal diamond the equivalent planes are packed in an ababab sequence. Many other (hypothetical) structures can be imagined by different sequences. In all cases, however, the nearest neighbor environment of a carbon atom is identical, i.e., it is surrounded by four tetrahedrally disposed atoms.

The densities of our ion deposited films were approximately 1.75 g/cm^3 . These densities were measured by direct measurement of mass, area and thickness of the films. However, in most situations it is much simpler to remove the film from the substrate and use a sink/float technique for determining the density.

Auger Spectroscopy. Auger spectroscopy was used both for elemental analysis and as a means for distinguishing between various forms of carbon. In Figure 7 the line shapes of the carbon Auger signal at 275 eV are shown for single crystal graphite, ion deposited carbon film and natural diamond. The line shape of the carbon film lies somewhere in between those of graphite and diamond. The pronounced shoulder at about 250 eV present in graphite is much smaller in the ion deposited film, but is missing entirely in the diamond. These spectra were taken on the "as-received" surfaces without any annealing in vacuum and without any sputtering.

Secondary Ion Mass Spectroscopy. SIMS spectra from diamond, an ion beam deposited film and a film deposited by RF deposition are shown in Figures 8, 9 and 10 respectively. (The latter film was grown by Mr. Stan Domitz of the NASA Lewis Laboratories.) The SIMS spectrum from the (111) surface of natural diamond is quite clean, with only a carbon peak at 12 atomic mass units and a smaller peak at 28 atomic mass units, which arises from silicon impurity. The spectrum from the ion beam deposited film shown in Figure 9 shows, in addition to the strong peak at 12 atomic mass units, a strong peak at 14 atomic mass units, which can be associated with CH_2 . In addition, a hydrogen peak at 1 atomic mass units is visible as well as a rich structure of peaks ranging from 23 to 29 atomic mass units. The peaks at 23 and 28 atomic mass units may arise from sodium and silicon respectively; however,

the other peaks in this range can be attributed to hydrocarbon fragments containing 2 carbon atoms. The spectrum of the carbon film deposited by RF discharge in a hydrocarbon, shown in Figure 10, is much simpler than the spectrum derived from the ion deposited films. The hydrogen peak at 1 atomic mass unit, the carbon peak at 12 and weaker hydrocarbon peaks at 13 and 14 atomic mass units are visible in addition to the impurity peaks for sodium, silicon and potassium. This might indicate that the film derived from the RF discharge contains less hydrogen than the ion beam deposited film; however, much more work would be required to confirm this speculation.

In Figure 11 the intensity of the SIMS signal at 28 atomic mass units is plotted versus sputtering time. The concentration of silicon increases at greater depths in the film. This silicon may have arisen from the substrate.

Infrared Spectroscopy. The ion deposited films were studied by Fourier Transform Infrared Spectroscopy. This technique is particularly useful in identifying functional groups that may be present in the carbon films. The first spectrum, shown in Figure 12 shows the infrared absorption spectrum of the uncoated silicon substrate. Figure 13 shows the spectrum of the same silicon substrate after one side was covered with an ion beam deposited carbon film. Note first that the large broad feature at approximately 3200 cm^{-1} appears at about half the intensity as in the uncoated substrate. This band arises from Si-O vibrations and, presumably, the carbon ion beam removed this film from the one side of the substrate. The broad double peak at approximately 2850 cm^{-1} which appears in Figure 13 arises from the carbon-hydrogen stretching modes. Additional structure arising from carbon-carbon skeletal modes also appears in Figure 13.

The spectrum of a carbon film deposited on KBr is shown in Figure 14. The carbon-hydrogen stretching modes are clearly visible near 2900 cm^{-1} . A strong feature at 1560 cm^{-1} , which can be tentatively signed to double bonded carbon, is also visible in Figure 14. Finally a detailed expanded spectrum in the region of the carbon-hydrogen stretching frequencies is shown in Figure 15. The double peak 2850 and 2916 cm^{-1} is characteristic of the symmetric and assymmetric stretching modes respectively of the methylene group.

A quantitative measure of the amount of methylenic hydrogen in the films was made by comparing the observed absorbances with a set of standards. Details of this procedure are given in reference (15) and (17). The results indicate that the atomic ratio of carbon to methylenic hydrogen is in the range from 10 to 50, with a most probable value of about 25.

The infrared results also indicate the presence of carbon-carbon double bonds and the absence of cumulene, polyyne, triply bonded carbon and aromatic hydrogen.

VI SUMMARY

Diamond-like films are at one end of a spectrum of films with progressively decreasing amounts of trigonal sp^2 bonding. A possible structure is an amorphous network with many areas of sp^3 bonding together with methylene, double bonded carbon and other linkages.

Diamond-like films are probably formed by preferential sputtering away of non- sp^3 structures by high energy impacts during film growth.

Positively charged carbon clusters do not appear to prefer a tetrahedral configuration.

Negatively charged carbon clusters or hydrogen on the surface may promote tetrahedral, sp^3 , bonding.

Resistance to chemical reagents, elemental analysis and density measurements are simple but powerful tools for characterization of carbon films.

Because of the wide variety of possible crystal structures which are consistent with sp^3 tetrahedral bonding, structural studies alone are not sufficient to characterize diamond-like carbon films. Particular attention should be paid to the chemical functional groups that are present in the films as well.

VII ACKNOWLEDGEMENTS

The carbon films were grown by Mr. Michael J. Mirtich. Professor Al Anderson and Mr. Jeffrey Segall performed the molecular orbital calculations. Others who contributed to the work were Mr. Bruce Banks, Mr. Stan Domitz, Dr. Ira T. Myers and Mr. Thomas Riley. The research was supported by the NASA Lewis Research Center, Cleveland, Ohio.

VIII REFERENCES

1. H. Schmellenmeier, Z. Phys. Chem. 205 (1956) 349.
2. S. Aisenberg and R. Chabot, J. Appl. Phys. 42 (1971) 2953-58.
3. S. Aisenberg and R.W. Chabot, J. Vac. Sc. and Tech. 10 (1973) 104.
4. L. Holland and S.M. Ojha, Thin Solid Films 38 (1976) L17-L19.
5. S.M. Ojha and L. Holland, Thin Solid Films 40 (1977) L31-L32.
6. L. Holland and S.M. Ojha, Thin Solid Films 48 (1978) L21-L23.
7. E.G. Spencer, P.H. Schmidt, D.C. Joy and F.J. Snasalone, Appl. Phys. Lett. 29 (1976) 118-20.
8. D.C. Joy, E.G. Spencer, P.H. Schmidt and F.J. Snasalone, Thirty-fourth Annual Electron Microscope Society of American Meeting, Aug. 1976, p. 646-47.
9. H. Vora and T.J. Moravec, J. Appl. Phys. 52 (1981) 6151-57.
10. T.J. Moravec, Thin Solid Films 70 (1980) L9-L10.
11. L.P. Anderson, S. Berg, H. Norstrom, R. Olaison and S. Towta, Thin Solid Films 63 (1979) 155-60.
12. S. Berg and L.P. Anderson, Thin Solid Films 58 (1979) 117-120.
13. Chr. Weissmantl, K. Bewilogua, S. Schurer, K. Breuer, and H. Zscheile, Thin Solid Films 61 (1979) L1-L4.
14. Chr. Weissmantl, C. Schurer, F. Frohlich, P. Grau and H. Lehman, Thin Solid Films 61 (1979) L5-L7.
15. J. C. Angus, NASA Contractors Report, NASA CR 165493, December 22, 1981.
16. J. C. Angus, NASA Contractors Report, NASA CR 165588, February 22, 1982.
17. J.C. Angus, M.J. Mirtich and E.G. Wintucky, in "Metastable Materials Formation by Ion Implantation", S.T. Picraux and W.J. Choyke eds., Elsevier, N.Y. 1982.
18. I.S. McLintock and J.C. Orr, "Evaporated Carbon Films", in Chemistry and Physics of Carbon, Vol. 11, P.L. Walker and P.A. Thrower, eds., p. 243, Marcel Dekker, N.Y., 1973.
19. E. Dornenburg and H. Hintenberger, Z. Naturforsch 14a (1959) 765-67.
20. E. Dornenburg, H. Hintenberger and J. Franzen, Z. Naturforsch 16a (1961) 532-34.
21. W.L. Baun and D.W. Fischer, J. Chem. Phys. 35 (1961) 1518-19.

22. E.A. Burgemeister, C.A.J. Ammerlaan and G. Davies, Diamond Conference Proceedings, Bristol, 1980, page 23.
23. G. Carter and J.S. Colligon, "Ion Bombardment of Solids", American Elsevier, N.Y., 1968, page 214.
24. L. Pauling, "The Nature of the Chemical Bond", Cornell University Press, 1960, page 85.
25. A.R. Ubbelohde and R. A. Lewis, "Graphite and Its Crystal Compounds", Clarendon Press, Oxford, 1960, page 71.
26. A.B. Anderson, J. Chem. Phys. 60 (1974) 2477.
27. A.B. Anderson, J. Chem. Phys. 62 (1975) 1187.
28. A.B. Anderson, J. Chem. Phys. 63 (1975) 4430.
29. A.B. Anderson, J. Am. Chem. Soc. 100 (1978) 1153.
30. A.B. Anderson and G. Fitzgerald, Inorg. Chem. 20 (1981) 3288.
31. J.J. Hauser and A. Staudinger, Phys. Rev. B 8(3), (1973) 607-15.
32. A.M. Sladkov, V.I. Kasatochkin, P. Yu. Kudryavtsev and V.V. Korshak, Izv. Akad. Nauk SSSR, Ser. Khim. 12 (1968) 2560 (English translation).
33. A. Ed Goresy and G. Donnay, Science 161 (1968) 363-64.
34. A.G. Whittaker and P.L. Kintner, Science 165 (1969) 589-91.
35. A.G. Whittaker and G.M. Wolten, Science 178 (1972) 54-56.

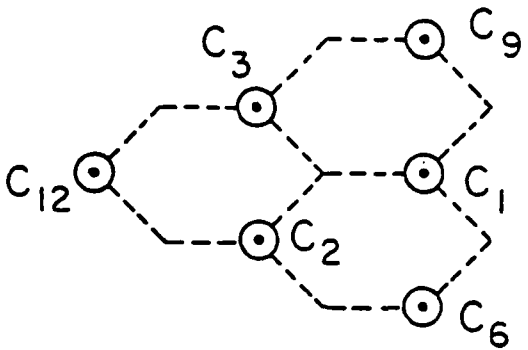


Figure 1 Surface model made up from three fused hexane rings, $C_{13}H_{16}$. Circles show available surface bonding sites. Bond angles are 109.47° . Bond distances are: C-H 1.09 \AA , C-C 1.54 \AA .

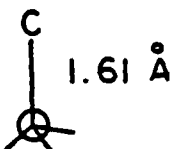


Figure 2 One carbon bonded to surface. Bond energy is 3.15 eV.

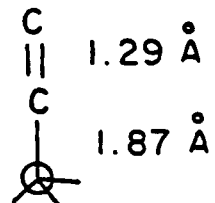


Figure 3 A C_2 nucleus bonded to surface with energy of 2.11 eV.

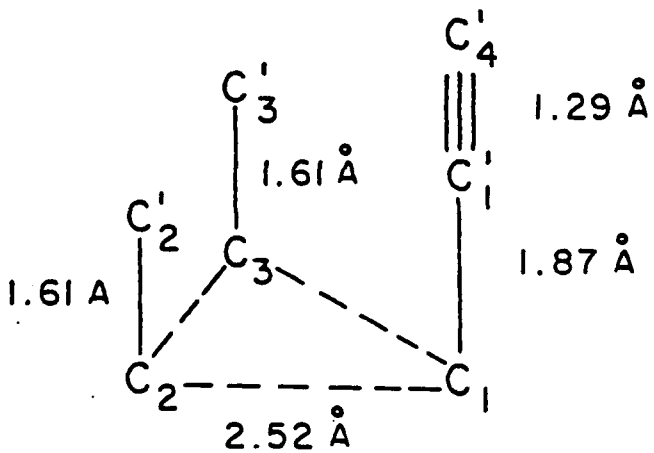


Figure 4 Less stable configuration of four carbon atoms on $C_{13}H_{16}$ surface model.

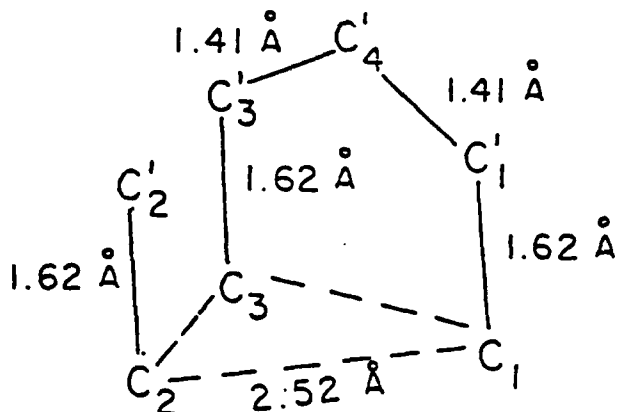


Figure 5 The "bridge and sentry" configuration of four carbon atoms on $C_{13}H_{16}$ surface model. Favored over configuration in Figure 4 by 0.48 eV. Moving C_4' towards C_2' will cause a four atom diamond nucleus of hexagonal symmetry to be formed. The $C_4'-C_1'-C_1$ angle is 109.47° ; The $C_1'-C_4'-C_3$ angle is 140° .

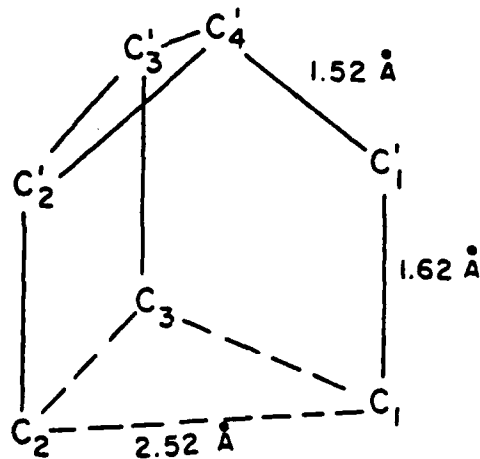


Figure 6 The four atom "tent" configuration on a $C_{13}H_{16}$ nucleus. Favored over the "bridge and sentry" configuration by 0.31 eV and 0.79 eV over the configuration in Figure 4.

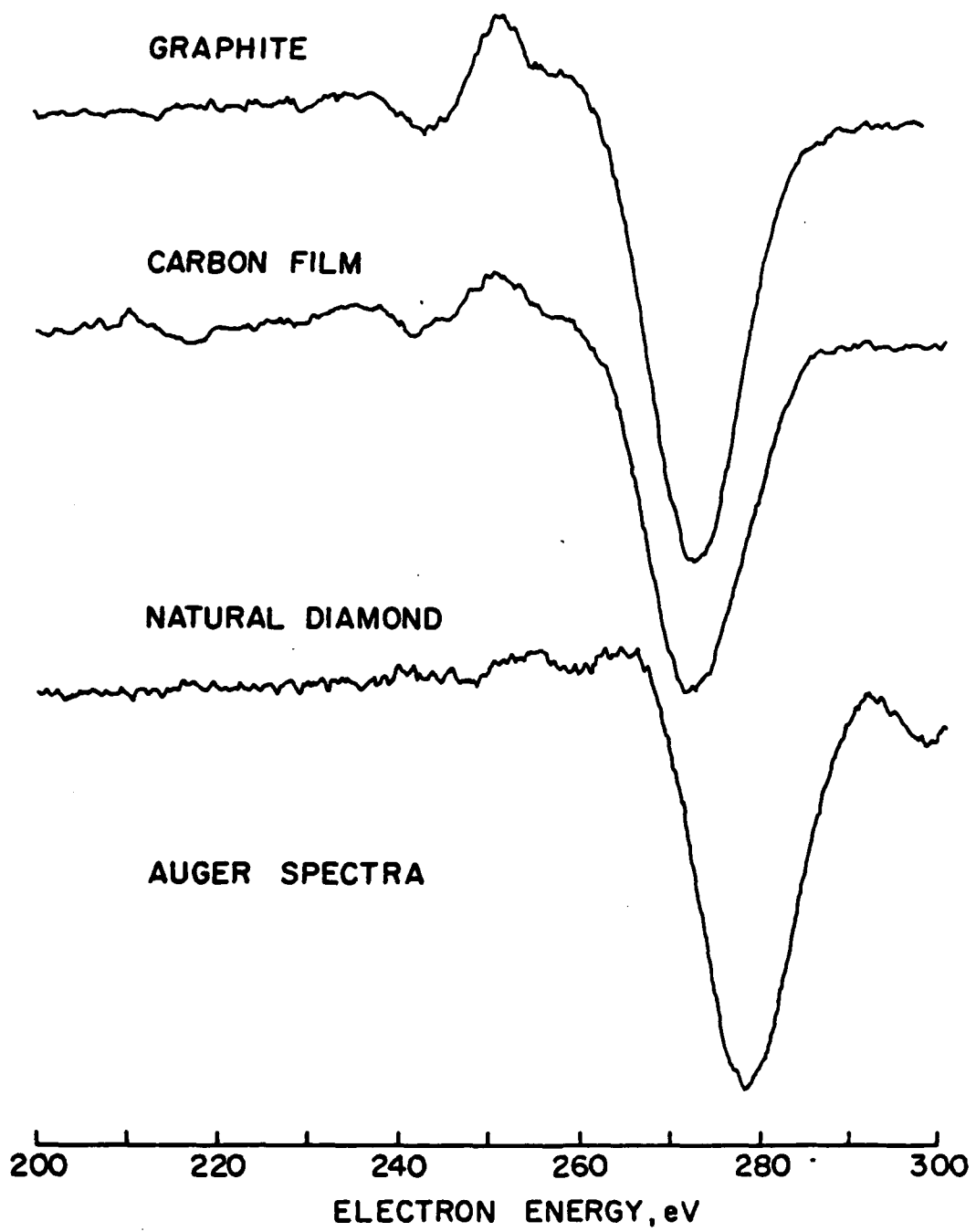


Figure 7 Auger spectra of pyrolytic graphite, ion deposited carbon film and natural diamond.

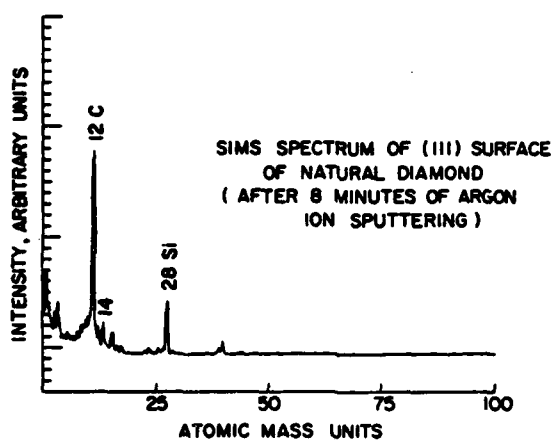


Figure 8 SIMS spectrum of (111) surface of natural diamond after 8 minutes of argon ion sputtering.

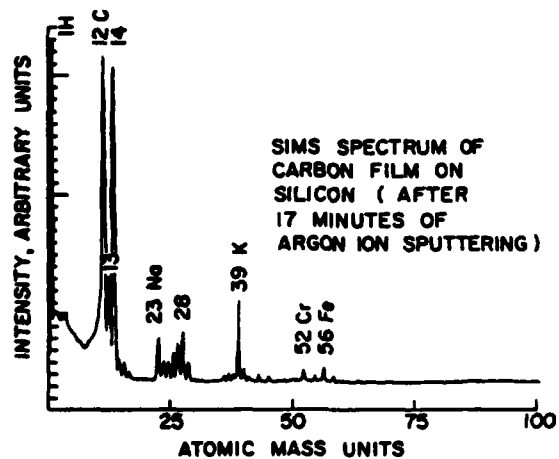


Figure 9 SIMS spectrum of ion deposited carbon film on silicon after 17 minutes of argon ion sputtering.

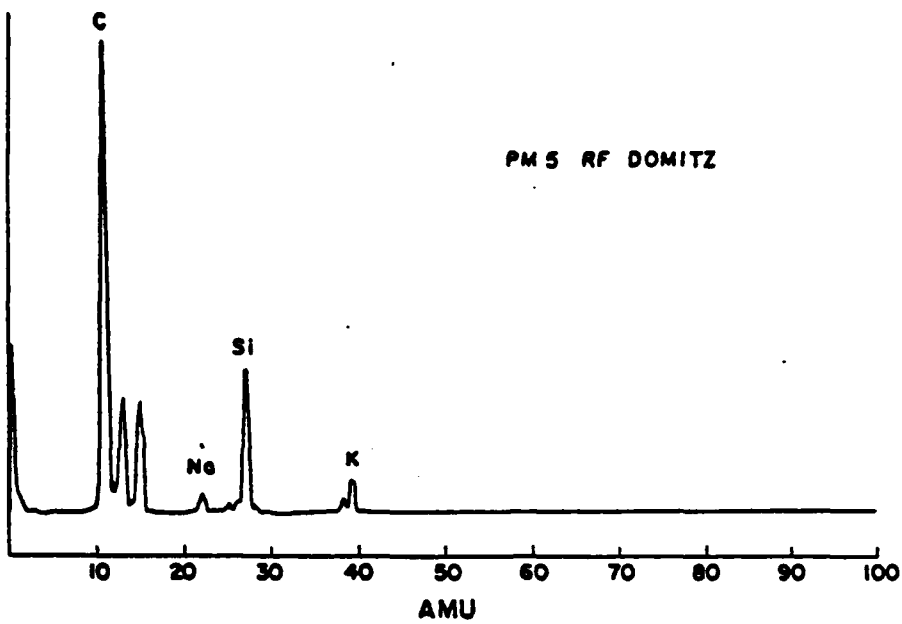


Figure 10 SIMS spectrum of carbon film obtained by RF discharge in CH_4 after 40 minutes of argon ion sputtering.

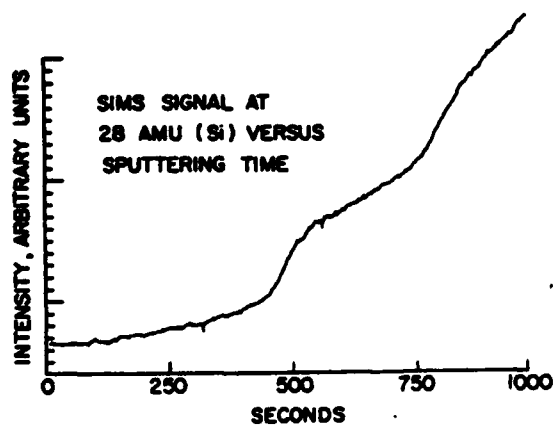


Figure 11 SIMS signal at 28 AMU (Si) versus sputtering time for carbon film on Si substrate.

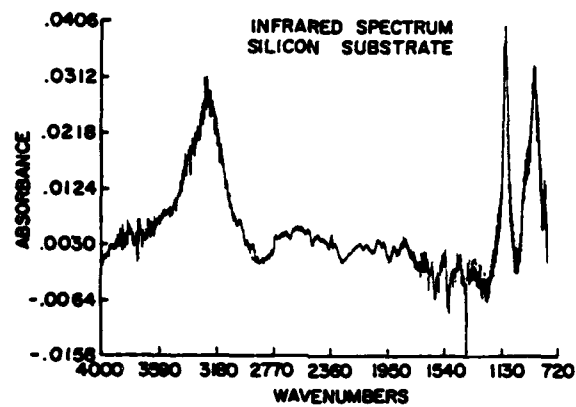


Figure 12 Transmission infrared spectrum of uncoated silicon substrate.

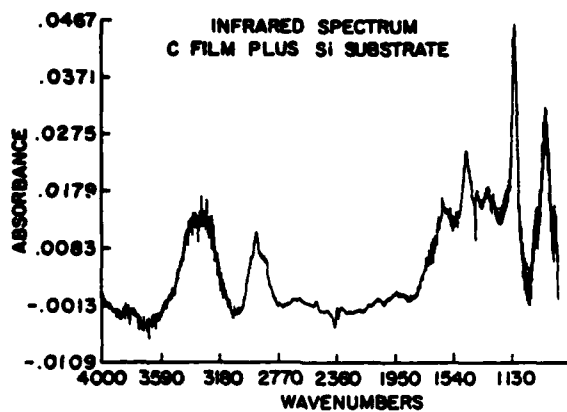


Figure 13 Transmission infrared spectrum of ion deposited carbon film plus silicon substrate.

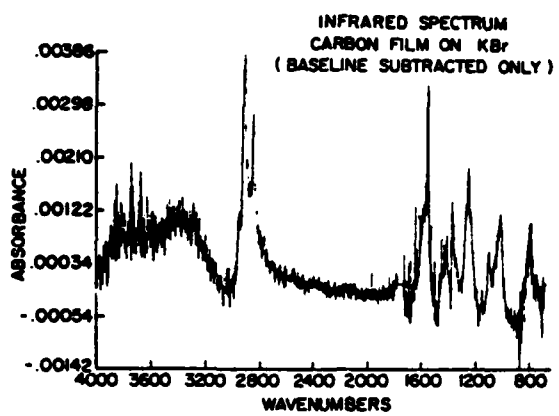


Figure 14 Transmission infrared spectrum of ion deposited carbon film on KBr.

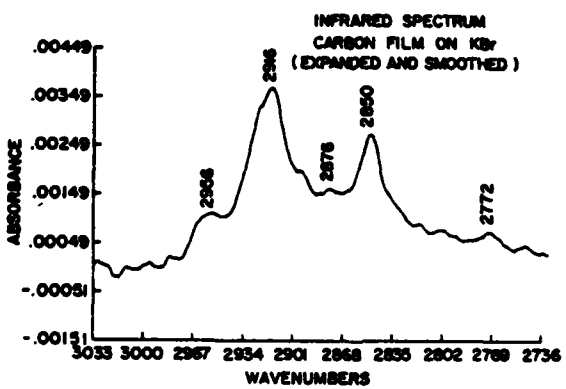


Figure 15 Transmission infrared spectrum of ion deposited carbon film on KBr (expanded and smoothed).

AD P002592



CARBON-COATED OPTICAL FIBERS

John M. Stevens
SpecTran Corporation
Sturbridge, MA

Martin Stein
Stein Associates
Bedford, MA

Presented By
Dr. Raymond E. Jaeger
SpecTran Corporation
Sturbridge, MA

BACKGROUND

This program was initiated approximately two and one half years ago as a cooperative development effort between Gulf & Western Applied Science Laboratories and Galileo Electro-Optics Corporation with Gulf & Western supplying the plasma coating technology and Galileo supplying the fiber drawing expertise and strength analysis. The project evolved out of an initial interaction with S. DiVita of the Army CECOM and H. Windsor at DARPA. The original funding sources were DARPA and the Air Force at RADC with follow-on tri-service funding. During 1981, a number of the key personnel left the program and the contract was ultimately terminated as of September 30, 1981. As a result, the data reported here are over one year old. More recently, SpecTran Corporation of Sturbridge, Massachusetts, received a service order from RADC to re-establish the experimental facility. That work is now in process.

INTRODUCTION

The overall goal of the program was to explore the use of in-line plasma ion deposited carbon films alone, and in combination with metals as a means of providing moisture protective coatings on optical fibers. The need for moisture proof fiber coatings can be demonstrated by examining briefly, the fracture mechanics of glass fiber. The strength distribution in most brittle materials

can be approximated by a Weibull distribution function given by Equation 1 and illustrated in Figure 1.

$$\ln \ln \frac{1}{1-F} = \ln \sigma_f + C \quad (1)$$

Where F equals $\frac{\text{rank number}}{N + 1}$,

m equals slope,

σ_f equals failure stress

The curves on the left hand side of Figure 1 represent results obtained in the early years of fiber strength development. These curves illustrate a bimodal strength distribution with an average slope of less than 10. In the last several years, much work has been dedicated to the achievement of a unimodal strength distribution with Weibull slopes greater than 40, as illustrated by the curves on the right hand side of Figure 1. These unimodal high strength distributions have been achieved through improvements in glass preform preparation, fiber draw and coating techniques.

Having accomplished such a high strength unimodal flaw distribution, attention must then be given to improving the static fatigue of the fiber; that is, the environmentally accelerated sub-critical crack growth that ultimately leads to failure of the fiber under an applied load. This static performance can perhaps best be explained through an understanding of the dynamic fatigue behavior of glass fiber, as described by Equation 2, and illustrated in Figure 2.

$$\ln \sigma_f = \frac{1}{n+1} \ln \sigma + K \quad (2)$$

where n is the stress corrosion coefficient. It is seen, therefore, that the higher the n value, the longer the life under a given applied stress and the less dependent the failure stress is on the stressing rate $\dot{\sigma}$.

The value of n is related to the time to failure under an applied stress by Equation 3,

$$\ln t_f = -n \ln \sigma_{ap} + B \quad (3)$$

where t_f is the time to failure and σ_{ap} is the applied stress. This static fatigue behavior is illustrated in Figure 3. Using Equation 4

$$n = \frac{\ln t_1 - \ln t_0}{\ln \sigma_0 - \ln \sigma_{ap}} \quad (4)$$

and incorporating an initial proof stress (σ_0) of 300kpsi and a time to failure (t_f) of 20 years, one can postulate that for an n value of 100 (hermetically coated fiber) the fiber could sustain an applied stress (σ_{ap}) over this period of time of approximately 250kpsi. At the same time, a plastic coated fiber having an n value of 20 could sustain an applied stress of only 100kpsi and survive the same time period.

EXPERIMENTAL APPROACH

With these latter numbers as a goal, we proceeded to coat fused silica fiber by the plasma ion beam technique using the apparatus shown schematically in Figure 4. The preform feed mechanism is mounted above a graphite resistance furnace and is continually flushed with filtered air. A diameter monitor, located between the furnace and the hermetic coating apparatus measures and controls the outside diameter of the fiber. Below the plasma deposition chamber is located a polymer coating applicator, curing oven, pinch wheel assembly, and spooling mechanism.

Figure 5 is a more detailed schematic of the hermetic coating chamber, showing the positions of the various differential pumping ports, irises and electrodes. The fiber enters the top of the chamber through a one millimeter diameter inlet orifice, which is shrouded in argon. Upon entering the actual deposition chamber, it experiences a low energy plasma polishing before carbon deposition. The carbon deposition is accomplished in the region of the upper electrode at a 20 to 30 micron argon/methane gas pressure. Upon exiting the

top electrode, the fiber is coated with approximately 200 Å of diamond-like carbon. It then enters the metal plasma deposition region (lower electrode) at the bottom of which is a ring shaped resistance heated evaporation boat containing indium metal. In this electrode region the carbon fiber is overlayed with a plasma deposited indium coating followed by an evaporation assisted plasma deposition of indium to a thickness of 1,000 - 2,000 Å. The fiber then exits the deposition chamber through the bottom differential ports and enters the polymer coating apparatus, where a UV curable acrylic resin is applied over the hermetic coating.

RESULTS AND DISCUSSION

Table I summarizes the best results obtained to date. The first set of data compares strength versus length for a polymer coated carbon fiber. The purpose of these control experiments were to determine that gage length which would ensure a unimodal strength distribution and minimize macroscopic flaw distribution effects. The Weibull slope and correlation coefficients indicate that this is achieved at gage lengths less than 10 centimeters. In order to ensure the elimination of macroscopic effects, a 1 centimeter gage length was selected for the remaining experiments.

The second set of data compares dynamic fatigue results over three orders of magnitude of strain rate. The median strength is seen to increase with increasing strain rate and yields an n value of 19.2, which compares well with literature reports on the static fatigue of fused silica.

The last two sets of test results are for fibers having a carbon-indium coating in combination and a carbon coating alone. For the carbon-indium combination, the median strength is reduced to 500kpsi, but yields an n value of 134. The apparent strength degradation may be the result of an interaction of the indium metal with the fused silica surface to form an oxide. This would only occur in the case of a discontinuous or too thin carbon coating.

The fiber with the carbon coating alone did not experience the same strength decrease as in the case of indium; however, the n value achieved was only 30. This result indicates either a discontinuous carbon coating or some

damage occurring to the coating as the fiber exits the lower orifice of the deposition chamber. Nonetheless, the fiber does exhibit improved stress corrosion characteristics.

CONCLUSIONS

We have demonstrated improved stress corrosion characteristics in fused silica fibers coated with carbon and indium metal alone and in combination. In the case where indium is used as a secondary coating, high n values ($n=134$) are achieved with some degradation in median strength that may be the result of a chemical reaction between the indium metal and the fused silica surface. With no indium present, there appears to be little decrease in median strength; however, the fiber exhibits only moderately improved stress corrosion behavior ($n=30$). The collective data appear to indicate that improved static fatigue properties may be achieved with much thicker carbon coatings, and the removal or enlargement of the entrance and exit orifices of the deposition chamber. The latter would eliminate the abrasion of the pristine and coated fiber surface. Indeed, this will be the direction of future experiments.

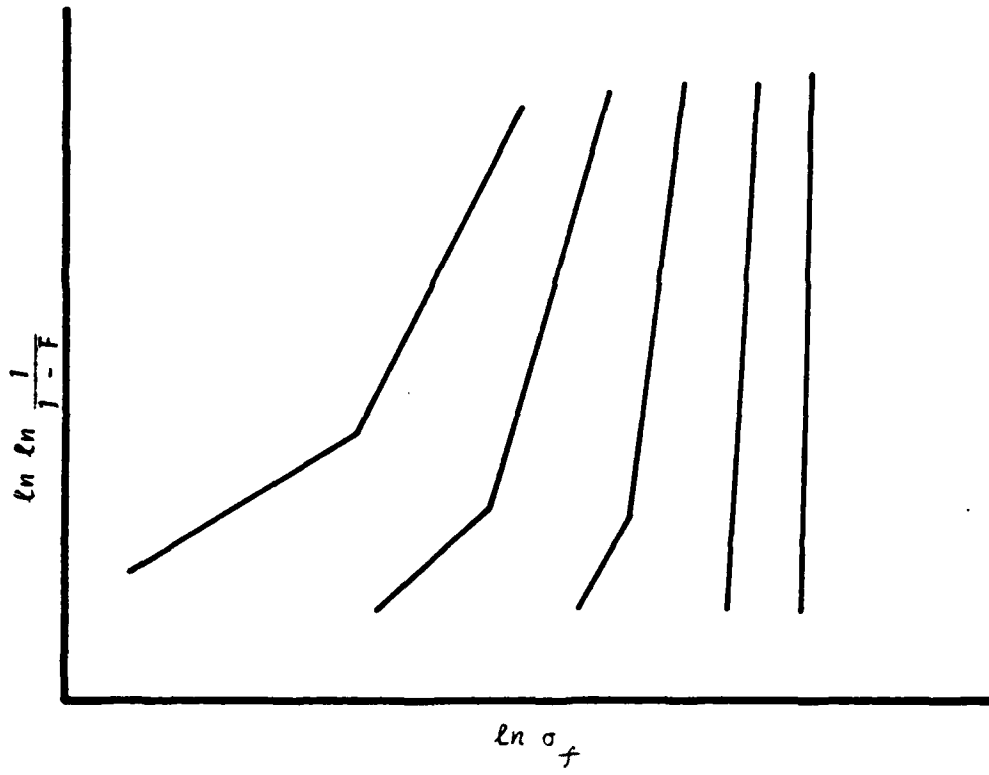


Figure 1

133

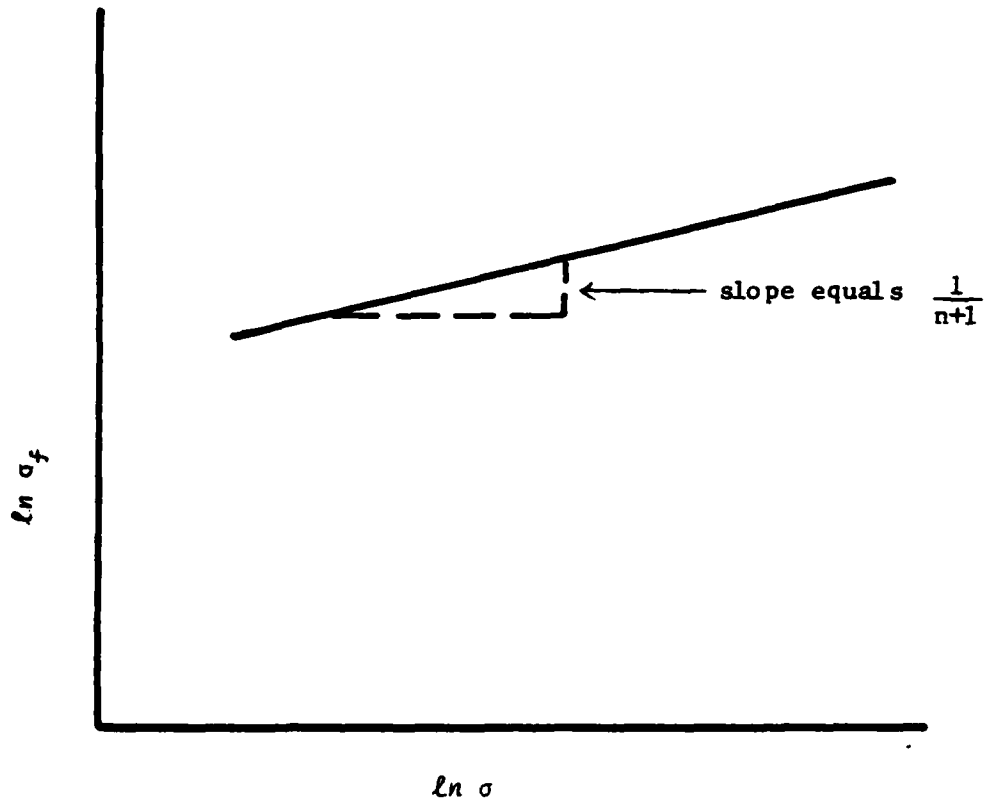


Figure 2

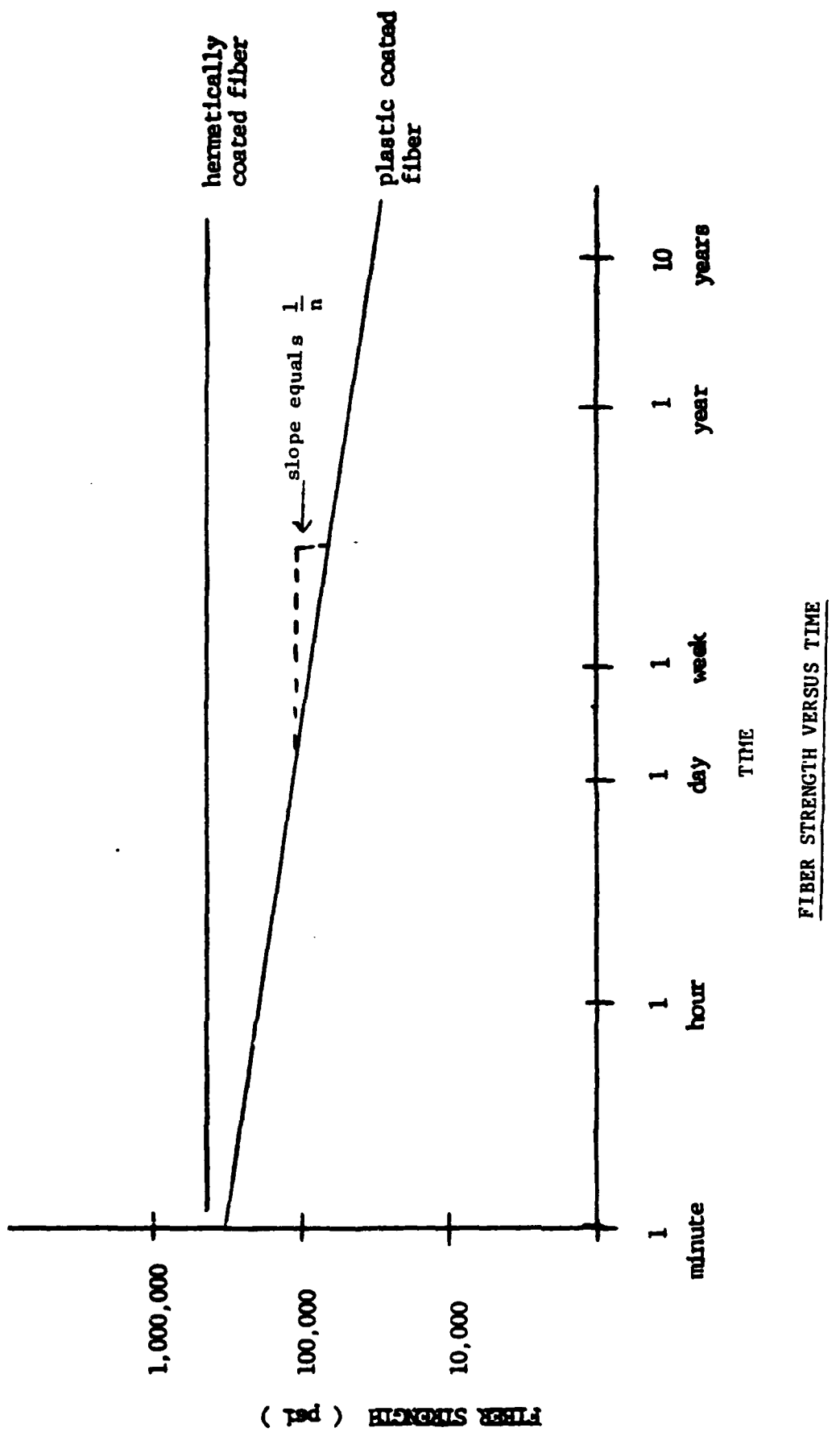
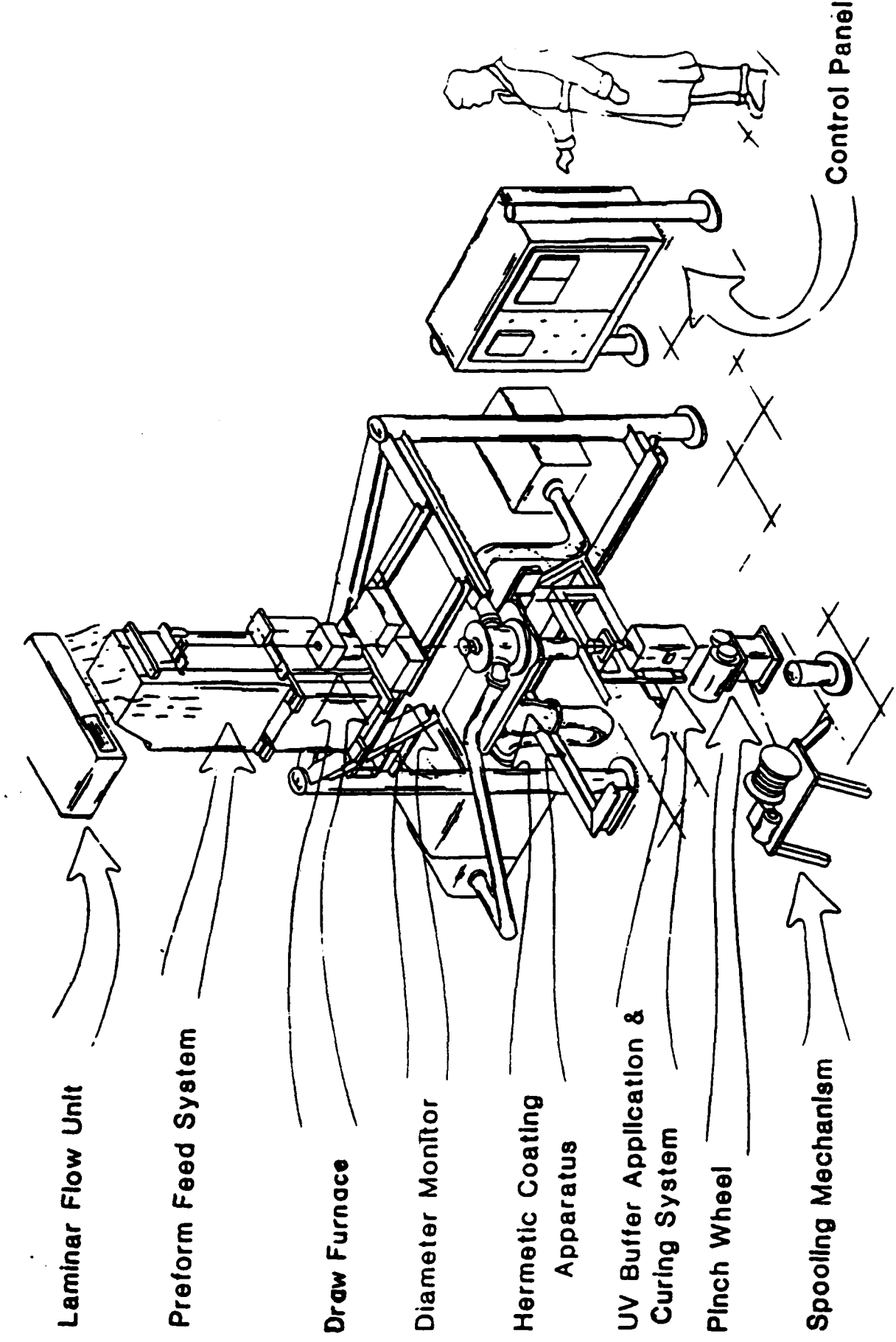
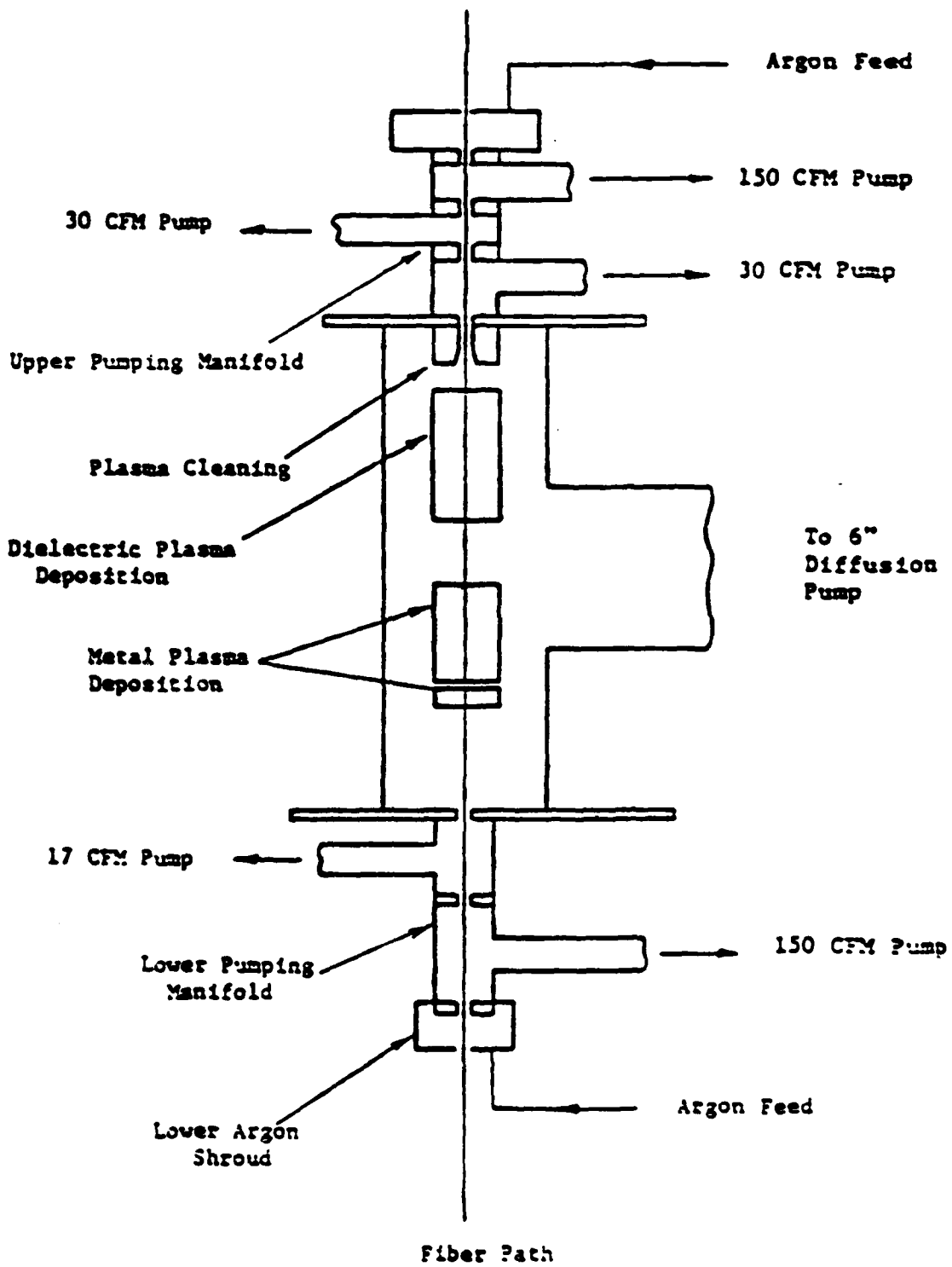


Figure 3



DRAW TOWER/ HERMETIC COATING APPARATUS

Figure 4



HERMETIC COATING APPARATUS SCHEMATIC

Figure 5

Test Parameter	TEST DATA			STRENGTH DATA					Static Fatigue Results	
	L ₀	c	N	Median kpsi	Std. Dev. kpsi	High kpsi	Low kpsi	Slope "m"	Coef. Coeff.	
	cm sec ⁻¹									
Control Fiber, Strength versus Length.	50	.85	29	807.5	47.7	832.4	617.9	14.4	.931	
	25	.85	30	815.7	60.1	867.6	557.0	11.1	.839	
	10	.85	34	816.4	21.8	851.1	735.5	41.8	.971	
	2.5	.85	31	816.4	25.6	896.8	772.7	34.7	.923	
Control Dynamic Fatigue Tests.	1.0	.085	18	679.2	18.4	730.4	666.9	40.1	.977	n = 19.20
	1.0	.85	17	791.5	25.9	833.3	720.9	32.4	.832	c.c. = 0.999
	1.0	8.5	23	878.7	25.8	914.6	772.7	30.5	.985	
Indium, Dynamic Fatigue Tests.	1.0	.085	26	507.1	14.8	528.3	480.2	36.5	.983	n = 134.5
	1.0	.85	29	508.3	39.8	575.1	415.8	13.7	.970	c.c. = 0.903
	1.0	8.5	27	523.8		593.7	463.6	13.24	.922	
Carbon, Dynamic Fatigue Tests.	1.0	.085	21	661.9	57.5	744.7	552.2	12.1	.967	n = 30.3
	1.0	.85	30	731.7	63.5	828.4	606.7	12.5	.983	c.c. = .979
	1.0	8.5	30	766.5	78.8	901.4	575.5	10.5	.987	

MOISTURE PROTECTION OF OPTICAL FIBERS

TABLE I

AD P00259C3

Electrical and Optical Properties of "Diamond-Like"
Amorphous Carbon Films

F.W. Smith
Department of Physics
City College of New York
New York, N.Y. 10031

Abstract

The electrical and optical properties of "diamond-like" amorphous carbon films, prepared via the dc glow discharge decomposition of ~~C₂H₂~~^{acetylene}, show a remarkable dependence on preparation conditions. In particular, as a function of the substrate deposition temperature T_d , the room temperature electrical conductivity of the films increases from 10^{-16} to $10^{-6} \text{ ohm}^{-1} \text{ cm}^{-1}$ and the optical energy gap decreases from 2.1 eV to 0.9 eV as T_d is increased from 25 to 375°C. The films would have essentially "graphitic" electrical and optical properties when deposited at $T_d > 400^\circ\text{C}$. For possible semiconductor applications, we have shown that these "diamond-like" films can be doped n- or p-type via incorporation of P or B atoms during deposition. This doping effect has been confirmed via thermopower measurements. At present we are studying the thermal stability of these films. Results obtained from a study of the effects of annealing on the optical properties of these films will be presented.

Amorphous semiconducting (or insulating) thin films prepared via the glow discharge decomposition of suitable gases have grown in importance within the last 5-10 years and promise to become of increasing interest in the 1980's as technological applications are further developed. Many of the films studied so far contain hydrogen as an important constituent (5-40 at %). The following is a partial list of films which have been prepared and studied primarily due to interest in their electrical and optical properties (with the primary constituent listed first): a-Si:H, a-Si:H:F, a-Si:B:H, a-Si:As:H, a-Si:C:H, a-Ge:H, a-Ga:As:H, a-P:H, a-Ge:C:H, and a-C:H. In addition, the following films have been prepared and studied due to interest in their mechanical or dielectric properties: a-Si:O, a-Si:N:H, a-C:H, and a-C:F.

Successful chemical modification of the electrical properties of these films (i.e. doping) has already been accomplished for the a-Si:H, a-Si:H:F, and a-Ge:H systems. We have shown that it is also possible to controllably modify the electrical properties of a-C:H films prepared from C_2H_2 via the incorporation of B and P atoms during growth of the films.¹⁻³

The a-C:H films studied have been prepared in a flow-through dc glow discharge apparatus. For optical absorption studies, quartz substrates were used. For conductivity studies, a 1000 Å thick Mo film evaporated onto glass slides (Mo/Glass) was used as a substrate. The discharge system was flushed with dry N_2 and then pumped to below 10^{-6} Torr, a flow of acetylene (Linde 99.6%) was established at 0.5-1.0 sccm, using a system pressure of 0.9 Torr. On the Mo/Glass substrates, a-C:H was deposited using a screen cathode 1cm above the substrate, the growth parameters being deposition temperature T_d =25 to 375°C, discharge current i_d =0.8 to 2 ma, with a deposition rate r_d =10 Å/sec. For deposition on glass, both i_d and r_d dropped by an order of magnitude. Resulting films were from 1500 to 7500 Å thick. The voltage necessary to maintain the discharge varied from 300 to 400 volts, decreasing with increasing T_d . The optical absorption studies,

from 1.65 to 4.eV, were performed using a GCA/McPherson Spectrophotometer.

The a-C:H films prepared on Mo/Glass substrates for $T_d < 200C$ were nearly transparent. As T_d was increased above 200C, the samples grew progressively darker, until they were a glossy black at $T_d=350C$. Films grown on glass were a faint tan, and highly transparent at $T_d=25C$. As T_d approached 350C, the films became deep brown, but were still moderately transparent. The a-C:H films were insoluble in a variety of organic solvents and acids, were quite hard, and proved extremely resistant to scratching. The films adhered well to both types of substrates for thicknesses of < 1 micron.

Representative electrical conductivity data for these samples are shown in Fig. 1, where σ is plotted versus $1/T$ on a logarithmic scale. The dependence of σ on T_d is quite strong, with the room temperature conductivity $\sigma(RT)$ varying from about 10^{-16} to $10^{-6} \text{ ohm}^{-1} \text{ cm}^{-1}$ as T_d is increased from 75 to 350C. Except for the $T_d=350C$ sample, σ does not have the simple activated form, $\sigma(T) = \sigma_0 \exp(-E_A/k_B T)$, with σ_0 and E_A independent of measuring temperature. Annealing the samples at 350C typically resulted in a decrease in $\sigma(T)$ by a factor of two, indicating that these a-C:H films are thermally stable (in vacuum) up to this temperature.

The measured energy dependence of the optical absorption coefficient α indicates that the optical absorption "edges" in these a-C:H films are quite broad. For the $T_d=300C$ sample, $\alpha \sim 10^4 \text{ cm}^{-1}$ at 1.6 eV, rising to 10^5 cm^{-1} at 3.3eV. The corresponding energies for the 150C sample are 2.25 and 3.9eV. Optical energy gaps E_{opt} have been determined for these samples by plotting $(\alpha E)^{1/2}$ versus E as a test of the expression $(\alpha E)^{1/2} = A(E_{opt} - E)$ where E is the photon energy, and A is a constant. E_{opt} , displayed in Fig. 2, was obtained from the

intercept of the extrapolation of the linear part of the curves to $(\propto E)^{1/2} = 0$. E_{opt} is observed to decrease from 2.1 to 0.9eV as T_d increases from 25 to 375C, with most of the decrease occurring for T_d greater than 250C. We note that a-C:H films can be prepared with $E_{opt} = 1.5$ eV, indicating a potentially good match to the solar spectrum, a prerequisite for their possible use in thin film photovoltaic solar cells. Preliminary infrared absorption studies of these a-C:H films have indicated a strong absorption due to C-H bond-stretching modes near 2900cm^{-1} , with little or no absorption due to C=O bonds observed in the region near 1700 cm^{-1} .

Doping of these a-C:H films was accomplished by adding B_2H_6 or PH_3 to the C_2H_2 discharge gas. In Fig. 3 $\sigma(\text{RT})$ is shown as a function of discharge gas concentration for films deposited at $T_d = 250\text{C}$. We observed that $\sigma(\text{RT})$ could be increased by five orders of magnitude by adding either 1% PH_3 or 10% B_2H_6 to the discharge gas. A shift of the Fermi level E_F of about 0.7eV through the energy gap has been inferred from changes in the "activation energy" of conduction. Somewhat enhanced doping efficiency has been observed in films prepared at $T_d = 325\text{C}$, where thermopower measurements³ also confirmed that doping to n- or p-type had actually occurred in these films.

Whether these a-C:H films find applications due to their interesting electrical or optical properties, it will be important to first establish their thermal stability. It is to be expected that, when exposed to sufficiently high temperatures, these films will evolve hydrogen and will likely become essentially graphitic. In this case their useful electrical, optical, and mechanical properties will undergo modification as graphitic amorphous carbon films are known to be soft, semi-metallic, and optically opaque. For this reason, we have undertaken an experimental study of the thermal stability of these "diamond-like" a-C:H films.

The film studied was deposited at $T_d = 250\text{C}$ onto a quartz substrate using pure C_2H_2 in the discharge. The as-deposited

film was measured to have $E_{opt} = 2.06\text{eV}$ and $\sigma(RT)$ about $10^{-10} \text{ ohm}^{-1} \text{ cm}^{-1}$. The reflectance R and transmittance T of the film were measured from 1.6 to 4.1eV following anneals from $T_a = 250$ to 700C , by steps of 50C . These anneals were carried out either in vacuum or in an inert atmosphere. The index of refraction n of the film was determined to be 1.8.

The absorption coefficient α is shown as a function of photon energy in Fig. 4 for the same film following anneals at temperatures T_a . It can be seen that the absorption in the film increases monotonically with increasing T_a , signalling the shrinkage or filling-in of the energy gap as hydrogen is evolved from the film.

The shrinkage of the energy gap is illustrated in Fig. 5 where E_{opt} determined in the usual way is given as a function of T_a . E_{opt} is essentially constant at 2.0eV for $T_a \leq 350\text{C}$. Following a rapid decrease for $350 < T_a < 500\text{C}$, E_{opt} falls linearly with increasing T_a , extrapolating to zero at $T_a = 750\text{C}$. We note that the film disintegrated during the anneal at $T_a = 750\text{C}$. For intermediate values of T_a , from 400 to 500C , there seem to be two values of E_{opt} for the films, indicating either sample non-uniformity or perhaps the coexistence and development of two types of short range order within the film as it is annealed.

The evolution of the increasing optical absorption of this a-C:H film as it is successively annealed at higher T_a is tentatively modeled as follows:

- 1) $250 \leq T_a \leq 350\text{C}$. The optical transitions involved are from extended states at the valence band edge to extended states at the conduction band edge (extended \rightarrow extended). There is some evidence for transitions involving localized states within the energy gap for lower photon energies.
- 2) $350 < T_a < 450\text{C}$.

In this range of T_a , we propose that hydrogen begins to be evolved from the film, leaving behind localized defect levels which

had previously been compensated by being bonded to the hydrogen. As these states are created in large numbers due to the evolution of hydrogen, particularly near the band edges, the energy gap shrinks and hence E_{opt} decreases. The optical transitions in this range will now involve both extended \rightarrow extended and extended \leftrightarrow localized states.

3) $450 < T_a < 550C$.

More hydrogen is evolved in this range of annealing temperatures, leading to the creation of further defect states. However, the simultaneous development of trigonal (3-fold, graphitic) short range order begins. As a result, more π -like electron states begin to appear near the top of the valence band. Again, optical transitions in this range will involve both extended and localized states.

4) $550 < T_a < 750C$.

Further development of trigonal short range order within the film occurs in this range of T_a as the film's electrical, optical, and mechanical properties approach those typically observed for graphitic amorphous carbon films prepared via evaporation of carbon. In the language of amorphous semiconductors, the mobility gap of the film is shrinking to zero as the optical gap also closes up.

From these annealing studies, we can conclude that the "diamond-like" amorphous carbon films can be considered thermally stable for annealing temperatures T_a up to approximately 350-400C, at which point their optical properties begin to be significantly altered due to the evolution of hydrogen.

In conclusion, we have for the last three years carried through an experimental study of the preparation and characterization of "diamond-like", hydrogenated amorphous carbon films. We have focussed our attention on the electrical and optical properties of these interesting amorphous semiconducting films, investigating their dependence on both deposition temperature T_d and subsequent

annealing temperature T_a . We have been able to demonstrate that these films can be doped n- and p-type, an important first step in their possible application in optoelectronic devices.

For the realization of applications of these films, two different approaches should be considered:

- 1) As hard, transparent surface coatings, effort must be made to further minimize optical absorption in these films in both the interesting visible and infrared regions;
- 2) As optoelectronic device material, significant photosensitivity in these films must be established.

To achieve these applications, possible areas of further investigation include:

- 1) determination of film structure, in particular the type of short range order and its dependence on deposition conditions.
- 2) clarification of the role of hydrogen in these films, including the amount and mode of its bonding within the films.
- 3) determination of the properties of a "second-generation" of films which could include additional elements such as nitrogen, fluorine, or silicon to achieve desired tuning of the film properties.

References

No attempt has been made to develop a complete set of references to work being done on "diamond-like" carbon films. For additional references, see citations listed in references 1-3 below, as well as the other contributions to this workshop.

1. "Electrical and Optical Properties of Hydrogenated Amorphous Carbon Films", B. Meyerson and F.W. Smith, J. Non-Cryst. Solids 35/36, 435 (1980).
2. "Chemical Modification of the Electrical Properties of Hydrogenated Amorphous Carbon Films", B. Meyerson and F.W. Smith, Solid State Comm. 34, 531 (1980).
3. "Thermopower of Doped Semiconducting Hydrogenated Amorphous Carbon Films", B. Meyerson and F.W. Smith, Solid State Comm. 41, 23 (1982).

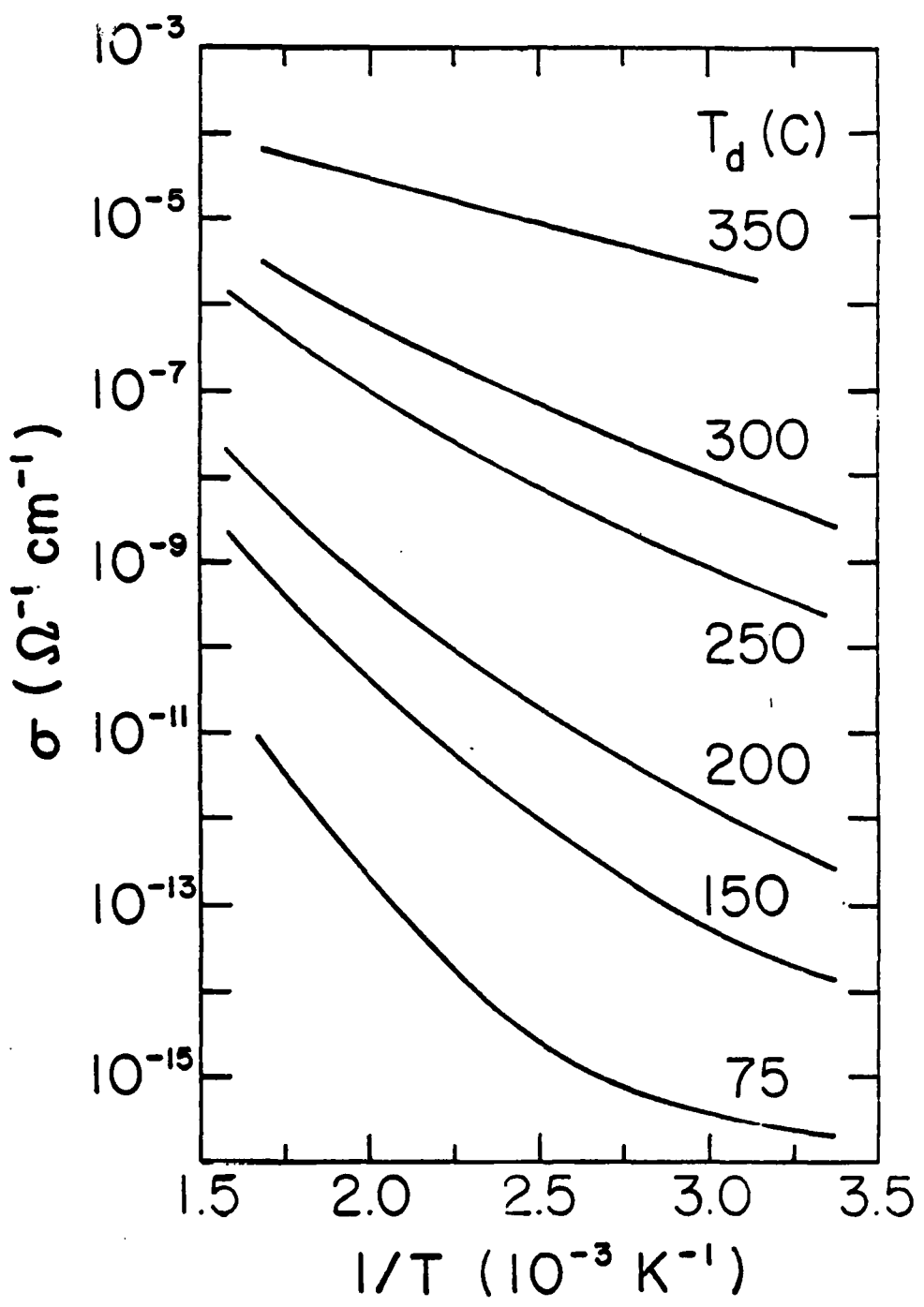


Fig. 1 Electrical conductivity σ as a function of $1/T$ for these a-C:H films. T_d = deposition Temperature

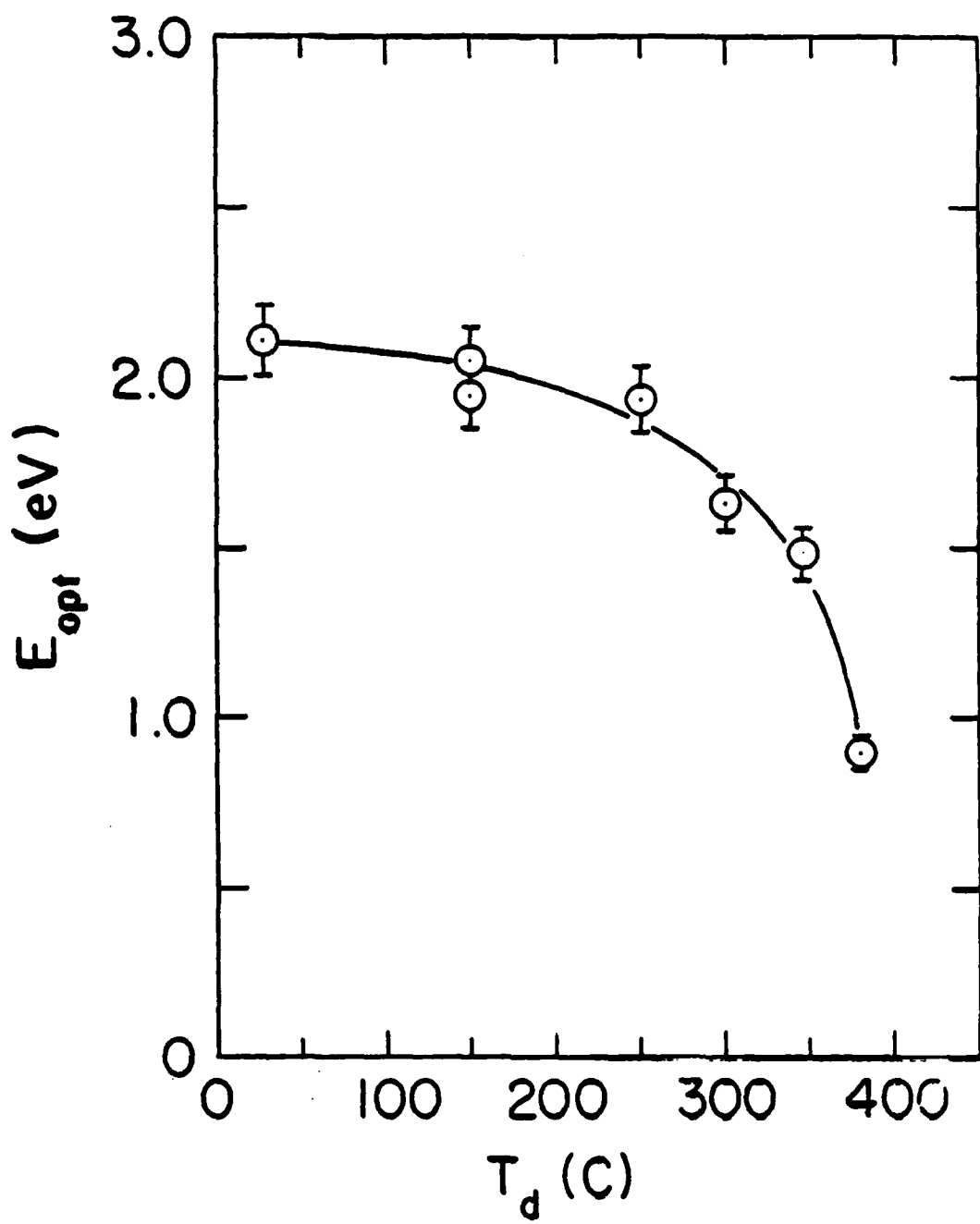


Fig. 2 Optical energy gap E_{opt} as a function of deposition Temperature T_d for these a-C:H films.

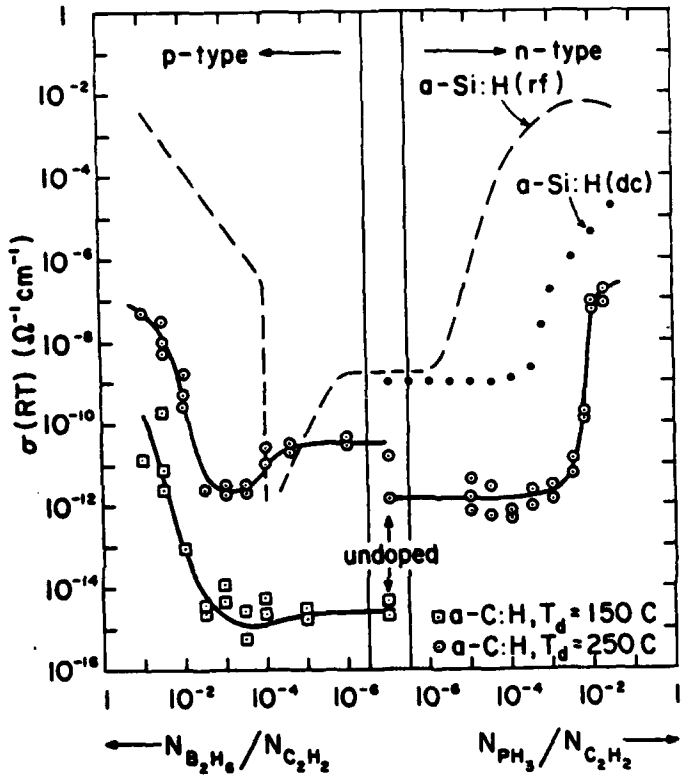


Fig. 3 Room Temperature electrical conductivity for n- and p-type a - C:H films deposited at $T_d = 150$ and 250°C , as a function of the composition of the discharge gas from which the films were deposited. Included for comparison are data for n- and p- type a - Si:H films prepared via rf or dc glow discharge Techniques (see Ref. 2 for details).

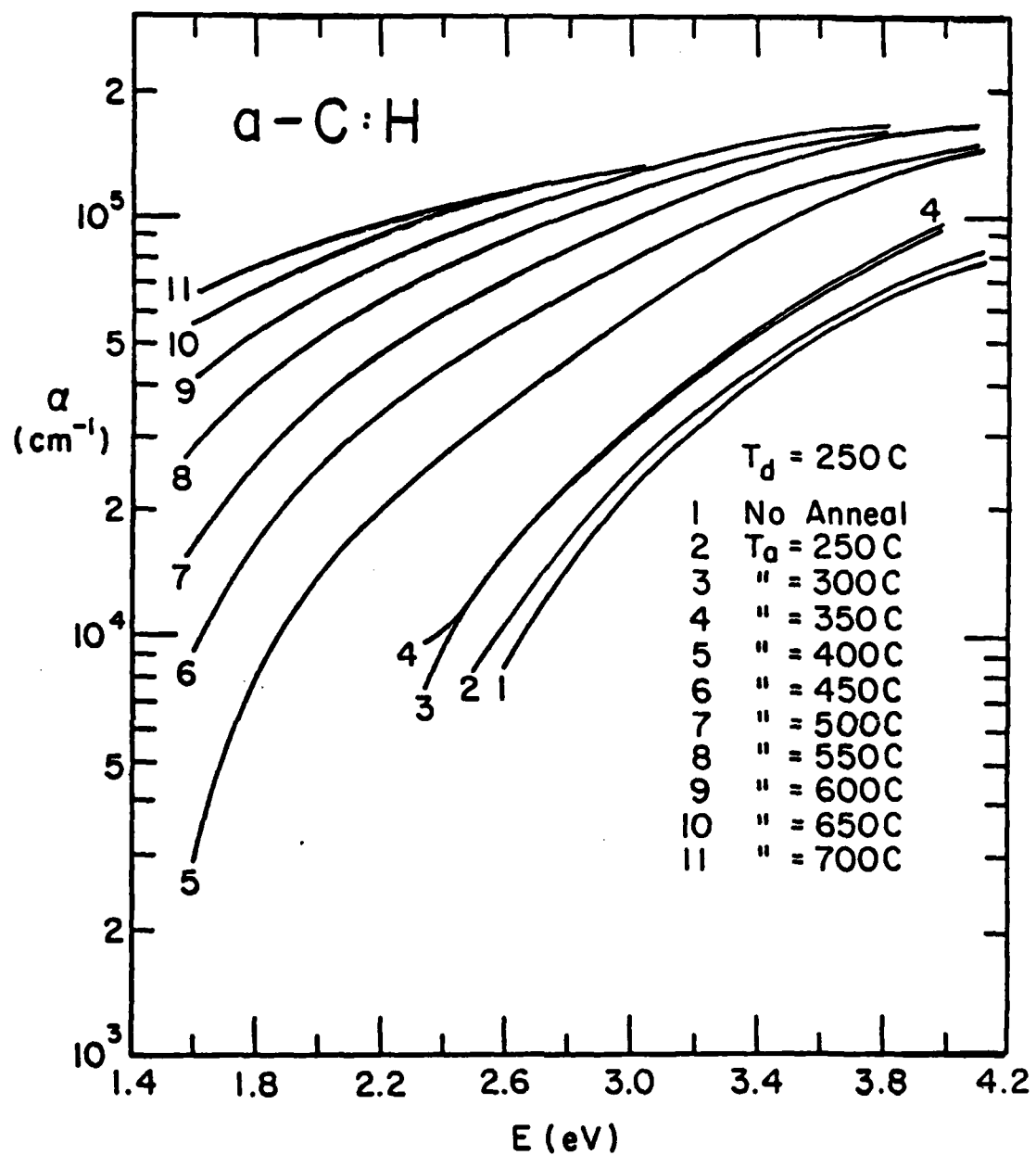


Fig. 4 Optical absorption coefficient α for a "diamond-like" a-C:H film versus photon energy E (eV). Curves are shown for the as-prepared film ($T_d = 250\text{C}$) with no anneal, curve 1, and for the same film following 1 hr. anneals at temperatures T_a from 250 to 700C , curves 2 - 11.

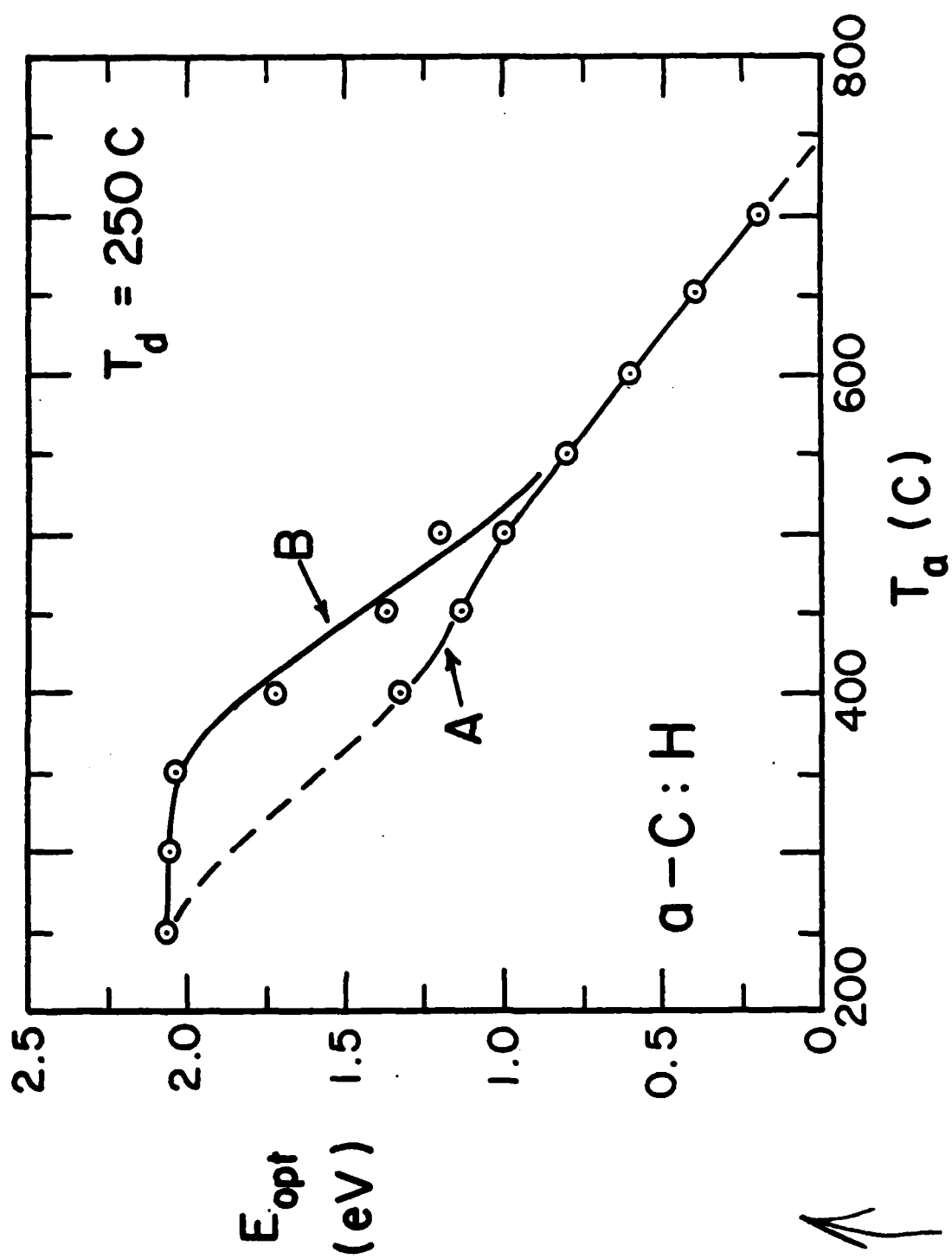


Fig. 5 Optical energy gap E_{opt} for an a-C:H film deposited at $T_d = 250\text{C}$ as a function of subsequent annealing Temperature T_a , see Fig. 4.

AD P002594



ULTRAVIOLET-LASER PHOTODEPOSITION*

D. J. Ehrlich and J. Y. Tsao
Lincoln Laboratory, Massachusetts Institute of Technology
Lexington, Massachusetts 02173

Ultraviolet laser light can be used to initiate low-temperature chemical processing of surfaces by reactions which are similar in many respects to those active in plasma techniques. Such processing has been under investigation at M.I.T. Lincoln Laboratory over the last several years. A series of new techniques have been developed for thin-film deposition, for etching, and for doping of semiconductors by processes based on photolytic reactions at a gas-solid interface. Gas-phase and surface chemical reactions are controlled by a UV laser, while the temperature of the surface is independently controlled and can typically remain near room temperature. Experiments on UV excimer laser deposition of similar materials suggest that the same approach may be useful for rapid deposition of hard carbon films. In this summary we will review this new technology.

A principle emphasis has been techniques for mask-free fabrication of thin-film and semiconductor microstructures for solid-state electronics. In these applications the photochemical reactions are confined to micrometer-scale areas on the substrate; spatial resolution and process rate become primary concerns since they determine, to a large extent, the range of applicability to device fabrication. The highly focused output of a frequency-doubled Ar-ion laser is typically used.

Other applications can make use of the efficiency of UV generation which has recently become possible with rare gas halide excimer lasers for processing of large surface areas. However the pulsed output and poor spatial-mode pro-

*This work was supported by the Department of the Air Force, in part under a specific program sponsored by the Air Force Office of Scientific Research, by the Defense Advanced Research Projects Agency, and by the Army Research Office.

erties of excimer lasers make them less suitable for high-spatial-resolution processes. The characteristics of these two laser sources, both used widely in laser photochemical processing, are listed in Table 1.

For specific electronics processing problems a variety of chemical mechanisms have been used; these are outlined in Table 2 and discussed in detail in the references. Table 3 lists the current rate and resolution limits of the new techniques. Figures 1-6 show representative microstructures produced.

TABLE I

UV LASERS

CW - Ar⁺ FREQUENCY DOUBLED, 257.2 nm

- A.) Focus: < 1 to 50 μm diameter
- B.) Intensity: < 1 kW/cm²

PULSED EXCIMER (ArF - 193 nm; XeF - 351 nm)

- A.) Focus: ~ 100 - 300 μm diameter
- B.) Fluence: 0.1 - 1.0 J/cm², 7 ns pulse, 1-1000 Hz PRF
- C.) Transient heating for diffusion
- D.) Multiple shots: ~ 25 - 100 for contacts

TABLE 2

CHEMICAL MECHANISMS

VOLUMETRIC PHOTOLYSIS REACTION

- A.) $\text{Cd}(\text{CH}_3)_2 + h\nu \rightarrow \text{Cd} + \text{C}_2\text{H}_6$
- B.) $\text{CH}_3\text{Br} + h\nu \rightarrow \text{Br} + \frac{1}{2}(\text{C}_2\text{H}_6)$

ADLAYER PHOTOLYSIS - PRENUCLEATION

LASER HEATING

- A.) Application: Alloying of Zn into Al, doping by diffusion
- B.) Collinear focus of 514.5 nm CW beam
- C.) Transient heating for excimer laser, $\sim 0.1 \mu\text{m}$ absorption depth

PYROLYSIS - LASER CVD

- A.) $\text{SiH}_4(\text{g}) \rightarrow \text{Si}(\text{s}) + 2\text{H}_2(\text{g})$

TABLE 3

PROCESS CHARACTERISTICS

<u>PROCESS</u>	<u>DEMONSTRATED RATE</u>	<u>DEMONSTRATED RESOLUTION</u>	<u>COMMENT</u>
III-V DRY ETCHING	0.01 $\mu\text{m/s}$	2 μm	AMBIENT TEMP.
III-V WET ETCHING	0.1 $\mu\text{m/s}$	1 μm	AMBIENT TEMP.
Si ETCHING	> 6 $\mu\text{m/s}$	3 μm	MECHANISM VARIES WITH TEMP.
PHOTODEPOSITION	0.1 $\mu\text{m/s}$	< 1 μm	AMBIENT TEMP.
PYROLYTIC DEPOSITION (Si)	15 $\mu\text{m/s}$	2 μm	> 600 C
III-V PHOTOCHEMICAL DOPING	$\sim 10^{11} \text{ cm}^{-2} \text{ s}^{-1}$ (cw)	2 μm	TWO BEAMS
	$\sim 10^{20} \text{ cm}^{-2} \text{ s}^{-1}$ (PULSED)	LARGE AREA	-----
Si PHOTODOPING	? (cw)	1 μm	-----
	$\sim 10^{20} \text{ cm}^{-2} \text{ s}^{-1}$ (PULSED)	LARGE AREA	-----
Al/Zn PHOTOCHEMICAL MICROALLOYING	$\sim 10^{15} \text{ cm}^{-2} \text{ s}^{-1}$ (cw)	5 μm	FOR Al ETCHING, 350-500 C

1. D. J. Ehrlich, R. M. Osgood, Jr. and T. F. Deutsch, "Laser Microphotochemistry for Use in Solid State Electronics," IEEE J. Quantum Electron. QE-16, 1233, (1980).
2. D. J. Ehrlich, R. M. Osgood, Jr., and T. F. Deutsch, "Photodeposition of Metal Films with Ultraviolet Light," J. Vac. Sci. and Technology. 21, 23 (1982).
3. D. J. Ehrlich, R. M. Osgood, Jr., D. J. Silversmith and T. F. Deutsch, "One-step Repair of Transparent Defects in Hard-Surface Photolithographic Masks Via Laser Photodeposition," Electron Device Lett. EDL-1 101 (1980).
4. J. Y. Tsao, D. J. Ehrlich, D. J. Silversmith and R. W. Mountain, "Direct-Write Metalization of Silicon Mosfets using Laser Photodeposition, IEEE Elect. Dev. Lett. EDL-3, 164 (1982).
5. D. J. Ehrlich, R. M. Osgood, Jr. and T. F. Deutsch, "Laser Microreaction for Deposition of Doped Silicon Films," Appl. Phys. Lett. 39, 957 (1981).
6. D. J. Ehrlich, R. M. Osgood, Jr. and T. F. Deutsch, "Laser Chemical Technique for Rapid Direct Writing of Surface Relief in Silicon," Appl. Phys. Lett. 38, 1018 (1981).
7. D. J. Ehrlich and J. Y. Tsao, "Submicrometer-LineWidth Doping and Surface Relief Definition in Silicon by Laser Controlled Diffusion," Appl. Phys. Lett. 41, 297 (1982).

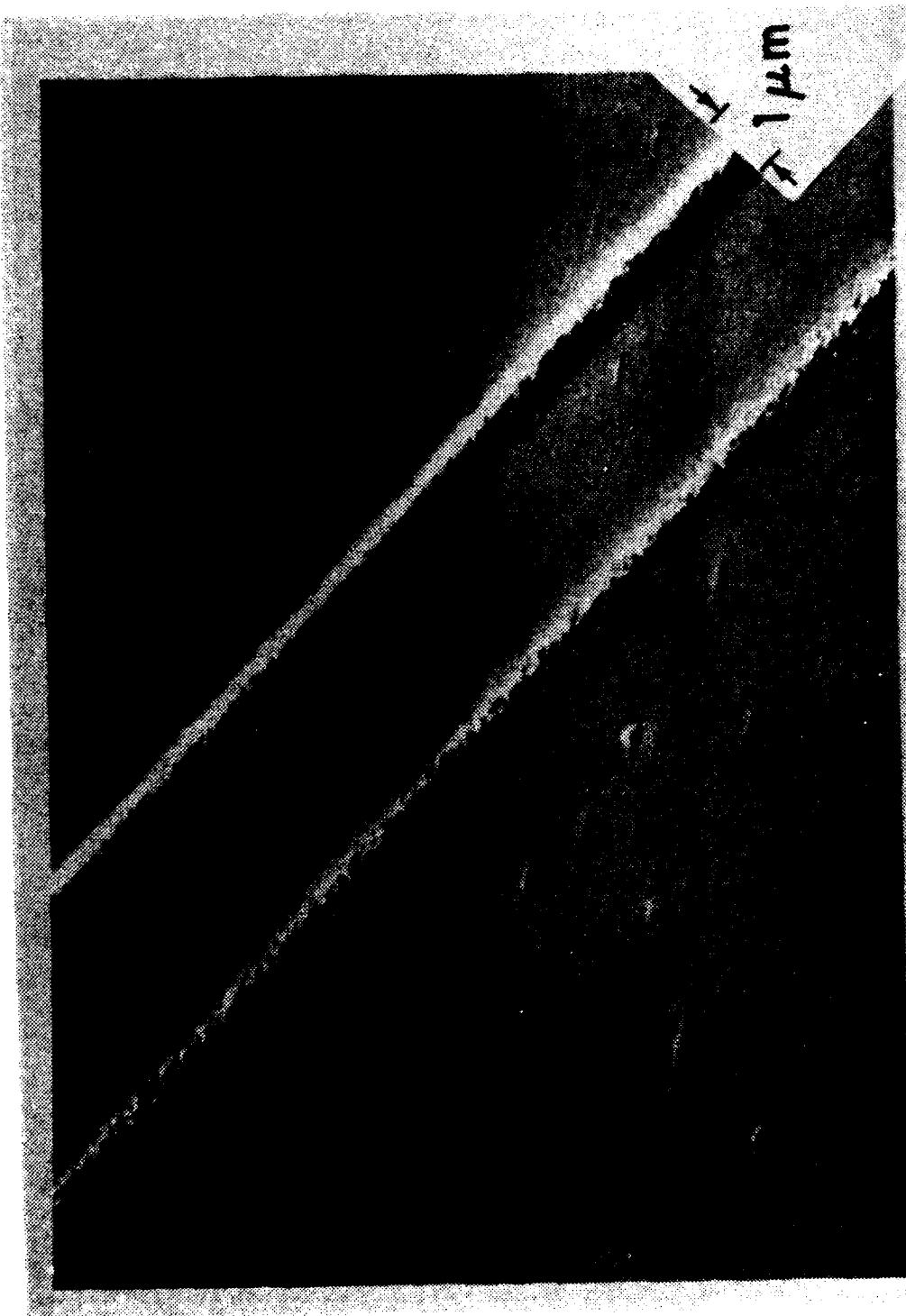


Figure 1. Submicrometer Metallization Lines Written by Laser Photodeposition.
Lines Deposited by Photolysis of $\text{Zn}(\text{CH}_3)_2$ Using a 257.2 nm Laser.
See Ref. 2.

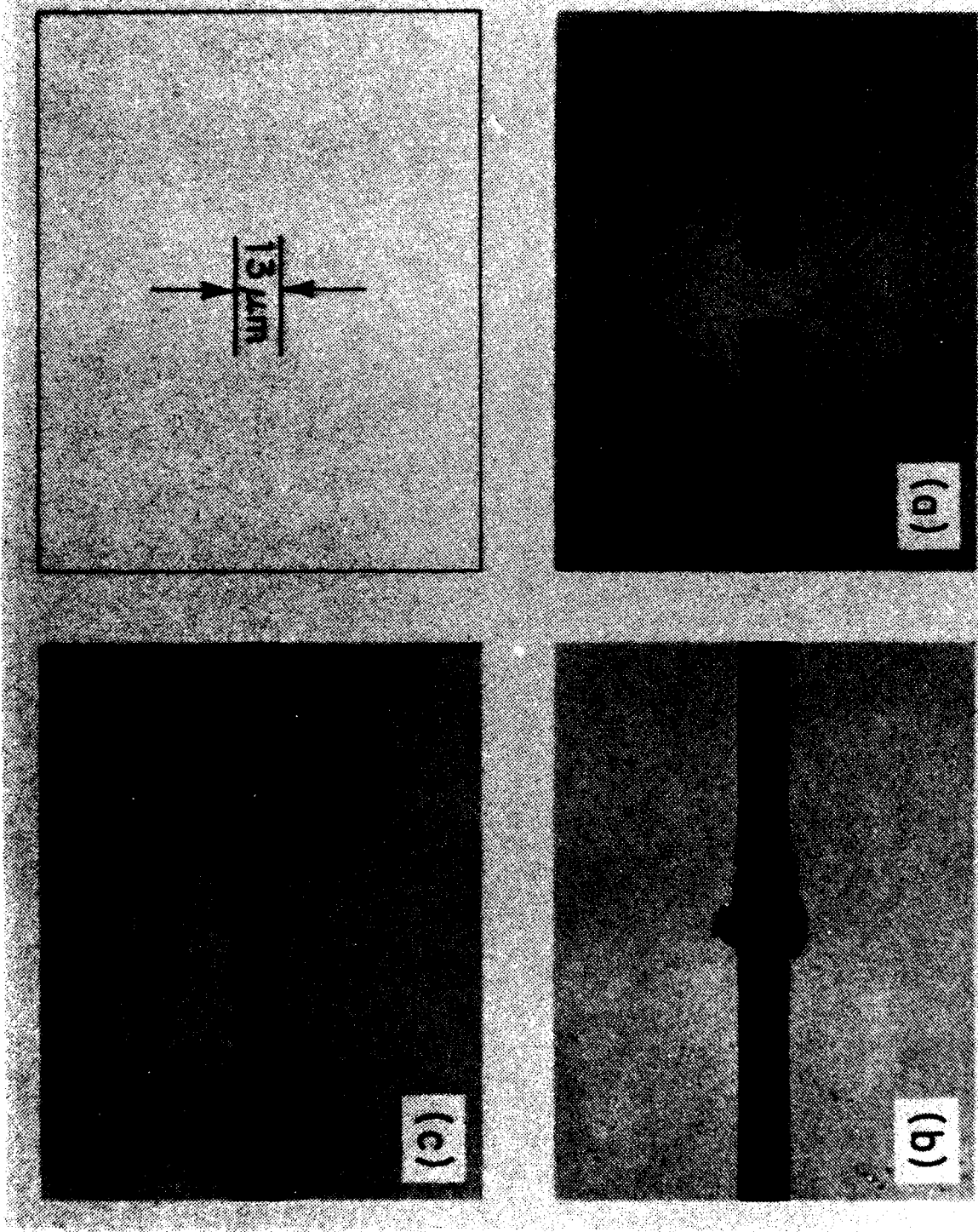


Figure 2. Photomask Repair Sequence: (a) Simulated Defect, (b) After Repair by Cd Photodeposition, (c) After Laser Trimming. See Ref. 3.

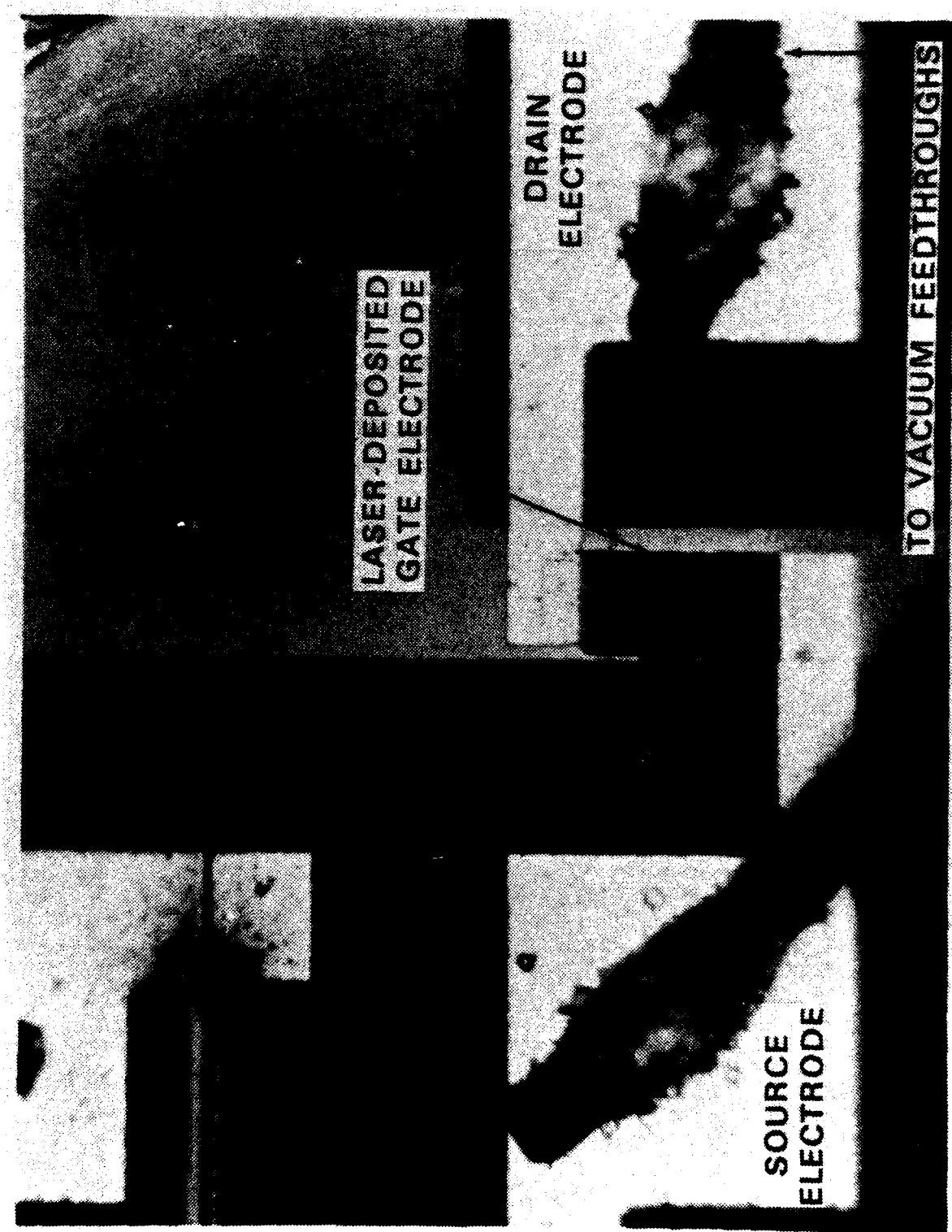


Figure 3. Laser-Photodeposited Gate Electrode on Operating Si MOSFET. Electrode Geometry Variations Are Used to Actively Tune the MOSFET Device Characteristics. See Ref. 4.

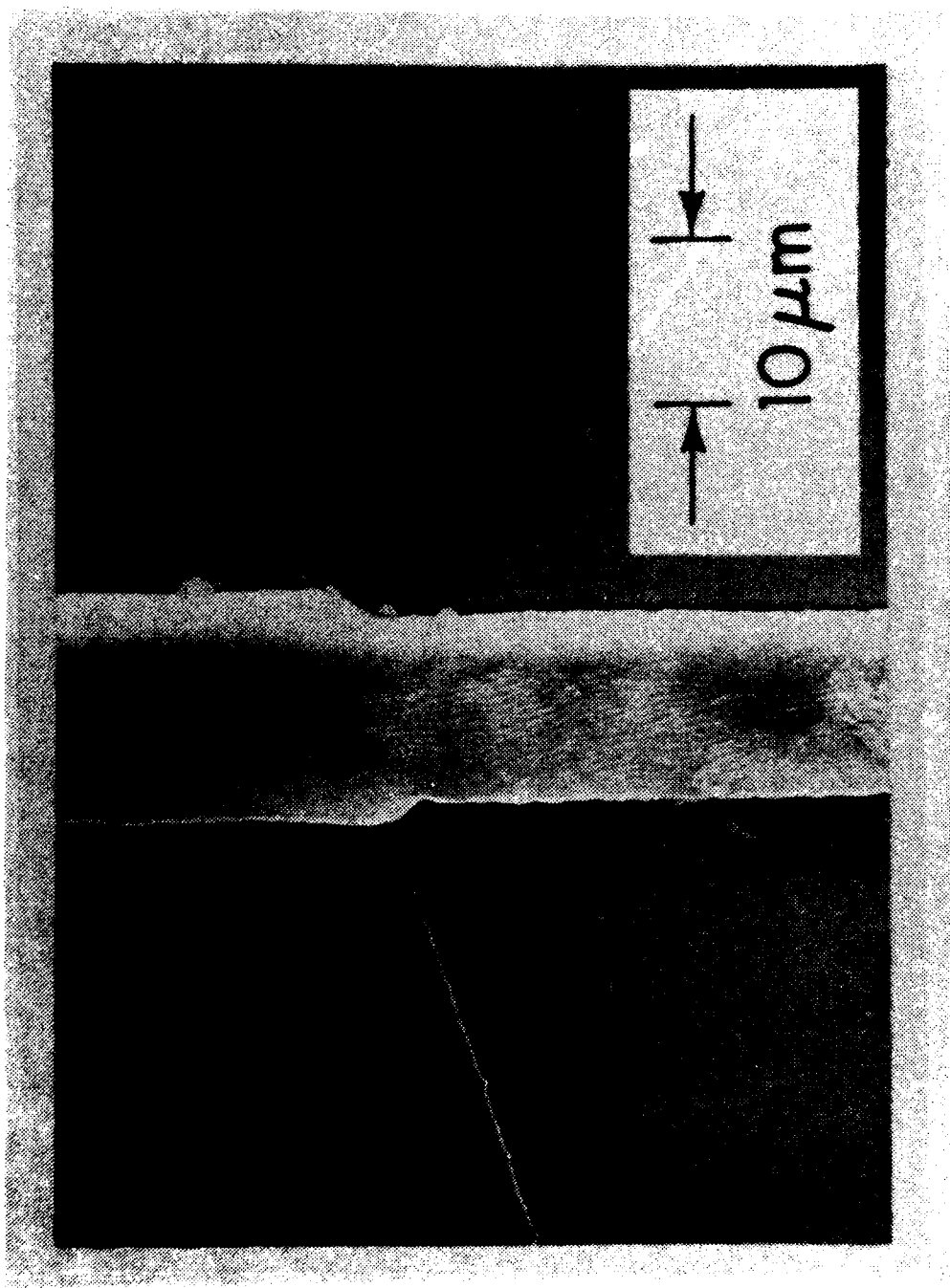
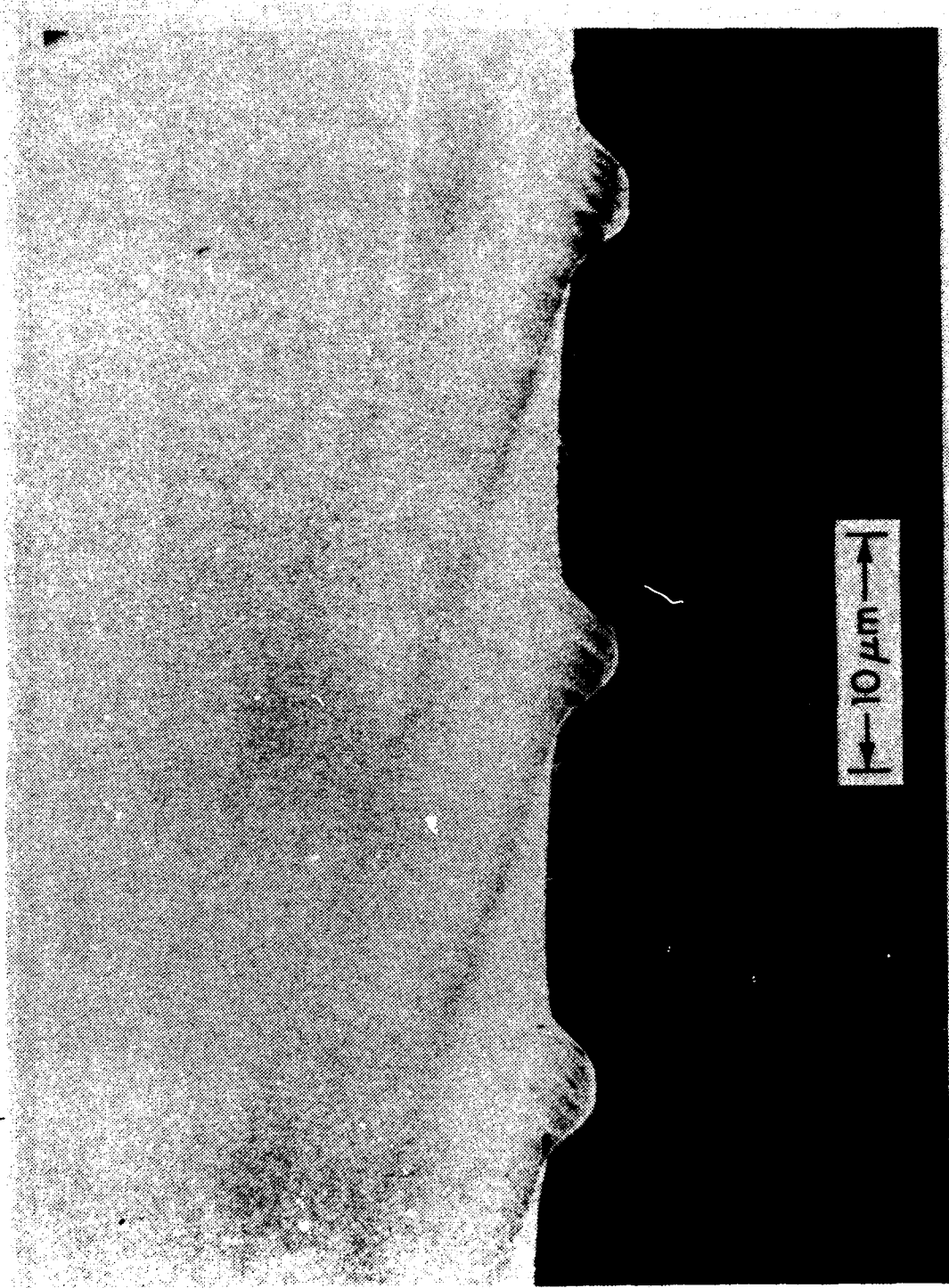


Figure 4. Laser Pyrolytically Deposited doped-Polysilicon Conductor Over Thermally Grown SiO_2 . See Ref. 5.

Figure 5. Laser Photochemically Etched Grooves in Silicon Using Cl₂ Vapor.
See Ref. 6.



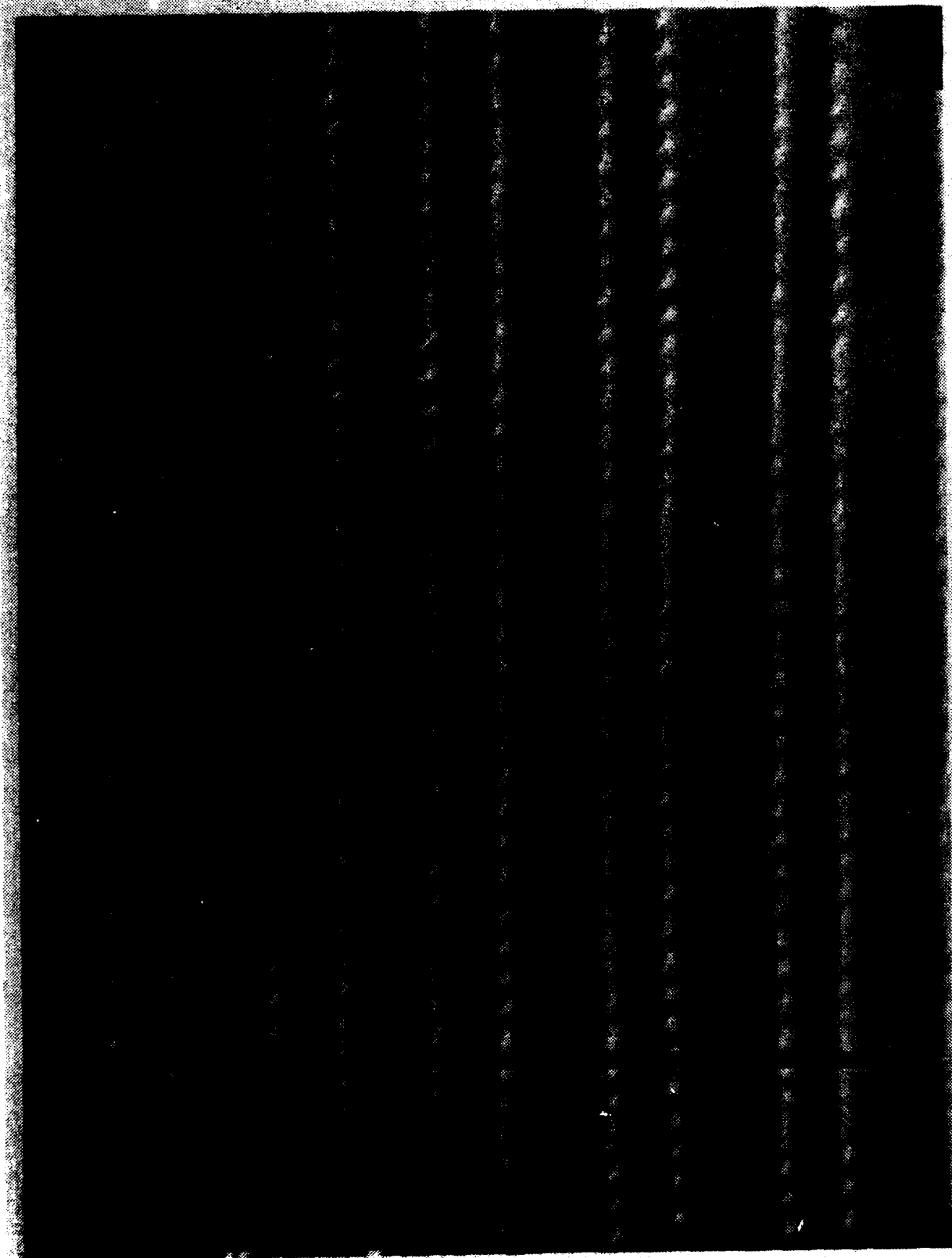


Figure 6. Boron-doped Lines in Silicon after Differential Etching. A $0.3 \mu\text{m}$ Resolution Has Been Obtained using 514.5 nm Laser Irradiation. See Ref. 7.

ADP002595

ABSTRACT

CARBON FILM RESEARCH AT AEROSPACE:
PREPARATION, CHARACTERIZATION, AND PULSED
DF LASER DAMAGE OF COATED OPTICS

S. T. Amimoto, J. S. Whittier, A. Whittaker, A. Chase
and R. Hofland, Jr.

The Aerospace Corporation
P. O. Box 92957
Los Angeles, CA 90009

April 1982

Pulsed laser damaged levels of well characterized carbon (carbyne) films produced by rapid quenching of laser heated carbon gas will be reported. These films have an average refractive index of 2, absorption coefficient varying from $8 \times 10^4 \text{ cm}^{-1}$ at $1 \mu\text{m}$ to $< 2 \times 10^3 \text{ cm}^{-1}$ at $10 \mu\text{m}$, excellent adhesion on a variety of substrates including CaF_2 , Ca , Pt, glass, Si, Ge and sapphire and high chemical resistance to corrosive acids including concentrated HF. Ion microprobe mass analysis reveal the presence of C_1^- to C_4^- carbon negative ions. For early samples produced at Aerospace, but not subjected to laser damage tests, diamond-like hardness (greater than B_4C) and adhesion strengths of $60 - 400 \text{ kg/cm}^2$ have been found.

Film thicknesses of $0.1 - 0.2 \mu$ were deposited on heated degreased bowl-feed polished 1" diameter CaF_2 windows and polished copper mirrors. Single pulsed damage levels were determined using a 2 ℓ electron-beam initiated $\text{D}_2\text{-F}_2$ chain laser. A transmission coupled unstable resonator with a soft spatial aperture gave uniform laser fluence at the optics test bench. Nominal $10 - 20 \text{ J}$ pulses in $0.6 - 0.9 \mu\text{s}$ (FWHM) were employed on fresh test sites on the half coated optics.

Single pulse DF damage levels of carbyne films on CaF_2 were determined to be 25 J/cm^2 on the best samples with damage confined primarily to localized spots containing graphitic particles. The origin of these particles was identified as the heated graphite rod used as the source of the hot carbon gas. With uncoated CaF_2 , damage levels of $21 - 27 \text{ J/cm}^2$ were measured.

For carbon films on copper, damage levels of $\sim 10 \text{ J/cm}^2$ were measured in marked contrast to uncoated OFHC Spawr copper mirrors of 58 J/cm^2 . Damage on copper was also initiated by numerous graphitic particulates. It thus appears that the removal of these particulates would result in higher pulsed damage levels in carbon films.

Despite the relatively unsophisticated technique for producing carbyne coatings, we have shown that carbyne films are attractive candidates for protective coating applications. For pulsed high energy laser applications such coatings must repetitively withstand high overpressures of 6 - 8 atmospheres of hot corrosive $\text{F}_2\text{-DF}$ gas mixtures at high laser fluence. At present no coatings are available that will simultaneously satisfy these requirements.

CARBENE FILM RESEARCH AT AEROSPACE:
PREPARATION, CHARACTERIZATION, AND PULSED DF
LASER DAMAGE OF COATED WINDOWS AND MIRRORS.

BY

S.T. AMIMOTO

THE AEROSPACE CORPORATION
P.O. BOX 92957
LOS ANGELES, CA 90009

PRESENTED AT

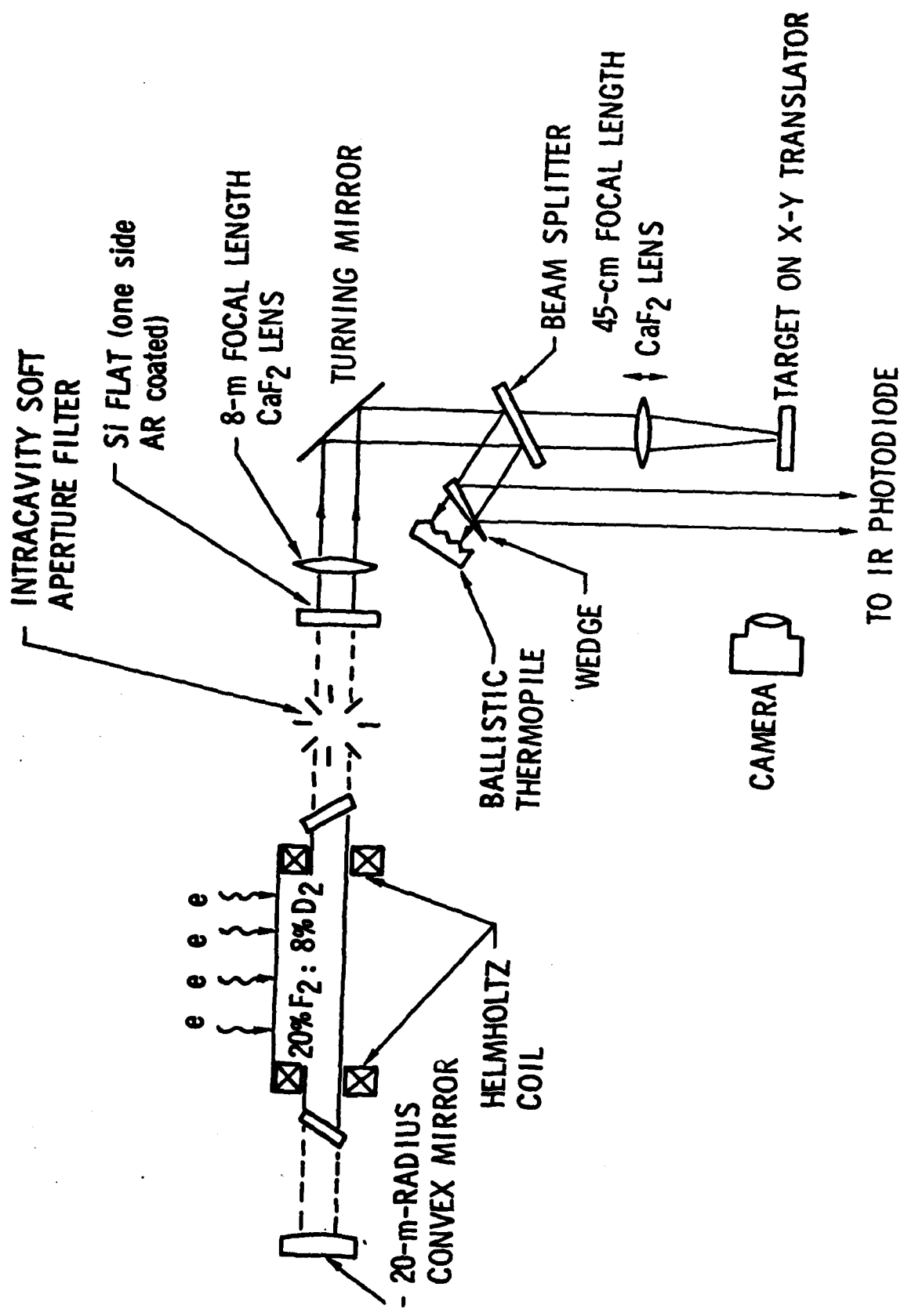
WORKSHOP ON DIAMOND-LIKE CARBON COATINGS
ALBUQUERQUE, NM

APRIL 19-20, 1982

OBJECTIVES

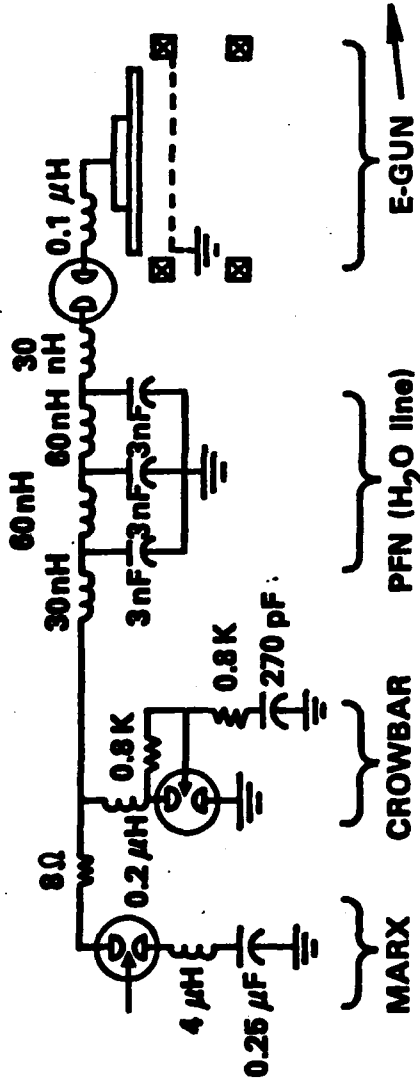
- PREPARE AND CHARACTERIZE CARBYNE FILMS ON CAF₂ AND COPPER OPTICS
 - UNDERSTAND PHYSICS OF PREPARATION
- MEASURE LARGE SPOT OF PULSED DAMAGE LEVELS USING E-BEAM INITIATED CHAIN D₂-F₂ LASER
- PROVIDE GUIDANCE TO PRODUCE MORE DAMAGE RESISTANT FILMS

EXPERIMENTAL



PULSED HF/DF LASER DEVELOPMENT

0.8 MTS MOIE / 0.5 MTS AFWL / 0.4 MTS NAVY / 0.8 MTS ARMY



(a) 20 kA, 200 kV ELECTRON GUN



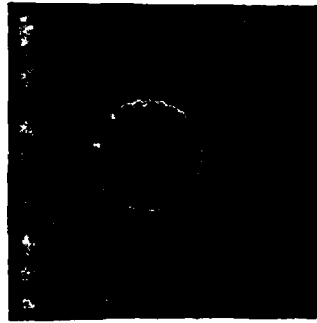
(a) PLASMA CATHODE, HELMHOLTZ COIL AND LASER CHAMBER



(b) MARX GENERATOR,
CROWBAR, AND PFN

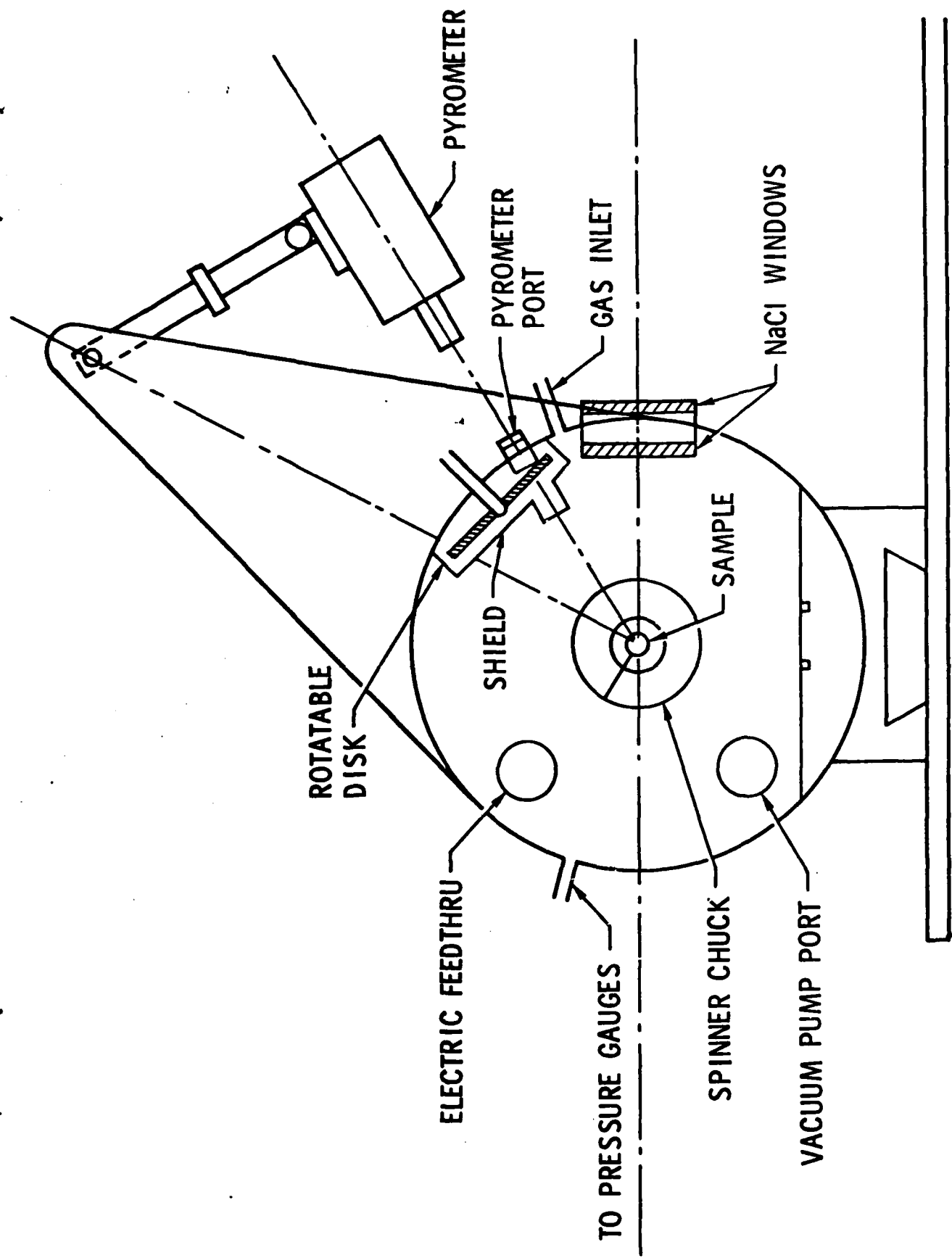
BEAM QUALITY

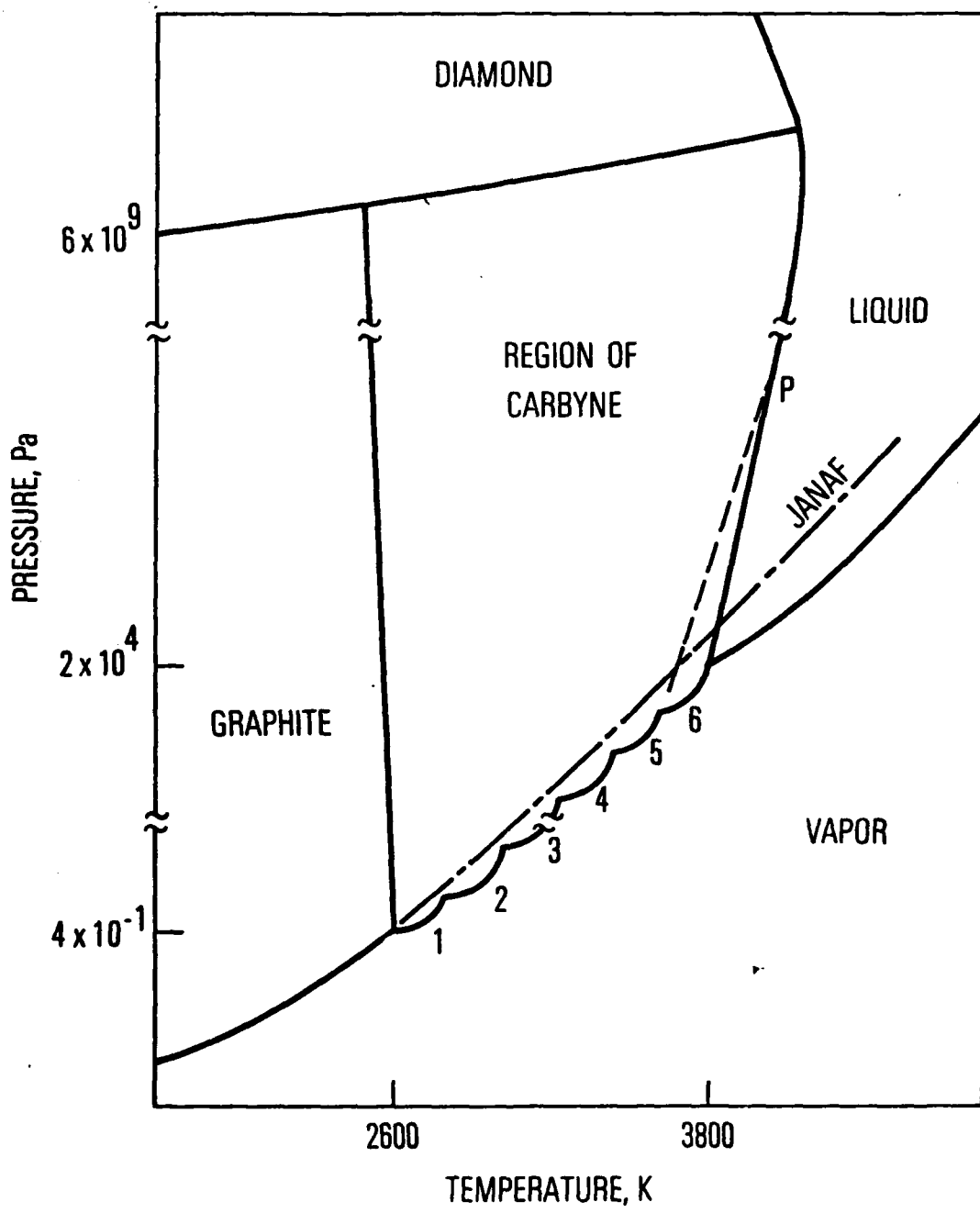
- RESONATOR
 - TRANSMISSION COUPLED; ELIMINATES MIRROR STRUTS
 - O.C. TRANSMISSION (SILICON, 1 SIDE ARC) = 70% TRANSMITTING
 - MAGNIFICATION = 1.25
- SOFT APERTURE
 - REDUCES DIFFRACTION FROM EDGE OF WINDOW HOLDERS
 - AVERAGES OVER SEVERAL FRESNEL ZONES
- FILM BURN FOR LARGE SPOT CHARACTERIZATION



3 J/cm²

DATA





AD-R136 766

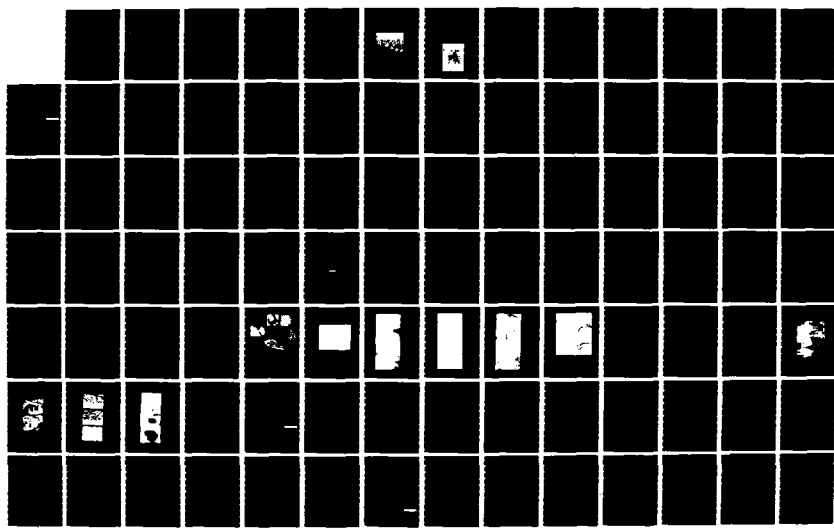
PROCEEDINGS OF THE DARPA (DEFENSE ADVANCED RESEARCH
PROJECTS AGENCY) WORK. (U) BDM CORP ALBUQUERQUE NM
B BENDOW 1982 MDA903-81-C-0151

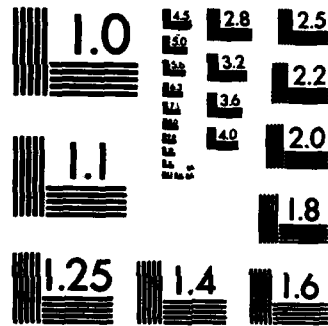
3/4

UNCLASSIFIED

F/G 11/3

NL

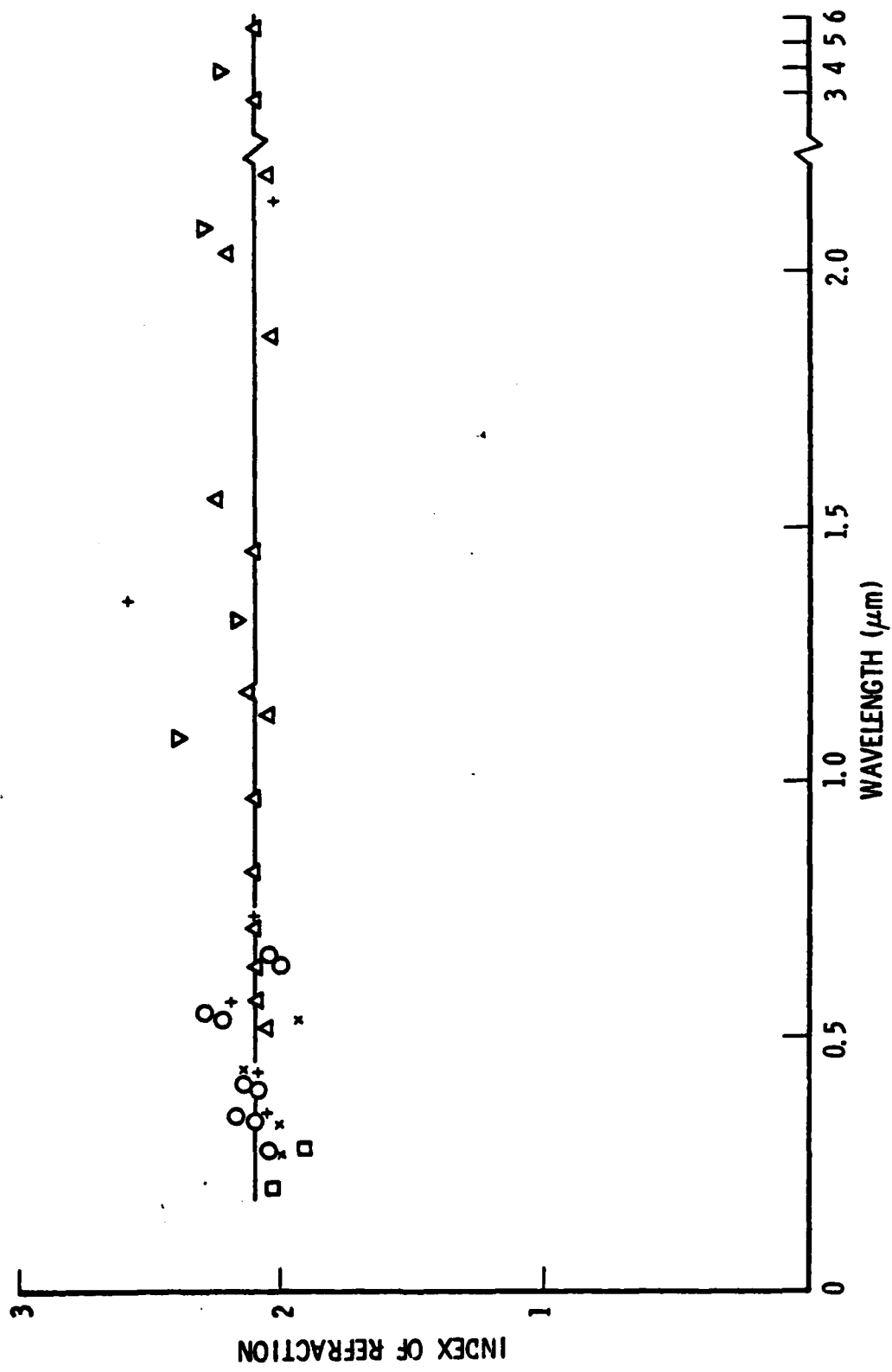




MICROCOPY RESOLUTION TEST CHART
NATIONAL BUREAU OF STANDARDS-1963-A

Film Index of Refraction vs Wavelength

CARBON FILM

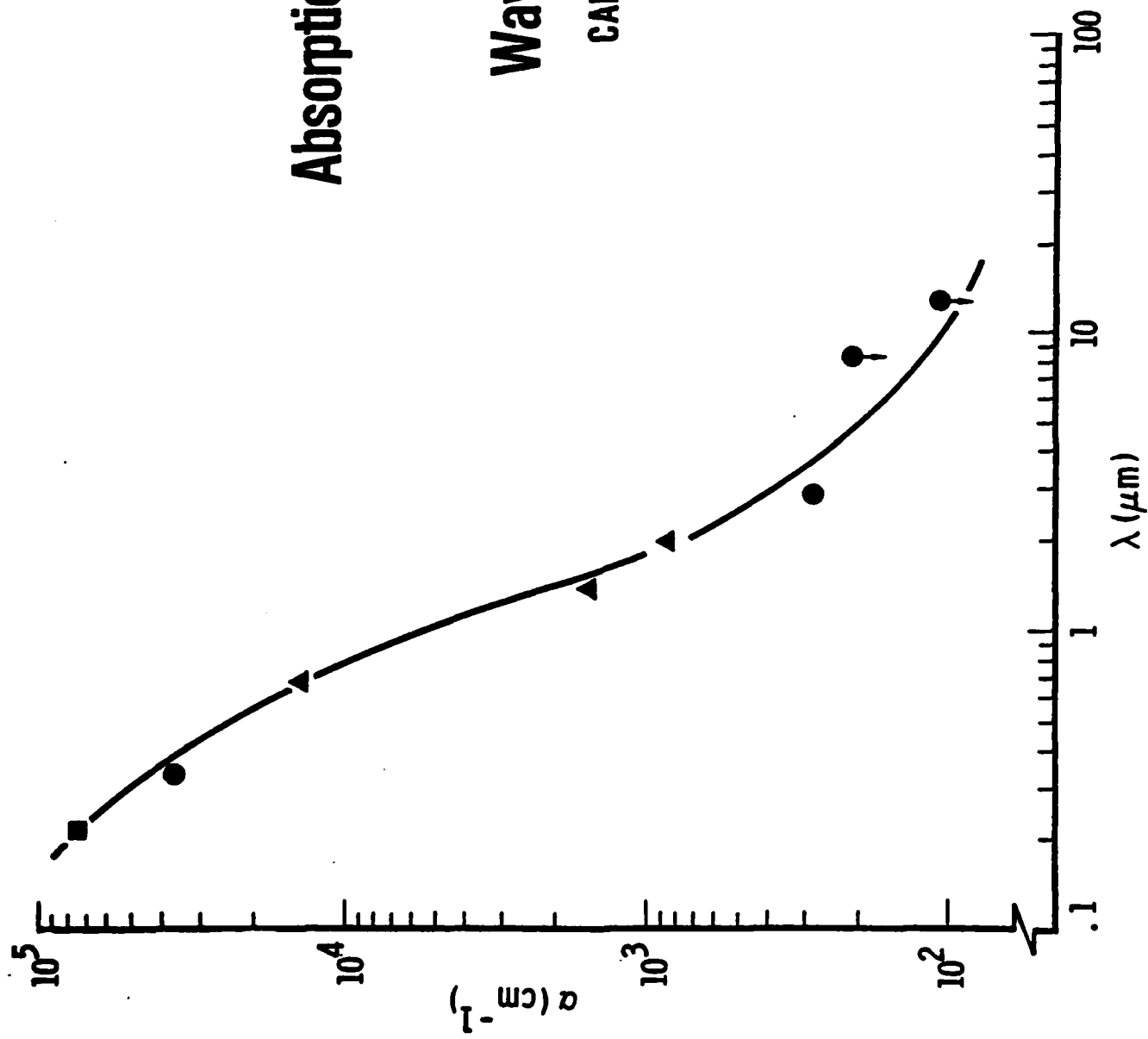


Absorption Coefficient

vs

Wavelength

CARBON FILM



CARBYNE FILM PROPERTIES

CaF_2 ADHESION: 60-440 KG/CM²

THICKNESS: 0.1-0.2 μ

IMMA: $C_1 < C_2$, $C_3 \approx C_4$

PYROMETER TEMP: 2820 K

BOWL FEED POLISH

CU THICKNESS: 0.1-0.2

PYROMETER TEMP: 2880 K

GENERAL PROPERTIES

INDEX = 2.1

HARDNESS UP TO BORON CARBIDE

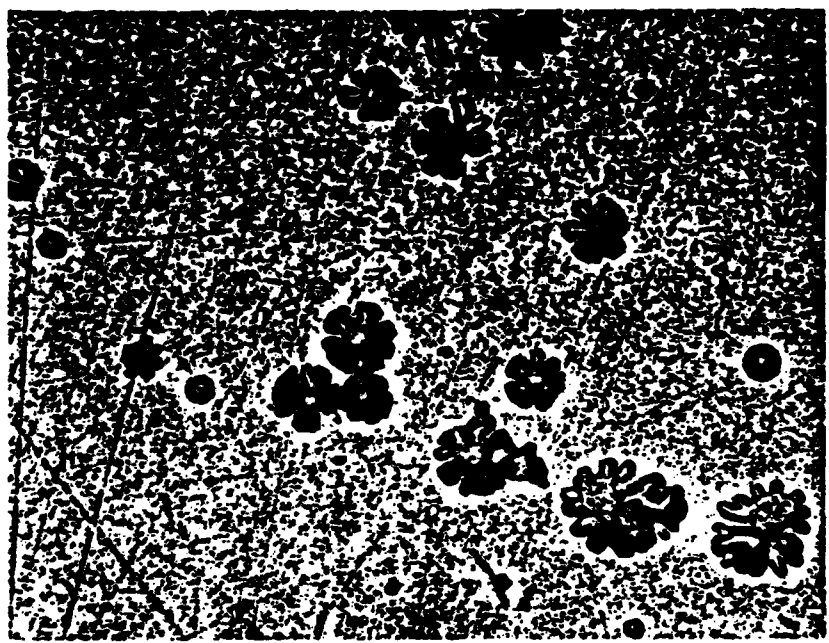
RESISTANT TO ACIDS, BASES, & ORGANIC SOLVENTS

ABSORPTION $10^2 - 2 \times 10^3 \text{ cm}^{-1}$

Table I. DF-Laser-Damage Summary Table

Substrate Thickness	Coating (Vendor)	Type of Damage	Fluence (J/cm ²)
CaF ₂ 5 mm	None	Exit surface and bulk damage at lens focus Entrance surface and bulk damage at lens focus	21 27
S ₁₈ N ₄ —	Carbyne (Aerospace) None (Spawr)	Small spot on entrance coating No visible damage Slight surface damage	14 25 58
Cu —	Carbyne (Aerospace)	Severe coating failure	9.5

CaF_2 + carbon film

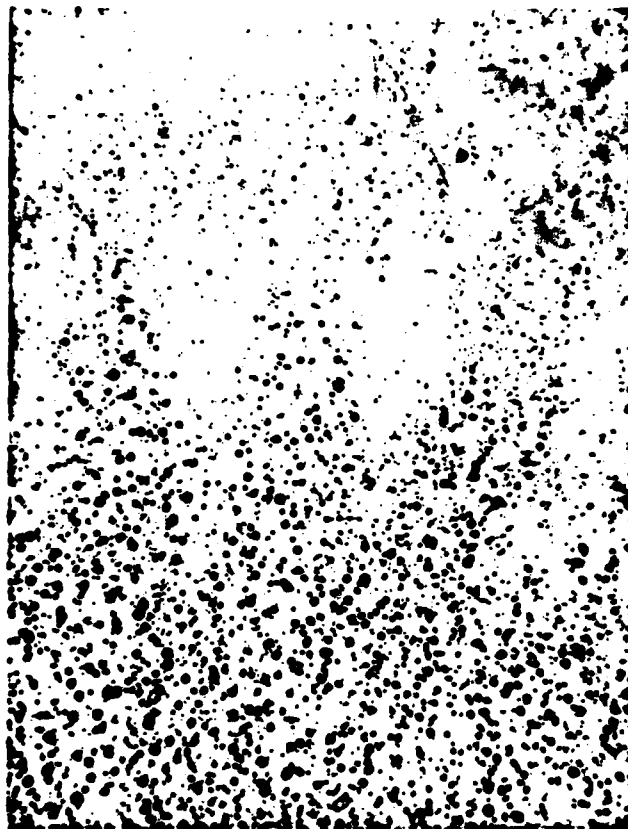


→ 100 μ ←

COATED

(a)

1 mm



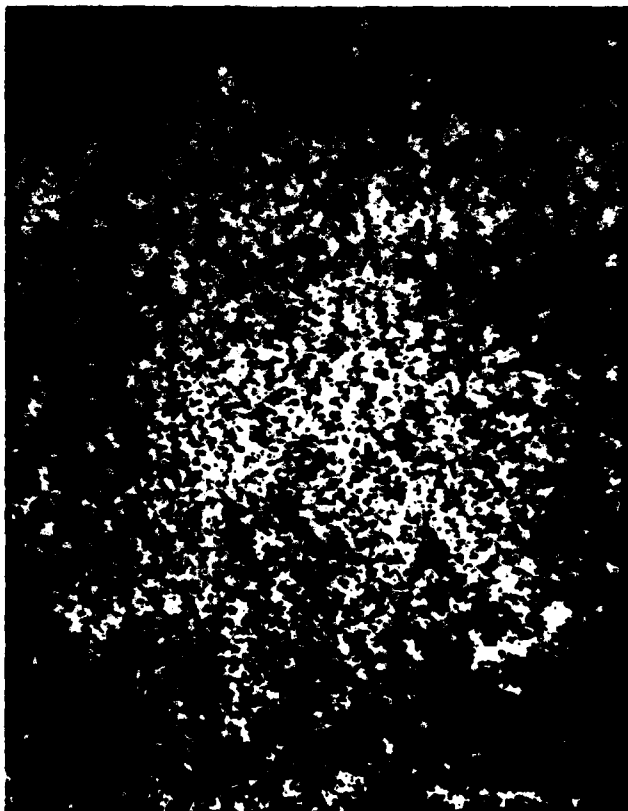
COPPER

IRRADIATED

UNCOATED

(b)

1 mm



CONCLUSIONS

- DETERMINED SINGLE PULSE DAMAGE LEVELS(0.6-0.9 μ s FWHM)
 - COATED CAF₂ 14-25 J/cm²
 - UNCOATED CAF₂ 25 J/cm²
 - COATED COPPER 10 J/cm²
 - UNCOATED COPPER 58 J/cm²
- IDENTIFIED CARBYNE FILM AS AN ATTRACTIVE PROTECTIVE FILM CANDIDATE
 - FURTHER DEVELOPMENT NECESSARY

ANNOTATIONS

VG 2 As a part of a damage evaluation study of coated optics, we have investigated the suitability of carbyne or diamond-like carbon films as window or mirror coatings. Carbon films were prepared using a laser coating process. Coated optics were then evaluated for optical damage at DF wavelengths using an electron-beam initiated D₂-F₂ chain laser. Results of this study should provide guidance in producing more damage resistance coatings.

VG 4 The laser used in this damage study was a 2 ω electron-beam-initiated pulsed chemical laser employing transverse magnetic confinement for the electron beam. An unstable resonator consisting of a convex copper mirror and a silicon flat with a soft aperture formed by an array of needles was used to obtain nearly uniform near-field pattern. A CaF₂ lens was used to vary the laser intensity at the target.

VG 5 Details of the electron accelerator are shown as an equivalent circuit. The four stage Marx bank is shown on the left. Variable pulselength is achieved with the crowbar circuit. A water coaxial line is used as a pulse forming network with a pre-pulse switch on the output (right side). A slotted cathode feed with a carbon felt cathode compatible with the confining magnetic field is used as the electron gun.

V6 6 The principles of a transmission coupled unstable resonator with a soft aperture for achieving uniform beam intensity in the near field are shown.

V6 7 Carbon film coatings are prepared using a CO₂ laser heated graphite rod held in a rotating chuck. The coating chamber pressure is typically 100 μ . Carbon gas temperature is monitored with a pyrometer.

V6 9 The phase diagram of carbon is shown. During the deposition of carbon films hot carbon gas at $\sim 2900^{\circ}\text{K}$ is quenched into the carbyne phase. The first 2 inflection points, the sixth inflection point between vapor and carbyne and the triple point have been verified. The many structures of carbynes have not been verified. The name, carbyne, originates from the presence of carbon-carbon triple bonds that have been assigned in observed spectra.. Carbon 6 is a known form of hard or diamond like carbon.

VG 10 The absorption coefficients have been measured using a spectrometer and a thickness stylus. The coefficients vary from $\sim 10^3$ cm^{-1} to 10^2 cm^{-1} as the wavelength increases from 1 to 10μ . This is consistent with observations by others. Laser calorimetry data provided by A. Hopkins is also consistent with these absorption coefficients.

VG 11 The refractive index of our carbon films is slightly larger than 2 with some scatter. These indices were measured from films placed on several substrate materials.

VG 12 The properties of carbyne films used in the present optical damage tests are listed in this vignograph. Adhesion is good on the best samples. Film thickness is 0.1 - 0.2 μ . The ion mass microprobe analyses (IMMA) showed that fragments of carbon up to a cluster of 4 atoms were present a good indication that hard carbon forms were not present.

Tests on best samples produced earlier indicate film hardness comparable to boron carbide (> Knoop 2750). Films were found to be pin hole free and resistant to acids, bases, and organic solvents; a drop of concentrated HF acid left on a sample until it evaporated produced no apparent effects.

YG 13 Damage thresholds of coated optics. Best carbon film coatings on CaF_2 were found to have damage thresholds identical to the substrate at 25 J/cm^2 . However, carbon coatings on copper were found to reduce the threshold from 58 to 10 J/cm^2 .

YG 14 Damaged areas on the best coated CaF_2 were confined to localized spots that were probably initiated by the presence of graphitic particles from the laser heated carbon rod at a fluence of 25 J/cm^2 . Production of these graphite particles from a heated graphite rod is known to occur. We believe that carbon films do show good promise as a protective film on high energy laser optics.

YG 15 On coated copper, damage was again initiated by the presence of graphite particles. In (a) the copper optics is coated but only the lower half is irradiated at 10 J/cm^2 . The uncoated portion (b) still shows the presence of graphite particles.

VG 16 The damage thresholds of coated & uncoated mirrors & windows are summarized.
We believe that carbyne films have been identified as an attractive candidate for
protective film applications. It is obvious that the graphite particles need
to be removed and that further research is required.

Coating Characterization

COATING CHARACTERIZATION

COATING CHARACTERIZATION

Thin Film Characterization Techniques Applicable to Diamond-Like Carbon Coatings

H. E. Bennett

 Michelson Laboratory, Physics Division
Naval Weapons Center, China Lake, California 93555

AD P002596

There are many properties which are of interest and should be characterized for optical thin films. Among the important parameters are (1) film thickness and index of refraction, (2) volume absorption coefficient of the film material, (3) surface absorption, (4) impurities and structure of the deposited film, (5) surface irregularities and defects, (6) light scattering, and (7) adherence, hardness, and resistance to chemical attack. Another parameter of importance in optical coatings applications is (8) thickness uniformity and resulting apparent optical figure. These various parameters and a few of the many ways to measure them will be discussed in this paper.

The film thickness and index of refraction determine its optical thickness and hence its interference characteristics. There are many ways of determining optical thickness, some of which are shown schematically in Fig. 1. One of the simplest is to run a trace of reflectance or transmittance as a function of wavelength on a spectrometer. Such a trace is shown in Fig. 2. If the film absorption is low, the depth and location in wavelength of the interference maxima or minima are determined entirely by the physical thickness and the index of refraction of the film. At the quarter-wavelength points, i.e., at the wavelength values where the film optical thickness is an odd multiple of a quarter wavelength, a maximum in reflectance will occur for a single film if the index of the film is higher than that of the substrate on which it is deposited and a minimum if it is lower. A second parameter is the magnitude of the reflectance. Since the physical thickness of the film does not vary with

wavelength, the reflectance variation can be used to track the variation in index with wavelength. In Fig. 2 a diamond-like carbon (DLC) film from RCA Laboratories is shown. It has an unusually high index which varies from nearly 2.4 at the shortest wavelengths to 2.2 at the longer wavelengths. If the film has significant absorption, the situation is more complicated. To verify the absence of significant absorption, note if the reflectance or transmission equals that of the uncoated substrate at the half-wave points on the spectral trace. If it does, the absorption coefficient of the film does not affect the measurement unless it has a strong spectral dependence.

A more precise method for determining film thickness is by interferometry, either utilizing Fizeau fringes at a single wavelength or Fringes of Equal Chromatic Order (FECO) over a range of wavelengths which is typically the visible spectrum. The commercially available Mireau interference microscope is a convenient Fizeau interferometer system for such measurements. The uncertainty in film thickness obtainable interferometrically is as low as 10 Å in the best cases. There is an ambiguity in film thickness because of the order of interference, so a preliminary value of film thickness is required. It can be obtained, for example, from the spectrophotometer measurements just described. To remove the effect of the index of refraction on the Fizeau or FECO measurements, the substrate, half of which is coated by the film, should be overcoated with an opaque layer of silver.

Another very precise method for determining film thickness and index of refraction is ellipsometry, which is also illustrated in Fig. 1. Again, the optical constants of the substrate should be well known or the substrate should be only half coated with the film. A very useful combination of measurements is ellipsometry plus interferometry. The absolute film thickness can be determined

interferometrically and then the optical constants for the film determined ellipsometrically with very high precision. Both the real and imaginary parts of the index of refraction can be determined in this way.

There are various other techniques for determining film thickness which could be mentioned. One of the more useful is taper sectioning, which can be used to determine the thicknesses of either single or multilayer films. An inclined plane is produced on the substrate, for example, by rotating an abrasive-covered ball, and the film thickness is simply read with a scanning microscope as shown schematically in Fig. 1.

Another key optical parameter is the volume absorption coefficient of the film. As discussed above, it can be determined from ellipsometry. Other techniques are illustrated in Fig. 3. Gross absorption can be determined from a spectrophotometer trace. Smaller absorption requires more precise measurement techniques. One of them, modulated spectroscopy using either the variation in reflectance with temperature or with wavelength, can detect absorption levels in favorable circumstances as low as a few parts in 10^5 . Emittance measurements, where the radiation from the sample is measured spectrally, have nearly the same sensitivity as modulation spectroscopy. Emittance measurements have the advantage that the absorption can be determined when the sample is at several hundred degrees centigrade. Perhaps the simplest appearing measurement technique is calorimetry. Light passes through the film-coated sample and also an uncoated portion of the sample and the temperature rise is noted. The absorption coefficient follows. Calorimetry is a very sensitive technique and can detect absorption levels of 10^4 or less. It is subject to various sources of systematic error, however, which, unless precautions are taken, limits its reliability. The most accurate calorimetric technique appears to be adiabatic calorimetry. Most sources of error are eliminated by maintaining the sample and

its environment at the same temperature and monitoring its rise in vacuum. Internal reflection spectroscopy and photoacoustic spectroscopy are two other very accurate techniques for measuring film absorption. Considerable interpretation of the data obtained is required, but the final results can be excellent. As a general practice, it seems best to use at least two of the above independent techniques. If the results agree, there is some confidence that they are not substantially in error.

Often ignored in absorption measurements on thin films is the presence of surface absorption. The absorbing layers are typically less than a hundred angstroms thick, so the absorption coefficients of these layers must be enormous. Some techniques for evaluating surface absorption are shown in Fig. 4. Calorimetry using a wedged film as a sample and extrapolating to zero film thickness is one very useful technique. Situations have occurred where virtually all of the absorption in the film was at the surface, and much effort has been expended to reduce the contaminant level in the evaporant powder when in fact it was not the problem at all. Various authors have studied the surface absorption problem. Dr. Paul Temple of Michelson Laboratory, Naval Weapons Center (NWC), has developed a calorimetric technique for not only separating bulk and surface absorption in films but also for determining at which surface the absorption occurs. Attenuated total reflection (ATR) spectroscopy is another technique for sampling surface absorption. By varying the angle of incidence near the critical angle, the penetration of the standing wave electric field can be varied and the absorption sampled as a function of film depth. The depth of the contaminant atoms causing surface absorption can be determined by two other techniques in use at NWC: nuclear resonance spectroscopy and profiling secondary ion mass spectroscopy. Both are illustrated in Fig. 4.

The identity of contaminant atoms causing either surface or volume absorption can be determined in various ways. Structural information about the film composition can also often be obtained using some of the techniques shown schematically in Fig. 5. The electron spectroscopies, such as secondary ion mass spectroscopy (SIMS), Auger electron spectroscopy (AES), and x-ray photoemission spectroscopy (XPS), sometimes called electron spectroscopy for chemical analysis (ESCA), can be used to evaluate surface layers only a few angstroms in depth. By incorporating a profiling argon-ion gun to penetrate the film, this analysis can be carried through the entire film structure. Structural information may be obtained from electron diffraction, either low energy (LEED) or reflection high energy (RHEED) spectroscopy. Structure can also be examined in detail using electron microscopy, either scanning electron microscopy (SEM) or transmission electron microscopy (TEM) combined with replication. A mass analyzer may be combined with an electron microscope to yield the identity of the atoms whose structure is being observed. Nuclear techniques such as Rutherford backscattering (RBS), neutron activation analysis (NAA), and the nuclear resonance techniques described previously can also be used to identify impurities and determine their position. One of the newest analysis techniques is laser desorption. Dr. J. O. Porteus of NWC, in collaboration with Dr. Susan Allen of the University of Southern California, has developed this technique and has used it to determine how tightly bound water is to a surface. The instrument is shown schematically in Fig. 6. A quadrupole mass analyzer (QMA) is used to detect the amount and composition of atoms desorbed from the sample surface by a laser beam of known intensity. A plot of water desorbed from a polished CaF_2 surface as a function of on-axis energy density of the laser beam operating at a wavelength of $2.7 \mu\text{m}$ is shown in Fig. 7. Much of the water is desorbed at very low energies, but

the last of the water does not desorb until the single-shot damage threshold of the sample is exceeded. Work relating these results to the binding energy of these contaminant atoms is in progress.

Surface irregularities and defects in a deposited film may be evaluated using optical microscopy or interferometry. To resolve height differences down to about 10 Å, an interference microscopy technique such as Nomarski differential interference contrast (DIC) is required. The Mireau interferometer is another approach to the problem. It employs two beam interference fringes from a very smooth reference mounted on the microscope objective as illustrated in Fig. 8. A heterodyne Mireau interferometer which evaluates surface irregularities and gives their height distribution and autocovariance functions has been developed by Professor J. Wyant of the Optical Sciences Center, University of Arizona, and will be set up at NWC this fall. Its operation will be checked using an NWC stylus profiling instrument, whose lateral resolution is as small as 0.1 µm. An alternate technique useful for determining the rms surface roughness of large areas is total integrated scatter (TIS) measurement. The rms roughness obtained using this technique is in good agreement with that obtained using FECO interferometry or stylus profiling measurements.

Scattered light is an important parameter in evaluating the performance of optical thin films. TIS can be measured using either a Coblentz sphere or an integrating sphere, as illustrated in Fig. 9. Often the imaging quality of the coated optic or its scatter in a given direction, rather than scatter in all directions, is the key parameter. In laser gyro systems, for example, back-scattering along the direction from which the beam has come is a limiting parameter governing laser gyro performance. The angular dependence of scattered light can be measured by determining the bidirectional reflectance distribution

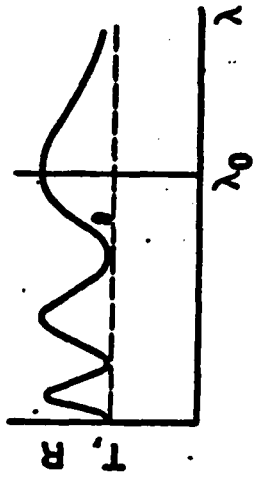
function (BRDF), as illustrated in Fig. 9. However, the imaging quality of a film is usually dependent on very near angle scattering and can best be determined by measuring the modulation transfer function (MTF) and the blur circle. Various kinds of MTF facilities are available commercially. At NWC we have the EROS-IV, a very large MTF instrument which is made for evaluation in the visible region. We also have an infrared MTF measurement facility for longer wavelength evaluations.

Most of this survey has addressed problems associated with the optical performance of a thin film coating. There are also many tests associated with its physical, mechanical, chemical, and thermal properties. Figure 10 describes some of these tests. Adhesion is an important film characteristic. The standard test for adhesion is the scotch tape test. The scratch test checks abrasion resistance. The sand erosion test is standardized and easily set up. Rain erosion tests or particulate tests are much more difficult and require specialized laboratory facilities. Humidity, salt spray, and corrosive gas tests are readily made. Film stress tests are important and can be made quantitatively using the cat's eye interferometer approach developed at Perkin-Elmer and now used in various laboratories.

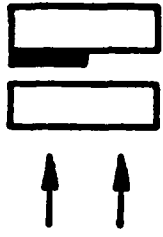
Thickness uniformity is an important parameter when thin film coatings are actually used on optical components. A change in thickness of only 1% can affect the phase change on reflection of a multilayer dielectric film and hence can change the effective optical figure of the component. Figure errors translate into wave front errors and hence focal spot intensity for the output laser beam. The coating conditions required to produce uniform films are thus important. Wave front errors can be determined interferometrically or photometrically using equipment operating at the wavelength of use. However, ellipsometry appears to be the method of choice.

This brief survey covers some of the techniques for thin film evaluation and characterization. Many are very powerful techniques; however, systematic errors can occur in all and it is prudent to use two or more independent techniques whenever possible to determine important thin film parameters.

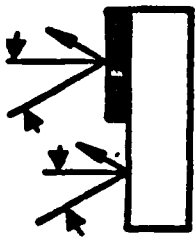
• SPECTROPHOTOMETER



• INTERFEROMETER



• ELLIPSOMETER



• TAPERSECTIONING

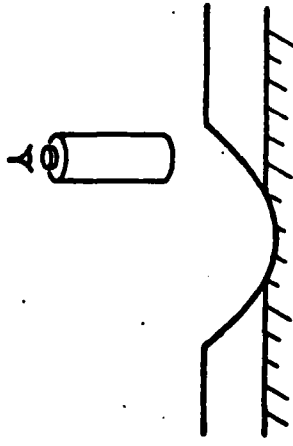


Figure 1. Thickness and Index

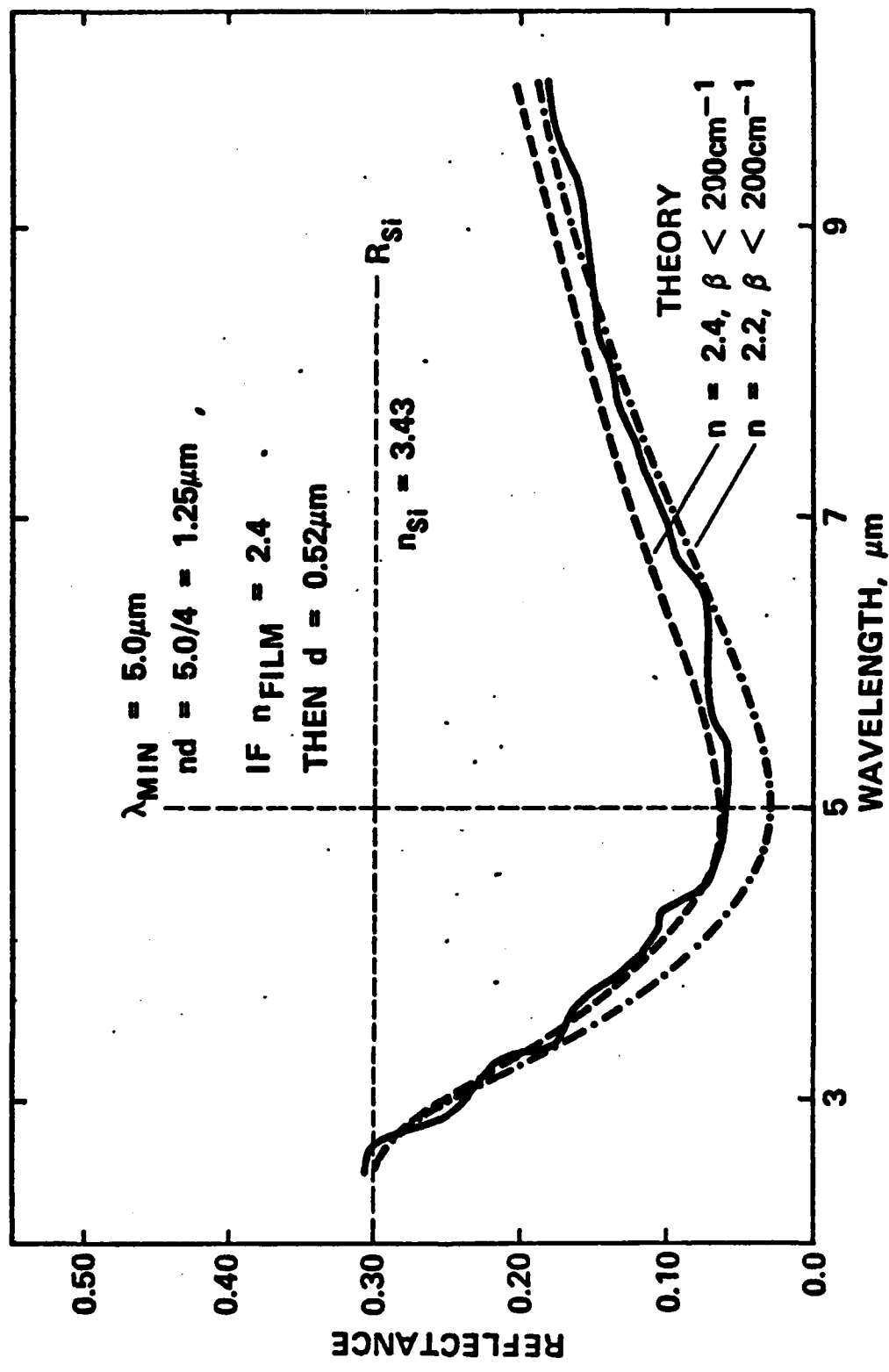


Figure 2. Optical Thickness of Hard Carbon Film on Silicon

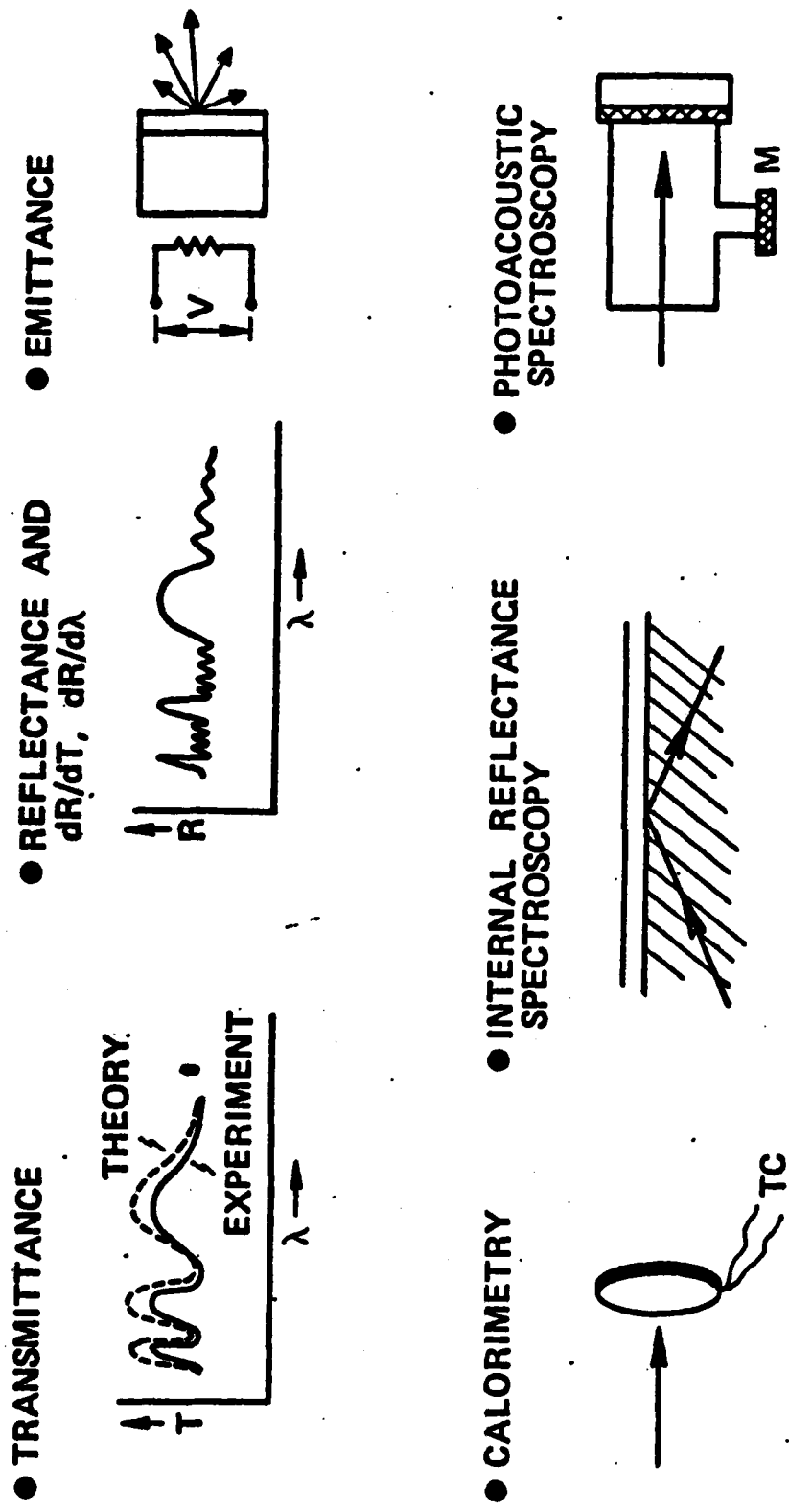
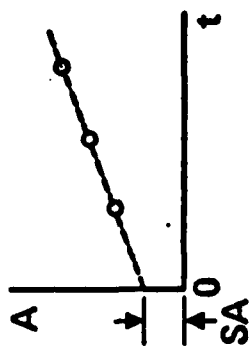
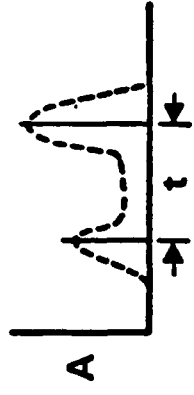


Figure 3. Absorption Coefficient

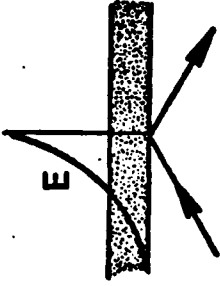
• CALORIMETRY



• NUCLEAR RESONANCE FOR H^+



• ATR

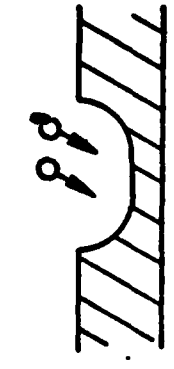


• PROFILING SIMS

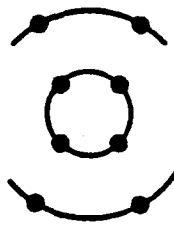


Figure 4. Surface Absorption

- ELECTRON SPECTROSCOPIES
AES, XPS (ESCA), SIMS
WITH PROFILING



- ELECTRON DIFFRACTION
LEED, RHEED



- ELECTRON MICROSCOPY
SEM, TEM, EPMA,
REPLICATION

- NUCLEAR TECHNIQUES
RBS, NAA, NUCLEAR
RESONANCE

- LASER DESORPTION

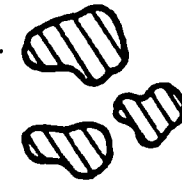
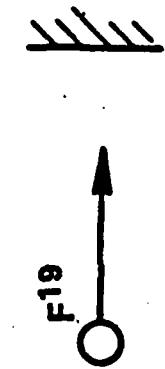


Figure 5. Impurities and Structure

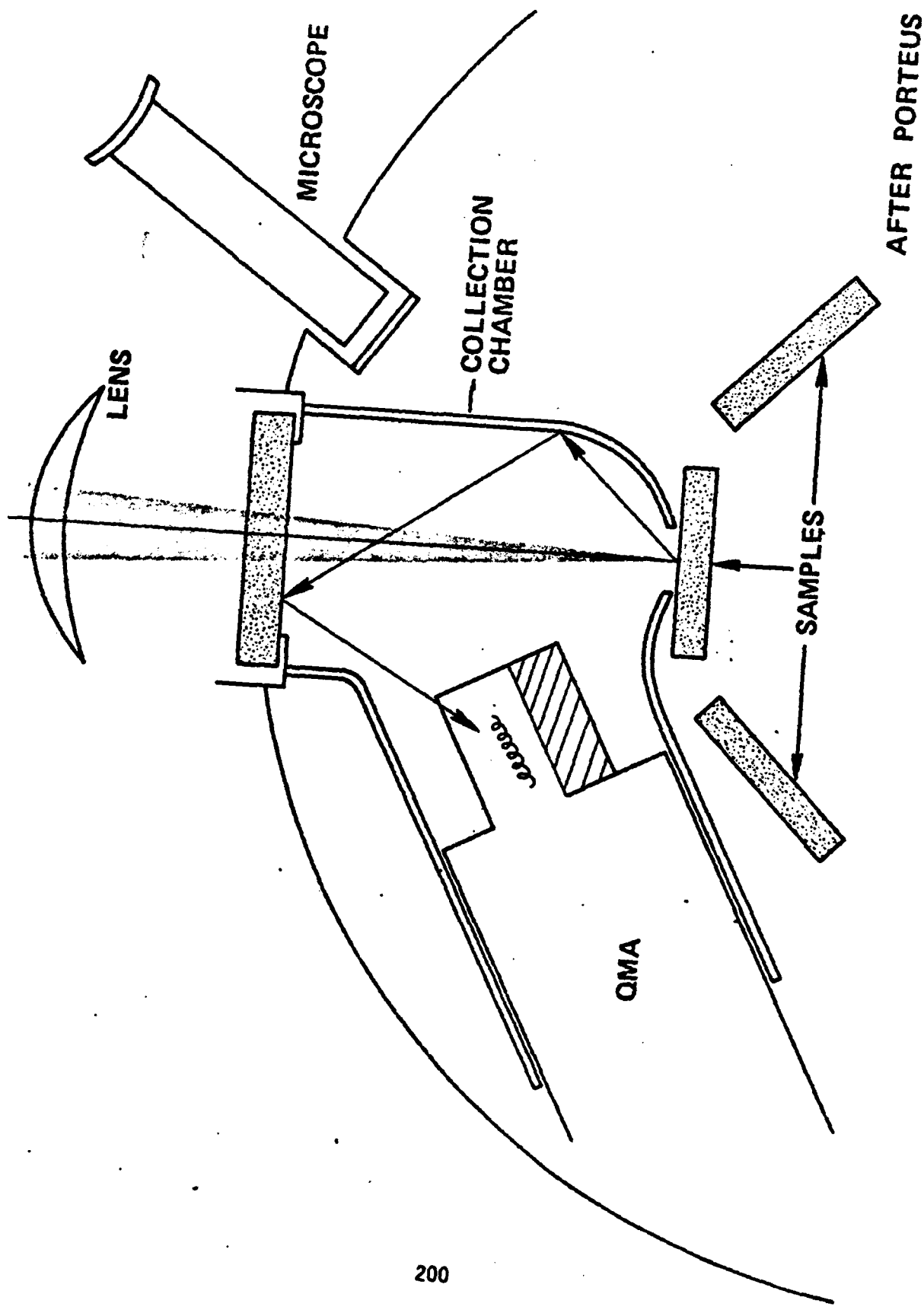


Figure 6. Laser Desorption Apparatus

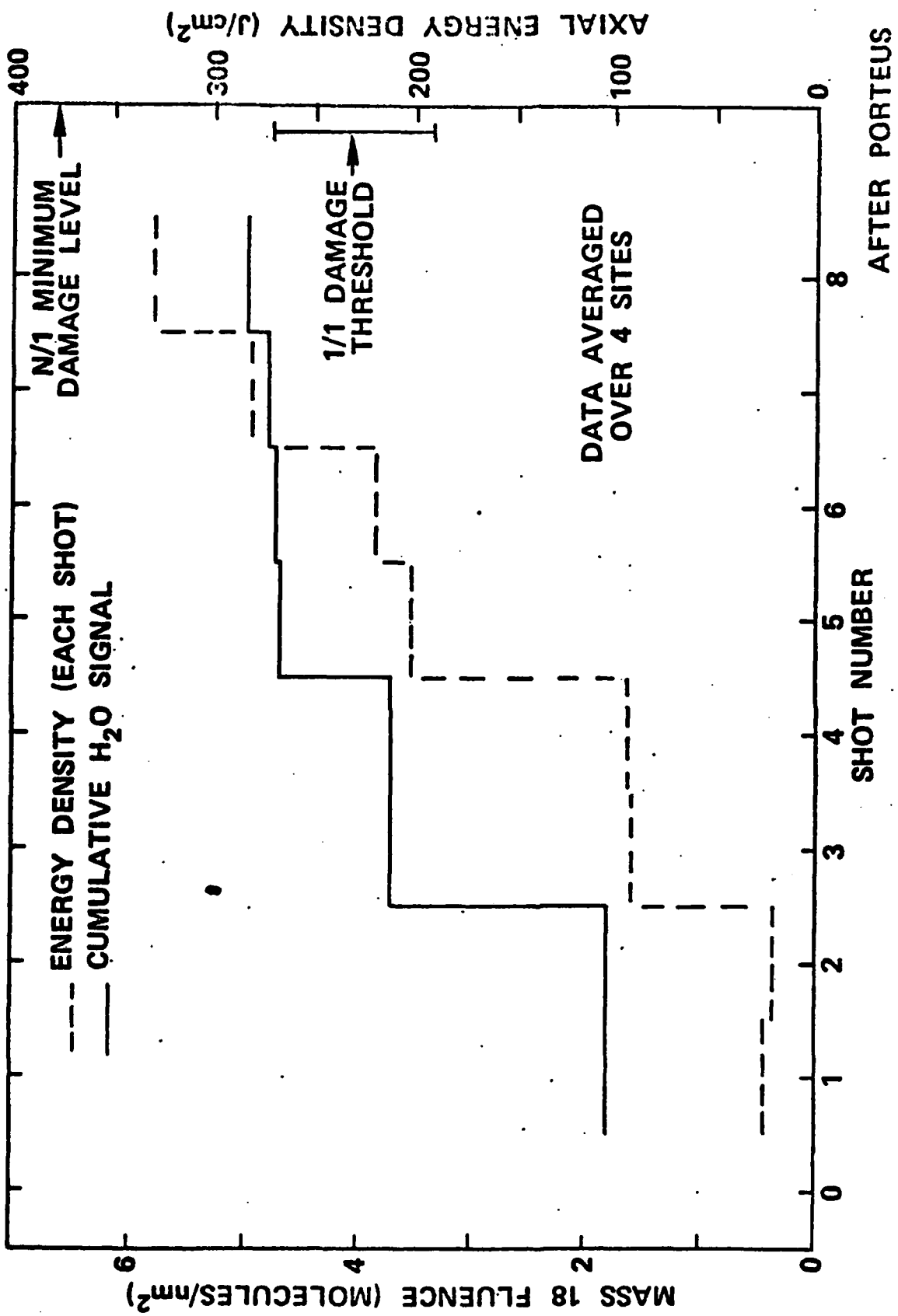
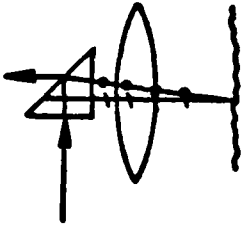


Figure 7. H_2O Desorption from CaF_2 at $2.7 \mu\text{m}$ (N/1)

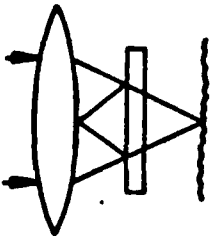
● DIC. (NOMARSKI)
MICROSCOPY



● FECO, FIZEAU
INTERFEROMETER



● MIREAU HETERODYNE



● STYLUS PROFILING



● TIS EVALUATION

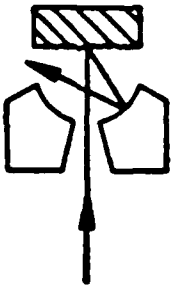


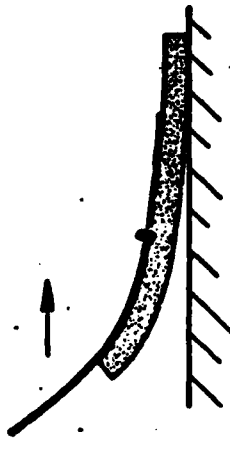
Figure 8. Surface Irregularities and Defects

- TOTAL INTEGRATED SCATTER (TIS)
- COBLENZ SPHERE
- INTEGRATING SPHERE
- ANGULAR DEPENDENCE OF SCATTER (BRDF)
- NEAR ANGLE SCATTER (MTF)

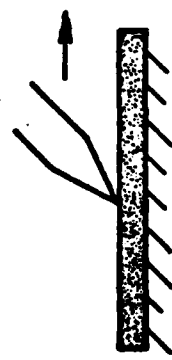
The figure contains five bullet points corresponding to different types of light scattering. Each point is accompanied by a small diagram. The first two diagrams show spheres with various patterns (grid, grid with central axis, shaded cone) to represent different measurement or conceptual models. The last three diagrams are graphs showing the angular dependence of scattering.

Figure 9. Light Scattering

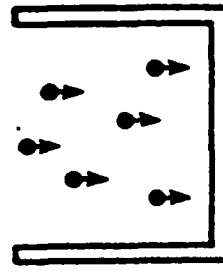
● SCOTCH TAPE TEST



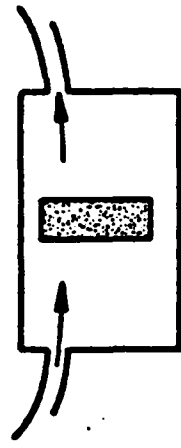
● SCRATCH TEST



● EROSION TESTS



● HUMIDITY CORROSIVE GAS



- DROPPING SAND
- WATER DROPLET
- ULTRASONIC IRRADIATION

Figure 10. Adherence, Hardness, and Resistance to Chemical Attack

DIAMONDLIKE CARBON FILMS IN OPTICAL COATINGS

H. A. Macleod

Optical Sciences Center
University of Arizona
Tucson, Arizona 85721

AD P 002597

The features of conventional thin films which are known to be of importance in optical coatings ~~are discussed as~~ might be useful indicators of properties which could be used as characterization parameters for diamondlike carbon films.

Once regions of transparency and optical constants have been determined, I believe that the most important characteristics for a useful optical thin-film material can all be classified under the heading of stability. I define a stable film as one which exhibits properties which are single valued functions of the film environment, which implies the classification of any variation of properties with time, or any hysteresis in the properties of a material, as a lack of stability. Most film materials in current use suffer from defects of stability, and a knowledge of their defects can guide us in assessing the potential of a new material, such as diamondlike carbon, in optical coatings. Note that a sensitivity of properties to environmental conditions is not classified as instability as long as it is single-valued and predictable.

Let us first of all consider the symptoms and causes of thin-film instability. Instability may take many forms, two of the principal ones being optical and mechanical. Optical instability shows itself first as a shift in the properties of a coating towards longer wavelengths when it is exposed to the atmosphere after deposition. The shift may be rapid, taking a few minutes, or slow, taking many days.^{1,2} This particular effect is caused by moisture adsorption. The moisture can desorb, especially during temperature cycling, which causes a shift towards shorter wavelengths competing with and usually exceeding the normal shift towards longer wavelengths with increasing temperature.³ Considerable hysteresis of quite unpredictable nature results. Laser damage phenomena are well known but there are also subtle effects which occur at very much lower values of flux, especially in the ultraviolet. Zinc sulphide and silicon oxide are two materials much studied in this respect.^{4,5}

Then there are mechanical effects such as lack of durability which can be classified as a lack of stability under mechanical stress. Perhaps the most frustrating and exasperating type of mechanical instability is delamination, an insidious problem which often creeps in some time after manufacture with no apparent change in environmental conditions. These two effects represent irreversible changes of the worst possible kind because the component is actually destroyed.

Delamination is of course an adhesion failure, but in thin films it is characterized by a progressive rather than sudden detachment of film material, otherwise known as peeling. In peeling, it is the work which must be done to cause the failure rather than the force which must be exerted which is the important quantity.⁶ Thus, although the forces which hold thin films to each other and to the substrate are extremely high, they are all short range forces, atom to atom or molecule, and the work which must be done to break them correspondingly small. We can equate the work which must be done, the work of adhesion, to the surface energy which is created by the exposure of the fresh surfaces in the failure, together with any energy lost in, for instance, plastic deformation of the film or substrate. In the case of Van der Waals bonds the new surface energy is of the order of 0.1J/m². Chemical bonds will be much greater, at least an order of magnitude or so. Thin films are usually in a state of some considerable stress which is accompanied by the storing of considerable strain energy. This stress is a mixture of intrinsic, which appears during deposition at constant temperature, and extrinsic which is a consequence of subsequent differential contraction or expansion of film and substrate. We can take a level of 10⁸Pa for intrinsic stress and assume, say, 5x10¹⁰Pa for Young's modulus.⁷ These figures are typical (and are within the range measured by Ledger and Bastien for ThF₄ films⁸). Then for a biaxial stress the strain energy is given roughly by

$$\frac{(10^8)^2}{5 \times 10^{10}} = 2 \times 10^5 \text{ J m}^{-3}$$

(assuming zero Poisson's ratio and neglecting any deformation of the substrate). This gives an energy for a 2μm thick film of 0.4Jm⁻² which is more energy than we need to balance the work which will be required to drive a peel adhesion failure with Van der Waals bonds. With chemical bonds which are bound to be involved in any durable thin film system, the energy will be required to be much higher, but differential contraction or expansion can easily double or triple the stress levels. Whether or not adhesion failures will actually take place depends on the magnitude of the forces acting to rupture the bonds and usually a stress concentrator is required which can be a defect in the film or even the edge of the film.

These different effects are closely related to film microstructure. Thin-film microstructure is a columnar one, the columns being more or less loosely packed so that pores exist between them, running through the thickness of the films in the direction of growth.^{9,10} In films of thicknesses typical of coatings for the visible region, we can infer the existence of these pores from adsorption isotherms which show features characteristic of capillary condensation in pores of radii around 2 to 5nm.¹¹ When a film is exposed to a humid atmosphere, the adsorption of moisture

of index around 1.33 replacing gas of index unity, increases the index of the film as a whole. Desorption of moisture, with decreasing index, occurs as the humidity falls, but there is usually considerable and largely unpredictable hysteresis and the tightly bound water, over the internal surface of the film, desorbs only at very high temperatures. The behavior of multilayer structures is more complex than single films. The interfaces between layers slow down the entry and emission of water which tends to penetrate into the multilayer at isolated sites and then spread out across the layers and many of the features of the optical instability of multilayers exposed to the atmosphere can be explained as a progressive widening of patches with optical characteristics shifted to a longer wavelength.¹

Moisture adsorption has serious mechanical consequences. It is the forces acting across the gaps between the grains which transmit the stress in the film, and indeed are now considered to be the origin of the intrinsic stress,¹² and it is these forces which help the films to resist the effects of abrasion. Anything which affects these forces will affect film durability and film stress level. Adsorbed moisture blocks these forces, usually reducing durability and stress. The most severe durability testing is that carried out on a thin film immediately after exposure to high humidity. Adsorbed moisture also affects film adhesion. Since moisture reduces the surface energy of freshly exposed surfaces, it can reduce the work necessary to cause the propagation of a peel adhesion failure, and in the case of the high energy solids, such as the oxides commonly used as thin film materials, the reduction can be severe. The water must be present at the actual site of the bond rupture and take part in a process of bond exchange rather than rupture followed by adsorption. Water is most likely to be present at the site of a failure when it occurs at the edge of a coating, and the progression of peeling from the edge towards the center is a common mode of failure. Another possible site is right in the center of a moisture adsorption patch where liquid water is present and where there is a water-admitting defect which might act as a stress concentrator. Blistering, which is a common form of delamination, appears to be initiated in this way.¹

What then are the implications for diamondlike carbon films as elements of optical coatings? After such things as optical constants, regions of transparency and consistency of production are established, I believe that the most important questions are concerned with the potential stability of the films and especially:

- (a) what is the packing density of the films?
- (b) what are the main features of the microstructure?
- (c) what is the adsorption behavior?

References

1. H. A. Macleod and D. Richmond, "Moisture penetration patterns in thin films," *Thin Solid Films* 37, 163 (1976).
2. T. M. Christmas and D. Richmond, "The durability and stability of evaporated thin film filters," *Optics and Laser Technology* 9, 109 (1977).
3. E. Pelletier, P. Roche and L. Bertrand, "On the limiting bandwidth of interference filters: influence of temperature during production," *Optica Acta* 21, 927 (1974).
4. G. Hass, J. B. Heaney, W. R. Hunter and D. W. Angel, "Effect of UV irradiation on evaporated ZnS films," *Appl. Opt.* 19, 2480 (1980).
5. A. P. Bradford, G. Hass, M. McFarland and E. Ritter, "Effect of ultraviolet irradiation on the optical properties of silicon oxide films," *Appl. Opt.* 4, 971 (1965).
6. E. Orowan, "The physical basis of adhesion," *J. Franklin Inst.* 290, 493 (1970).
7. K. L. Chopra, Thin Film Phenomena, McGraw Hill Book Co., New York and London (1969).
8. A. M. Ledger and R. C. Bastien, "Intrinsic and thermal stress modeling for thin-film multilayers," Technical Report, Contract DAA25-76-C-0410 (DARPA), The Perkin-Elmer Corporation, Norwalk, CT, June 1977.
9. H. A. Macleod, "Microstructure of optical thin films," *In Optical Thin Films*, R. I. Seddon (ed.), Proceedings of the Society of Photo-Optical Instrumentation Engineers 325, 21 (1982).
10. K. H. Guenther, "Columnar and nodular growth of thin films," Paper 346-02 in the Washington meeting on thin films 1982 (to be published in the Proceedings of the SPIE).
11. S. Ogura and H. A. Macleod, "Water sorption phenomena in optical thin films," *Thin Solid Films* 34, 371 (1976).
12. H. K. Pulker, "Stress, adherence, hardness and density of optical thin films," *In Optical Thin Films*, R. I. Seddon (ed.), Proceedings of the Society of Photo-Optical Instrumentation Engineers 325, 84 (1982).



Surface Analysis of Diamond-like Carbon Films

A. K. Green and Victor Rehn
Naval Weapons Center
China Lake, California 93555

AD P002598

There has been considerable interest recently in carbon films because of several unusual properties reported. Some of these properties, such as the optical absorption edge¹⁻² and the valence-band structure,³⁻⁴ are similar to those of diamond. Thus the appellation "diamond-like carbon" (DLC) films has developed, along with a host of suggested applications for films with such unusual properties. DLC films have been shown to be much harder than graphite or amorphous-carbon films, suggesting application in wear reduction.⁵⁻⁶ The wide band gap suggests application as an optical, passivating or insulating coating.^{1,5} Their good physical strength and low atomic number has led to the use of DLC films as free-standing windows for high-energy ion beams.

In this report we discuss several surface-analysis techniques as applied to study the chemical and structural properties of DLC films, and present results obtained from several films from four different laboratories. We have studied the fine structure of the carbon KLL Auger spectra for DLC films, natural diamond and SiC after various heating or cleaning treatments. We have also studied the natural diamond with low energy electron diffraction (LEED). None of the DLC films show the characteristic fine structure of the C KLL Auger line observed in diamond, although the insipient formation of SiC on the DLC surface produced a similar fine structure. Thus we find no evidence to suggest a tetrahedrally coordinated diamond structure in DLC films, and conclude that their structure must be an intermediate one between diamond and graphite as has been suggested previously.⁷

Three of the most popular surface analysis methods are XPS (X-Ray Photoelectron Spectroscopy), SIMS (Secondary Ion Mass Spectroscopy), and AES (Auger Electron Spectroscopy). XPS has the inherent capability to reveal bonding differences. However, for the specific case of carbon, there is a very small energy shift from one form to another, e.g., the carbon 1s for graphite has a binding energy of 284.3,⁸ while that of diamond is 284.4.³ This small shift makes it very difficult to use XPS to differentiate between diamond and other forms of carbon. We have used XPS for survey scans on samples for which AES was made difficult due to charging by the electron beam. SIMS will not provide direct evidence of diamond-like character, as it is primarily a trace-element tool. SIMS has been used to reveal chemical composition by the composition of fragment ions. The hard carbon films in general contain significant amounts of hydrogen, and C_xH_y fragments are observed with SIMS. Vora and Moravec⁹

have reported a correlation between hardness and the ratio of C_3 to C_3H_3 fragments.

With AES it is possible to distinguish tetrahedrally bonded carbon (diamond) from other forms. There are easily observed differences in the KLL Auger line shapes for amorphous carbon, graphite and natural diamond. This chemical effect has been clearly demonstrated.^{10,11} Figure 1 illustrates the carbon KLL Auger peak from these three forms of carbon. If diamond crystallites are formed in the DLC film, then it should be evident in the C KLL fine structure. Because AES samples only the outer 10 - 20 Å surface layer, it is critical that we obtain a clean surface that is chemically representative of the bulk of the film.

LEED work on natural diamond was reported in the 1960's. We have reproduced the most pertinent conclusions in order to be convinced that we have a reliable procedure to clean diamond. Marsh and Farnsworth¹² found that the best clean diamond LEED pattern was obtained in their apparatus by heating the diamond to 700°C in 10^{-3} torr of hydrogen for 1-2 hours. A clean diamond surface was defined by them to exhibit a sharp $\frac{1}{2}$ order LEED pattern. They also found that if they heated diamond in vacuum without an intentional hydrogen leak that the LEED pattern would deteriorate. They attributed this to a carbonization of the diamond surface. In addition, they found that ion bombardment would totally eliminate the LEED pattern. Lander and Morrison¹³ confirmed their results with the exception of being able to heat much higher without carbonization. One explanation for this could be that Lander and Morrison's vacuum system was cleaner than Marsh and Farnsworth's. The fact that Marsh and Farnsworth could get clean diamond by heating in hydrogen would imply that at 700°C they were removing contamination at a faster rate than it was being deposited. This indicates that even a heavily contaminated film should be cleanable by heating in a clean vacuum with an intentional hydrogen leak.

Our experiments were performed in a bakeable all stainless steel ion-pumped vacuum system. A base pressure of 5×10^{-11} torr is routine. LEED optics, ion gun, single-pass cylindrical mirror analyzer for AES and a gas inlet manifold are attached. The sample can be rotated in-situ to position for any of the experimental procedures. The specimens were mounted on a 0.001" Ta foil. The Ta could be resistively heated and the temperature monitored with a W 5% Re vs. W 26% Re thermocouple or with an optical pyrometer.

As shown in Figure 1, we have reproduced the previously reported characteristic AES fine structure from amorphous carbon, graphite and natural diamond. We have also correlated the LEED pattern with the diamond Auger fine structure. A natural (111) diamond surface that has been cleaned to produce a sharp LEED pattern will also exhibit the diamond AES fine structure. Conversely, if the AES fine structure is destroyed by contamination or ion bombardment the LEED pattern is also destroyed.

We were unable to obtain the diamond AES fine structure from the films investigated. These films were prepared at NWC, Westinghouse, Gulf and Western and RCA-Princeton. A similar fine structure was observed from films on a silicon substrate heated to $\sim 900^{\circ}\text{C}$, but was found to be a precursor to the formation of silicon carbide on the DLC surface. Figure 2 shows the development of the carbon KLL Auger spectrum from a DLC film that was deposited on a silicon substrate and subsequently annealed in UHV. Annealing at temperatures below approximately 600°C did not change the fine structure from that of amorphous carbon. Heating above 900°C causes the diamond-like fine structure to develop as shown in Figure 2(B) and (C). This is correlated with the appearance of a silicon Auger peak, however, showing that silicon is diffusing through the DLC film from the substrate. This fine structure converts to that reported for SiC¹⁰ at about 1100°C , shown in Figure 2(D). These temperatures are approximate and appear to vary significantly from film to film. The films prepared at RCA-Princeton were noteworthy for their high resistivity. It was very difficult to perform AES on these films because of charging produced by the electron beam on the highly insulating DLC film.

In conclusion, we have not observed diamond-like fine structure in AES from DLC films. Films that have been carefully cleaned by heating in ultrahigh vacuum show a weak graphite-like shoulder on the AES C KLL line, but the fine structure duplicates none of the curves of Fig. 1. Figure 3 illustrates the comparison of a representative clean DLC lineshape with the amorphous carbon and graphite lineshapes. This is in general agreement with Moravec and Orent,¹⁴ and suggests that DLC films do not have the tetrahedral C-C bonding configuration of natural diamond, or the graphite trigonal bond. Instead, another intermediate structure⁷ must be responsible for the unusual diamond-like properties.

Acknowledgements

We gratefully acknowledge the following individuals for providing their DLC films for analysis:

W. J. Choyke and R. Hoffman of Westinghouse R&D Center, Pittsburgh, PA 15235,
Martin Stein of Gulf and Western, Waltham, MA 02154,
and J. Zelez of RCA-Princeton, Princeton, NJ 08540.

We also want to thank F. A. Raal of DeBeers Diamond Research Laboratories, Johannesburg 2000, South Africa, for supplying the natural diamond used in these experiments.

References

1. S. I. Vakula, V. G. Padalka, V. E. Strel'nitskii, A. O. Vsokin, Zh. Tekh. Fiz. (USSR) 5, 1362 (1979). Translation: Sov. Tech. Phys. Lett. 5, 573 (1979)
2. D. F. Edwards, E. Ochoa, J. Opt. Soc. Am. 71, 607 (1981)
3. R. G. Cavell, S. P. Kowalezyk, L. Ley, R. A. Pollak, B. Mills, D. A. Shirley, and W. Perry, Phys. Rev. B 7, 5315 (1973)
4. J. J. Cuomo, J. L. Freeouf, P. Oelhafen, Bull. Am. Phys. Soc. 27, 147 (March 1982)
5. J. J. Hauser, J. R. Patel, J. W. Rodgers, Appl. Phys. Lett. 30, 129 (1977)
6. See various papers presented at the Tenth Conference on Carbon published in Carbon 10 (1972)
7. V. E. Strel'nitskii, M. M. Matushenko, A. A. Romanov, V. T. Tolok, Dopov. Akad. Nauk, UkrSR, Ser. A (USSR), No. 8, 760 (1977)
8. K. Hamrin, G. Johansson, U. Gelius, C. Nordling and K. Siebahn, Phys. Scr. 1, 277 (1970)
9. H. Vora and T. J. Moravec, J. App. Phys. 52, 6151 (1981)
10. T. W. Haas, J. T. Grant and G. J. Dooley III, J. App. Phys. 43, 1853 (1972)
11. P. G. Lurie and J. M. Wilson, Surface Science 65, 476 (1977)
12. J. B. Marsh and H. E. Farnsworth, Surface Science 1, 3 (1964)
13. J. J. Lander and J. Morrison, Surface Science 4, 241 (1966)
14. T. J. Moravec and T. W. Orent, J. Vac. Sci. Technol., 18 266 (1981)

Figure Captions

Fig. 1 Auger carbon KLL spectra from: A) amorphous carbon, B) graphite and C) natural diamond.

Fig. 2 Auger carbon KLL spectra from a DLC film on silicon, after 30 minute UHV anneals: A) $\sim 500^\circ\text{C}$, B) $\sim 900^\circ\text{C}$, C) $\sim 1000^\circ\text{C}$, D) $\sim 1100^\circ\text{C}$. Note: Curves B, C and D are accompanied by increasing amounts of Si on the carbon surface, as detected by the Si Auger spectrum.

Fig. 3 Auger carbon KLL spectra from: A) DLC film cleaned in UHV, B) amorphous carbon, C) graphite.

FIG 1

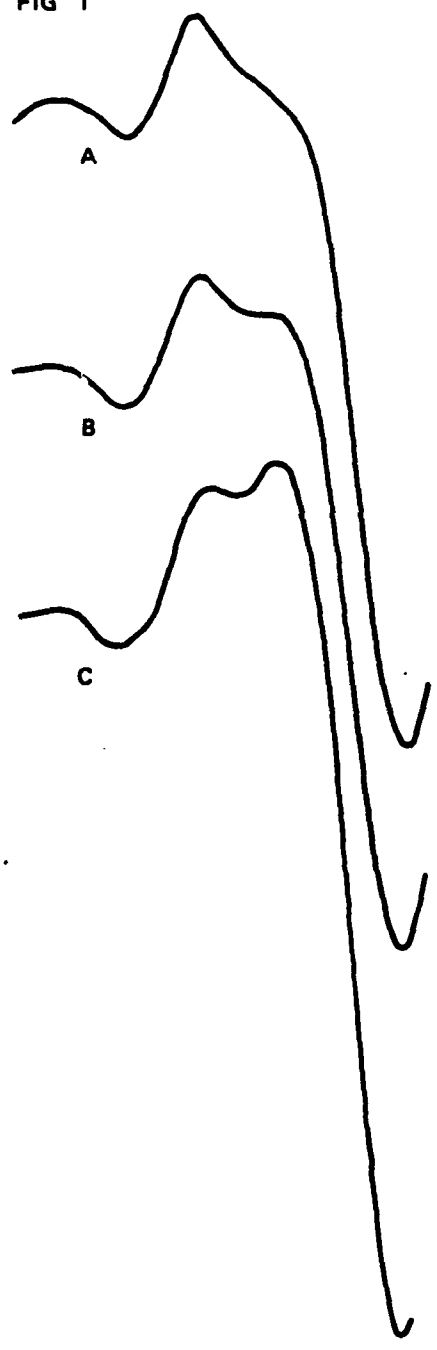
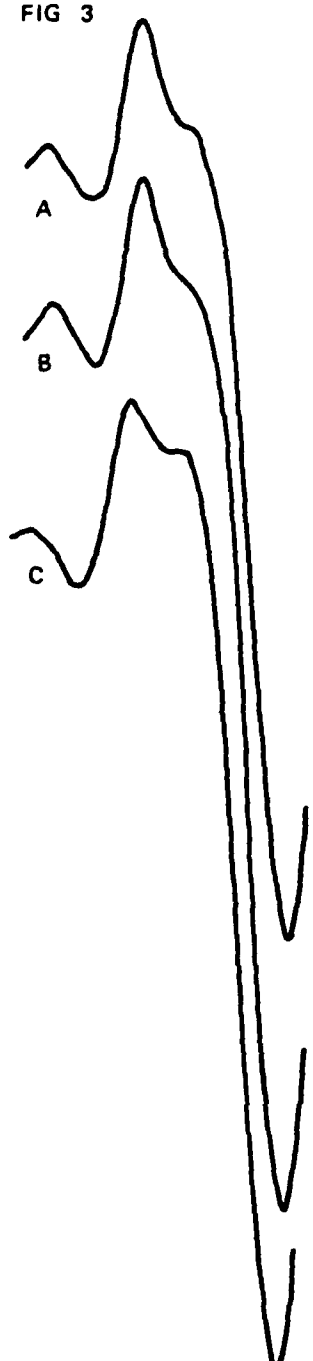


FIG 2



FIG 3



ADP002599

RAMAN SCATTERING AS A PROBE OF THIN-FILMS*

S. R. J. Brueck

Lincoln Laboratory, Massachusetts Institute of Technology
Lexington, Massachusetts 02173

Abstract

Raman scattering provides a nondestructive probe of thin-film properties such as local structure, degree of crystallinity, microcrystal grain size and local strain fields. We have carried out a series of measurements on Si films with thicknesses as small as 20 \AA and with a transverse spatial resolution of $\sim 0.5 \mu\text{m}$. Applications to the characterization of "diamond-like" carbon films will be discussed.

about 0.5 micrometers.

*This work was supported by the Department of the Air Force, in part with specific funding from the Air Force Office of Scientific Research, and by the Office of Naval Research.

Introduction

In this paper several examples of the use of Raman spectroscopy for the probing of thin-solid films are presented. The applications that we have been investigating are predominantly related to electronic materials and device characterization and have been largely carried out on Si films. These techniques are also applicable to thin carbon films and will provide a valuable diagnostic tool to supplement the electron spectroscopies that are discussed elsewhere in this volume. Here applications of Raman scattering to the characterization of stress in Si-on-sapphire (SOS) device structures and of ultra-thin (< 3 nm) Si films will be discussed briefly. More detailed accounts of this work are reported elsewhere.^{1,2} Finally, the applications to the characterization of "diamond-like" carbon films are discussed.

High-Spatial Resolution Measurements

Device structures fabricated from high-quality silicon films deposited on insulating substrates are of great interest for VLSI applications due to improved isolation between densely packed devices as compared with bulk silicon material. Silicon-on-sapphire (SOS) material grown by vapor phase epitaxy is commercially available; a number of alternate growth techniques and material systems are currently under development.^{3,4}

For these heterogeneous material systems there is often an inherent two-dimensional stress on the Si film caused by the differential thermal contraction of the Si and the substrate material upon cooling from the growth temperature of 1000-1400 C to room temperature. This stress results in variations of the silicon energy-level structure and electronic transport properties which can affect device characteristics. Specifically, for the two-dimensional compressive stress characteristic of SOS the conduction band energy level structure is altered and the heavy-mass directions of the electronic structure are lowered relative to the light-mass directions.⁵ This results in a higher effective mass and, consequently, a reduced electron mobility⁶ than for bulk Si. For other materials systems such as silicon-on-fused quartz, the stress is tensile rather than compressive resulting in a higher effective mobility.⁷

In addition to these changes in the electronic properties, the stress-induced strain modifies the lattice characteristics. For a two-dimensional stress, the triply-degenerate zone-center phonon modes in unstressed Si are split into a singlet and a doublet. The frequencies of both of these modes shift linearly with applied stress.^{8,9} For the <100> wafers used for many device configurations, the singlet is Raman active and the Raman frequency can be used to monitor the local stress. The Raman linewidth provides a monitor of the local defect density.

Previously, determinations of this stress have been limited to large-area wafers of the silicon-on-insulator material rather than to actual fabricated devices. Significant variations in the stress may be expected to occur near the edges of Si structures because of the thermal cycling involved in fabricating devices from these materials. In particular the effects of this cycling on the very small structures, with linear dimensions of less than 2 μm , currently being fabricated for VLSI applications have not been investigated.

Raman scattering provides a powerful nondestructive technique for monitoring these stress variations since it can provide a spatial resolution down to approximately the pump laser wavelength ($\sim 0.5 \mu\text{m}$ for this experiment). This should be contrasted with more conventional techniques such as x-ray analysis which typically have a spatial resolution of several millimeters. An additional advantage of the Raman technique is that alignment onto particular device structures is quite straightforward using the visible pump-laser beam for illumination.

We report on the use of Raman scattering to probe stress profiles across $\sim 6\text{-}\mu\text{m}$ wide Si stripes on Al_2O_3 patterned as part of n-channel MOSFETS. The experiment is shown schematically in Fig. 1. The 5145-A argon-ion pump laser beam was reflected from a dichroic mirror and focused onto the Si device with a 60X-microscope objective. A spot size of less than 1- μm diameter was inferred from the measured scattering intensity profiles. Typically, laser powers of less than 2 mW, corresponding to power densities of $\sim 500 \text{ kW/cm}^2$, were used. The Raman spectra were insensitive to laser power at this level. The Raman scattered light was collected by the same objective, transmitted through the dichroic filter, analyzed with a 3/4-meter computer-controlled

double monochromator and detected with a small-area, S-20 surface, photomultiplier using photon-counting electronics. The spectral resolution was approximately 2 cm^{-1} . The computer also controlled a stepping motor which translated the sample across the laser beam focal position with steps as small as $0.25 \mu\text{m}$; Raman spectra were obtained at each position. These spectra were then least-squares fitted to a Lorentzian lineshape to obtain the integrated Raman intensity, the Raman frequency, and the linewidth (FWHM) as a function of position.

Figure 2 shows the Raman parameters that were measured in a scan across a $6\text{-}\mu\text{m}$ gate width device fabricated by a complete-island-etch isolation technique. The penetration depth of the 5145 \AA pump laser light is comparable to the $0.5\text{-}\mu\text{m}$ Si thickness so that the Raman scattering probes the entire Si film. The integrated intensity of the Raman scattering is shown in the upper curve; the rapid changes in intensity at the edges of the structure indicate that a spatial resolution of ~ 1 micron has been achieved. The enhanced scattering just at the edges of the device is a repeatable effect that becomes more pronounced as the laser beam spot size is decreased. Changes are also observed in both the transmitted and reflected laser power at corresponding positions. The corresponding Raman frequencies are shown in the bottom trace of Fig. 2. As a result of the compressive stress of SOS the Raman frequencies are shifted to a higher frequency than that of bulk Si. In the center of the $6\text{-}\mu\text{m}$ structure, only a very small relaxation from the frequency of a nearby $50\text{-}\mu\text{m}$ wide structure is observed. At the edges of the structure, however, there is a significant shift of the Raman frequency towards the frequency of bulk Si indicating that a substantial relaxation of the stress has occurred. The stress variation and the corresponding relative electron mobility variation^{6,7} deduced from these Raman frequency shifts are also shown in the figure. The measured stress variation corresponds to a 20% stress-induced mobility variation across the stripe. The actual mobility variation may be different as a result of defect variations.

Raman Spectra of Ultrathin Si Films

Raman scattering in crystalline materials such as semiconductors involves the interaction of an incident photon of energy $\hbar\omega_i$ with a phonon

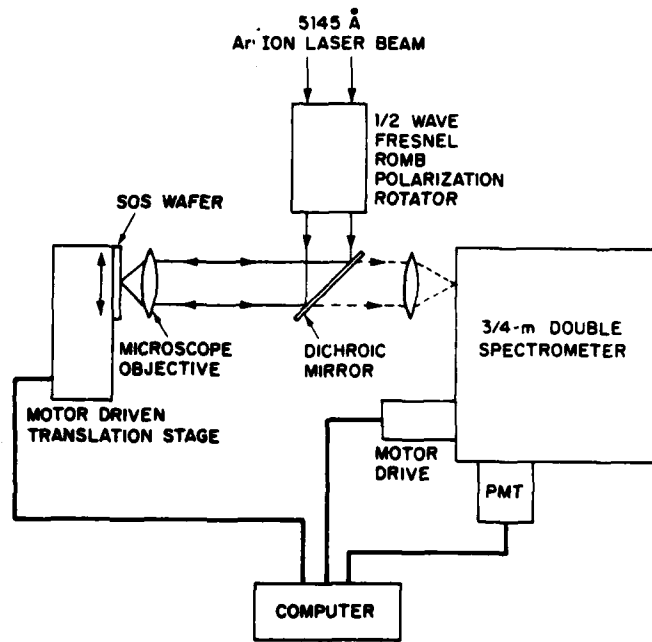


Fig. 1. Experimental apparatus for measuring Raman spectra with high-spatial resolution.

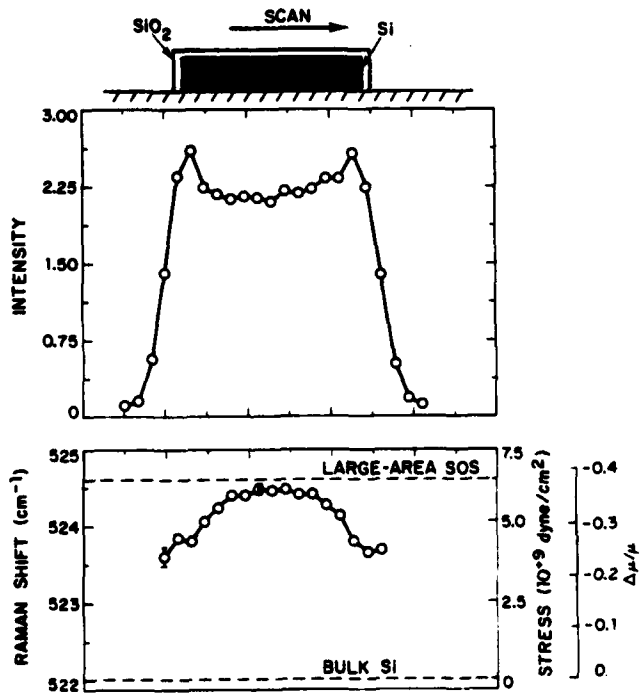


Fig. 2. Raman intensity and frequency shift as a function of position across a 6-μm wide Si stripe on a Al₂O₃ substrate.

of energy $\hbar\omega_q$ to produce a scattered photon of energy $\hbar\omega_s = \hbar\omega_i - \hbar\omega_q$ (Stokes scattering). In crystals of macroscopic size the requirement of momentum conservation allows only long wavelength optical phonons with wavevectors near the Brillouin zone center to participate in the scattering process. For crystal sizes approaching typical lattice dimensions, however, this momentum conservation requirement is relaxed, and phonons with non-zero wavevectors contribute to the Raman spectrum, resulting in the broadening and shifting of the optical phonon line. Raman spectroscopy therefore provides an indication of the size of crystalline samples and has been employed to characterize polycrystalline semiconductor films that have been incompletely recrystallized from the amorphous state.^{10,11} However, no quantitative explanation of the dependence of the observed Raman spectra on crystallite size has been presented. We report here the preliminary results of our study of sample size effects on the Raman spectrum of the optical phonons in Si (at 520 cm⁻¹ in bulk Si) using Si films that have long-range crystalline order in two dimensions but are very thin in the third dimension (down to 3 nm). This system is easily characterized with well-known optical constants and is more accessible to simple modeling than are films consisting of crystallites of random size and orientation. A quantitative understanding of the effect of sample size on Raman lineshape will enhance the utility of Raman spectroscopy as a diagnostic technique for characterizing polycrystalline material. These measurements are also important for understanding the modifications that must be made in conventional physical models of semiconductor devices in order to scale to ultrasmall dimensions.

Thin Si films were prepared from commercially obtained <100> Si epitaxially grown on 2" diameter polished sapphire substrates. The Si was uniformly oxidized until a thin Si layer of the desired thickness range remained under a thick SiO₂ cap. The individual layer thicknesses of the resulting Al₂O₃-Si-SiO₂ structure were determined by fitting to theory experimental transmission spectra recorded over the 0.4 to 3 μm wavelength range. Because of the nonuniform thickness of the starting SOS material, the thickness of the Si layer used for the measurements varied from 0 to > 65 nm, with a linear wedge of 3.5 nm/mm across the wafer. It was therefore possible to investigate a wide range of Si film thicknesses using a

single wafer. Raman spectra measured as a function of Si film thickness over a thickness range of 19 to 3 nm exhibit the following general behavior: (1) as the Si thickness decreases, the Raman line broadens and develops a low-frequency tail extending as far as 70 cm^{-1} from line center; (2) the peak position of the Raman line does not shift significantly ($<1\text{ cm}^{-1}$) from its value for $0.5\mu\text{m}$ SOS even for a Si thickness as small as 2.8 nm. This second observation is in contrast to results obtained with polycrystalline Si for which large shifts in Raman linewidth have been reported and attributed to dimensional effects in small crystallites.¹⁰ Spectra recorded for the thicknesses of 2.8 and 19 nm are shown in Fig. 3. The spectrum of the 2.8-nm thick film clearly exhibits an unshifted, broad, central peak and a low-frequency tail. The Raman linewidth of the 190-A film is broadened because of laser heating; its low power value of 5.9 cm^{-1} is the same as that obtained for $0.5\text{-}\mu\text{m}$ SOS. Dramatic broadening of the Raman line does not occur for film thicknesses greater than approximately 10 nm, as can be seen from the summary of linewidth measurements in Fig. 4, which displays the central peak linewidth as a function of the film thickness.

Broadening of the Raman line toward lower frequency is expected to accompany the relaxation of phonon wavevector selection rules in crystals of finite size because of the participation in the scattering process of lower energy phonons with wavevectors extending into the Brillouin zone. In amorphous Si, where there is no long-range order and all phonons are able to participate in the scattering process, the Raman line is extremely broad and centered at 480 cm^{-1} . It is interesting to note that the 3-nm film is only 6 lattice constants thick but nevertheless has a spectrum that is much closer to that of bulk Si than to that of amorphous Si. Part of the observed broadening may be due to increased phonon scattering at the film boundaries.

Application to Carbon Films

The Raman scattering frequency is sensitive to the local atomic structure. Thus, substantial frequency differences are expected between tetrahedral diamond-like bonding (frequency $\sim 1330\text{ cm}^{-1}$) and trigonal graphite-like bonding (frequency $\sim 1580\text{ cm}^{-1}$). Such variations have been observed¹³ and provide a valuable complement to Auger spectroscopy and X-ray photo-electron spectroscopy. A major advantage of Raman spectroscopy is that it

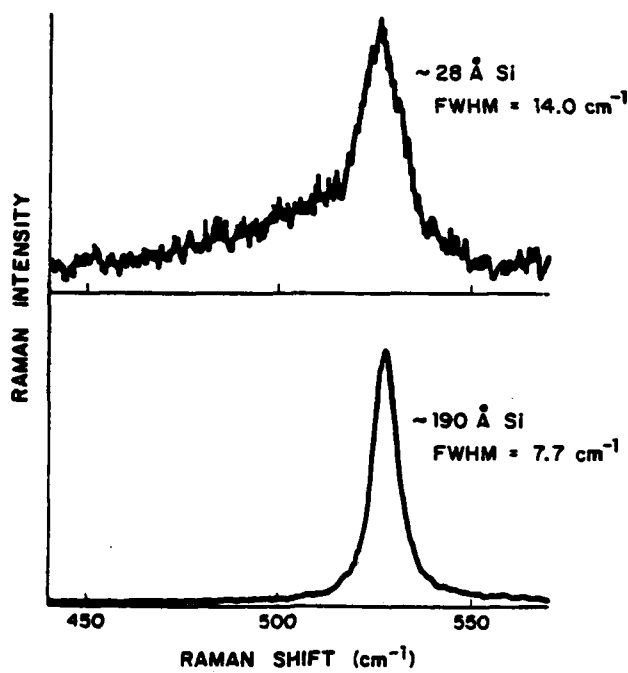


Fig. 3. Si Raman spectra for film thicknesses of 28 \AA and 190 \AA .

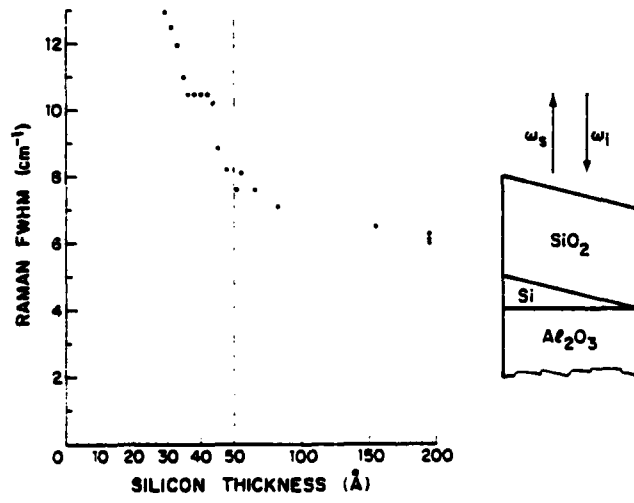


Fig. 4. Variation of the Raman linewidth with film thickness for thin Si films.

is a nondestructive technique requiring no special sample preparation or high vacuum conditions. It can therefore be applied to in situ measurements during film growth. Using an optical multichannel analyzer system in place of the PMT detection scheme discussed here sufficiently rapid analysis capability is available to provide a real-time monitor of the film growth.

Acknowledgment

This work was carried out in collaboration with T. F. Deutsch, John C. C. Fan, D. V. Murphy, D. J. Silversmith, D. D. Rathman and B-Y. Tsaur.

REFERENCES

1. S. R. J. Brueck, B-Y. Tsaur, John C. C. Fan, D. V. Murphy, T. F. Deutsch and D. J. Silversmith, *Appl. Phys. Lett.* 40, 895 (1982).
2. D. V. Murphy, S. R. J. Brueck and D. D. Rathman, Solid State Research, Lincoln Laboratory, M.I.T. (1982:1); and to be published.
3. J. C. C. Fan, M. W. Geis and B-Y. Tsaur, *Appl. Phys. Lett.* 38, 365 (1981).
4. E. W. Maby, M. W. Geis, Y.-L. LeCoz, D. J. Silversmith, R. W. Mountain and D. A. Antoniadis, *IEEE Electron Device Lett.* EDL-2, 241 (1981).
5. J. Hynecek, *J. Appl. Phys.* 45, 2631 (1974).
6. H. Schlotterer, *Solid State Electron.* 11, 947 (1968).
7. B-Y. Tsaur, J. C. C. Fan, and M. W. Geis, *Appl. Phys. Lett.* 40, 322 (1982).
8. I. I. Novak, V. V. Baptizmanskii, and L. V. Zhosa, *Opt. Spectrosc. (USSR)* 43, 145 (1977).
9. Th. Englert, G. Arbstreiter, and J. Pontcharra, *Solid-State Electron.* 23, 31 (1980).
10. J. F. Morhange, G. Kanellis and M. Balkanski, *Solid State Commun.* 31, 805 (1979).
11. R. P. Salathe, H. P. Weber and G. Badertscher, *Phys. Lett.* 80A, 65 (1980).
12. cf. M. Stein and S. Aisenberg, paper presented at this meeting.



Microstructure-Property Relations in Sputtered Films

Russell Messier
Materials Research Laboratory
The Pennsylvania State University
University Park, PA 16802

ABSTRACT

The mechanical and chemical properties of thin films depend at least in part on their microstructure. A structure zone model common to all vapor deposition methods has been developed to classify the various physical microstructures found^(1,2). In this model the microstructure is related to a normalized temperature, T/T_m where T = temperature of the film during preparation and T_m = the melting point of the material ($^{\circ}$ K). Thornton⁽²⁾ extended this model to the case of sputtered films in which a second important variable, the pressure of the sputtering gas (eg., P_{Ar}) was demonstrated. It has been shown that the densest, most crystalline structures are obtained at high T/T_m and low P_{Ar} .

Recently we have shown the effectiveness of this model in understanding the complex relations between chemical, mechanical, and electronic properties and the detailed physical structure for the amorphous semiconductors a-Ge^(3,4), a-Si⁽⁵⁾, and a-Si:H⁽⁶⁻⁸⁾. In particular, the effects of positive ion-bombardment of the growing film have been shown to be most important^(6,7) and directly related to decreasing gas pressure. In effect, the bombardment is producing a second source of temperature, albeit a non-equilibrium temperature, at the growing film. Thus the "effective T/T_m " can be increased without increasing the temperature of the workpiece. This process is seen to be especially important for materials with a high T_m (such as carbon) since it allows dense structures to be achieved at relatively low equilibrium, external heater temperatures.

Physical Structure of Thin Films

It is generally recognized that thin films show a wide range of microstructures and resulting film properties, both of which are highly dependent of preparation conditions. The Structure Zone Model (SZM), which relates thin film microstructure to a reduced temperature (T/T_m), where T = film temperature during deposition and T_m = material melting point, has been invoked to classify the various microstructures observed in thin films^(1,2). As T/T_m increases, the microstructure is controlled by shadowing effects (Zone 1), surface diffusion (Zone 2), and bulk diffusion (Zone 3). Such a classification scheme explains the independence of microstructure on the preparation method, e.g., sputtering, evaporation, chemical vapor deposition, electrodeposition⁽²⁾. Although the SZM was developed primarily on the basis of metallic crystalline films, there have been several recent reports on its application to amorphous and/or dielectric films such as those used for optical coatings^(9,10). Since optical coatings are usually deposited at fairly low temperatures ($T/T_m < 0.3$), the film microstructure is generally Zone 1, which

is a columnar structure with fairly large void regions separating the columns(10).

The term microstructure has been used rather broadly to include the columnar⁽¹¹⁻¹³⁾ and nodular⁽¹⁴⁾ growth patterns generally observed in optical films thicker than $\sim 1\mu\text{m}$ and observable by scanning electron microscopy and TEM replica techniques. In addition, microstructure at the atomic level (3-30nm) has also been reported extensively (e.g., Refs. 15 and 16). The relations between these various observed "microstructures," however, have not been generally recognized. Indeed, it is usually considered that "microstructure" covers a wide range of sizes from $\sim 3\text{nm}$ to several μm , with a continuous variation in size related to preparation conditions.

Nodular growths, however, are exceptions in that they consist of a bundle of smaller columns which originate at a submicron level due to spontaneous and copious nucleation⁽²⁾ and grow to much larger lateral sizes. These smaller columns initially grow in all directions but, due to the constraints of the surrounding films, are forced toward the direction of the impinging vapor stream. The net result is the characteristic parabolic nodular shape in which the size increases with increasing film thickness^(10,17). Nodules usually originate at the substrate/film interface and are often related to surface impurities or asperities⁽¹⁰⁾.

The SZM, as developed to date, has been applied exclusively to microstructure, $>100\text{nm}$ in size in thick films ($>1\mu\text{m}$). The smaller, 10nm diameter columns viewed in thinner films by TEM⁽¹⁶⁾ and field ion microscopy⁽¹⁸⁾ have not been explained in the framework of the SZM. This latter physical structure might better be considered nano-structure. Recently, we have developed a composite model, encompassing both the microstructure and nano-structure of the thin films (prepared at $T/T_m < 0.5$), based on extensive preparation and characterization studies of both thick ($1-10\mu\text{m}$) and thin ($0.1 - 1\mu\text{m}$) films of the tetrahedrally bonded amorphous semiconductors. In this temperature range, shadowing effects, and to an extent surface diffusion, control the columnar nature of thin films and applies to both crystalline and amorphous films.

In this evolutionary model⁽⁸⁾ at least three distinct structural units are recognized; nano-, micro- and macro-columns and associated nano-, micro-, and macro-voids^(3,19). Figure 1 shows both a schematic representation of these interrelated structural units along with representative micrographs for amorphous Ge (a-Ge) films. The voids, actually lower density regions, surrounding the columns⁽⁴⁾ are the primary controlling factors. For very thin films only the nano-columns ($\sim 10\text{nm}$ dia.) are found. As film thickness increases, the initially uniform nano-columns undergo incomplete coalescence resulting in somewhat larger voids in addition to

the nano-voids. These larger voids are more widely spaced, begin to dominate the structure as film thickness increases, and lead to the dense Zone T microstructure with a characteristic \sim 100nm diameter micro-column size. [The detailed reasons for these characteristic sizes (\sim 10nm nano-columns and \sim 100nm micro-columns) is unknown even though it has been observed in a wide range of materials.] Finally, macro-columns (Zone 1) evolve from the incomplete coalescence of micro-columns (Zone T) and have been related to low substrate temperature, substrate roughness, and gas phase scattering effects. The gas phase scattering effects lead to a uniform array of macro-columns (\sim 1000nm dia.) which are bundles of micro-columns⁽²⁾. Roughness effects associated with surface preparation procedures (generally uniform roughness) vary widely, of course, but again are bundles of micro-columns⁽³⁾. Zone 1 structures usually result in which macro-column sizes mimick the surface roughness. The more isolated surface roughnesses (e.g., spits, asperites, surface contaminants) have been shown to initiate nodular structures of the macro-columnar type^(10,20) which increase considerably in size with increasing film thickness, unlike the other effects. Thus, due to these various origins, macro-structure does not have a characteristic size. The evolution of Zone 1 microstructure in a-Si:H films prepared under low mobility (low T/T_m) conditions, and on various substrate types and roughness is shown in Figs. 2-6 (taken from Ref. 8).

Since optical coatings are almost always prepared in this lower temperature range ($T/T_m < 0.5$)⁽¹⁰⁾, this evolutionary model for columnar structure should apply. Although the model is developed mainly upon results for amorphous semiconductor films, studies of oxide (Messier and Bholagir, unpublished) and other dielectric coatings^(9,11) suggest that this model has general applicability. Furthermore, this model shows that film thickness defines the evolutionary stage of the structure and that, even though it may not be observable in thinner films (<1μm) by SEM, the structure does originate at the substrate/film interface and is still present, as evident by field ion microscopy (FIM)^(4,18) and TEM⁽¹⁶⁾. Films of interest in the present study are in this thickness range (\sim 100-1000nm) and, therefore, characterization of physical structure will require high resolution.

Bombardment Processes

Positive ion-bombardment of the growing film has been recognized as an important parameter in controlling film physical microstructure and crystal structure. Both imposed-biasing (i.e., bias-sputtering and ion plating)⁽²¹⁻²³⁾ and self-biasing resulting from sputter-deposition processes^(6,7) have been related to a suppression of Zone 1 structures and enhancement of Zone T structures. The self-bias floating potentials are usually not measured, yet generally reach high

negative values (<-20V) at low sputtering gas pressures (<10-20m Torr)⁽²⁴⁾. Such potentials lead to direct bombardment of the growing film by positive ions from the plasma (e.g., Ar⁺, Ar⁺⁺, H⁺) and the resulting densification of the film's physical structure.

Another possible source of film bombardment results from negative-ion formation at the sputtering target in which the negative species gain nearly the full cathode potential, become neutralized in the negative glow region, and impinge on the growing film⁽²⁵⁾. This, of course, leads to atomic rearrangement at the film surface and, in the extreme case, complete resputtering of the film. Such an effect has not yet been related to the resulting physical structure in terms of the SZM. Since negative-ion effects occur mainly for materials with a highly electronegative element (e.g., oxides and fluorides)⁽²⁵⁾, this factor could be important in oxide laser coatings produced by sputtering.

A third source of film bombardment during sputtering is due to elastically backscattered ions (e.g., Ar⁺, H⁺) from the sputtering target. The degree of this bombardment is inversely related to the ratio M_i/M_t , where M_i = mass of incident ion and M_t = mass of the target atom and can be a predominate effect for low ratios. Thus in the case of H⁺ incident ions, a high percentage can be back-reflected with energies comparable to their incident energy.

Each of these film bombardment processes increases with effective surface temperature. Although other, generally less important, bombardment processes are possible, they will not be discussed here. Such processes result in increased atom mobility or even desorption at the growing film surface. This, then, provides an alternate route to obtaining microstructure representative of a higher T/T_m than could otherwise be obtained through direct heating of the substrate. Since optical components and multilayer coatings are often limited in the temperature range to which they can be subjected, the use of bombardment effects may be the best, or perhaps only, route to obtaining dense film microstructures (Zone T in the SZM notation).

Examples

Several examples of the first bombardment process (V_s -induced Ar⁺-bombardment) will be given from our direct experience. First, in the preparation of a-Si:H films by sputtering we have measured the substrate floating potential (V_s) using electrostatic probe techniques (Fig. 7) and have found^(6,7) a direct relation between the V_s -induced Ar⁺-bombardment and the resulting film microstructure (Fig. 8) and properties (Fig. 9). In particular, a series of films prepared at a substrate heater temperature of 200°C and at varying sputtering gas pressures

(along line in Fig. 8) displayed zone-structures in close agreement with a modified structure zone model developed by Thornton⁽²⁾ on the basis of crystalline, metallic films. It is noted in Fig. 8 that the shape of the Zone 1 - Zone T boundary and the shape of $-V_s$ (both as a function of argon sputtering gas pressure, P_{Ar}) are quite similar, indicating the direct relation between bombardment and micro-structure.

The second example involves the deposition of SiC films by sputtering a ceramic SiC target in pure Ar. As in the case of a-Si:H, and for that matter many other materials, we find a similar sharp dependence of V_s with P_{Ar} (see Fig. 10). By preparing films over this relatively large range in Ar^+ bombarding potentials (relative to bond strengths and sputtering yields of most materials) we have shown that the physical structure goes from a Zone T all the way to a Zone 2 (possibly Zone 3) structure (see Fig. 11 a-e) for films deposited directly onto an α -SiC ceramic substrate (Fig. 11 e). Films deposited over this same range of V_s but onto glass slides showed only a change from Zone 1 to Zone T (Fig. 12), indicating an epitaxial relation in the former case. Although bulk substrate heating will result from secondary electron bombardment (primary effect on V_s) and Ar^+ bombardment, this temperature never exceeded $\sim 500^\circ\text{C}$ since the soda-lime glass substrates neither shattered (from thermal shock or thermal differentials) nor softened. This example of very low bulk temperature epitaxy is the direct result of film surface bombardment during deposition.

Conclusion

Our research on the preparation-characterization-physical structure relations of a-Ge^(3,4,18,27-31), a-Si⁽¹⁹⁾ and a-Si:H⁽⁶⁻⁸⁾ sputtered films, as well as unpublished work on a-WO₃ (Messier and Bholagir) and SiC films has led to the evolutionary model of film physical structure as described in detail above. In addition to using the standard techniques (e.g., SEM of top surfaces and fractured edges, TEM) for viewing directly the structure of thin films, we have developed two new techniques; a) anisotropic etching to reveal micro-structure and macro-structure^(3,19,31), and b) direct imaging and mass analysis of the nano-structure of thin films by atom probe field ion microscopy (APFIM)^(4,18,32,33). Also, we are currently developing the spectroscopic ellipsometry technique as a non-destructive characterization technique for characterizing the surface roughness and internal structure in a-Si:H films (1-10 μm thick) in particular and thin film structure in general.

References

1. B.A. Movchan and A.V. Demchishin, Phys. Met. Metallogr. 28, 83 (1969).
2. J.A. Thornton, Ann. Rev. Mat. Sci. 7, 239 (1977).
3. P. Swab, S.V. Krishnaswamy, and R. Messier, J. Vac. Sci. Technol 17, 362 (1980).
4. S.V. Krishnaswamy, R. Messier, Y.S. Ng, T.T. Tsong, and S.B. McLane, J. Non-Cryst. Solids 35-36, 531 (1980).
5. R. Messier, S.V. Krishnaswamy, L.R. Gilbert, and P. Swab, J. Appl. Phys. 51, 1611 (1980).
6. R.C. Ross and R. Messier, J. Appl. Phys. 52, 5329 (1981).
7. R.C. Ross and R. Messier, AIP Conf. Proc. 73, 53 (1981).
8. R. Messier and R.C. Ross, J. Appl. Phys. (in press).
9. K.H. Guenther, Thin Solid Films 77, 239 (1981).
10. K.H. Guenther, Appl. Opt. 20, 1034 (1981).
11. K.H. Guenther and H.K. Pulker, Appl. Opt. 15, 2992 (1976).
12. J.A. Thornton, J. Vac. Sci. Technol. 11, 666 (1974).
13. J.A. Thornton, J. Vac. Sci. Technol. 12, 830 (1975).
14. T. Splavins and W.A. Brainard, J. Vac. Sci. Technol. 11, 1186 (1974).
15. A.G. Dirks and H.J. Leamy, Thin Solid Films 47, 219 (1977).
16. S. Nakahara, Thin Solid Films 45, 421 (1977).
17. T. Splavins, Thin Solid Films 64, 143 (1979).
18. S.V. Krishnaswamy, R. Messier, Yee S. Ng, T.T. Tsong, Appl. Phys. Lett. 35, 870 (1979).
19. R. Messier, S.V. Krishnaswamy, L.R. Gilbert and P. Swab, J. Appl. Phys. 51, 1611 (1980).
20. A.M. Ledger, Appl. Opt. 18, 2979 (1979).
21. D.M. Mattox and G.J. Kominak, J. Vac. Sci. Technol. 9, 528 (1972).
22. R.D. Bland, G.J. Kominak and D.M. Mattox, J. Vac. Sci. Technol. 11, 671 (1974).
23. J.W. Patten and E.D. McClanahan, J. Appl. Phys. 43, 4811 (1972).
24. R. Messier and R. Roy, J. Non-Cryst. Solids 28, 107 (1978).
25. J.J. Cuomo, R.J. Gambino, J.M.E. Harper, J.D. Kuptsis and J.C. Webber, J. Vac. Sci. Technol. 15, 281 (1978).
26. L.R. Gilbert, R. Messier and S.V. Krishnaswamy, J. Vac. Sci. Technol. 17, 389 (1980).
27. R. Messier, T. Takamori and R. Roy, Solid State Commun. 16, 311 (1975).
28. R. Messier, T. Takamori and R. Roy, J. Vac. Sci. Technol. 13, 1060 (1976).
29. T. Takamori, R. Messier and R. Roy, Appl. Phys. Letts. 20, 201 (1972).
30. T. Takamori, R. Messier and R. Roy, J. Mat. Sci. 8, 1809 (1973).
31. L.R. Gilbert, R. Messier and R. Roy, Thin Solid Films 54, 149 (1978).

32. S.V. Krishnaswamy, S.B. McLane, Y.S. Ng, T.T. Tsong and R. Messier, *Thin Solid Films* 79, 21 (1981).
33. S.V. Krishnaswamy, R. Messier, C.S. Wu, S.B. McLane and T.T. Tsong, *J. Vac. Sci. Technol.*, 18, 309 (1981).

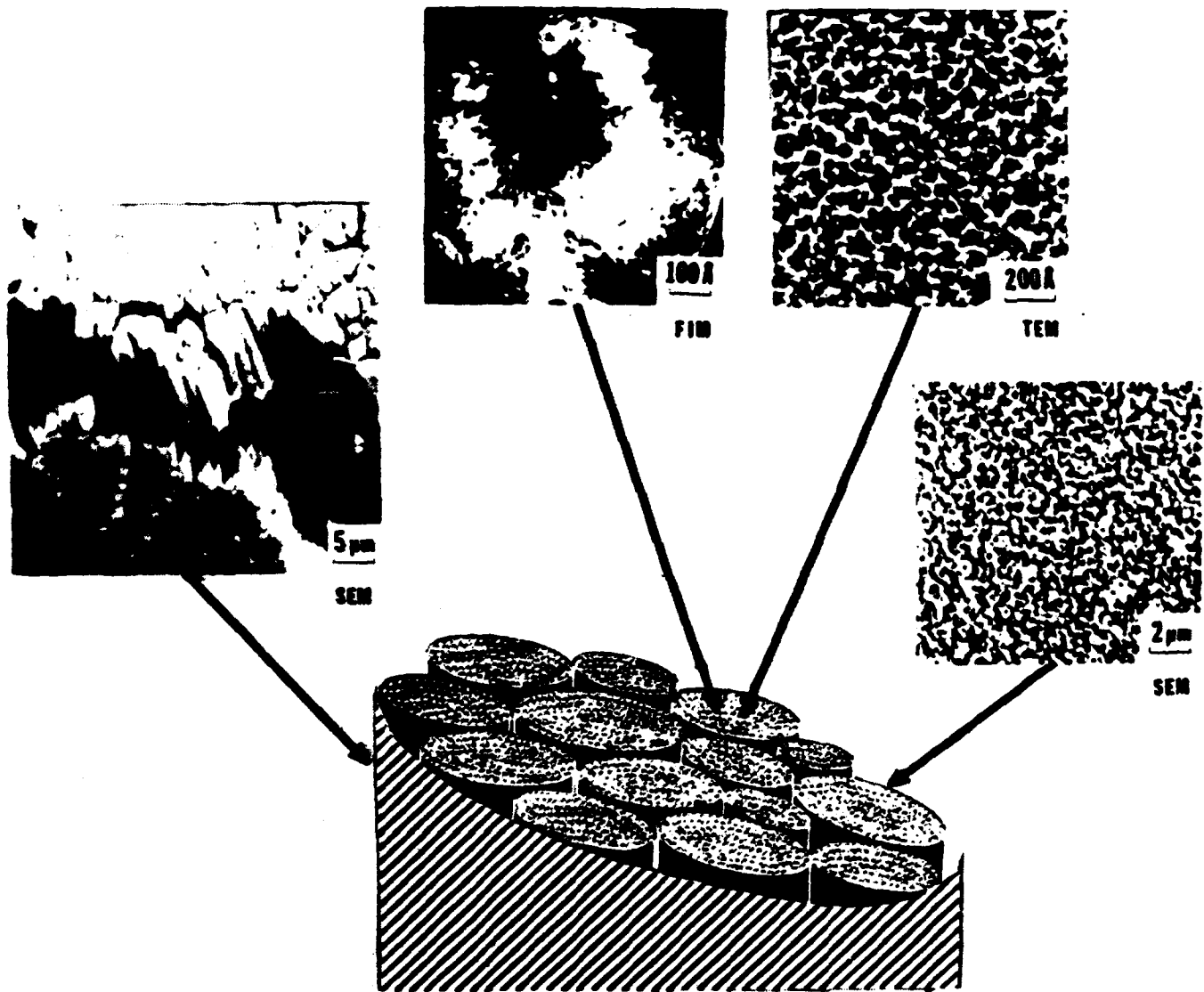


Fig. 1 Schematic of various levels of physical structure in a-Ge sputtered films and corresponding micrographs showing macrostructure (SEM, on left), microstructure (SEM, on right), and nanostructure (TEM and FIM, top).

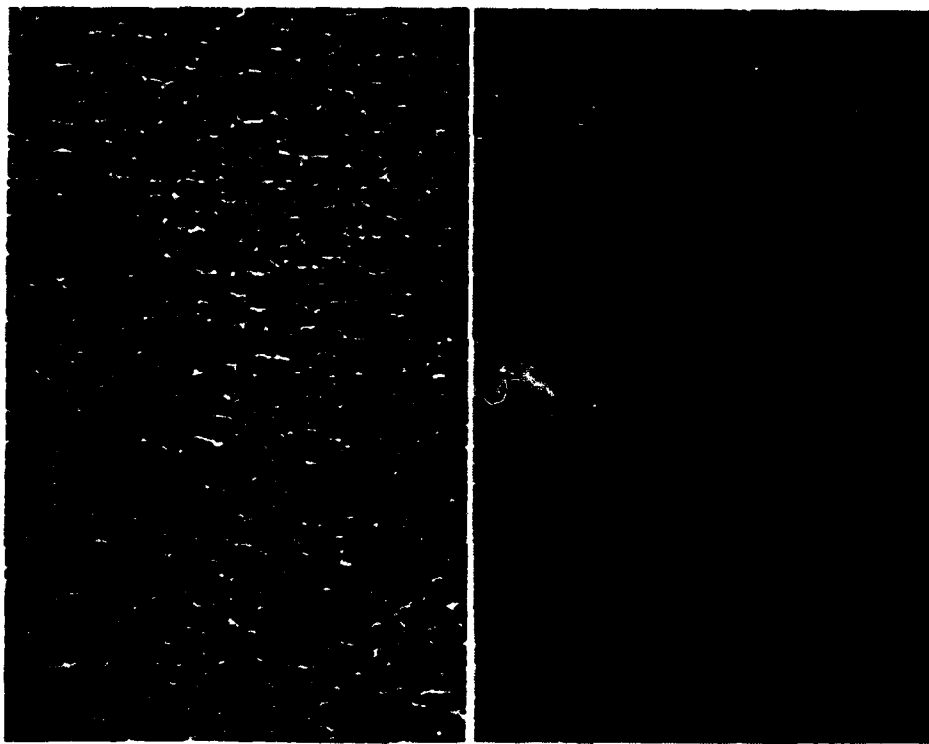


Fig. 2 Underfocused phase-contrast TEM micrographs comparing the void network structures of identically prepared films ($t = 600 \text{ \AA}$) onto evaporated carbon (right) and KCl (left). (Marker = 500 \AA)

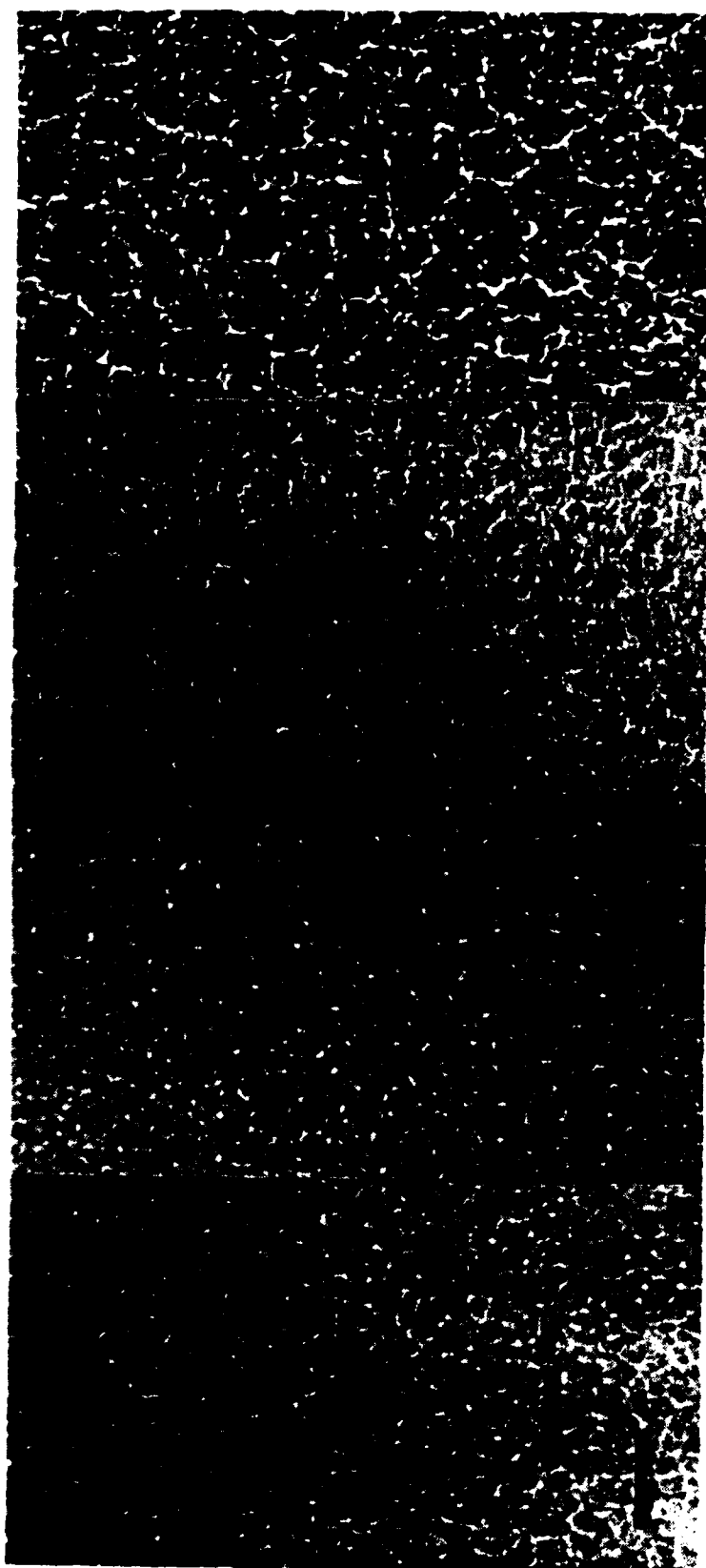


Fig. 3 Underfocused phase-contrast TEM micrographs of a-Si:H films. Film thickness is 150 Å, 300 Å, 600 Å, and 1200 Å (from left to right) (Marker = 500 Å)

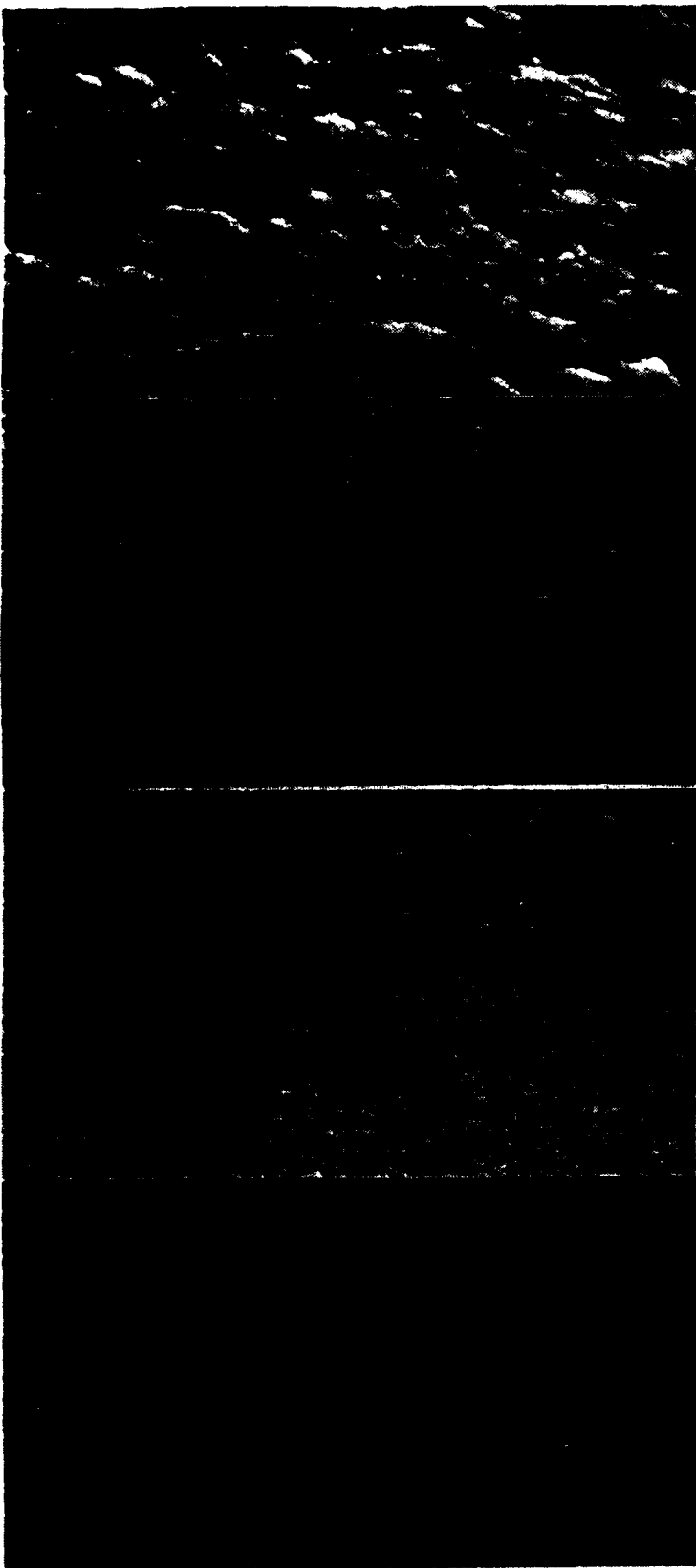


Fig. 4 SEM micrographs of top surface (at 45° tilt) of films deposited on KCl. Thickness is 1200 Å, 3000 Å, 1 µm, and 10 µm. (from left to right) (Marker = 5000 Å)

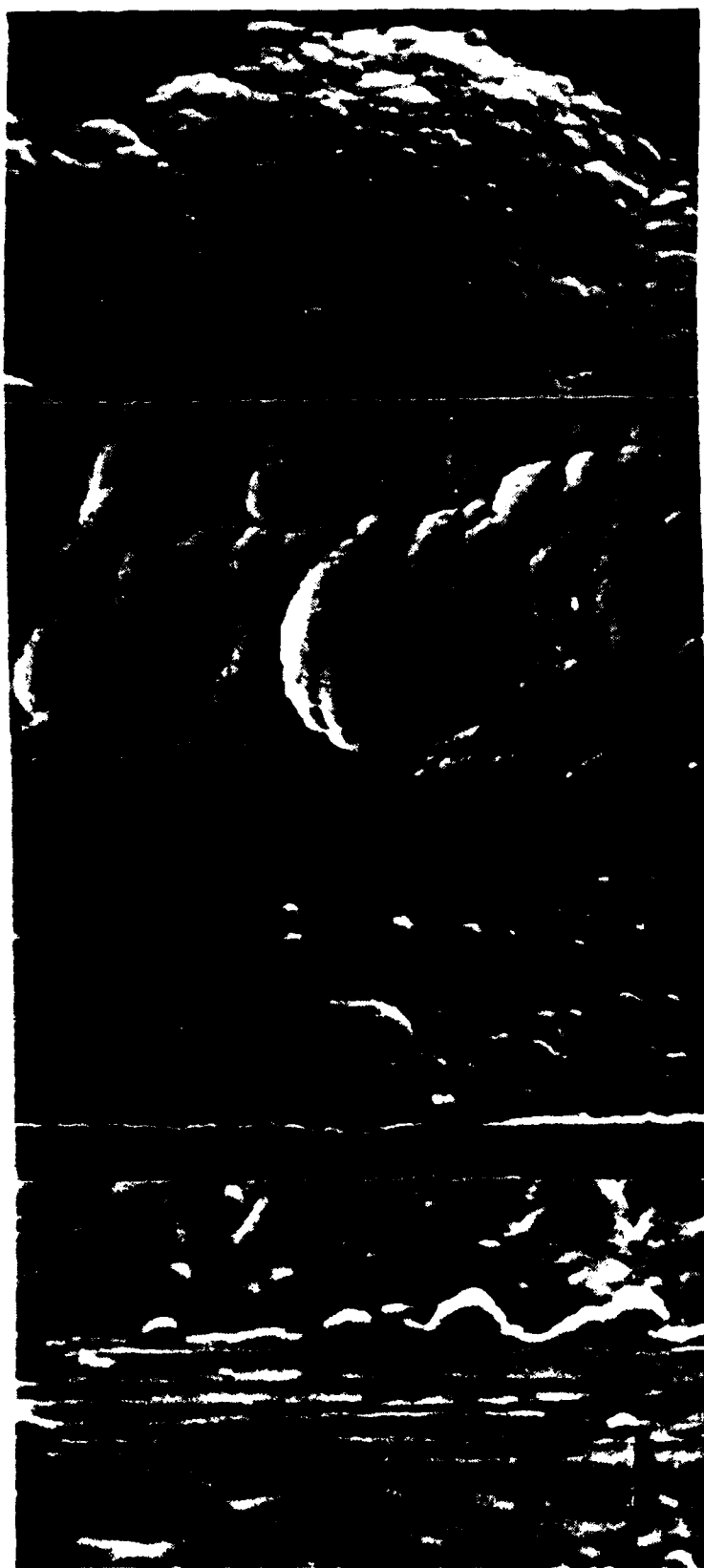


Fig. 5 SEM micrographs of top surface (at 45° tilt) of films on mechanically roughened KCl. The film thicknesses and sequence are the same as in Fig. 3. (Marker = 5000 Å)

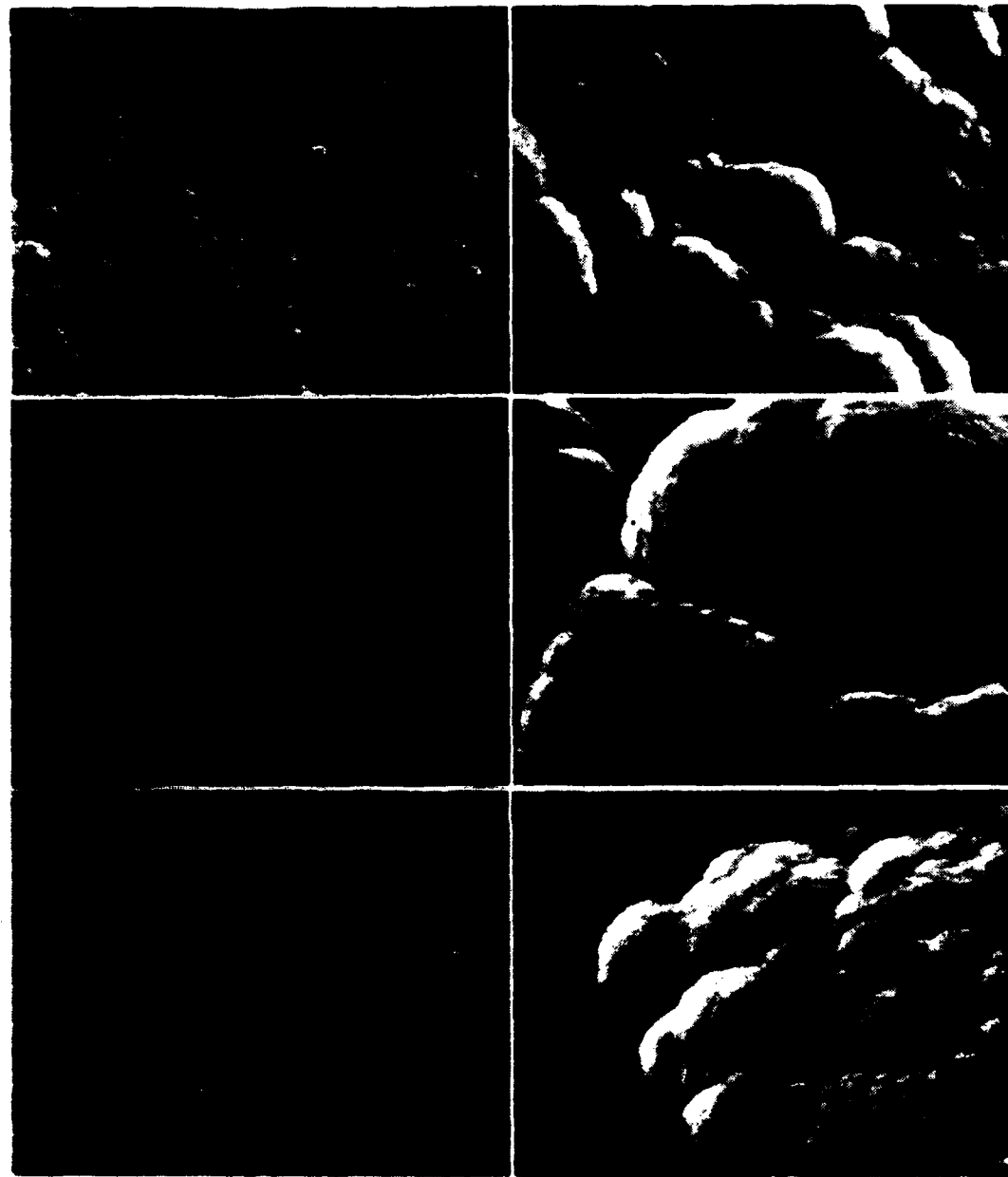


Fig. 6 SEM micrographs of top surface (at 45° tilt) of films deposited in the same run ($t = 1 \mu\text{m}$) onto various smooth (left column) and roughened (right column) substrates. The substrates (from bottom to top) are polished Si single crystal wafer, air-cleaved KCl, and glassy carbon. (Marker = 5000 Å)

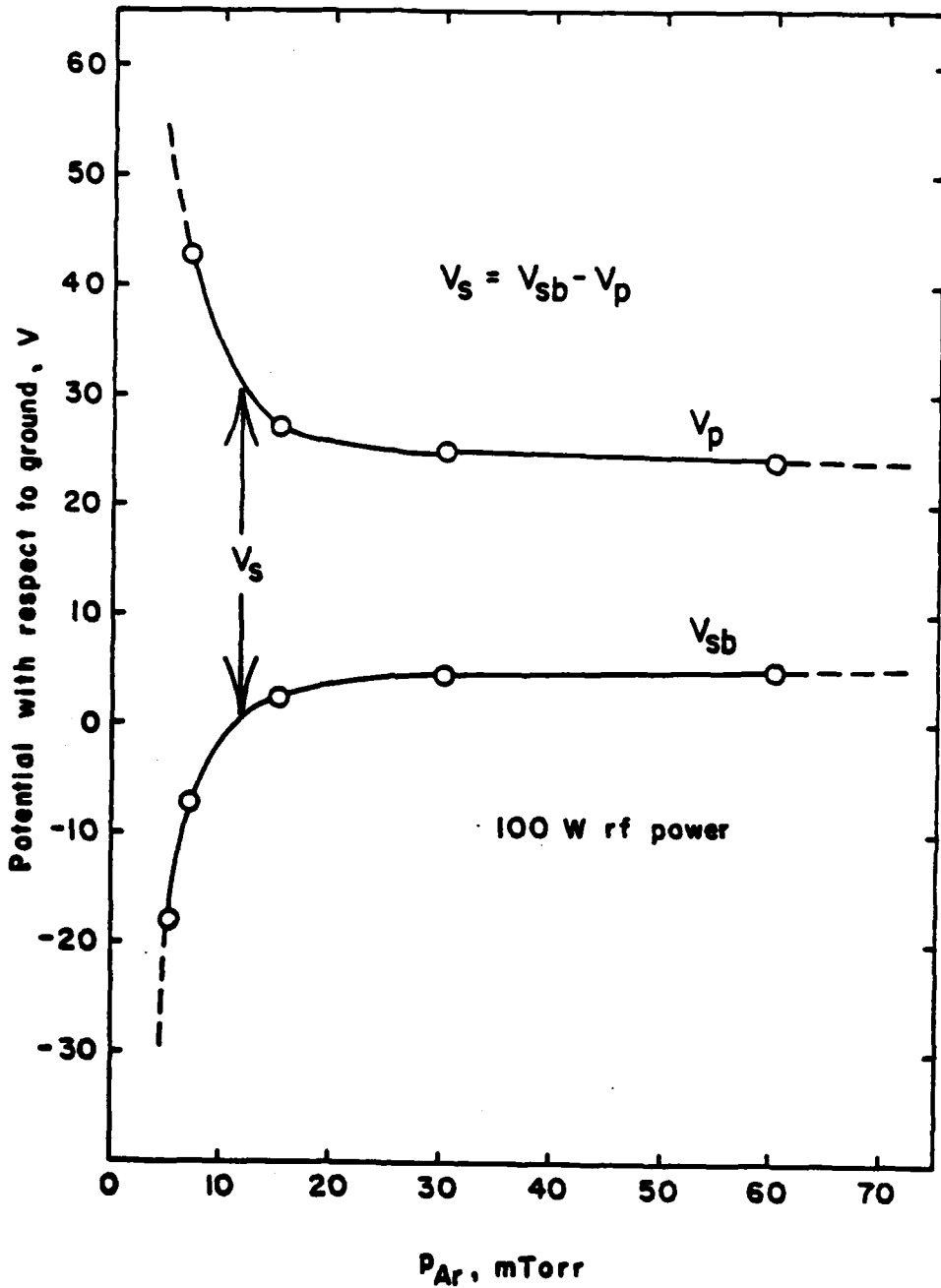


Fig. 7 Plot of substrate potential (V_{sb}) and plasma potential (V_p) with respect to ground as a function of P_{Ar} . The substrate floating potential ($V_s = V_{sb} - V_p$) determines the energy of positive ions extracted from the plasma and assumes a large negative value at low P_{Ar} .

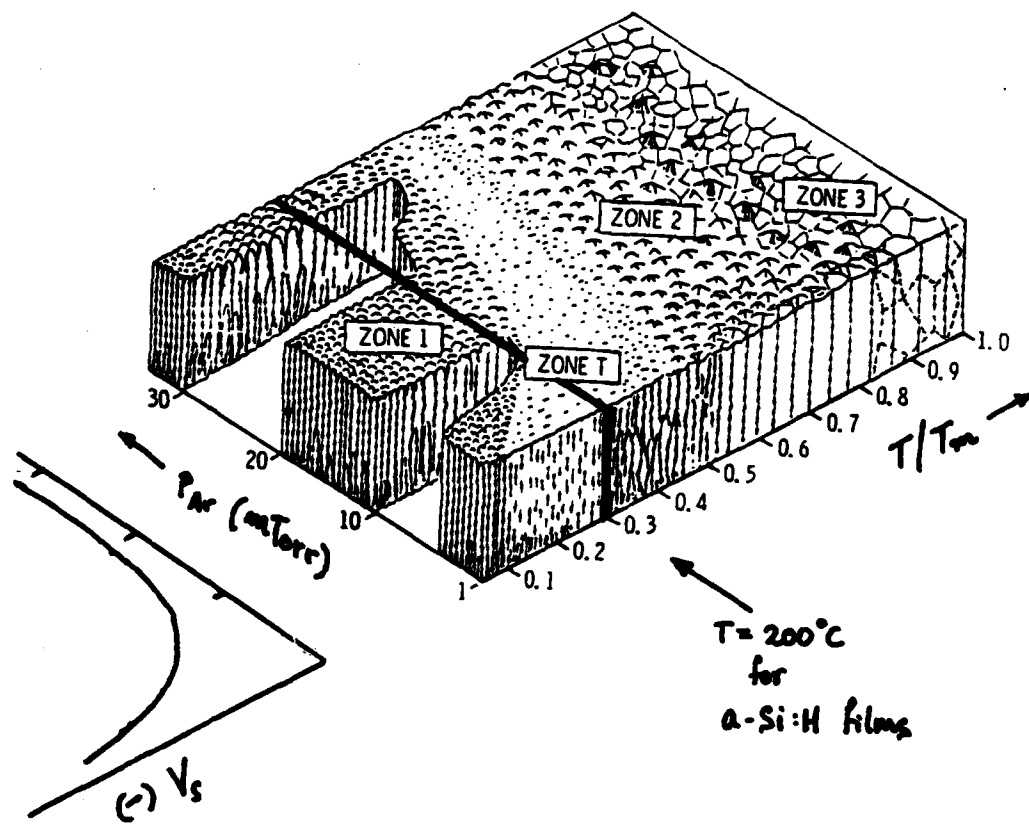


Fig. 8 Structure zone model (reprinted with permission of J.A. Thornton) with the additions of floating self-bias voltage (general dependence) and substrate temperature for a-Si:H film preparation series.

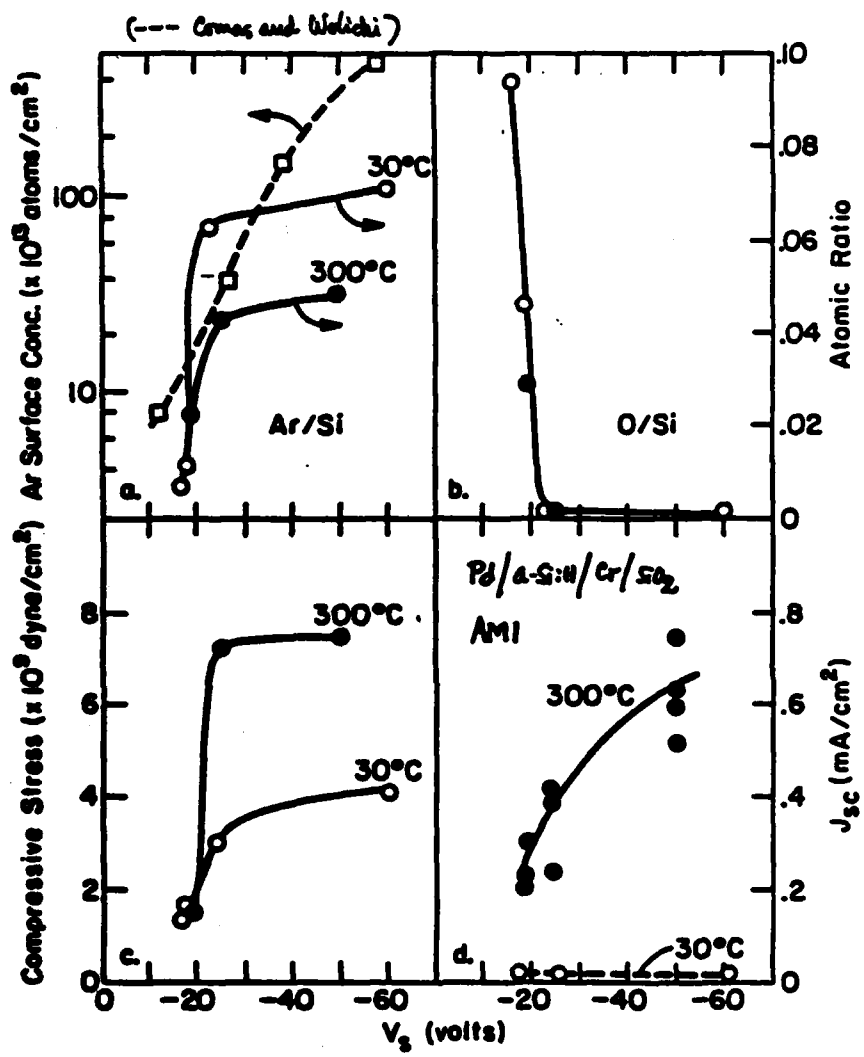


Fig. 9 Threshold type dependence of film properties upon the substrate floating potential, V_g : (a) Ar/Si atomic ratio, (b) O/Si atomic ratio, (c) intrinsic compressive stress, (d) J_{sc} at AML for Pd/a-Si:H/Cr/glass. Dashed line in (a) is Ar surface concentration in c-Si from low energy implantation studies (from reference 9). Data in (a-c) is for films prepared with no H: samples prepared at various P_{H_2} followed similar trends.

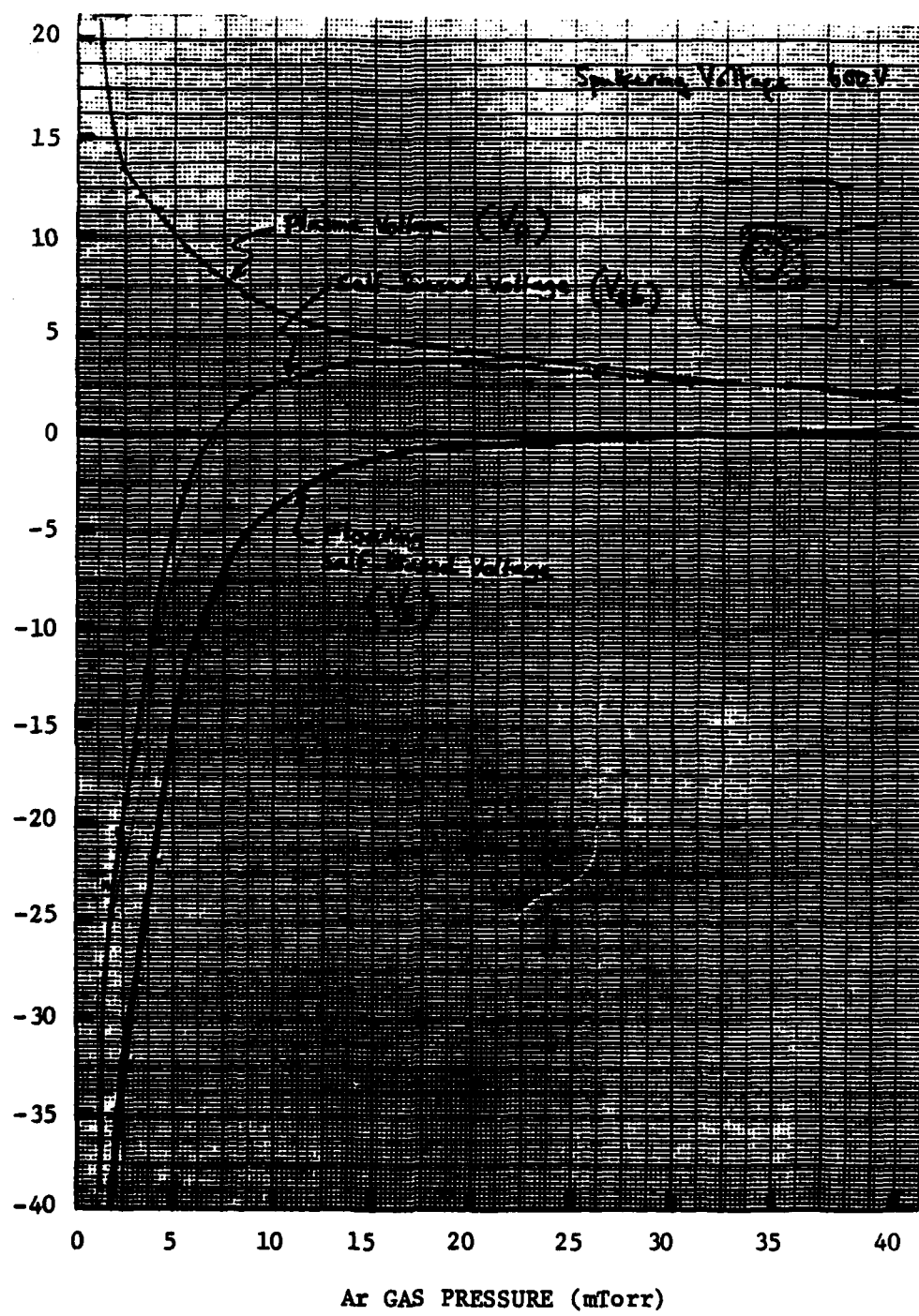


Fig. 10 Plasma, self-biased, and floating self-bias voltage at the substrate during sputtering a TiC target as a function of Ar sputtering gas pressure.

Sputtered SiC film
on
 α -SiC Ceramic Substrate

(a)



Substrate floating
potential (V_s)
during deposition

$$V_s = -0.7 \text{ V}$$

(b)



$$V_s = -3 \text{ V}$$

Fig. 11 Microstructure of SiC sputtered films on α -SiC ceramic substrate are a function of substrate floating self-bias voltage (V_s). V_s is non-linearly related to P_{Ar} as shown in Fig. 10.

(c)



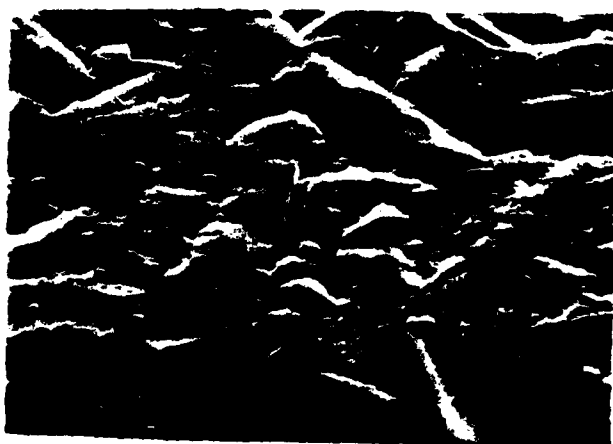
$V_s = -41 \text{ V}$

(d)



$V_s = -52 \text{ V}$

(e)



$\alpha\text{-SiC}$
Substrate

(uncoated)

5 μm

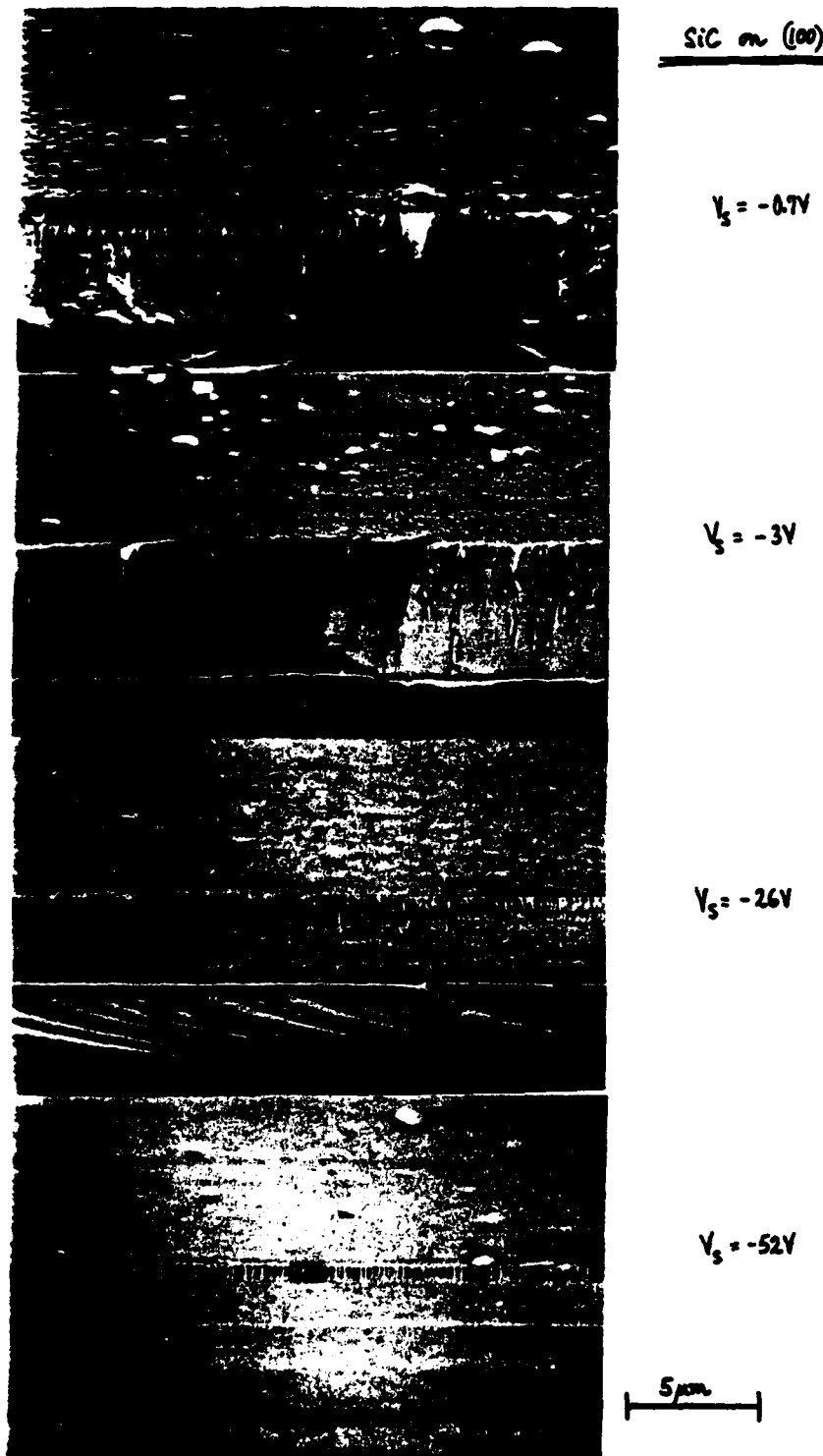


Fig. 12 Microstructure of SiC films on (100)Si substrates (native oxide not removed) as a function of V_s .

Appendix A Program and Abstracts

APPENDIX A

APPENDIX A
PROGRAM AND ABSTRACTS

PROGRAM AND ABSTRACTS

WORKSHOP ON
DIAMOND-LIKE CARBON COATINGS

APRIL 19 - 20, 1982
THE BDM CORPORATION CONFERENCE CENTER
ALBUQUERQUE, NEW MEXICO 87106

SPONSORED BY DEFENSE ADVANCED RESEARCH PROJECTS AGENCY

B. BENDOW
THE BDM CORPORATION, WORKSHOP COORDINATOR

D. GRISCOM
DARPA POINT-OF-CONTACT

WORKSHOP ON DIAMOND-LIKE CARBON COATINGS

FINAL PROGRAM

Monday, April 19

REQUIREMENTS AND POTENTIAL APPLICATIONS

Chairman: Al Hopkins, AFWAL

Opening Remarks, D. Griscom, DARPA (15 minutes)

Air Force Requirements, H. V. Winsor, AFOSR (15 minutes)

Possible Applications of Diamond-Like Carbon Coatings for
Missile Systems and Lasers, H. E. Bennett, NWC
(15 minutes)

Requirements for Laser-Damage Resistant Coatings, A. H. Guenther,
AFWL (15 minutes)

Non-Conducting Hermetic Coatings for Optical Fibers, H. E. Rast,
NOSC (15 minutes)

PREPARATION AND PROPERTIES

Chairman: O. El-Bayoumi, RADC

Hard Carbon Coatings for IR Optical Components, A. Bubenzer,
B. Dischler and P. Koidl, Fraunhofer Inst. (25 minutes)

The Properties of Hard, Insulating Carbon Coatings and Areas
of Future Efforts, T. Moravec, Honeywell (25 minutes)

Diamond-Like Carbon Films Research at NASA Lewis Research Center,
B. Banks, NASA (25 minutes)

High Energy Ion Deposited Carbon Films, M. Stein and S. Aisenberg,
Gulf & Western (25 minutes)

Hard Carbon for Environmental Protection of FLIR Optics,
A. Hendry, L. Taub and H. Gurev, OCLI (25 minutes)

PREPARATION AND PROPERTIES, cont'd

Chairman: R. Jaeger, Spectran Corp.

Some Aspects of the Growth and Characterization of "Diamond-Like"
Carbon Films, J. C. Angus, Case Western Res. Univ. (25 minutes)

Carbon-Coated Optical Fibers, J. M. Stevens, Spectran Corp., and
M. Stein, Gulf & Western (20 minutes)

Another Method of Obtaining Hard Carbon Coatings, G. K. Wehner,
Univ. of Minnesota (20 minutes)

Electrical and Optical Properties of "Diamond-Line" Amorphous
Carbon Films, F. W. Smith, City College of NY (25 minutes)

Ultraviolet-Laser Deposition, D. J. Ehrlich and J. Y. Tsao,
Lincoln Lab (15 minutes)

Carbon Film Research at Aerospace: Preparation, Characterization
and Pulsed DF Laser Damage of Coated Optics, S. Amimoto,
et al, Aerospace Corp., (15 minutes)

COATING CHARACTERIZATION

Chairman: P. Miles, Raytheon

Thin Film Characterization Techniques Applicable to Diamond-Like Carbon Coatings, H. E. Bennett, NWC (20 minutes)

Diamond-Like Carbon Films in Optical Coatings, H. A. Macleod, Univ. of Arizona (20 minutes)

Surface Analysis of Diamond-Like Carbon Films, A. K. Green and V. Rehn, NWC (15 minutes)

Raman Scattering as a Probe of Thin Films, S. Brueck, Lincoln Lab (15 minutes)

Microstructure - Property Relations in Sputtered Films, R. Messier, Penn State University (15 minutes)

ROUNDTABLE DISCUSSIONS

1. Preparation Techniques and Preparation/Properties Relationships for Diamond-Like Carbon Coatings
Moderators: B. Banks, NASA, and B. Bendow, The BDM Corporation
2. Directions for Future Research and Technology Transfer
Moderators: D. Griscom, DARPA, and H. E. Bennett, NWC

Tuesday, April 20

GOVERNMENT ONLY SESSIONS

WORKSHOP ON DIAMOND-LIKE CARBON COATINGS

ABSTRACTS

NON-CONDUCTING HERMETIC COATINGS FOR OPTICAL FIBERS

H. E. Rast
Naval Ocean Systems Center
San Diego

A number of military systems incorporating fiber optics require long lengths of high strength fibers. These fibers, like other silicate derived glasses, suffer from the phenomenon of stress corrosion or static fatigue. The observed fatigue occurs when fibers are subject to tensile stresses in a humid environment. None of the currently used organic buffer and overcoating materials is impermeable to water and, therefore, to provide hermetic protection, one must look to other materials. Among the more promising materials are metals, silicon nitride, and diamond-like carbon. The requirements and possible behavior of suitable coatings will be discussed in terms of performance, expected reliability, and economic considerations.

HARD CARBON COATINGS FOR IR-OPTICAL COMPONENTS

A. Bubenzer, B. Dischler and P. Koidl
Fraunhofer-Institute für Angewandte Festkörperphysik,
Eckerstr. 4, D-7800 Freiburg, West-Germany

Hydrogenated amorphous carbon films (a-C:H) were deposited on glass, silicon and germanium substrates. The films are transparent in the IR and are extremely hard. The a-C:H films were homogeneously deposited at a rate of about 500 Å/min in an RF excited discharge from benzene vapour. The characteristic features of this deposition method are discussed.

Thickness, short wavelength absorption, refractive index (at 0.3 μm and 2 - 10 μm) and relative hydrogen content were determined. Variations in short wavelength absorption, IR-refractive index and relative hydrogen content could be correlated with deposition conditions. The refractive index of a-C:H can be tuned to be exactly 2, thus a-C:H is an ideal one

layer AR-coating for germanium ($n = 4$). Laser calorimetric measurements of optical absorption at $10.6 \mu\text{m}$ give a loss as low as 4% for a $1.3 \mu\text{m}$ coating on germanium ($\lambda/4$ for $n = 2$ at $10.6 \mu\text{m}$). a-C:H coatings were tested for thermal shock resistance with a cw CO_2 laser.

THE PROPERTIES OF HARD, INSULATING CARBON COATINGS AND AREAS OF FUTURE EFFORTS

Thomas J. Moravec
Honeywell, Inc.
10701 Lyndale Ave. South
Bloomington, NM 55420

The electrical, optical, and mechanical properties of hard, insulating carbon coatings will be reviewed from data collected over the last several years at Honeywell. Then areas of future research efforts will be discussed that will be important for the application of these coatings to different substrates. These areas include stress and adhesion of these films.

DIAMOND-LIKE CARBON FILMS RESEARCH AT NASA LEWIS RESEARCH CENTER

Bruce Banks
NASA Lewis Research Center
Cleveland, OH 44135

NASA Lewis has been investigating a variety of approaches to produce diamond-like carbon films. Experiments have been performed or are in the process of being constructed to examine deposition by DC and RF discharges, single and dual ion-beam sources, vacuum carbon arc, and coaxial carbon plasma gun. Experimental results, including film characteristics, will be presented.

HIGH ENERGY ION DEPOSITED CARBON FILMS

M. Stein and S. Aisenberg
G+W Applied Science Labs
Watham, MA

Extensive work has been performed by G+W Applied Science Laboratories to demonstrate and investigate the process of high energy carbon ion deposition. This work includes production of carbon coatings, as well as ion implantation and surface modification. The resulting processes are designed to produce very hard, uniform, strongly adhering, transparent coatings. The particular issue addressed is the energy dependence of ion deposited carbon and observed properties as a function of this dependency.

HARD CARBON FOR ENVIRONMENTAL PROTECTION OF FLIR OPTICS

A. Hendry*, L. Taub* and H. Gurev**

The coating of hard carbon on germanium windows for land vehicle service will be described. Environmental test data, including abrasion results, will be presented.

* OCLI - Hillend, Dunfermline, Fife, Scotland

**OCLI - Santa Rosa, CA

SOME ASPECTS OF THE GROWTH AND CHARACTERIZATION OF "DIAMOND-LIKE" CARBON FILMS

John C. Angus
Chemical Engineering Department
Case Western Reserve University
Cleveland, Ohio

Carbon films can be grown by many varied techniques including: chemical vapor deposition from hydrocarbons; evaporation (carbon arc, resistance or electron beam); ion beams; RF and glow discharge in hydrocarbons; and various types of sputtering processes. Although properties of the films vary widely, they can be grouped, roughly, into those produced by low energy or thermal sources (chemical vapor deposition and evaporation) and those produced in a non-thermal, higher energy environment (ion beams, discharge processes and sputtering).

The differences between these films are summarized in the Table below. In not all cases do the films fall neatly in one category or the other. For example, diffraction maxima at both 1.16 \AA and 3.36 \AA are sometimes found.

**Properties of Films Produced by Thermal
and Non Thermal Processes**

Thermal Films

electrically conductive, 1-10 Ωcm
greater optical absorption, $\sim 10^5 \text{cm}^{-1}$
less resistant to chemical attack,
 $3\text{H}_2\text{SO}_4/\text{HNO}_3$
softer
less dense (?)
presence of $\sim 3.36\text{\AA}$ diffraction line

Non Thermal Films

electrical insulators, $10^{12}\text{-}10^{16} \Omega\text{cm}$
less optical absorption, $\sim 10^4 \text{cm}^{-1}$
very resistant to chemical attack,
 $3\text{H}_2\text{SO}_4/\text{HNO}_3$
harder
more dense (?)
absence of $\sim 3.36\text{\AA}$ diffraction line
presence of $\sim 1.16\text{\AA}$ diffraction line

The most logical and simplest explanation for the differences is that the "thermal" films are dominated by sp^2 , trigonal type graphitic bonds, whereas the films produced by non-thermal means are dominated by sp^3 , tetrahedral diamond-like bonding. In the former case growth occurs from molecules and molecular fragments with relatively low energies, i.e., less than 1 eV. On the other hand with non-thermal sources the surface is continually bombarded with energetic species, e.g., 10 to 500 eV depending on the process. This unusual growth environment is likely responsible for the production of films dominated by sp^3 tetrahedral structure. Other structures, e.g., graphitic, olefinic, cumulene, are sputtered away by the high energy ions impinging on the surface.

Most diamond-like carbon films are amorphous and hence it is difficult to get detailed structural information from diffraction experiments. However, a great deal of information can be obtained from relatively simple tests, e.g., elemental analysis (Auger and SIMS) together with a measurement of density. Because a carbon atom has only a relatively few possible bonding schemes available to it, inferences can be made about the possible structure of the films. Further information can be obtained from infrared absorption measurements and from chemical dissolution tests.

The results of these measurements on several types of films grown at the NASA Lewis Research Center will be discussed.

Molecular orbital calculations have been made which permit a preliminary determination of the most stable two, three and four atom clusters on a (111) diamond surface. The most stable dimer has a linear configuration normal to the surface. The bond to the surface is longer, i.e., less strongly bound, than that of a single carbon adatom, and hence this dimer would appear to be more susceptible to sputtering. Three adatoms can form a bridged structure. Four adatoms can form a "bridge and sentry" or, more preferably, a tent configuration which is essentially an extension of the diamond lattice. These results tend to support the simple idea that non sp^3 (non tetrahedral) structures may be preferentially sputtered away.

CARBON-COATED OPTICAL FIBERS

John M. Stevens
SpecTran Corporation
Sturbridge, MA

Martin Stein
G+H Applied Science Laboratory
Waltham, MA

We review progress in the use of carbon as a hermetic coating for optical fibers and indicate prospects for future performance.

ANOTHER METHOD OF OBTAINING HARD CARBON COATINGS

G. K. Wehner
Electric Engineering Department
University of Minnesota
Minneapolis, MN 55455

Graphite is sputtered in a low pressure triode plasma. Those atoms which leave the target surface obliquely have higher kinetic energy than those leaving perpendicularly. One obtains hard carbon coatings when one catches on a substrate only the obliquely ejected carbon atoms.

ELECTRICAL AND OPTICAL PROPERTIES OF
"DIAMOND-LIKE AMORPHOUS CARBON FILMS

F. W. Smith
Professor of Physics
Dept. of Physics
City College of N.Y.
New York, N.Y. 10031

The electrical and optical properties of "diamond-like" amorphous carbon films, prepared via the dc glow discharge decomposition of C₂H₂, show a remarkable dependence on preparation conditions¹. In particular, as a function of the deposition temperature T_d, the room temperature electrical conductivity increases from 10⁻¹⁶ to 10⁻⁶ ohm⁻¹ cm⁻¹ and the optical energy gap decreases from 2.1 to 0.9 eV as T_d is increased from 25 to 375°C. The deposited films would have essentially "graphitic" electrical and optical properties when deposited at T_d > 400°C. For possible semiconductor applications, we have shown that these "diamond-like" films can be doped n- or p-type via incorporation of P or B atoms during deposition². This doping effect has been confirmed via thermopower measurements³. At present we are studying the thermal stability of these films. The effect of annealing (in vacuum or an inert atmosphere) on the electrical and optical properties of these films will be discussed.

¹ B. Meyerson and F. W. Smith, J. Non-Cryst. Solids 3/36, 435 (1980).

² B. Meyerson and F. W. Smith, Solid State Comm. 34, 531 (1980).

³ B. Meyerson and F. W. Smith (to be published in Solid State Comm.).

ULTRAVIOLET-LASER PHOTODEPOSITION*

D. J. Ehrlich and J. Y. Tsao
Lincoln Laboratory, Massachusetts Institute of Technology
Lexington, Massachusetts 02173

Ultraviolet laser light can be used to initiate low-temperature chemical processing of surfaces by reactions which are similar in many respects to those active in plasma techniques. We have recently

*This work was supported by the Department of the Air Force, in part under a specific program sponsored by the Air Force Office of Scientific Research, by the Defense Advanced Research Projects Agency, and by the Army Research Office.

demonstrated a series of new techniques¹ for thin-film deposition, for etching, and for doping of semiconductors by processes based on photolytic reactions at a gas-solid interface. Gas-phase and surface chemical reactions are controlled by a UV laser, while the temperature of the surface is independently controlled and can typically remain near room temperature. Extensions to laser deposition of carbon films by neutral or ion photochemical channels will be discussed.

¹D. J. Ehrlich, R. M. Osgood, Jr. and T. F. Deutsch, IEEE J. Quantum Electron., Vol. QE-16, pp. 1233-1243, Nov. 1980.

CARBON FILM RESEARCH AT AEROSPACE:
PREPARATION, CHARACTERIZATION, AND PULSED
DF LASER DAMAGE OF COATED OPTICS

S. T. Amimoto, J. S. Whittier, A. Whittaker, A. Chase
and R. Hofland, Jr.

The Aerospace Corporation
P. O. Box 92957
Los Angeles, CA 90009

Pulsed laser damaged levels of well characterized carbon (carbyne) films produced by rapid quenching of laser heated carbon gas will be reported. These films have an average refractive index of 2, absorption coefficient varying from $8 \times 10^4 \text{ cm}^{-1}$ at $1 \mu\text{m}$ to $< 2 \times 10^3 \text{ cm}^{-1}$ at $10 \mu\text{m}$, excellent adhesion on a variety of substrates including CaF_2 , Cu, Pt, glass, Si, Ge and sapphire and high chemical resistance to corrosive acids including concentrated HF. Ion microprobe mass analysis reveal the presence of C_1^- to C_4^- carbon negative ions. For early samples produced at Aerospace, but not subjected to laser damage tests, diamond-like hardness (greater than B_4C) and adhesion strengths of $60\text{-}400 \text{ kg/cm}^2$ have been found.

Film thicknesses of $0.1 - 0.2 \mu$ were deposited on heated degreased bowl-feed polished 1" diameter CaF_2 windows and polished copper mirrors. Single pulsed damage levels were determined using a 2 ω electron-beam initiated $\text{D}_2\text{-F}_2$ chain laser. A transmission coupled unstable resonator with a soft spatial aperture gave uniform laser fluence at the optics test bench. Nominal 10-20 J pulses in $0.6 - 0.9 \mu\text{s}$ (FWHM) were employed on fresh test sites on the half coated optics.

Single pulse DF damage levels of carbyne films on CaF_2 were determined to be 25 J/cm^2 on the best samples with damage confined primarily to localized spots containing graphitic particles. The origin of these particles was identified as the heated graphite rod used as the source of the hot carbon gas. With uncoated CaF_2 , damage levels of $21\text{-}27 \text{ J/cm}^2$ were measured. For carbon films on copper, damage levels of $\sim 10 \text{ J/cm}^2$ were measured in marked contrast to uncoated OFHC Spawr copper mirrors of 58 J/cm^2 . Damage on copper was also initiated by numerous graphitic particulates. It thus appears that the removal of these particulates would result in higher pulsed damage levels in carbon films.

Despite the relatively unsophisticated technique for producing carbyne coatings, we have shown that carbyne films are attractive candidates for protective coating applications. For pulsed high energy laser applications such coatings must repetitively withstand high overpressures of 6-8 atmospheres of hot corrosive $\text{F}_2\text{-DF}$ gas mixtures at high laser fluence. At present no coatings are available that will simultaneously satisfy these requirements.

THIN FILM CARACTERIZATION TECHNIQUES APPLICABLE TO DIAMOND-LIKE CARBON COATINGS

H. E. Bennett
Naval Weapons Center
China Lake, CA

Parameters which should be evaluated for diamond-like films include (1) film structure, including both microscopic properties such as the existence of columnar structure, density and porosity, and crystallographic properties, (2) film thickness and thickness uniformity, (3) mechanical properties such as hardness, strain, stress, adhesion, (4) compositional properties including the phase and chemical state of the carbon and also the presence of impurities, (5) physical imperfections such as aggregates, nodules, film microroughness and correlation to substrate microroughness, the parameter which determines optical scattering behaviour, and (6) optical properties including index of refraction, absorption coefficient, interfacial absorption, high temperature properties and possible optical

inhomogeneity or anisotropy. Other properties of interest may be the environmental stability, resistance to chemical attack, radiation resistance, laser damage threshold, diffusion rate of possible contaminants, presence of dangling bonds, sensitivity to absorption and many others. A brief survey of some of the experimental techniques which are in use at Michelson Laboratory and elsewhere for evaluating such film properties will be given.

DIAMOND-LIKE CARBON FILMS IN OPTICAL COATINGS

H. A. Macleod
Optical Sciences Center
Tucson, AZ

The features of conventional thin films which are known to be of importance in optical coatings might be useful indicators of properties which could be used as characterization parameters for diamond-like carbon films.

SURFACE ANALYSIS OF DIAMOND-LIKE CARBON FILMS

A. K. Green and Victor Rehn
Naval Weapons Center
China Lake, CA 93555

Auger Electron Spectroscopy (AES), X-ray Photoelectron Spectroscopy (XPS) and Secondary Ion Mass Spectroscopy (SIMS) have been applied to a limited number of diamond-like carbon films. Both AES and XPS have the potential to reveal chemical bonding as well as chemical composition. SIMS is mainly used for trace element detection.

Diamond-like carbon films prepared at Westinghouse Research Labs and Gulf & Western Applied Science Labs have been studied. Comparison spectra have been taken from amorphous carbon films prepared at NWC and graphite. Ion-beam sputtering and heating were tried as in-situ surface cleaning procedures. The fine structure of the carbon KLL Auger transition was monitored as an indication of diamond-like character. Lurie and Wilson¹ have reported that a clean undamaged diamond surface

¹P. G. Lurie and J. M. Wilson, Surface Science 65, 476 (1977).

exhibits four peaks in the carbon KLL spectra while graphite has three peaks and amorphous carbon has two peaks. Our results indicate that diamond-like carbon films, if properly cleaned in UHV, have carbon KLL spectra similar to a diamond surface.

RAMAN SCATTERING AS A PROBE OF THIN-FILMS*

S. R. J. Brueck
Lincoln Laboratory, Massachusetts Institute of Technology
Lexington, Massachusetts 02173

Raman scattering provides a nondestructive probe of thin-film properties such as local structure, degree of crystallinity, microcrystal grain size and local strain fields. We have carried out a series of measurements on Si films with thicknesses as small as 20 Å and with a transverse spatial resolution of $\sim 0.5 \mu\text{m}$. Applications to the characterization of "diamond-like" carbon films will be discussed.

*This work was supported by the Department of the Air Force, in part with specific funding from the Air Force Office of Scientific Research, and by the Office of Naval Research.

MICROSTRUCTURE-PROPERTY RELATIONS IN SPUTTERED FILMS

Russell Messier
Materials Research Laboratory
The Pennsylvania State University
University Park, PA 16802

The mechanical and chemical properties of thin films depend at least in part on their microstructure. A structure zone model common to all vapor deposition methods has been developed to classify the various physical microstructures found^(1,2). In this model the microstructure is related to a normalized temperature, T/T_m where T = temperature of the film during preparation and T_m - the melting point of the material ($^{\circ}\text{K}$). Thornton⁽²⁾ extended this model to the case of sputtered films in which a second important variable, the pressure of the sputtering gas (e.g., P_{Ar}) was demonstrated. It has been shown that the densest, most crystalline structures are obtained at high T/T_m and low P_{Ar} .

¹B. A. Movchan and A. V. Demchishin, Phys. Met. Metallogr. 28, 83 (1969).

²J. A. Thornton, Ann. Rev. Mat. Sci. 7, 239 (1977).

Recently we have shown the effectiveness of this model in understanding the complex relations between chemical, mechanical, and electronic properties and the detailed physical structure for the amorphous semiconductors a-Ge⁽³⁾, a-Si⁽⁴⁾, and a-Si:H⁽⁵⁾. In particular, the effects of positive ion-bombardment of the growing film have been shown to be most important⁽⁵⁾ and directly related to decreasing gas pressure. In effect, the bombardment is producing a second source of temperature, albeit a non-equilibrium temperature, at the growing film. Thus the "effective T/T_m" can be increased without increasing the temperature of the workpiece. This process is seen to be especially important for materials with a high T_m (such as carbon) since it allows dense structures to be achieved at relatively low equilibrium, external heater temperatures.

In addition to reviewing this above work⁽³⁻⁵⁾, we will present recent unpublished results on SiC and BN films in which similar bombardment effects are related to epitaxial growth and film hardness. Relation between our work and that reported for diamondlike carbon films, will be made. Finally, methods we have used for characterizing the physical structure of thin films in detail, from the micron-level (microstructure) to the atomic-level (nanostructure), will be described.

³P. Swab, S. V. Krishnaswamy, and R. Messier, J. Vac. Sci. Technol. 17, 326 (1980); and; S. V. Krishnaswamy, R. Messier, Y. S. Ng, T. T. Tsong, and S. B. McLane, J. Non-Cryst. Solids 35-36, 531 (1980).

⁴R. Messier, S. V. Krishnaswamy, L. R. Gilbert, and P. Swab, J. Appl. Phys. 51, 1611 (1980).

⁵R. C. Ross and R. Messier, J. Appl. Phys. 52, 5329 (1981); and R. C. Ross and R. Messier, AIP Conf. Proc. 73, 53 (1981).

Appendix B

Workshop Attendance List

APPENDIX B

APPENDIX B
WORKSHOP ATTENDANCE LIST

WORKSHOP ON DIAMOND-LIKE CARBON COATINGS

April 19-20, 1982
The BDM Corporation Conference Center
Albuquerque, NM 87106

ATTENDANCE LIST

S. Amimoto
Aerospace Corporation
P. O. Box 92957
Los Angeles, CA 90009

Bruce Banks
NASA Lewis Research Center
Mail Stop 77-4
21000 Brookpark Road
Cleveland, OH 44135

Mike Bayne
Hewlett Packard
P. O. Box C-006
Vancouver, WA 98668

Dr. Bernard Bendow
The BDM Corporation
1801 Randolph Road, SE
Albuquerque, NM 87106

H. E. Bennett
Naval Weapons Center
China Lake, CA 93555

Dr. V. W. Biricik
Northrop Res. & Tech. Center
One Research Park
Palos Verdes Peninsula, CA 90274

Dr. S. R. J. Brueck
MIT Lincoln Laboratory
244 Wood Street
Lexington, MA 02173

A. Bubenzer
Fraunhofer Institute IAF
Eckerstr.4
d-78 Freiburg
W-Germany

Ronald E. Bullock
General Atomic Company
P. O. Box 81608
San Diego, CA 92138

Patrick Colardelle
S. A. T.
41 Rue Cantagrel
75013 Paris, France

John Cooney
General Dynamics
Convair Division
P. O. Box 80847
San Diego, CA 92138

Donald Dalton
UTRC
West Palm Beach, FL

Charles DeLuca
SpecTran Corporation
P. O. Box 650, Hall Road
Sturbridge, MA 01566

C. W. Deneka
Corning Glass Works
Sullivan Park
Corning, NY 14831

Richard Denton
Denton Vacuum
Cherry Hill Indus Center
Cherry Hill, NJ 08003

Michael DiMano
The Rochester Corporation
P. O. Box 312
Culpeper, VA 22701

Sam Divita
U.S. Army CECOM
DRSEL/COM/RML
Ft. Monmouth, NJ 07703

Stan Domitz
Lewis Research Center, NASA
21000 Brookpark Road
Cleveland, OH 44135

T. M. Donovan
Naval Weapons Center
Physical Optic & Thin Films Branch
Code 3818
China Lake, CA 93555

David F. Edwards
Los Alamos National Laboratory
MS-J564
Los Alamos, NM 87545

D. J. Ehrlich
MIT Lincoln Laboratory
Lexington, MA 02173

Osama El-Bayoumj
U. S. Air Force
RADC/ES17
Hanscom AFB, MA 01731

Mr. Richard E. Engdahl
Deposits & Composites Inc.
318 Victory Drive
Herndon, VA 22070

Robert Giglia
American Cyanamid
1937 W. Main Street
Stanford, CT 06904

A. K. Green
Naval Weapons Center
Code 3813
China Lake, CA 93555

Dave Griscom
DARPA
1400 Wilson Blvd
Arlington, VA

Dr. H. S. Gurev
OCLI
P. O. Box 1599
Santa Rosa, CA 95402

Gottfried Haacke
American Cyanamid
1937 West Main Street
Stanford, CT 06904

Hiroshi Hashimoto
Nippon Kogaku K.K.
6-3, Nishi-oi, 1-Chrome
Shinagawa-Ku, Tokyo
Japan 140

Mr. S. J. Holmes
Northrop Res. & Tech. Center
One Research Park
Palos Verdes Peninsula, CA 90274

Dr. Alan K. Hopkins
AFWAL/Materials Laboratory
Wright-Patterson AFB, OH 45433

Dr. Raymond Jaeger
SpecTran Corporation
P. O. Box 650, Hall Road
Sturbridge, MA 01566

G. T. Johnston
Rocketdyne Division
Rockwell International
P. O. Box 5670
Kirtland AFB, NM 87185

Mr. R. William Jones
U.S. Army Missile Command
ATTN: DRSMI-RHST
Redstone Arsenal, AL 35898

Milton N. Kabler
Optical Probes Branch
Code 6510
Naval Research Lab
Washington, D.C. 20375

Gary F. Knutson
Vector/Schlumberger
555 Industrial Road
Sugar Land, TX 77478

Dr. Peter Koidl
Fraunhofer Institute for
Applied Solid State Physics
Eckerstrasse 4
D-7800 Freiburg, W-Germany

W. J. Lackey
Oakridge National Laboratory
Oakridge, TN 37830

Peter C. LaDelfe
Los Alamos National Laboratory
CMB-6/MS-770
P. O. Box 1663
Los Alamos, NM 87545

John J. Larkin
RADC/CSM
Hanscom AFB
Bedford, MA 01731

H. Angus Macleod
Optical Sciences Center
University of Arizona
Tucson, AZ 85721

Jean Marie Mackowski
Institut Physique Nucléaire de Lyon
Université Claude Bernard
43 Boulevard du 11 Novembre 1918
69621 Villeurbanne, France

Tim McGrath
Laser Focus Magazine
3109 Flowers
Palo Alto, CA 94306

Carl J. McHargue
Oak Ridge National Laboratory
Metals and Ceramics Division
P.O. Box X
Oak Ridge, TN 37830

R. C. McNamara
General Dynamics/Convair
P.O. Box 80847
San Diego, CA 92138

Bob McNeill
UNM
Electrical Engineering Department
Albuquerque, New Mexico 87131

Dr. James A. Merritt
Research Directorate
US Army Missile Laboratory
Redstone Arsenal, AL 35898

Russell Messier
Pennsylvania State University
265 Materials Research Laboratory
University Park, PA 16802

David Millam
Lawrence Livermore National Laboratory
P.O. Box 5508, L-470
Livermore, CA 94550

Peray A. Miles
Ratheon Company
Hartwell Road Bedford, MA 01730

Mr. R. C. Monachan
Barr and Stroud Limited
Caxton Street, Anniesland, Glasgow G13
Scotland

Thomas J. Moravec
Honeywell
10701 Lyndale Avenue S
Bloomington, MN 55420

Dr. Yoshihara Namba
The University of New Mexico
Department of Physics and Astronomy
Albuquerque, New Mexico 87131

Mr. James L. Parham
US Army Missile Command
Attn: DRSMI-RLM
Redstone Arsenal, AL 35898

Russ Parsons
UTRC
5301 Central, NE - Suite 306
Albuquerque, NM 87108

Ricardo C. Pastor
Hughes Research Labs
3011 Malibu Canyon Road
Malibu, CA 90265

Dr. Walter T. Pawlewicz
Battelle - Pacific Northwest
Laboratory
Box 999
Richland, WA 99352

Kevin Probst
The BDM Corporation
1801 Randolph Rd. S. E.
Albuquerque, New Mexico 87106

Mehnet Rona
A D Little Inc.
Acorn Park
Cambridge, MA 02140

Dr. Earl Rudisill
Laser Power Optics
11211 Suite U
Sorrento Valley Road
San Diego, CA 92121

Dr. Lyn Skolnik
The BDM Corporation
1801 Randolph Rd. S. E.
Albuquerque, New Mexico 87106

Frederick W. Smith
Physics Department
City College of N. Y.
New York, New York 10031

Mr. Martin Stein
G&W Applied Science Labs.
335 Bear Hill Road
Waltham, MA 02154

Dennis Strauss
Rockwell International
Science Center
1049 Camino Dos Rios
Thousand Oaks, California 91360

Derek B. Webb
British Embassy
3100 Massachusetts Ave. N.W.
Washington, D. C. 20008

G. K. Wehner
University of Minnesota
E. E. Department
Minneapolis, MN 55455

R. T. Williams
Naval Research Laboratory
Code 6511
Washington, D. C. 20375

Charles Wood
Jet Propulsion Laboratory
Bldg. 277-102
4800 Oak Grove Dr.
Pasadena, CA 91103

John C. Angus
Case Western Reserve Univ.
Cleveland, OH 44106

Troy W. Barbee Jr.
Stanford University
Department of Materials & Sciences &
Engineering
Stanford, CA

Harry Winsor
AFOSR/NE
Bolling AFB, D. C. 20332

V. Nathan
AFWL/ARAO
Kirtland AFB, NM 87123

Amy Luck
AFWL/ARAO
Kirtland AFB, NM 87117

Ron Lusk
AFWL
Kirtland AFB, NM 87117

A. Guenther
AFWL/CA
Kirtland AFB, NM 87117

A. B. Chase
Aeorspace Corporation
P. O. Box 92957
Los Angeles, CA 90009

D. J. Nagal
Naval Research Lab
Washington, D.C. 20375

H. E. Rast
NOSC
271 Catalina Blvd.
San Diego, CA 92152

Keith Shillito
AFWL/ARAO
Kirtland AF8, NM 87117

F. J. Vascola
Penn State University
265 Materials Research Laboratory
University Park, PA 16802

Bruce Pierce
AFWL
Kirtland AFB, NM 87117

Myron Maclin
AFWL
Kirtland AFB, NM 87117

Kenneth Jungling
University of New Mexico
Albuquerque, NM 87106

B-6

AD-A136 766

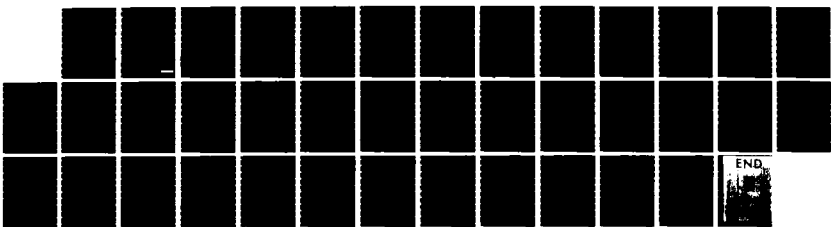
PROCEEDINGS OF THE DARPA (DEFENSE ADVANCED RESEARCH
PROJECTS AGENCY) WORK. (U) BDM CORP ALBUQUERQUE NM
B BENDOW 1982 MDA983-81-C-0151

4/4

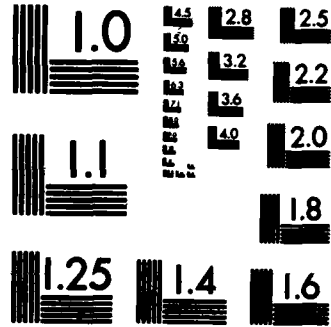
UNCLASSIFIED

F/G 11/3

NL



END



MICROCOPY RESOLUTION TEST CHART
NATIONAL BUREAU OF STANDARDS-1963-A

**Appendix C
Partial Bibliography on
Diamond-Like Coatings**

APPENDIX C

APPENDIX C
PARTIAL BIBLIOGRAPHY ON
DIAMOND-LIKE CARBON COATINGS

PRIMARY REFERENCES

Hard Carbon Coatings with Low Optical Absorption
B. Dischler, A. Bubenzer, and P. Koidl
Fraunhofer-Institut fur Angewandte Festkorperphysik
Eckerstrasse 4, D-7800 Freiburg, West Germany

Hydrogenated amorphous (a-C:H) films were prepared by RF-plasma deposition from benzene vapor. Complete optical absorption spectra from the UV to the IR (0.2-20.0 μm) have been measured. The optical gap depends linearly on hydrogen content and E_{opt} can be varied between 0.8 and 1.8 eV. For energies below E_{opt} the films are almost transparent and absorption is specially low in the 2-6 μm region (e.g. $\alpha = 15 \text{ cm}^{-1}$ at $\lambda = 2.8 \mu\text{m}$). Sharp C-H stretch absorption bands occur near 3.4 μm , giving insight into the microstructure of the films. A newly reported weak band at 3.03 μm is first evidence for C=C triple bonds (sp^1 hybridization) in a-C:H, where sp^3 (single) and sp^2 (double) C-C bonds dominate.

Hydrogenated Carbon Films Produced by Sputtering in Argon-Hydrogen Mixtures

D. R. McKenzie, R. C. McPhedran, L. C. Botten, N. Savvides, and R. P. Netterfield
University of Sydney, School of Physics
Sydney, N.S.W. 2006, Australia
Journal: Applied Optics, Vol. 21, No. 20, page 3615
October 15, 1982

Carbyne Forms of Carbon: Do They Exist?

Journal: Science, Vol. 216, page 984
May 28, 1982

Almost 15 years have passed since carbynes entered the literature as new forms of elemental carbon. They recently attracted attention as possible interstellar dust constituents and as carriers of presolar noble gases in meteorites. Their existence and that of the related mineral chaoite are questioned, and a reevaluation of previous data is suggested.

Optical Characterization of Plasma-Deposited Hard Carbon Coatings
B. Dischler, A. Bubenzer, P. Koidl, G. Brandt, O. F. Schirmer
Fraunhofer-Institut fur Angewandte Festkorperphysik
Eckerstrasse 4, D-7800 Freiburg, West Germany

Hydrogenated amorphous carbon films (a-C:H) have been deposited on Ge, Si, and glass substrates in a RF excited flow discharge from benzene vapor. These films are hard, chemically inert and IR-transparent and therefore very promising for protective and anti-reflective coatings for IR-optical components. We report on the optical properties of a-C:H and their quantitative dependence on

deposition parameters. Absorption spectra of a-C:H coatings in the wavelength range 0.2-20 μm have been extracted from transmission and reflection measurements. In addition, CO₂ laser damage thresholds are reported. For a-C:H with refractive index $n=1.93$ the following absorption coefficients have been measured: 250, 25, 15, 200, and 780 cm^{-1} at wavelengths of 10.6, 3.8, 2.8, 1.3, and 1.06 μm , respectively. The increased short wavelength absorption and its possible dependence on dangling bond density--as determined by electron spin resonance--is discussed.

Key Words: Absorption, Amorphous Hydrogenated Carbon, Hard Coating, Infrared, Laser Damage, Optical Properties, Plasma Deposition, Thin Films.

On the Short Range Atomic Structure of Non-Crystalline Carbon

D. F. R. Mildner

University of Missouri Research Reactor, Columbia, MO 65211

J. M. Carpenter

Pulsed Neutron Source Program, Argonne National Laboratory,

Argonne, IL 60439

July 16, 1981

Neutron diffraction data show there is little tetrahedral bonding in glassy carbon, and correspond to the Stenhouse-Grout structure factor model for amorphous carbon taking the degenerate case in which the amount of tetrahedral bonding is negligible. This is in contrast to the X-ray results of Noda and Inagaki. Further analysis of the radial distribution function from the neutron diffraction data is presented. A brief summary of other X-ray diffraction measurements on a variety of amorphous carbons is given, all of which confirm the predominantly trigonal coordination. The disagreement of the earlier X-ray and electron diffraction measurements is due to the poor resolution and normalization of the data, and also perhaps the method of preparation. The amount of tetrahedral bonding present in amorphous carbon requires careful diffraction measurements at large scattering vectors to enable better resolution of the peaks in the radial distribution function.

Characterization of Diamondlike Films

John C. Angus

Angus Research Corporation

302 N. Buchanan St., Spring Lake, MI 49456

December 22, 1981 (63 pages)

Carbon films formed by ion deposition from methane/argon using the NASA 30 cm ion source were characterized. The films were deposited on silicon, quartz, and potassium bromide substrates using nominal conditions of 100eV beam energy and 300 $\mu\text{A}/\text{cm}^2$ current density. Growth rates of approximately 0.3 $\mu\text{m}/\text{hour}$ were achieved.

Electron microscopy and electron diffraction show the films to be featureless and amorphous. Elemental analysis by Auger and secondary ion mass spectroscopy show only carbon and hydrogen present in significant amounts, with small amounts of argon, oxygen, and silicon present in some films. The

densities of two of the films, determined by direct measurement of area, thickness, and mass, were 1.78 ± 0.21 g/cm³. Analysis by Fourier transform infrared spectroscopy indicates the hydrogen is present mainly in methylene groups. The atomic ratio of carbon to methylenic hydrogen is between 10 and 50.

The films appear yellowish in transmission; the absorbance uniformly increases from 7,000 Å in the visible to 2,000 Å in the ultraviolet. The films survive prolonged attack by a solution of 3H₂SO₄/1 HNO₃ at 80°C and are not attacked by 3HNO₃/1 HF/1 HAc mixtures. The index of refraction as measured by ellipsometry was in the range from 1.75 to 2.30.

The films are clearly not diamond; however, some of their properties, e.g., carbon Auger line-shape, transparency, chemical inertness, resistivity, and index of refraction, are similar to those of diamond. Other properties such as density and carbon/hydrogen ratio indicate the film is a hydrogen-deficient polymer.

One possible structure, consistent with the data, is a random network of tetrahedrally coordinated carbon atoms and methylene linkages.

Key words: Carbon Films, Diamond Like Films, Ion Beam Deposition, Characterization of Films.

Ion Beam Deposition of Amorphous Carbon Films with Diamondlike Properties

John C. Angus

Case Western Reserve University, Cleveland, OH 44106

Michael J. Mirtich and Edwin G. Wintucky

NASA Lewis Research Center

21000 Brookpark Road, Cleveland, OH 44135

November 19, 1981

Carbon films were deposited in silicon, quartz, and potassium bromide substrates from an ion beam. Growth rates were approximately 0.3 m/hour. The films were featureless and amorphous and contained only carbon and hydrogen in significant amounts. The density and carbon/hydrogen ratio indicate the film is a hydrogen-deficient polymer. One possible structure, consistent with the data, is a random network of methylene linkages and tetrahedrally coordinated carbon atoms.

Pulsed D₂-F₂ Chain-Laser Damage to Coated Window and Mirror Components

S. T. Amimoto, J. S. Whittier, A. Whittaker, A. Chase,
and R. Hofland, Jr.

The Aerospace Corporation, Los Angeles, CA 90009

M. Bass

USC Center for Laser Studies, Los Angeles, CA 90009

November 1981

Large-spot laser damage thresholds have been measured for bowl-feed-polished CaF₂ and sapphire windows (bare and antireflection-coated) and for highly-polished copper mirrors (bare and carbyne-coated) at DF chain-laser wavelengths (3.58-4.7 μm). The chain reaction between F₂ and D₂ was initiated by a magnetically-confined electron beam, producing DF-laser outputs

of 10-20 J in pulses of a 0.6-0.9 μ sec (FWHM) duration. Energy extracted from a transmission-coupled unstable resonator was focused using a CaF₂ lens. A soft-aperture technique was employed to suppress effects of Fresnel diffraction so that uniform (top-hat) intensity profiles were obtained along the focusing beam. With this laser system, commercially available antireflection-coated CaF₂ and Al₂O₃ samples were measured to have damage thresholds in the range 21-27 J/cm². Significantly larger damage thresholds were found for uncoated, polished samples of Al₂O₃, but damage resistance of uncoated polished CaF₂ was measured to be equal to that of the best antireflection-coated CaF₂ samples. A highly polished copper mirror was found to have the highest damage threshold of all the materials tested (58 J/cm²). Carbyne films of diamond-like hardness, a type of carbon coating, were applied to polished copper mirrors and bowl-feed-polished CaF₂ surfaces. Such carbyne coatings as were prepared in this work contained numerous carbon-bearing particles that were easily damaged (\sim 10 J/cm²). However, regions of the irradiated carbyne film that were free of carbon particles withstood high laser fluences (25 J/cm²), suggesting that improvements in carbyne film preparation would yield attractive protective coatings of high damage resistance at DF wavelengths.

Key words: Carbone (carbon) Coatings, Laser Windows, Laser Mirrors, Laser Damage, DF-Chain Laser, Coating Absorption, Adhesion Strength, Acid Resistance.

Structural Investigation of Thin Films of Diamondlike Carbon

H. Vera and T. J. Moravec

Honeywell Corporate Technology Center

10701 Lyndale Avenue South, Bloomington, MN 55420

June 30, 1981

Diamondlike carbon films produced both by ion-beam technique and by radio-frequency (RF) plasma decomposition of hydrocarbon gases (C₄H₁₀, C₂H₆, C₃H₈, and CH₄) have been examined using the technique of transmission electron microscopy. Although these examinations indicate that these films are predominantly amorphous, both single-crystal and polycrystalline diffraction patterns have been obtained from films of both types that indicate formation of several different phases. Some of these phases appear to be cubic and could be new forms of carbon. The results of secondary ion mass spectrometric analysis of carbon films produced by RF plasma decomposition of hydrocarbon gases are also discussed.

Infrared Reflectors

(Patent): European Pat. Appl.: EP 30792, Britain

Alan Herold Lettington

National Research Development Corporation

June 24, 1981 (11 pages)

Language: English.

**Deposition of Thin Films of Materials with High Melting Points on
Substrates at Room Temperature Using the Pulse Plasma Method**

M. Sokolowski, A. Sokolowska, A. Michalski, Z. Romanowski,

A. Rusek-Mazurek, and M. Wronikowski

Technical University, Warsaw, Poland

Proceedings of The International Conference on Ion and Plasma Assist.

Tech., Amsterdam, Netherlands, Jun 30-Jul 2, 1981 (pages 249-254)

The pulse plasma method was used to deposit thin films of diamond, borozone, Al//20//3, Ta//20//t and other materials. The main advantage of this method is the possibility that films with good adhesion to the substrate can be prepared under low temperatures and at pressures attainable with a rotary pump. The main disadvantage of this method in its present stage of development is that the purity of the films produced is insufficient for their application as semiconductors in electronic devices.

Key Words: Semiconductor Diodes, Light Emitting, Thin Films, Aluminum Compounds, Tantalum Compounds, Plasmas.

Diamond Film Formation

(Patent): Japan Kikai Tokkyo Koho; JP 8122616

Nippon Telegraph and Telephone Public Corporation

March 3, 1981 (4 pages)

Language: Japanese

Ion-Beam Deposited Protective Films

Michael J. Mirtich

NASA, Lewis Research Center, Cleveland, OH

Proceedings of 15th International Electr. Propul. Conference, Las Vegas,
NV, 21-23 Apr 1981

1981 (11 pages)

A 30-cm-diameter argon ion source was used to sputter deposit metallic films on H-13 steel. Some materials protect the steel by reducing thermal fatigue and increase die lifetime. Tests were performed to optimize conditions to produce diamondlike films. A dual beam ion source was used to increase the mobility of the condensing atoms during film deposition. The beam shield incorporated in the mercury ion thruster to be flight tested on the P80-1 satellite was coated with molybdenum coating.

Key Words: Protective Coatings, Sputtering, Propulsion, Aerospace Applications, Spacecraft, Power Supply.

Vapor Phase Diamond Growth Technology

J. C. Angus

Case Western Reserve University, Cleveland, OH

Dept. of Chemical Engineering, National Aeronautics and Space
Administration, Washington, D.C.

January 30, 1981 (17 pages)

Key Words: Carbon, Crystal Growth, Ion Beams, Thin Films, Vapor Deposition, Crystal Structure, Ionization Chambers, Spectroscopic Analysis.

The Protection of Front Surfaced Aluminum Mirrors with Diamondlike Carbon Coatings for Use in the Infrared

A. H. Lettington, G. J. Ball

Royal Signals and Radar Establishment, Malvern, England

Defence Research Information Centre, Orpington, England

January, 1981 (11 pages)

It has recently been shown that aluminum mirrors protected with a variety of thin passivation layers have severe reflectivity losses in the 8-12 micrometer spectral region when used at oblique incidence. This memorandum presents measurements and calculations illustrating this effect and derives the condition that the loss will occur if $\cos \phi < (\text{in sub } 1 \text{ sq} + k \text{ sub } 1 \text{ sq})^{-1/2}$ where ϕ is the angle of incidence. Its main purpose is to propose the use of an infrared transmitting diamondlike carbon coating for metallic reflectors in the 8-12 micrometer band. These coatings, in addition to being abrasion-resistant and chemically durable, do not exhibit a reflectivity loss at angles of incidence of practical importance.

The use of an infrared transmitting diamondlike carbon coating for metallic reflectors to correct for reflectivity losses in the 8-12 micron band is proposed. Many thin passivation layers have severe reflectivity losses when used at oblique incidence. Measurements and calculations illustrating this effect are presented. The destructive interference appears at angles lower than a limit related to the refractive index and the extinction coefficient. An expression for that limit is given. Carbon overcoating of metallic reflectors is shown to upgrade the reflectivity in the 8-12 micron band, at angles of incidence of 45 and 60 degrees. Applications such as catadioptric telescopes permanently exposed to the atmosphere can be envisaged using this technique.

Key Words: Protective Coatings, Mirrors, Infrared Equipment, Aluminum, Carbon, Diamonds, Reflectance, Infrared Spectra, Low Loss, Infrared Optical Systems, Infrared Reflection, Mirrors, Dielectrics, Incidence, Refractivity, Spectral Reflectance, Telescopes.

Identifiers: Foreign Technology, NTISDODXA, NTISFNUK, NTISDODXA, NITSFNUK, NTISNASAE.

Carbon Film Formation by Laser Evaporation and Ion Beam Sputtering

Susumu Fujimori, Toshio Kasai, Takahiro Inamura

Ibaraki Electr. Communications Laboratory

Nippon Telegraph and Telephone Public Corporation, Ibaraki, Japan

Journal: Iongen to Ion o Kiso Toshita Oyo Gijutsu, Shinpojumu (pages 319-26)
1981

Publisher: Ion Kogaku Kondankai, Kyoto, Japan

Language: English

Structure of Carbon Films Formed During Fast-Ion Deposition

A. S. Bakai, V. E. Strel'nitskii

U.S.S.R.

Journal: Zh. Tekh. Fiz., Vol. 51, No. 11 (Pages 2414-16)

1981

Language: Russian

Precipitation of Diamond Films from Ionic Carbon Beams

E. F. Chalkovskii, V. M. Puzikov, A. V. Semenov

Vses. Nauchno-Issled. Inst., Monokrist., Kharkov, U.S.S.R.

Journal: Kristallografiya, Vol. 26, No. 1 (pages 219-22)

1981

Language: Russian

Studies of Diamondlike Carbon Coatings for Protection of Optical Components

M. L. Stein and S. Aisenberg

Gulf + Western Applied Science Laboratories

335 Bear Hill Road, Waltham, MA 02154

B. Bendow

The BDM Corporation

1801 Randolph Road, S.E., Albuquerque, NM 87106

1981 Boulder Symposium

Ion-deposited diamondlike carbon is a promising candidate for thin protective coatings for optical components. Recent studies have been directed to ascertaining several key properties of the coating, and verifying its protective nature.

Tests performed on coated discs of CaF₂ indicated improved resistance to environmental attack by acids, bases, and solvents. Hermeticity was corroborated by comparing the effects of HF-acid on coated and uncoated surfaces. The tenacity to substrates such as glass and CaF₂ was demonstrated by the difficulty to remove the coating with standard techniques, such as exposure to HF and water. Also, a marked decrease in abrasion was found (by measuring forward optical scatter) for the coated portion of a disc.

Optical measurements performed on these coated discs indicated that the coating neither significantly decreased transmission as measured from 2 to 6 microns, nor induced visible scatter. High resolution scanning and transmission electron micrograph studies indicate that the films are partly amorphous with a partial ordering of carbon atoms; while Raman studies indicated both graphite as well as microcrystalline diamond-type behavior. ESCA studies indicated a C to CaF₂ gradient throughout the coating indicative of ion implantation. Thickness determinations were made by substrate dissolution and surface profile measurements.

Surface Structures of Synthetic Diamonds

H. Kanda, M. Akaishi, N. Setaka, S. Yamaoka, O. Fukunaga

J. Mater. Sci. (GB) (JMTSAS), Vol. 15, No. 11 (pages 2743-8)

November 1980

Electron Spectroscopy of Ion Beam and Hydrocarbon Plasma Generated Diamondlike Carbon Films
Proceedings of the 27th National Symposium of the American Vacuum Society, Detroit, MI, 13-17 Oct. 1980
T. J. Moravec, T. W. Orent

Synthesis of Metastable Materials by Sputter Deposition Techniques
T. W. Barbee, Jr., D. L. Keith
TMS/AIME, 420 Commonwealth Drive, Warrendale, PA 15085
October 9, 1980

The application of sputter source techniques to the synthesis of metastable phases (Cu-Zr, Cu-Ag) is considered. Factors intrinsic to vapor deposition that make it a powerful process for synthesis of metastable phases are discussed. Also, as sputter deposition is a complex process, the effects of factors (vapor source--deposition surface coupling, energy distribution of incident adatoms, ambient atmosphere in the deposition system, condensation energy of the adatoms, energies of formation or mixing in multicomponent alloys, geometry of the vapor source--substrate configurations, substrate characteristics) are systematically explored. Particular emphasis is placed on synthesis of noncrystalline or amorphous metastable phases including diamondlike carbon. It is shown that a separation of experimental variables is possible and that the effects of sputter deposition process parameters can be qualitatively isolated as a result of advances in sputter source technology. Hence, it is now possible to control and thereby purposefully use these extrinsic factors to synthesize designed metastable phases.

Key Words: Sputtering, Copper Base Alloys, Phases (state of matter), Synthesis; Zirconium, Alloying Elements; Silver, Alloying Elements; Amorphous Structure.

Identifiers: Cu-48Zr, Cu-48Ag, CU

The Structural Characteristics of Some Allotropes of Carbon Using Surface Secondary Electron Emission Spectroscopy
H. G. Maguire, P. J. Schonning
Proceedings of the Fourth International Conference on Solid Surfaces and the Third European Conference on Surface Science, 22-26 Sept. 1980, Cannes, France
Societe Francaise du Vide, Paris, France, 1981
Language: English.

Secondary electron emission measurements on various carbons consisting of diamond, highly oriented stress annealed pyrolytic graphite, vitreous C, and variously prepared evaporated C films were performed in a conventional UHV (// 10 -- 9 torr) LEED/Auger chamber under identical conditions. Differences between the various carbons were observed in all regions of the secondary emission spectrum. X-ray examination of the thick amorphous films complements the secondary emission results.

Key Words: Graphite, Atomic Properties, Diamonds, Atomic.

The Use of Ion-Beam Deposited Diamondlike Carbon for Improved

Optical Elements for High Powered Lasers

S. Aisenberg and M. Stein

Applied Science Laboratories

335 Bear Hill Road, Waltham, MA 02154

Journal: NBS Spec. Publ., Vol. 620 (pages 313-23)

1981

The use of thin films of ion-beam deposited diamondlike carbon (DLC) appears to provide a number of properties that could result in improved optical elements (windows, mirrors) for high powered lasers. Many of these properties have already been described.

Of particular importance for high powered lasers is the ultra-smooth nature of the ion-beam deposited DLC plus its transparency, chemical inertia, and barrier properties. Several mechanisms predict and explain why DLC films are observed to be smoother than the substrate, and can result in improved transmission and reflection coefficients. The problem of high power surface breakdown associated with microscopic irregularities in the substrate can be reduced as a result of the ion-beam deposition energy and the smoothing effects of a film of ion-beam diamondlike carbon. The relationship of DLC to high power breakdown at surface defects, as well as plasma breakdown will be discussed to show how the ion-beam diamondlike carbon coating can improve performance.

Key Words: Diamondlike Carbon, Thin Films, Ion-Beam Deposition, Surface Smoothness, Barrier Properties.

Optical Properties of Hydrogenated Amorphous Carbon (a-C:H) - A Hard Coating for IR-Optical Elements

A. Bubenzer and B. Dischler

Fraunhofer-Institut fur Angewandte Festkoerperphysik, Freiburg, FRD

A. Nyaiesh

School of Engineering and Applied Sciences

University of Sussex, Falmer, Brighton, England

1981 Boulder Damage Symposium (to be published)

Hydrogenated amorphous carbon films a-C:H were deposited on glass and germanium substrates. The films are transparent in the IR and are extremely hard (Mohs's hardness of about 8). The a-C:H coatings were prepared according to the method of Holland in an RF excited discharge sustained by various hydrocarbon gases.

Thickness, density, refractive index (at 0.3 μm and 2-10 μm) and relative hydrogen content were determined. Variations in IR-refractive index and relative hydrogen content could be correlated with deposition conditions. With a refractive index of approximately 2, a-C:H is an ideal AR-coating for germanium ($n=4$). Laser calorimetric measurements of optical absorption at 10.6 μm give a loss as low as 4 percent for a 1.3 μm thick coating on germanium ($\lambda/4$ for $n=2$ at 10.6 μm). Preliminary damage tests with a CO₂ laser (600 W, cw) were performed.

Key Words: Amorphous Hydrogenated Carbon, AR Coating, Germanium, Hard Coating, Infrared, Laser Calorimetry, Plasma Deposition.

Structure and Properties of Quasi-Amorphous Films Prepared by Ion Beam Techniques

C. Weissmantel, K. Bewilogua, D. Dietrich, H. J. Erler, H. J. Hinneberg,
S. Klose, W. Nowick, G. Reisse

Proceedings of International Conference on Metallurgical Coatings,
San Diego, CA, 21-25 April, 1980

Tech. Hochsch., Karl-Marx-Stadt, East Germany
September 15, 1980

Ion beam deposition techniques offer interesting possibilities for the preparation of metastable quasi-amorphous films owing to a high local activation and rapid quenching on an atomic scale. This is demonstrated in the context of new results obtained with the following materials: (1) i-carbon with diamondlike properties; (2) film-forming processes and the layer properties observed are interpreted by a first approximation model based on the concept of rapidly collapsing thermal spikes.

Key Words: Ion Plating; Amorphous Structure; Hardness, Cooling Effects; Ion Beams, Thin Films; Microstructure, Quenching (cooling); Carbon, Mechanical Properties; Silicon; Hydrogenation; Boron Nitride, Mechanical Properties.

Identifiers: Quasi-Amorphous Films, BN, CPD.

Color Chart for Diamondlike Carbon Films on Silicon

T. J. Moravec

Corp. Mater. Sci. Cent., Honeywell Inc., Bloomington, MN 55420

Journal: Thin Solid Films, Vol. 70, No. 1 (pages L9-10)

July 15, 1980

Language: English

The so-called i-C ("ionized carbon") films, with hardness, inertness, and resistance characteristics resembling those of diamonds, were deposited on single-crystal Si wafers by the butane-decomposition and ion-beam techniques. A tabulation of 16 colors relatable with given film thickness in the range 300-2700 Å, and therefore applicable to speedy thickness estimations, is presented. In view of refractive-index similarities, the chart is also valid for films on GaP and InP substrates.

Key Words: Carbon, Physical Properties, Hardness; Resistivity, Ion Beams, Thin Films, Physical Properties, Reactions (chemical), Thickness Measurements, Substrates, Silicon, Coating, Color.

Electron Tunneling Devices Using Diamondlike Amorphous Carbon as a Barrier

E. I. Alessandrini, R. J. Gambino, C. C. Tsuei, J. M. Viggiano

IBM Tech. Disclosure Bulletin (IBMTAA), Vol. 23, No. 1

(pages 387-92)

June 1980

Spin Resonance Spectroscopy of Amorphous Carbon Films

R. J. Gambino, J. A. Thompson

IBM Thomas J. Watson Res. Center, Yorktown Heights, NY

Solid State Commun., Vol 34, No. 1

April 1980

Spin resonance has been used to study the unpaired spins in amorphous carbon films prepared by the plasma decomposition of propane. The properties of amorphous carbon prepared by this method are very diamondlike. The ESR signal shows saturation effects and a fairly large positive G shift ($G=2.003 \pm .0003$). Both of these characteristics are associated with unpaired spins in a delocalized system, e.g., aromatic radicals. The authors conclude that there is appreciable trigonal bonding in this form of amorphous carbon which causes some delocalization into a pi molecular orbital.

Key Words: Carbon, Amorphous State, Infrared Spectra of Inorganic Solids, Hardness, Paramagnetic Resonance, Bonds (chemical), Plasma Deposited Coatings.

Identifiers: Unpaired spins, Plasma Decomposition, Propane, ESR Signal, Saturation Effects, G Shift, Aromatic Radicals, Trigonal Bonding, Pi Molecular Orbital, Amorphous C Films, Delocalized Systems, IR Spectra, Hardness.

Diamondlike Three-Fold Coordinated Amorphous Carbon

N. Wada, P. J. Gaczi, S. A. Solin

James Franck Institute, University of Chicago, Chicago, IL

Proceedings of the 8th International Conference on Amorphous and Liquid Semiconductors, Cambridge, MA, 23-27 Aug 1979

Journal: J. Non-Cryst. Solids, Vols. 35-36, No. 1 (pages 543-48)

February 1980

Language: English

Evaporated and sputtered Alpha-C films deposited at LN temperature were prepared and studied as a function of annealing using Raman, electron energy loss, and ESR techniques. The reduced Raman spectra of virgin films reflect the one phonon density of states of graphite. No evidence for diamond bonding is found from the electron energy loss experiment. Upon annealing, graphic structural correlations develop within bounded islands of carbon atoms. This picture is consistent with ESR measurements which yield $3 + 10^{19}/\text{spins}/\text{cm}^3$ independent of annealing but a resonance line ($G=2.002 \pm .0005$) that narrows with annealing. A model based solely on a three-fold coordinated random network structure is presented to explain the "diamondlike" physical properties of A-C films and their changes with annealing.

Key Words: Carbon, Annealing, Raman Spectra of Inorganic Solids, Electron Energy Loss Spectra, Paramagnetic Resonance, Noncrystalline State Structure, Vibrational States in Disordered Systems, Vacuum Deposited Coatings, Sputtered Coatings.

Identifiers: Alpha-C Films, Annealing, Electron Energy Loss, ESR, Raman Spectra, Phonon Density of States, Graphic Structural Correlations, Evaporated Film, Sputtered Film, Diamondlike Three-Fold Coordinated.

**Deposition of Carbene and Diamondlike Films in the Plasma of an RF
Gas Discharge**

E. I. Zorin, V. V. Sukhorukov, D. I. Tetel'baum
Zh. Tekh. Fiz. (U.S.S.R.) (ZTEFA3) Vol 50, No. 1 (pages 175-7)
January 1980

**Microtexture of Mesophase Spheres as Studied by High Resolution Conven-
tional Transmission Electron Microscopy (CTEM)**

D. Auguie, M. Oberlin, A. Oberlin, P. Hyvernat
Carbon (GB) (CRBNAH) Vol. 18, No. 5 (pages 337-46)
1980

Electrical and Optical Properties of Hydrogenated Amorphous Carbon Films

B. Meyerson and F. W. Smith

Department of Physics
The City College of New York, New York, NY 10031
1980

We have measured the electrical conductivity (25 to 350C) and optical absorption (1.65 to 4 eV) of a series of hydrogenated amorphous carbon (a-C:H) films prepared via dc glow discharge decomposition of acetylene (C_2H_2) at deposition temperatures T_d between 25 and 375C. The electrical conductivity is not simply activated, and varies by over 11 orders of magnitude for the samples studied. Optical energy gaps inferred from optical absorption data lie between 0.9 and 2.1 eV, decreasing with increasing T_d . It can be inferred from these measurements that the films will be "graphitic" in their electrical and optical properties for T_d greater than about 425C.

**Chemical Modification of the Electrical Properties of Hydrogenated
Amorphous Carbon Films**

B. Meyerson and F. W. Smith

Department of Physics
The City College of New York, New York, NY 10031
1980

Semiconducting films of hydrogenated amorphous carbon (a-C:H), prepared via the dc glow discharge decomposition of C_2H_2 , have been successfully doped via incorporation of B and P during growth. The doping efficiency achieved was comparable to that achieved in a-Si:H produced in a like manner. For a-C:H films deposited at $T_d=250C$, $\sigma(RT)$ increased from 10^{-12} to $10^{-7} \text{ ohm}^{-1} \text{ cm}^{-1}$ when either 1 percent PH_3 or 10 percent B_2H_6 were added to the C_2H_2 . A shift of the Fermi level E_F of about 0.7 eV is inferred from changes in the activation energy of conduction.

Carbon Thin Film Preparation by Laser Evaporation

Susumu Fujimori

Ibaraki Electr. Commun. Laboratory

Nippon Telegraph and Telephone Public Corporation, Ibaraki, Japan

Journal: Shinku, Vol. 23, No. 7, (pages 333-38)

1980

Language: Japanese

Highly Efficient Source of Pure Carbon Plasma

I. I. Aksenov, S. I. Vakula, V. G. Padalka, V. E. Strel'nitskii,

V. M. Khoroshikh

Fiz.-Tekh. Institute, Kharkov, U.S.S.R.

Journal: Zh. Tekh. Fiz., Vol. 50, No. 9 (pages 2000-4)

1980

Language: Russian

Effect of Graphitization on the Properties of Diamondlike Carbon Coatings

S. I. Vakula, V. E. Strel'nitskii

Khar'k. Fiz.-Tekh. Institute, Kharkov, U.S.S.R.

Journal: Sverkhtverd. Mater., No. 4 (pages 3-6)

1980

Language: Russian

Study of the Gas-Phase Deposition of Carbon Onto a Diamond Substrate

Under Conditions of Moderate Pressure

O. P. Bespal'ko, O. N. Andreev

Inst. Sverkhtverd. Mater., Kiev, U.S.S.R.

Journal: Sverkhtverd. Mater., No. 5 (pages 21-22)

1980

Language: Russian

Precipitation of Carbene and Diamondlike Films in a Gaseous HF

Discharge Plasma

E. I. Zorin, V. V. Suknorukov, D. I. Tetel'baum

Gor'k. Issled. Fiz.-Tekh. Inst., Gorkiy, U.S.S.R.

Journal: Zh. Tekh. Fiz., Vol. 50, No. 1 (pages 175-77)

1980

Language: Russian

Optical Properties of Diamondlike Carbon Films

S. I. Vakula, V. G. Padalka, V.E. Strel'nitskii, A. I. Usoskin

Khar'k, Politekh. Inst., Kharkov, U.S.S.R.

Journal: Sverkhtverd, Mater., No. 1 (pages 18-22)

1980

Language: Russian

Frictional Properties of Diamondlike Carbon Layers

K. Enke, H. Dimigen, H. Huebsch

Forschungslab. Hamburg, Phillips G.m.b.H., 2000, Hamburg, FRG

Journal: *Appl. Phys. Lett.*, Vol. 36, No. 4 (pages 291-2)

1980

Language: English

Mode of Hydrogen Entrance Into Synthetic Diamond Films

L. D. Kislovskii, B. V. Spitsyn

Inst. Kristallogr., Moscow, U.S.S.R.

Journal: *Kristallografiya*, Vol. 25, No. 2 (pages 414-15)

1980

Language: Russian

Carbon Layers with Diamondlike Properties

(Patent): East Germany; DD 138678

Christian Weissmantel, Christian Schuerer, Klaus Bewilogua, Lienhard Pagel,
Uwe Scheit, Bernd Rau, Ingolf Loeschner, Dietmar Fabian

German Democratic Republic

November 24, 1979 (13 pages)

Language: German

Properties and Coating Rates of Diamondlike Carbon Films Produced

by RF Glow Discharge of Hydrocarbon Gases

L. P. Andersson, S. Berg, H. Norstrom, R. Olaison, S. Towta

University of Uppsala, Sweden

Proceedings of International Conference on Metallurgical Coatings,

San Diego, CA, 23-27 April 1979, Vol. 63, No.1 (pages 155-160)

October 15, 1979

Language: English

The properties of films produced by cracking various hydrocarbon gases in an RF glow discharge were studied. Mass spectrometry studies and optical spectroscopy of the glow discharge were performed during the experiments. The production rates for the films increased with molecular weight for gases having the same structural form, e.g., C₄H₁₀ had a higher coating rate than CH₄ under the same plasma conditions. Also, the sputter-etch rate of the films depended on both the substrate material and the hydrocarbon gas used. Films several microns thick were manufactured onto steel substrates and showed a microhardness of more than 3,000 kgf/mm².

Key Words: Carbon, Coatings, Glow Discharges, Alkanes, Microhardness, Growth Rate, Amorphous Materials, Mechanical Properties, Adhesion, Steels.

Diamondlike Carbon

(Patent): United States, US 4228142

Cressie E. Holcombe, James B. Condon, D. H. Johnson

August 31, 1979 (5 pages)

Language: English

Film Preparation Using Plasma or Ion Activation

C. Weissmantel

Proceedings of International Congress on Thin Films, Loughborough,
England, 11-15 Sep 1978, Vol 58, No. 1 (pages 101-105)

Tech. Hochsch, Karl-Marx-Stadt, East Germany

March 15, 1979

It has been established that reactive layer growth can be enhanced by using plasma or ion activation. The capabilities of these techniques are discussed in connection with results obtained for the following film deposition processes: (1) the formation of silicon layers by plasma-induced chemical vapor deposition (CVD) from $\text{SiCl}_4\text{-H}_2$; (2) the synthesis of $\text{Si}_x\text{N}_y\text{-H}_z$ coatings by plasma-induced CVD from Si-NH_3 ; (3) the preparation of hard and transparent (diamondlike) carbon films by the condensation of ionized organic species.

Key Words: Films, Preparation; Silicon Compounds, Thin Films; Electric Discharges, Plasmas.

Identifiers: Chemical Vapor Deposition.

Structure and Properties of Diamond Films Grown on Foreign Substrates

B. V. Deryagin, B. V. Spitsyn, L. L. Builov, G. V. Aleksandrov,

G. G. Aleksnadrov, V. P. Repko, A. E. Gorodetskii,

Z. E. Sheshenina

Inst. Fiz. Khim, Moscow, U.S.S.R.

Journal: Dokl. Akad. Nauk SSSR, Vol. 244, No. 2 (pages 388-89)

1979

Language: Russian

Evaluation of Carbon Deposited from Gas Phase on Diamond

Mutsukazu Kamo, Yoichiro Sato, Nobuo Setaka

Natl. Institute for Research of Inorganic Matter, Tokyo, Japan

Journal: Koen Yoshishu-Jinko Kobutsu Toronkai, 24th (pages 49-50)

1979

Language: Japanese

Some Properties of Diamondlike Carbon Coatings and Possible Fields of Their Use

I. I. Aksenov, V. G. Padalka, V. E. Strel'nitskii, V. T. Tolok,
V. P. Zubov, M. F. Semko

Khar'k, Fiz.-Tekh. Inst., Kharkov, U.S.S.R.

Journal: Sverkhvred. Mater., No. 1 (pages 25-28)

Language: Russian

Synthesis of Diamond Epitaxial Layers and Some of Their Properties

B. V. Spitsyn, B. V. Deryagin

Journal: Probl. Fiz. i Teknol. Shirokozon. Poluprovodnikov,
2-e Vses. Soveshch. po Shirokozon, Poluprovodn., Leningrad,
U.S.S.R. (pages 22-34)

1979

Language: Russian

Plasma Deposition of Optical Thin Films for Infrared Use

L. Holland

Unit for Plasma Materials Processing, University of Sussex
Palmer, Sussex, England

Proceedings of 5th Conference of Modern Utilization of Infrared
Technology, 29-30 Aug 1979, San Diego, CA, Vol. 197
(pages 319-23)

Work on three types of plasma deposition processes is reviewed. The processes which afford film thickness growth rates of several hundred angstroms per minute are plasma polymerization of hydrocarbon, silicone, and fluorocarbon gases. the growth of amorphous carbon and silicon films in hydrocarbon and silane plasmas, respectively, and the formation of oxides and nitrides by plasma gas reactions. These processes have potential use for preparing anti-reflection films and polymer moisture protective films on halide crystals. It is proposed that interference systems based on A-Si/A-C layers could be made by plasma chemical processes.

Key Words: Optical Films, Plasma Deposition, Polymerization, Antireflection Coatings, Protective Coatings.

Identifiers: Optical Thin Films, Infrared, Plasma Deposition Processes, Plasma Polymerization, Plasma Gas Reactions, Moisture Protective Films, Interference Systems, Amorphous C.

Effect of Residual Atmosphere on Properties of Diamondlike Coatings

Produced by Vacuum-Plasma Technology

V. E. Strel'nitskii, S. I. Vakula, V. Y. Kolot, V. V. Mozgin,
V. N. Bondarenko

Fiz.-Tekh. Inst., Kharkov, U.S.S.R.

Journal: Sint. Almazy, No. 2 (pages 11-14)

1979

Language: Russian

Diamondlike Carbon Films Produced in a Butane Plasma

S. Berg, L. P. Andersson

Inst. Technology, University of Uppsala, Uppsala, Sweden

Proceedings of 4th International Congress of Thin Films, Loughborough,
England, 11-15 Sep 1978

Journal: Thin Solid Films, Vol. 58, N. 1 (pages 117-20)

1979

Language: English

Diamondlike carbon films produced in an RF butane plasma were characterized by X-ray photoemission analysis of the deposits. It was confirmed that films produced at low deposition rates were more diamond-like than films produced at high deposition rates. An investigation of the electrical properties of the films showed that the low deposition rate films were highly insulating whereas the high deposition rate films were conducting.

Key Words: Carbon-Thin Films, Diamonds, Films, X-Ray, Analysis, Electric Conductivity, Electric Insulating Materials.

Reactive Pulse Plasma Crystallization of Diamond and Diamondlike Carbon

M. Sokolowski, A. Sokolowska, B. Gokiel, A. Michalski

A. Rusek, Z. Romanowski

Institute of Mater. Sci., Warsaw Tech. University, Warsaw, Poland

Journal: J. Cryst. Growth, Vol. 47, No. 3 (pages 421-26)

1979

Language: English

Substrate Sputtering During Plasma Deposition of Diamondlike Carbon Films

H. Norstroem, R. Olaison, L. P. Andersson, S. Berg

Inst. Technol., University of Uppsala, Upssala, Sweden

Journal: Vide, Couches Minces, Vol 196 (pages 11-19)

1979

Language: English

Phase Transformation in Thin Carbon Layers

D. V. Fedoseev, V. P. Varnin

Inst. Fiz. Khim, Moscow, U.S.S.R.

Journal: Sb. Dokl. Konf. Poverkhn. Silam, Vol. 6, No. Poverkhn.

Sily Tonkikh Plenkakh (pages 203-6)

1979

Language: Russian

Properties of Diamondlike Carbon Coating Produced by Plasma Condensation

V.E. Strel'niskii, I. I. Aksenov, S. I. Vakula, V. G. Padalka,

V. A. Belous

Journal: Pis'ma V Zh. Tekh. Fiz. (U.S.S.R.), Vol. 4, Nos. 21-22

(pages 1355-58)

November 1978

Some Trends in Preparing Film Structures by Ion Beam Methods

G. Gautherin, C. Weissmantel

University of Paris, Orsay, France

Journal: Thin Solid Films, Vol. 50 (pages 135-44)

May 1, 1978

Film deposition by ion beam sputtering or condensation offers interesting possibilities for the preparation of special layer structures because activation energy can be supplied to the growing film in a defined manner. Some results of recent work on the ion beam sputtering of $Nv//xGe//y$ under ultrahigh vacuum conditions using insitu diagnostics and on the dual deposition of $S1//3N//4$ and diamondlike carbon are presented. Further trends are discussed in connection with methods of condensing low energy ions.

Key Words: Niobium Germanium Alloys, Thin Films; Ion Beams; Films, Preparation; Sputtering.

Synthesis of Diamond Crystals

(Patent): Japan Kokai Tokkyo Koho; JP 79131590

Yoshinari Miyamoto, Shushei Kuge

April 4, 1978 (6 pages)

Language: Japanese

The Growth of Carbon Films with Random Atomic Structure from Ion Impact Damage in a Hydrocarbon Plasma

L. Holland, S. M. Ojha

Unit For Plasma Materials Processing

University of Sussex, Falmer, Brighton, England

Journal: Thin Solid Films (Switzerland), Vol. 58, (pages 107-11)

March 15, 1978

The authors describe experiments on the coating of germanium targets on a water-cooled electrode in a butane RF plasma (13.56 MHz) with the electrode capacitively coupled to the supply to provide a negative bias to enhance ion impact. Films prepared at a low power input-to-pressure ratio of $1.2 \text{ W cm}^{-2}/\text{torr}$ were polymers with some oxygen contamination as shown by their infrared absorption bands. Raising the ratio to $40 \text{ W cm}^{-2}/\text{torr}$ produced carbon films without absorption in the measured region $\lambda=2-20 \mu\text{m}$. The films were amorphous with a refractive index of 1.9-2.0 and a resistivity of $10\text{ }\Omega\text{ cm}$. At higher power-to-pressure ratios or target temperatures the film resistivity fell with loss of the infrared transparency. A critical ratio exists at which energetic ion impact is sufficient to rupture all C-H bonded species reaching the target and to damage any structure ordering which may otherwise arise. At high ratios the target cooling is considered to be insufficient to prevent the film temperature rising and resulting in a transition from a metastable to a graphite form. In conclusion, the properties of vacuum-deposited carbon and the nature of some reported defects in diamond are considered in relation to the characteristics of ion impact films.

Key Words: Carbon, Insulating Thin Films, Ion-Beam Effects, Electronic Conduction in Insulating Thin Films, Refractive Index, Plasma Deposition, Impurities, Infrared Spectra of Inorganic Solids.

Identifiers: Growth, Random Atomic Structure, Ion Impact Damage, Butane, RF Plasma, Polymers, Infrared Absorption Band, Refractive Index, Resistivity, Critical Ratio, C-H Bonded Species, Target Cooling, Metastable to Graphite Transition, $O/\text{sub}/2$ Contamination, Power Input to Pressure Ration, Amorphous Films.

**Properties of the Diamondlike Carbon Film Produced by the Condensation
of a Plasma with an RF Potential**

V. E. Strel'nitskii, V. B. Padalka, S. I. Vakula

Journal: Soviet Phys. Tech. Phys., Vol. 23, No. 2 (pages 222-24)

February 2, 1978

Certain properties of the diamondlike film produced in the condensation of a carbon plasma stream in vacuum are studied. The deposition conditions are also studied. The properties of the carbon condensate are compared when dc and RF potentials are applied to the substrate. The RF potential yields a diamondlike coating with a higher electrical resistivity.

Key Words: Diamonds, Thin Films; Films, Preparation; Plasmas, Application; Carbon, Thin Films.

**Ultra-Microhardness of Vacuum-Deposited Films, Ultra-Microhardness
Tester**

Mineo Nishibori, Koreo Kinosita

Journal: Thin Solid Films, Vol. 48 (pages 325-31)

February 1, 1978

Language: English

Key Words: Thin Films, Mechanical Properties; Diamond Pyramid Hardness Tests, Microhardness

Epitaxial Synthesis of Diamond by Carbon-Ion Deposition at Low Energy

J. H. Freeman, W. Temple, G. A. Gard

Harwell, England

Journal: Nature (London), Vol. 275, No. 5681 (pages 634-35)

1978

Language: English

**Some Properties of Diamondlike Carbon Coatings Produced by Condensation
of Matter from a Plasma Phase**

**V. E. Strel'nitskii, I. I. Aksenov, S. I. Vakula, V. B. Padalka,
V. A. Belous**

**Journal: Pis'ma Zh. Tekh. Fiz., Vol. 4, No. 22 (pages 1355-58)
1978**

Language: Russian

On Energy Spectrum and Graphitization of Diamondlike Carbon Form

V. E. Strel'nitskii, S. I. Vakula, N. N. Matushenko

Journal: Ukr. Fiz. Zh., Vol. 22, No. 3 (pages 430-32)

March 1977

Language: Russian

Electrical, Structural, and Optical Properties of Amorphous Carbon
J. J. Hauser
Bell Lab, Murray Hill, NJ
Journal: Non Cryst. Solids, Vol., 23, No. 1, (pages 21-41)
January 1977

The planar and transverse electrical resistivity of amorphous carbon (a-C) films getter-sputtered at low temperature (77-95 K) is examined. Films thinner than 600 Å display a two-dimensional hopping conductivity from which one deduces a density of states $N(E/F)$ at the Fermi level of $10.1.8 \text{ eV}^{-1} \text{ cm}^{-3}$ and a radius of the localized wave functions (a) of 12 Å. Tunneling experiments and optical absorption measurements are consistent with a pseudogap of approximately 0.9 eV.

Diffraction Intensities and the Structure of Amorphous Carbon
B. J. Stenhouse, P. J. Grout
Physics Department, The Blackett Laboratory
Imperial College, Prince Consort Road, London, SW7 2BZ, UK
July 4, 1977

A model structure of amorphous carbon is investigated incorporating layered domains connected by means of a random network, the relative proportions of the two regions being a variable of the model. It is shown that for a certain relative proportion of the two regions there is good agreement between the predicted and experimentally observed electron and X-ray scattering intensities. The effects of covalent bonding are also studied and shown to be significant for small k .

Structure and Morphology of Autoepitaxial Diamond Films
A. E. Alekseenko, B. V. Deryagin, A. Gorodetskii, A. P. Zakharov,
M. D. Kliya, B. V. Spitsyn, L. L. Builov
Inst. Fiz. Khim. Moscow, U.S.S.R.
Journal: Tezisky Dokl. Vses. Soveshch. Rostu Krist., Vol. 1 (pages 122-23)
1977
Language: Russian

Diamondlike Carbon Films - Factors Leading to Improved Biocompatibility
S. Aisenberg
Gulf & West. Applied Science Lab., Waltham, MA
Journal: Ext. Abstr. Program - Bienn. Conf. Carbon, Vol. 13
(pages 87-89)
1977
Language: English

Coating with Diamondlike Carbon
(Patent): Japan Kokai Tokkyo Koho; JP 76128686
Yoichi Murayama, Yoichi Matsuda, Yoshimasa Hiruma, Toshihiro Takao
Orient Watch Co., Ltd., Japan
November 9, 1976 (3 pages)

Ion-Beam-Deposited Polycrystalline Diamondlike Films
E. G. Spencer, P. H. Schmidt, D. C. Joy, F. J. Sansalone
Applied Phys. Lett. (U.S.A.) (APPLAB), Vol 29, No. 2 (pages 118-20)
March 1976

X-ray and electron beam diffraction analyses have been carried out on thin films deposited from a beam of carbon ions. Results show that the films consist of a polycrystalline background of cubic diamond with a particle size of 50-100 Å with single-crystal regions up to 5 μm in diameter.

Epitaxial Diamond-Graphite Films
B. V. Deryagin, D. V. Fedoseev, N. D. Polyanskaya,
E. V. Statenkova
Inst. Fiz. Khim., Moscow, U.S.S.R.
Jurnal: Kristallografiya, Vol. 21, No.2 (pages 433-34)
1976
Language: Russian

Structure of Autoepitaxial Diamond Films
B. V. Deryagin, B. V. Spitsyn, A. E. Gorodetskii, A. P. Zakharov,
L. L. Builov, A. E. Alekseenko
Dep. Surf. Phenom., Inst. Phys. Chem., Moscow, U.S.S.R.
Journal: J. Cryst. Growth, Vol. 31 (pages 44-48)
1975
Language: English

Growth of Polycrystalline Diamond Films from the Gas Phase
B. V. Deryagin, D. V. Fedoseev, V. P. Varnin, A. E. Gorodetskii,
A. P. Zakharov, I. G. Teremetskaya
Inst. Fiz. Khim., Obninsk, U.S.S.R.
Journal: Zh. Eksp. Teor. Fiz., Vol 69, No. 4 (pages 1250-52)
1975
Language: Russian

Structure of Diamond Films Obtained from the Gaseous Phase Under Low Pressures
B. V. Deryagin, B. V. Spitsyn, A. E. Alekseenko, A. E. Gorodetskii,
A. P. Zakharov
Trans. of Akademiya Nauk SSSR, Doklady, Vol. 213, No. 5 (pages 1059-61)
March 29, 1974

Key Words: Diamonds-Crystal Structure, Films, Electron Diffraction, Low Pressure Research, Refractive Index, Density (Mass/Volume), Hardness, Translations, U.S.S.R.
Identifiers: JPRS

Low Pressure Vapor Growth of Diamond
John C. Angus, Nelson C. Gardner
Chemical Engineering Division, Western Reserve University,
Cleveland, OH
Final Technical Report, 25 Jun 69-24 Jun 72
March 16, 1973

Key Words: Diamond-Crystal Growth, Methane, Hydrogen, Mathematical Models, Vapor Plating, Deposition, Semiconducting Films, Diboranes, Reaction Kinetics, Doping

Identifiers: Vapor Deposition, SD.

Optical Spectra of Thin Films of Carbon - Effects of Thermic Treatments
C. Levy-Mannheim, J. Merin
CNRS, Orleans, France
Journal: Carbon (GB), Vol. 10, No. 5 (pages 505-18)
October 1972
Language: French

The optical study of turbostratic carbons was undertaken after having succeeded in making transparent carbon films of different thicknesses. The fundamental optical spectra $\epsilon_{\text{sub} 1}$ and σ have been plotted as a function of the energy $\hbar\omega$ of the incident photons in infrared range. When these films are heated in vacuum up to 900°C , their structure changes into an oriented model of turbostratic carbon ($1,000^{\circ}\text{C}$). Their electronic properties can be compared with those of graphite. The optical conductivity σ comes close to that of graphite while $\epsilon_{\text{sub} 1}$ takes lower (and always negative) values than before the heat treatment. This fact shows that the free carriers are more numerous than in graphite because of the presence of a great number of defects which act as electron traps. These results agree fairly well with the scheme proposed by Mrozowski for graphitizable carbons.

Key Words: Carbon-Films, Solid Optical Properties, Spectra, Inorganic Solids, Optical Constants, Crystal, Electron States Impurity, States Effects, Heat Treatment

Identifiers: Optical Study, Turbostratic Carbons, Transparent Carbon Films, Fundamental Optical Spectra, Energy, Incident Photons, Infrared Range, Vacuum, Structure, Oriented Model, Electronic Properties, Graphite, Optical Conductivity, Heat Treatment, Free Carriers, Defects, Electron Traps, Mrozowski, Graphitizable Carbons.

Deposition of Carbon Films with Diamond Properties (in Abstracts of Papers Presented at the 10th Conference on Carbon, Bethlehem, PA, 28 Jun-2 Jul 1971)

S. Aisenberg, R. Chabot
Carbon (GB) (CRBNAH), Vol. 10, No. 3.
June 1972 (356 pages)

Plasma Apparatus for the Deposition of Thin Films
(Patent): Germany Offen., DE 2113375
Sol Aisenberg
Whittaker Corp.
October 7, 1971 (19 pages)

Ion-Beam Deposition of Thin Films of Diamondlike Carbon
S. Aisenberg, R. Chabot
Whittaker Corporation, Waltham, MA
Journal: Applied Physics, Vol 42, No. 7 (pages 2953-58)
June 1971

An ion-beam deposition technique has been developed and was used to deposit thin films of insulating carbon on room-temperature substrates. It was established that the carbon films deposited using this technique are insulating and have many characteristics similar to that of carbon in the diamond form.

Thickness Estimation of Carbon Films by Electron Microscopy of Transverse Sections and Optical Density Measurements
R. C. Moretz, H. M. Johnson, D. F. Parsons
Dept. of Biophysics, Roswell Park Memorial Inst., Buffalo, NY
Journal: Applied Physics, Vol. 39, No. 12 (pages 5421-24)
November 1968

Rapid and convenient method for accurate determination of thickness of carbon films from their optical density is described; linear relationship was found between optical density and film thickness; optical-density-thickness curve was calibrated by direct measurement of thickness of transverse sections of carbon films embedded in epoxy resin; method can probably be extended to thin films of soft metals and other inorganic films having significant optical density and capable of being sectioned with diamond knife; pertinent to quantitative electron microscopy.

Key Words: Films-Thickness Measurement.

Optical Absorption Edge of Evaporated Carbon Films in the Near Infrared Region
Sanchi Mizushima, Yoshiko Fujibayashi
Keio University, Koganei, Japan
Journal: Carbon (Oxford), Series: 6, Issue 1 (123 pages)
1968

Key Words: Evaporated C Films Absorption, Carbon Films, Absorption, IR Absorption C Films, Optical Absorption.
Identifiers: Properties Films Carbon.

H. Schmellenmeier, Z. Phys. Chem. 205, 349 (1955)

Electron Diffraction Study of Evaporated Carbon Films

J. Kakinoki, K. Katada, T. Hanawa, T. Ino

The Institute of Polytechnics

Osaka City University, Osaka, Japan

August 11, 1959

The structure of evaporated carbon films has been studied by electron diffraction using a camera with a rotating sector. Films of 100 \AA thickness were used. Eleven halos were observed in the range of $s = (4\pi/\lambda) \sin\theta < 33\text{\AA}^{-1}$. Both the radial distribution and the correlation methods were applied to the analysis of dta.

Results obtained are as follows. Two kinds of bond distances exist in the film. One is the graphite-like 1.41 \AA , and the other is the diamondlike 1.55 \AA . The number of the diamondlike distances is somewhat larger than that of the graphite-like distances. Mean deviations of these equilibrium distances are 0.11 ~ 0.12 \AA , which are about twice as large as those found in free molecules. The atomic distribution around any atom becomes uniform beyond several Angstrom units. The probable atomic arrangement in the film is a three-dimensional random network consisting of graphite-like and diamondlike configurations. A model of such atomic arrangement is proposed and compared with structure of other amorphous carbons.

SECONDARY REFERENCES*

Optical Properties of Diamond: Index of Refraction and Absorption Coefficient
David F. Edwards
Handbook of Optics, E. D. Palik, Editor
(1983, to be published)

Infrared Refractive Index of Diamond
David F. Edwards and Ellen Ochoa
Los Alamos National Laboratory
University of California, Los Alamos, NM 86545
November 25, 1980

The refractive index of natural Type IIa diamond is reported for the spectral region of 1.5-15 μ m. The data have been fitted to a Herzberger-type dispersion formula with a quality of fit of a few places in the fifth decimal place. The resultant index uncertainty is about 10^{-3} .

Diamond Cyrstallites
(Patent): East Germany, DD 143070
Klaus Bewilogua, Klaus Breuer, Dietmar Fabian, Christian Schuerer,
Guenter Reisse, Christian Weissmantel
July 30, 1980 (6 pages)
Language: German

Diamond Coatings for Increased Wear Resistance
H. Wapler, T. A. Spooner, A. M. Balfour
Journal: Tribol Int., Vol. 13, No. 1 (pages 21-24)
February 1980

The use of small diamond particles in metal (nickel) matrix composite wear coatings is discussed, and the control that can be maintained of the size and shape of the particles is described. The physical properties of the diamond coating used and the effect of particle shape, particle concentration, and operating temperature on its performance under test conditions are investigated, and the results obtained for a range of applications are presented.

Key Words: Protective Coatings-Nickel and Alloys, Metallic Matrix Composite, Diamonds.

*These references, although not directly on diamond-like carbon coatings, may be of interest for a variety of related reasons.

A Correlation Between the Infrared Absorption Features and the Low Temperature Thermal Conductivity of Different Types of Natural Diamonds

J. W. Vandersande

Physics Department

University of the Witwatersrand, Johannesburg, South Africa

Journal: Phys. C (GB), Vol. 13, No. 5 (pages 759-64)

1980

The low-temperature thermal conductivity of three different types of natural diamond has been measured between 0.5 and 20 K. It has been attempted to relate the infrared absorption features of the diamonds with their thermal conductivity.

Study of Cathodoluminescence of Diamond Epitaxial Films

V. S. Vavilov, A. A. Gippius, A. M. Zaitsev, B. V. Deryagin,

B. V. Spitsyn, A. E. Alekseenko

Fiz. Inst. Lebedeva, Moscow, U.S.S.R.

Journal: Fiz. Tekh. Poluprovodn. (Leningrad), Vol. 14, No. 9
(pages 1811-14)

1980

Language: Russian

Study of Growth Kinetics and Doping of Semiconductor Films by Computer Simulation

L. N. Aleksandrov, A. N. Kogan, V. I. D'yakonova

Inst. Semicond. Phys., Novosibirsk, U.S.S.R.

Proceedings of 8th International Vac. Congress

Journal: Vide, Couches Minces, Vol. 201, No. Suppl. (pages 137-40)
1980

Language: English

Surface Structures of Synthetic Diamonds

H. Kanda, M. Akaishi, N. Setaka, S. Yamaoka, O. Fukunaga

Journal: Mater. Sci. (GB) (JMTSAS), Vol. 15, No. 11 (pages 2743-48)

1980

Optical Absorption and Luminescence in Diamond

J. Walker

Groupe de Phys. des Solides de l'Ecole Normale Superieure

University of Paris VII, Paris, France

Journal: Rep. Prog. Phys. (GB), Vol. 42, No. 10 (pages 1605-59)

October 1979

This review outlines some relevant aspects of theoretical physics-molecular orbital and other calculation of the properties of point defects, symmetry and group theory, zero-phonon lines, and the configuration coordinate

diagram. The experimentally observed spectra can conveniently be divided into infrared (<1 eV), which are observed in absorption and are mainly vibrational, and visible (1-5.5 eV), which are vibronic and are observed in both absorption and luminescence. Visible spectra include those present naturally, those induced by irradiation, and those induced by irradiation plus annealing. This review covers all the important point defects observed optically in diamond and includes some results that are not generally available. The relevance of the experimental results to the current controversy about how to calculate the properties of point defects is brought out.

Key Words: Diamond, Luminescence of Inorganic Solids, Photoluminescence, Visible and Ultraviolet Spectra of Inorganic Solids, Infrared Spectra of Inorganic Solids, Impurity and Defect Absorption Spectra of Inorganic Solids, Lattice Phonons, Point Defects, Elemental Semiconductors, Reviews

Identifiers: Luminescence, Diamond, Review, Point Defects, Symmetry, Group Theory, Molecular Orbital Calculations, IR Spectra, Zero Phonon Lines, Optical Absorption Spectra, Elemental Semiconductors.

Diamond and Carbide Get It Together

Anonymous

Journal: Mach. Prod. Eng., Vol. 134, No. 3460 (pages 26-27)
May 2, 1979

One of the most recent developments in cutting tool materials concerns the marrying of diamond and carbide. By coating a tungsten carbide substrate with fine-grained synthetic diamond, an extremely hard and tough composite is produced. It can be made into blanks and used for cutting tools, wire drawing dies, drill crowns and wear resistant parts. Examples are cited which show that this new composite material has performed well under true production conditions, particularly in the turning field. However, the material can also be used for wire drawing dies and tests have shown it to be successful for operations with most nonferrous metals. For drawing copper and aluminum, for example, die bore life is said to be up to 200 times better than with a tungsten carbide die and between 3 and 5 times greater than that of a diamond single-crystal die.

Key Words: Cutting Tools, Composite Materials.

Coatings Produced by Vacuum Condensation of Plasma Streams (Method of Condensation With Ionic Bombardment)

I. I. Aksenov

Journal: Ukr. Fiz. Zh., Vol. 24, No. 4 (pages 515-25)
April 1979

Language: Russian

An account is presented of arc erosion sources of metallic plasma with self-stabilization and magnetic retention of the cathode spot on the cathode working surfaces. A description is given of the plasma-optics devices required

to focus and separate the generated sources of plasma streams. The proposed devices can be used in equipment for the deposition of coatings by vacuum condensation with ionic bombardment. Data are presented on condensates of complex composition (based on nitrides and carbides), obtained by introducing nitrogen or carbonaceous gases into the chamber; the condensation of carbon-bearing plasmas produces diamondlike materials. The phase constitution, microstructure, microhardness, and surface structure of the resulting coatings are considered in relation to the basic parameters of the condensation process (active gas pressure, substrate temperature, ion energy).

Key Words: High Speed Tool Steels, Coating, Plasma (Physics), Vacuum-Deposited Coatings, Surface Structure, Microstructure, Ion Plating

Identifiers: Alloy Index.

Ion-Beam Evaporation Method

(Patent): Japan Kokai Tokkyo Koho; JP 79124879
Nippon Telegraph and Telephone Public Corp., Japan
February 28, 1979 (4 pages)

Language: Japanese

Compact-Grained Diamond Material

(Patent): United States, US 4142869
L. F. Vereshchagin, A. A. Semerchan, T. T. Gankevich, M. E. Dmitriev,
V. P. Modenov
U.S.S.R.
March 6, 1979 (4 pages)

Language: English

Magnetic Study of Absorption on the Surface of Diamondlike Semiconductors

I. S. Kirovskaya, L. N. Pimenova
Izd. Nauka, Moscow, U.S.S.R.
Journal: Sorbtsiya Khromatogr. (pages 54-57)
1979

Language: Russian

IR Spectroscopy Studies of Oxygen Surface Compounds on Carbon

J. Zawadski
Chemical Inst., Nicholas Kopernicus University, Torun, Poland
Journal: Carbon (CG), Vol. 16, No. 6 (pages 492-97)
1978

Spectral studies of oxidation process were carried out on carbon films prepared by carbonization of polyfurfuryl alcohol and of cellulose. Investigation of the oxygen role on the initial stages of carbonization shows that oxygen surface compounds formed during such process have different chemical structure from those produced during oxidation of carbonic film previously

absorbed at 600°C. Chemisorption of oxygen at room temperature on the carbonic film (desorbed previously at 600°C) occurs with the participation of PI electrons of condensed aromatic systems. Iono-radical structures formed during that process show absorption bands in the range of 1590 cm⁻¹. Oxidation of the carbon films carbonized at 800°C causes a decrease in the absorption coefficient, and oxygen surface compounds formed show absorption bands at about 1760, 1600, and 1260 cm⁻¹. The carbon films as a model substance give possibilities for broader application of IR spectroscopy in studies of carbon, carbonization, and activation processes, sorption effects, and catalytic mechanism.

Key Words: Infrared Spectra of Inorganic Solids, Surface Chemistry, Oxidation,

Thin Films, Carbon

Identifiers: Carbonization, Chemical Structure, Oxidation of Carbonic Films, Participation of PI Electrons, IR Spectroscopy, Activation Processes, Sorption Effects, Catalytic Mechanism, C Films.

Hard Conducting Implanted Diamond Layers

J. J. Hauser, J. R. Patel, J. W. Rodgers

Journal: Appl. Phys. Lett. (USA) (APPLAB), Vol. 30, No. 3
(pages 129-30)

February 1, 1977

Intermediate Form of Crystalline Carbon

V. E. Strel'nitskii, N. N. Matyushenko, A. A. Romanov, V. T. Tolok
Kharkov Phys.-Tech. Inst., Kharkov, U.S.S.R.

Journal: Dopov. Akad. Nauk Ukr. RSR, Fiz.-Mat. Tekh., No. 8 (pages 760-62)
1977

Language: Ukrainian

Growth of Diamond from Methane at a Temperature Over 1100 Degrees

D. B. Fedoseev, I. G. Varshavskaya, A. Lavrent'ev, B. V. Deryagin
Inst. Fiz. Khim., Moscow, U.S.S.R.

Journal: Izv. Akad. Nauk SSSR, Ser. Khim., No. 4 (pages 928-31)
1977

Language: Russian

**Charge Transfer and Nature of the Acceptor in Semiconductor Epitaxial
Diamond Layers**

A. E. Alekseenko, V. S. Vavilov, B. V. Deryagin, M. A. Gukasyan, T. A.
Karatygina, E. A. Konorova, V. F. Sergienko, B. V. Spitsyn,
S. D. Tkachenko

Inst. Fiz. Khim., Moscow, U.S.S.R.

Journal: Dokl. Akad. Nauk SSSR, Vol 233, No. 2 (pages 334-47)
1977

Language: Russian

**Photoconductivity and Electron Paramagnetic Resonance in Defects in
Epitaxial Diamond Films**

**N. D. Samsonenko, L. L. Builov, T. A. Karpukhina, B. V. Spitsyn,
V. I. Timchenko**

Donetsk. Gos. Univ., Donetsk, U.S.S.R.

Journal: Sint. Almazy, No. 2 (pages 6-8)

1977

Language: Russian

**Characteristic K-Shell Low-Energy Electron Loss Spectra from Diamond,
Graphite, and Evaporated Carbon Surfaces**

Journal: Phys. C (GB) (JPSQAW), Vol. 9, No. 5 (pages L135-38)

March 14, 1976

**Concomitant Particulate Diamond Deposition in Electroless Plating
(Patent): United States, US 3936577**

Theodore P. Christini, Albert L. Eustice, Arthur H. Graham

E. I. DuPont de Nemours and Co.

February 3, 1976 (26 pages)

A Method for Synthesizing Diamonds

(Patent): Japan Tokkyo Koho; JP 7607639

Japan

Hiroshi Ishizuka

March 9, 1976 (6 pages)

Nonmetallic Coatings for Diamond and Kubonit Powders

A. E. Shilo

Inst. Sverkhverd. Mater., Kiev, U.S.S.R.

Journal: Sint. Almazy, No. 6 (pages 20-21)

1976

Language: Russian

New Data on the Absorption of Synthetic Diamonds in the One-Phonon Region

V. G. Malogolovets, A. S. Vishnevskii

Inst. for Very Hard Materials

Academy of Sciences, Kiev, Ukrainian S.S.R.

Journal: Dokl. Akad. Nauk SSSR, Vol. 225, Nos. 1-3 (pages 319-21)

Trans. In: Sov. Phys.-Dokl. (USA), Vol. 20, No. 11 (pages 721-23)

November 1975

A UR-20 infrared spectrophotometer has been used to study previously unconsidered absorption bands in synthetic diamond crystals. It is also suggested that a certain lattice disruption, the D centre, contributes to the 1135 cm^{-1} band normally attributed to the concentration of paramagnetic nitrogen in the C centre.

Key Words: Diamond, Infrared Spectra of Inorganic Solids, Lattice Phonons, Colour Centres

Identifiers: Absorption Bands, Synthetic Diamond Crystals, Lattice Disruption, D-Centre, C-Centre Paramagnetic N, One-Phonon Region.

Diamond M - Partner in Productivity

Proceedings of Technical Symposium, Washington, DC, 11-12 Nov 1974
Ind. Diamond Assoc. of Am. Inc., Morristown, NJ (202 pages)

Twenty-three papers by various authors are presented. The topics discussed are: tool blanks, superhard materials, sintered diamond, micron abrasives, surface finishing, capping and polishing, grinding, wheels, coolants, glass generating fluids electroplated tools, composite coatings, drill cutting agents, diamonds in glass industry, grinding wheels, history of diamond uses, roller dressers, filter substrates, manufactured diamonds, cutting with wire, abrasive machining. Individual papers are indexed separately.

Key Words: Diamonds-Cutting Tools, Diamond, Grinding Wheels-Diamond.

Properties and Applications of Composite Diamond Coatings

William F. Sharp

DuPont, Gibbstown, NJ

Diamond M - Partner in Productivity Tech. Symp., Washington, DC

11-12 Nov 1974 (pages 121-26)
1974

A unique new wear-resistant coating has been developed that can be economically applied to many metal and nonmetal surfaces. The coating consists of micron-size particles of shock-synthesized diamond, uniformly dispersed in a plated metal matrix. Laboratory and field tests have demonstrated that composite diamond coatings have wear resistance and are suited for many industrial applications as a replacement for conventional wear-resistant materials. Tables and diagrams show properties.

Key Words: Diamonds-Synthethic, Coating Techniques.

X-Ray Photoemission Studies of Diamond, Graphite, and Glassy Carbon Valence Bands

F. R. McFeely, S. P. Kowalozyk, L. Ley, R. G. Cavell, R. A. Pollak.

D. A. Shirley

Journal: Phys. Rev. B (USA) (PLRBAQ), Vol. 9, No. 12 (pages 5268-78)
June 15, 1974

A Scanning Auger Microscope for Thin Film Analysis

James Martin Kroyer

U.S. Air Force Institute of Technology

Wright-Patterson AFB, Ohio School of Engineering

December 1973 (74 pages)

Key Words: Auger Electron Spectroscopy, Spectrum Analysis, Films, Surfaces, Electron Guns, Metals, Alloys, Carbides, Diamond, Graphite, Theses
Identifiers: Scanning Auger Microscopes, AF.

A Diamond Cermet Diamond
(Patent): Japan Tokkyo Koho; JP 7310922
Tatsuo Kuratomi
April 9, 1973 (4 pages)

Synthesis of Diamonds
National Institute for Research in Inorganic Materials
Sakura, Japan
Journal: Muki Zaiken Nuysu, Vol. 22 (pages 4-5)
1973
Language: Japanese

Surface Passivation of Diamonds
(Patent): Germany Offen.; DE P2121320
Werner Langheinrich
Licentia Patent-Verwaltungs-G.m.b.H.
November 9, 1972 (9 pages)

Polycrystalline Coagulated Diamond Powder
(Patent): Japan Tokkyo Koho; JP 7249807
Tatsuo Kuratomi
December 14, 1972 (5 pages)

X-Ray Photoelectron Spectrum of Diamond
T. Gora, R. Staley, J. D. Rimstidt, J. Sharma
Journal: Phys. Rev. B (USA) (PRVBAK), Vol. 5, No. 6 (pages 2309-14)
March 15, 1972

Synthesis and Physical Properties of Diamond Crystals
A. Yu. Litvin, E. V. Sobolev, V. I. Lisoivan, V. P. Butozov,
N. D. Samsonenko
Journal: Eksp. Issled. Mineraloobrazov. Sukhikh Okisnykh Silikat. Sist.
(pages 3-8)
1972
Language: Russian

Identifiers: EPR Synthetic Diamond, IR Spectra Synthetic Diamond, UV Spectra
Synthetic Diamond, Diamond Synthetic Spectra

High-Resolution Infrared Spectra of Diamond

W. A. Runciman, T. Carter

Aere, Harwell, Didcot, England

Australian ACAD, SCI

Abstracts of 8th Australian Spectroscopy Conference, 16-20 Aug 1971,

Clayton, Australia

1971

Narrow absorption lines have been observed in the room temperature spectra of several natural Type 1A diamonds. Lines have been observed at 1405 cm⁻¹ (7.115 μ; 174.2 MeV) and 3107 cm⁻¹ (3.218 μ; 385.2 MeV), with half-widths of 2 and 4 cm⁻¹, respectively. These two lines can be explained as due to the bending and stretching vibrations of an X-11 bond. The stretching mode is expected to be stronger in intensity than the deformation mode and this fits the observed pattern. The lines showed no strong temperature variation from 77°K to 250°C. No strain splitting was observed when strains up to 0.1 percent were obtained by applying uniaxial pressure to oriented diamond blocks. This tends to favor the view that the lines are vibrational rather than electronic in origin.

Key Words: Spectra/Inorganic Solids, Diamonds, Bonds, Crystals/Lattice Mechanics

Identifiers: Diamond, Strain Splitting, High Resolution IR, Spectra, Bond Bending, Bond Stretching Vibrations.

New Methods Aim at Deposition

T. H. Malim

Journal: Iron Age, Vol. 207, No. 20 (page 61)

May 20, 1971

It is noted that at least one blade maker is depositing coatings by vacuum sputtering. Others are currently evaluating an even newer technique, ion deposition. The new technique has also drawn the interest of tool--steel and turbine--blade manufacturers. Ion deposition is said to differ from vacuum sputtering in not using an inert gas. Of all the forms of depositing in vacuum, ion deposition sends the ions down at the highest rate of energy and at an energy rate that can be controlled. A number of tests show that the film is similar to diamond. The coating is transparent, has a high index of refraction, and can scratch glass.

Key Words: Films-Razors, Blades, Cutting Tools.

Investigations of the Structure of Thin Fluorocarbon Films by X-Ray Diffraction and Infrared Spectroscopy

H. Giegengack, D. Hinze

Sekt. Phys./Elektron Bauelen., Tech. Hochsch

Karl-Marx-Stadt, Karl-Marx-Stadt, East Germany

Journal: Phys. Status Solidi A, Series 8, Issue 2 (pages 513-20)

1971

Identifiers: Fluorocarbon Film Diffraction, IR Fluorocarbon Film.

Graphitization of Micropowders of Synthetic Diamonds Studied from IR Absorption Spectra

V. G. Malogolovets, E. G. Gatilova

Journal: Sin. Almazy, Series 2, Issue 4 (pages 29-32)

1970

Language: Russian

Identifiers: Graphitization, Diamond IR Spectra.

Thermally Induced Strains in Diamond Cubic, Tetragonal, Orthorhombic, and Hexagonal Films

F. Witt, R. W. Vook

Pitman-Dunn Research Labs, Philadelphia, PA

Journal: Applied Physics, Vol. 40, No. 2 (pages 709-19)

February 2, 1969

When thin films adhere to substrate that has different thermal expansion coefficient, changing temperature of composite will induce strains in both film and substrate; calculations of strain and strain energy have been made for various films on substrates which are assumed to be undeformable and to have isotropic thermal expansion and elastic properties in directions parallel to surface of substrate; computer programs were developed to calculate above quantities for diamond cubic semiconductors Ge and Si, tetragonal metals Be, Cd, Co, Mg, Ti, Za, and Zr.

Key Words: Films-Metallic, Semiconductors-Films.

Structure of Carbon

S. Ergun

Journal: Carbon (GB), Vol. 6, No. 2 (pages 141-59)

May 1968

Infrared Absorption of the Carbonyl Group of Semicarbazides, Semi-carbazones, and Pyrazolecarboxamides

Tze Seng Wang

T.R. Evans Research Center, Diamond Shamrock Corp., Painesville, OH

Journal: Appl. Spectrosc., Series 22, Issue 3 (pages 167-69)

1968

Key Words: IR Absorption Carbonyl Groups, Semicarbazides Carbonyl Groups, Semicarbazones Carbonyl Groups, Pyrazolecarboxamides Carbonyl Groups, Infrared Spectra, Carbonyl Group, Semicarbazones

Identifiers: Spectrum, IR band, Semicarbazide Derivs. Band, Pyrazolecarboxamides, Semicarbazides.

**Electron Paramagnetic Resonance Spectra of Natural Diamonds and
Their Relation with Optical Properties**

E. B. Sobolev, N. D. Samsonenko, V. F. Dvoryankin
Journal: Radiospektrosk. Iverd. Tela (pages 334-37)

1967

Language: Russian

Key Words: Diamond Spectra, IR Diamond, UV Diamond, EPR Diamond, Optical Properties, Electron Spin Resonance, Spectra-Visible and Ultraviolet, Spectra-Infrared

Identifiers: Diamond ESR Relation, Diamonds, IR Spectrum, UV Effect, Nitrogen Content.

Diamonds, II - Infrared Absorption

Swami P. Tandon

Physics Lab., University of Jodhpur, Jodhpur, India

Journal: Proc. Rajasthan Acad. Sci., Series 11, No. Pt. 1-2
(pages 37-39)

1967

Key Words: IR Spectra Diamonds, Diamonds IR Spectra, Spectra, Infrared

Identifiers: Diamond Spectrum IR.

Lattice Dynamics of Diamond

K. G. Aggarwal

Indian Institute of Technology, Kanpur, India

Journal: Proc. Phys. Soc., London, Series 91, Issue 2 (pages 381-389)
1967

Key Words: Force Constants

Identifiers: Diamond Lattice Dynamics, Diamond Born von Karman 2, Neighbor Model, Crystal Lattice Vibrations Consts., Phonon Spectrum.

Infrared Spectra of Diamond Coat

Richard M. Chrenko, R. S. McDonald, Kenneth A. Darrow

General Electric Research & Development Center, Schenectady, NY

Journal Nature (London), Series 213, Issue 5075 (pages 474-76)
1967

Key Words: Crystallization, Infrared Spectra

Identifiers: Diamond Coat IR Spectra, Properties Spectral Bands, IR Diamond Coat, Impurity Effects, Carbonate Nitrate Water.

Deposition of Carbon on Diamond Seed Crystals

John C. Angus, Herbert A. Will

Case Institute of Technology, Cleveland, OH

Journal: U.S.C.F.S.T.I., AD Rep., No. AD 642786 (14 pages)

1966

Language: English

Lattice Dynamics and Infrared Absorption of Diamond
Ronald Wehner, H. Borik, W. Kress, Anthony R. Goodwin, Stanley D. Smith
Inst. Theoret. Phys., Frankfurt/M, Germany
Journal: Solid State Commun., Series 5, Issue 4 (pages 307-09)
1967

Key Words: Phonons, Infrared Spectra
Identifiers: Lattice Dynamics Diamond, Crystal Vibrations, IR Spectrum,
Absorption Diamond Bands.

Diamond Reinforced Coatings and Method of Preparing Same
(Patent): United States, US 3295941
James. E. Spellman
E. I. DuPont de Nemours and Co.
January 3, 1967 (3 pages)

END

FILMED

2-84

DTIC